A High-Resolution Hurricane Analysis for the Southeastern United States

by

Christopher Whatley

A thesis submitted to the Graduate Faculty of
Auburn University
in partial fulfillment of the
requirements for the Degree of
Master of Science in Natural Resources

Auburn, Alabama
May 6, 2023

Keywords: Hurricane, Climate Change, Trend Analysis, HURDAT2, Precipitation

Approved by

Dr. Sanjiv Kumar (Chair), Assistant Professor
College of Forestry, Wildlife and Environment (CFWE)
Dr. Christopher Anderson (Committee Member), Professor, CFWE
Dr. Latif Kalin (Committee Member), Professor, CFWE

Abstract

This study investigated hurricane trends in the Southeastern United States. First, we developed a high-resolution gridded hurricane dataset, GRID-HURDAT2, and calculated Accumulated Cyclone Energy (ACE) index in three spatial domains: the Southeastern U.S., the Eastern U.S., and the entire Atlantic Basin along with the mainland United States. We found little change in ACE over land since 1900, though we did find an increasing trend over the ocean. We then investigated if Atlantic Multidecadal Oscillation (AMO), Pacific Decadal Oscillation (PDO), and El Nino Southern Oscillation (ENSO) were factors relevant to tropical cyclone activity in the Atlantic Basin, and they appear to be, especially AMO. From 1900 to 2019, we found that AMO positively impacted cyclonic activity ($r = 0.45$), and PDO and ENSO negatively impacted cyclonic activity ($r = -0.23, -0.24$, respectively). In the second phase, we used the GRID-HURDAT2 dataset along with gridded precipitation data from The National Oceanic and Atmospheric Administration (NOAA) to analyze the precipitation along the paths of hurricanes. We found an increasing trend in each year's greatest magnitude precipitation events with a p-value of 0.02. To further support the precipitation analysis, we used another metric, Extreme Rainfall Multiplier (ERM), for comparison and found an increasing trend with a p-value of 0.03.

Acknowledgments

First and foremost, I would like to thank my professor, Dr. Sanjiv Kumar, for guiding me throughout my Master of Science program and teaching me. His kindness and patience were indispensable in completing this research project. I'm grateful, as well, to Dr. Anderson and Dr. Kalin for serving on my committee. They both provided constructive feedback on my writing and helpful insight into my research. My friend, Thomas Kavoo, was also quite helpful in learning to use some of the programs I needed.

This project wouldn't have been possible without the data provided at no cost from multiple sources: the National Oceanic and Atmospheric Administration and the Climate Prediction Center. Apart from using these data sources, I used the TroPYcal Python package created by Dr. Sam Lillo at the University of Boulder, Colorado, and the Cheyenne supercomputer managed by the National Center for Atmospheric Research.

My appreciation extends further to the National Academy of Sciences GULF Research program for financing this project and my friends and family for providing me with moral support and inspiring confidence in me.

Table of Contents

List of Figures

List of Tables

List of Equations

Chapter 1:

Introduction

Hurricanes are powerful storms that often form in the Atlantic Basin and then travel westward to strike Central America, the Caribbean, and North America. For example, Fig. 1 shows storm tracks for the 2018 hurricane season, taken from the National Weather Service; most hurricane activity is found over the ocean, in this case, the North Atlantic. Further, global warming can increase hurricane risk and associated heavy precipitation events due to increased water vapor in the atmosphere and decreased translation speeds, which is the rate of movement of the cyclone system as a whole, as more precipitation can fall over an area if the cyclone moves more slowly (Kossin 2018). Hence, a global context is necessary to understand the changing hurricane risk to the Emerald Coast (Box region in Fig. 2), as it is an area of high economic activity.

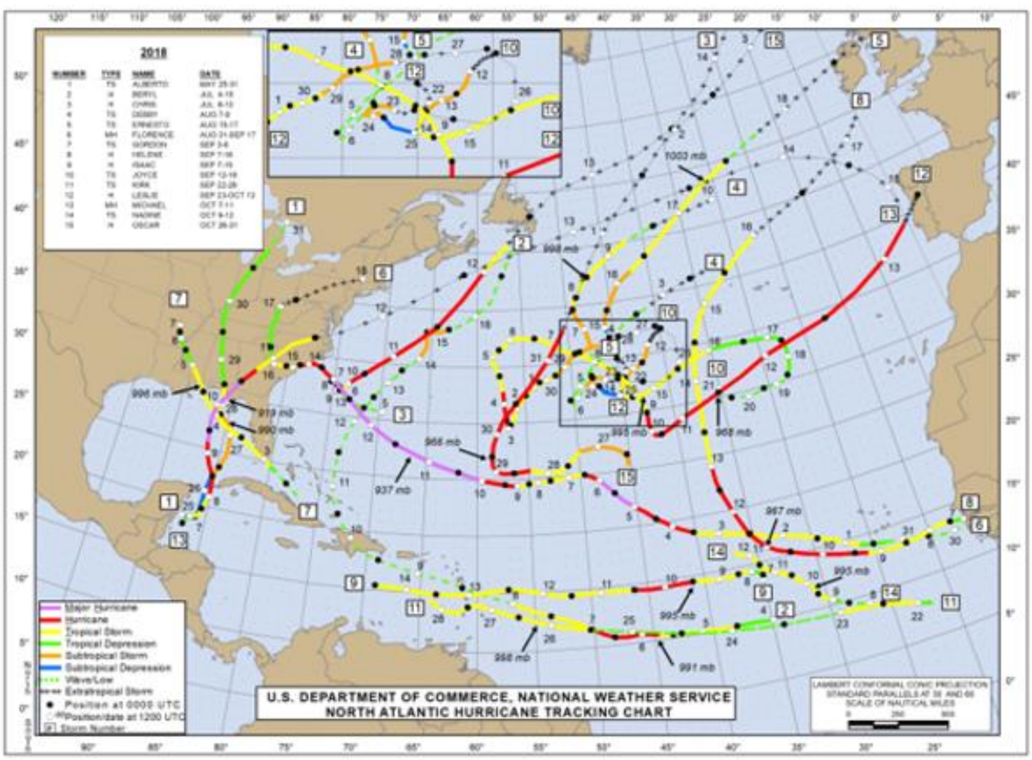

Figure 1: North Atlantic Hurricane Tracks in Year 2018. Source: National Weather Service.

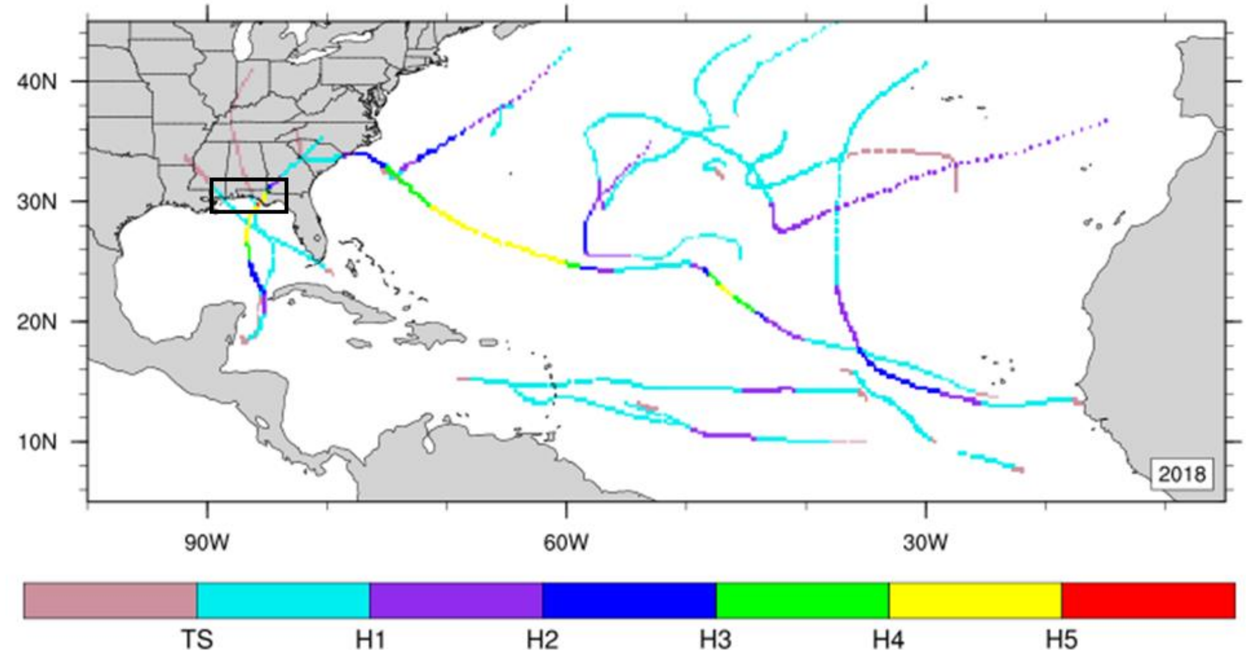

Figure 2: Hurricane Season 2018. In the Atlantic Basin and the Eastern United States with GRID-HURDAT2 Data (developed in this study). The Emerald Coast region is shown using the box. TS – Tropical Storm, H1 to H5 – Hurricane Category 1 to 5 based on the wind speed (see text).

Hurricanes bring wind-related damages and heavy precipitation, causing an average economic loss of almost $16.1 billion annually in the United States (Weinkle et al. 2018). In addition, when passing over land, they affect the areas they pass over by dropping significant amounts of precipitation and through the force of their winds. The precipitation they release can have beneficial and detrimental effects on the areas they cross over; beneficial in that it can replenish aquifers and soil moisture, and detrimental in that it can cause flooding and erosion, as just two examples. (Li and Tsai 2020).

Hurricane Data

One of the primary datasets used in working with hurricanes is HURDAT2, managed by the National Hurricane Center (NHC) (Landsea and Franklin 2013). It includes information such as location through time, the system's status, e.g., tropical system, hurricane, or an extratropical cyclone, maximum sustained wind speed, minimum pressure, and the wind speed in the four quadrants of the system. All this is measured at points in time every six hours, unaveraged, with additional measurements being taken at the time of landfall for some but not all of the systems. An issue with the HURDAT2 dataset is that historical data are less reliable. They are much more reliable, advancing through time, owing to societal changes and the advancement of tracking abilities due to newer science and technology, such as satellites, drones, and improved sensors. The reliability of the data especially improved after the beginning of the use of satellite technology to track tropical cyclones, the beginning of the satellite era often being taken as 1979 (Nnamchi et al. 2020)

Hurricane Metrics

Table 1: The Saffir-Simpson Hurricane Wind Scale (Saffir 1973).

Hurricane Category	Sustained wind speed
Tropical depression (T.D.)	0-62 km/h
Tropical Storm (T.S.)	63-118 km/h
Hurricane Category 1 (H1)	119-153 km/h
Hurricane Category 2 (H2)	154-177 km/h
Hurricane Category 3 (H3)	178-208 km/h
Hurricane Category 4 (H4)	209-251 km/h
Hurricane Category 5 (H5)	≥ 252 km/h

Saffir-Simpson Hurricane Wind Scale: A hurricane's intensity is categorized based on wind speed using the Saffir-Simpson Hurricane Wind Scale (Table 1) (Taylor et al. 2010). A hurricane is a class of tropical cyclones with a maximum sustained wind speed of at least 119 kilometers per hour. A tropical cyclone with a maximum sustained wind speed ranging from 63 to 118 kilometers per hour is called a tropical storm (T.S.), and anything less than 62 kilometers per hour is a tropical depression (T.D.). Although tropical depressions may not have destructive wind speeds, they can still drop significant amounts of precipitation and potentially cause harm through flooding (Shepherd et al. 2007). Hence, Tropical Cyclone (T.C.) is a more general term encompassing tropical depressions, tropical storms, and all five categories of hurricanes.

Accumulated Cyclone Energy: Another method of quantifying the power of a hurricane is Accumulated Cyclone Energy (ACE) (Bell and Chelliah 2006). ACE is calculated by squaring the maximum wind speed of the system every six hours and adding them (discussed later). Because the wind speed is squared, ACE increases exponentially with wind speed, as does the destructive potential of the storm system (Yu et al. 2009).

Extreme Rainfall Multiplier (ERM): This hurricane-related precipitation metric expresses T.C. rainfall as a multiple of climatologically derived 2-year return period maximum rainfall event, i.e., the median of annual maximum precipitation time series (Bosma et al. 2020). The ERM metric better assesses the precipitation impact than the wind-scale-based metric. For example, Hurricane Harvey produced record-breaking rainfall of 45 to over 50 inches (five days total) in Southeast Texas, including the Houston metropolitan area (https://www.weather.gov/hgx/hurricaneharvey, accessed May 5, 2022). Using the ERM scale, Hurricane Harvey ranks the highest (ERM = 6.4), although Harvey was a low-category storm (H1 and T.S.) in the Southeast, TX, according to the Saffir-Simpson wind scale (Bosma et al. 2020).

Literature Review

Hurricane Trends – History, Projections, and Societal Risk

Hurricane frequency varies across decades. There was greater than average hurricane activity in the 1940s, 1950s, and 1960s but relatively less in the 1970s, 1980s, and 1990s (Pielke and Landsea 1998). Although the number of major hurricanes has increased since the mid-nineties, that is not necessarily indicative of secular trends and could be due to multidecadal variability. Low-frequency variability in hurricane time series makes it more difficult to discern the influence of anthropogenic climate change.

No significant trend has been observed for tropical cyclones making landfall in the United States from 1900 to 2019. More broadly, no significant change in frequency has been found globally (Knutson et al. 2019). The frequency of tropical cyclones of lower categories, such as 1,2 and 3, is projected to decrease due to global warming, whereas the frequency of higher categories, 4 and 5 is expected to increase, as indicated in several relevant studies (Knutson et al. 2019)

Elsner et al. (2008) have found that there has been an increase in intensity among the most intense hurricanes in the past three decades. Climate model projections show the intensification of T.C.s due to global warming, particularly hurricanes of greater intensity (Elsner et al. 2008)

Best-track data refer to data developed after the passage of a hurricane season using the best possible estimates of tropical cyclone position, intensity, and other relevant variables. Heterogeneities in best-track data for tropical cyclones can complicate ascertaining trends in the relevant datasets, as the methods used vary with time, and so does the accuracy. Hurricane trends are more significant in the best-track data than homogenized gridded data, suggesting heterogeneity in the best-track data from technological changes (Kossin et al. 2020). The increases in the intensity of tropical cyclones vary between ocean basins and are most significant in the North Atlantic, the area to which this study is confined.

Large-scale climate variability can affect regional climate in regions outside the region of variability, e.g., PDO and ENSO can affect Atlantic Basin hurricanes (Lupo et al. 2008). For example, Lupo et al. (2008) found that Atlantic hurricanes are less intense during an El Niño year. Atmospheric variability is higher than variability in sea surface temperatures (SSTs), so it can be challenging to sort out the noise in analyzing individual tracks (Kossin et al. 2020).

Much is unknown about hurricanes and future trends, but some trends have become apparent, especially trends in factors relevant to the formation and activity of hurricanes. For example, SSTs have increased, and the atmosphere can hold more water vapor (Cane et al. 1997; Trenberth et al. 2005). Although models disagree on future trends, the abovementioned factors are expected to increase hurricane intensity and precipitation (Trenberth 2005). Additionally, there may be an increase in rainfall from hurricanes but not in the frequency of tropical storms and hurricanes (Knutson et al. 2008).

Changes in risk to society are driven primarily by changes in societal vulnerability, not by changes in the trends of storm events. For example, if the population is higher, there is a greater potential for loss of life, and if people have more wealth, there is a greater potential for economic damages (Pielke Jr et al. 2005).

The latest Intergovernmental Panel on Climate Change (IPCC) report finds that the precipitation associated with hurricanes may increase and that hurricane translation speeds, the speed at which the system moves, as opposed to wind speed, could decrease, which could lead to more precipitation along the storm path and a greater number of stalling events, as with Hurricane Harvey (Seneviratne et al. 2021). This metric is also less sensitive to data issues because it does not require precise measurements of a cyclone's absolute intensity. Kossin (2018) found that the average translation speeds of tropical cyclones decreased from 1949 to 2016.

A tropical cyclone has an inner region of convective activity and an outer region without convective activity. The size of a storm is necessary to analyze associated risks, such as precipitation and area of influence (Chavas et al. 2016). Tropical cyclone size has been somewhat neglected compared to other relevant metrics such as intensity. Between 1981-2011 there has been no significant change in the size of tropical cyclones within the North Atlantic Basin or globally (Knaff et al. 2014). Smaller tropical cyclones are more likely to undergo rapid intensification when the cyclone's intensity increases sharply over a relatively short period than the larger cyclones (Carrasco et al. 2014).

Impacts of Hurricanes on Society

The fact that hurricanes can cause significant economic losses on a wide scale has been well established, and it can be seen clearly from the scale of the destruction of property they cause and the lives lost. One of the prime examples of the economic cost is Hurricane Katrina, which caused the most enormous monetary loss to the United States of any hurricane in history until it struck in 2005. It was costly in terms of monetary damages and human costs; e.g., an estimated 1,836 lives were lost (Knabb et al. 2005). Because more well-developed areas tend to have higher property values, they also tend to suffer larger economic losses, although the overall impact on society is lower since they usually are more prepared for natural disasters and can do more to mitigate their harmful effects (Baade et al. 2007).

Ecological Impacts

Ecological disturbances are when forces or processes alter ecological systems or their components in reference to their normal state (Beever et al. 2019). Many kinds of disturbances can occur due to hurricanes. For example, when hurricanes occur, they can alter the populations of different organisms in diverse ways because some are much more vulnerable to such events than others (Witman 1992). One instance is that of coral communities in Florida, which were heavily affected by both Hurricanes Hugo and Gilbert (Witman 1992). Populations were affected in unexpected ways due to the severity of the disturbance and the time intervals at which they occurred. A hurricane of greater severity, Hurricane Hugo, was expected to have a more severe impact. Still, contrary to expectations, the comparatively less severe Hurricane Gilbert had a greater impact due to the fact that hurricanes had not impacted the area it struck in 54 months. Sponges had accumulated on the reef (Witman 1992).

The relative influence of a tropical storm on a community can vary based on the community and the tropical storm. Some storms are much more severe than others and have more potential to influence a community. For example, some areas might lose more or fewer trees to hurricanes based on topographic factors such as slope, elevation, and aspect, and other non-topographic factors such as soil type and density of streams (Wang and Xu 2009). Some areas could then be more or less fire-prone based on those changes in tree density. For another example, hurricanes can clear out some sites, which leaves them more available for other species to invade (Sousa 1984). In South Florida, for example, Hurricane Andrew profoundly affected the ecology of subtropical hardwood forests through alterations in the density and relative abundance of various native and exotic species after their regeneration from seed banks. (Kwit et al. 2000).

Epidemiological Significance of Tropical Cyclones

Among the myriad effects of tropical cyclones are those concerning the spread of contagious diseases. Tropical cyclones can often contribute to the spread of contagious diseases, especially waterborne diseases, and those spread by organisms that require water to reproduce and spread, particularly mosquitos (Naqvi 2010). Human factors such as land use, how buildings are designed, how people respond to the disaster, and how well people evacuate interact with storm factors such as the severity of winds, rain, flood, and storm surge to determine how contagious diseases spread (Shultz et al. 2005).

After the passing of a storm, there may be suffering from damage to buildings and infrastructure, people's homes, and healthcare infrastructure such as hospitals, especially; problems with transportation, economic issues, and others associated with that. Overall, some regions of the world suffer more from the effects of tropical cyclones, particularly those that are not as well developed, as more-developed areas have a greater capacity for handling tropical cyclones and their consequences (Shultz et al. 2005).

One of the most obvious ways to assess losses is to look at mortality. An estimated 1,836 people died as a result of Hurricane Katrina, for example (Knabb et al. 2005). Regarding the differences between how such disasters are handled in developed versus developing countries, deaths due to flooding are generally a larger proportion of overall mortality since developing countries often do not have robust emergency, warning, and evacuation systems in place compared to more developed countries. To describe this in terms of the phases of the disaster, developed countries frequently suffer a greater proportion of injuries in the phase after the storm has passed compared to the phase where the storm is making impact, and developing countries suffer more during the storm (Shultz et al. 2005).

Hurricane Modeling

A model is a conceptual/mathematical representation of a real system, and various diverse models are used across multiple domains. There are numerical models for a variety of climatic phenomena (Ford 2009). Climate models describe soil moisture, temperature, precipitation patterns and other phenomena. This study focuses on modeling tropical cyclones. Understanding and predicting tropical cyclones is necessary because of their profound impacts on society, and tropical cyclone modeling is useful to scientists and society because of its utility in understanding the behavior of tropical cyclones, which can be difficult to understand and predict through other means. (Vickery et al. 2009).

Tropical cyclone modeling has already been used to determine several vital things, such as wind speed maps in the United States and other world regions. Given that winds can damage property and infrastructure, those wind speed maps are also relevant to determining regulations in areas such as building construction and insurance (Huang et al. 2001). In the past half-century, models for tropical cyclones have improved notably. In making models for tropical cyclones, a few parameters are commonly used to identify them and describe their behavior, low sea surface pressure and high wind speed being two of the most common. Although the modeling of hurricanes in individual sites has existed for half a century, modeling entire hurricane tracks is a somewhat newer development (Vickery et al. 2009).

Vickery developed a new way of modeling hurricanes that allowed him to track a hurricane for its complete duration through the Atlantic Ocean. Their method is based principally on determining the central pressure of the system as a function of the sea surface temperature (Vickery et al. 2000; Vickery et al. 2009). Many other researchers conducted studies using his innovations. Emanuel et al. (2006) made further strides by using different models together to create many storm tracks and then synthesizing them together (Vickery et al. 2009).

Extreme Rainfall Multiplier.

Bosma et al. (2020) developed ERM (Extreme Rainfall Multiplier) as an intuitive metric for understanding extreme rainfall events. It is a hurricane-related precipitation metric that expresses tropical cyclone rainfall as a multiple of the climatologically derived 2-year return period rainfall event of a given duration, i.e., the median of annual maximum precipitation time series. To put this another way, at a given location, d-days duration (1-day) annual, maximum rainfall events in a year are ranked by their magnitude for all years, e.g., 1948 to 2021, then the median within that series is used as a baseline for comparison for tropical storms. A metric commonly used to access tropical cyclone intensity is maximum wind speed, but it does not consider their precipitation, as ERM does. Another advantage is that it shows the severity of a storm in reference to 2-year return period event, which can make it easier to understand for the public (Bosma et al. 2020)

Three Patterns of Sea Surface Temperature Oscillation: Atlantic Multidecadal Oscillation, Pacific Decadal Oscillation, and El Nino Southern Oscillation

Atlantic Multidecadal Oscillation (AMO) is a pattern of multidecadal warming and cooling SSTs in the North Atlantic Ocean that is linked with multiple climatic phenomena in different regions of the world. The cycle is about 65-80 years with a range of 0.4 degrees Celsius. Although the signal for AMO is most prominent in the North Atlantic Ocean, the signal is global and present in the North Pacific Ocean, as well (Enfield et al. 2001). AMO is detrended, so anthropogenic warming should not influence the signal. The region is between 0-70 degrees latitude in North Atlantic. Multiple warm and cold phases have been observed since 1860, but although SSTs in the North Atlantic Basin have been higher than average since 1995, it cannot be determined yet if this is a warm phase in the AMO pattern (McCabe et al. 2004). Pacific Decadal Oscillation (PDO) is another pattern of oscillating SSTs in the Pacific Ocean that may be driven by several physical processes working together (Newman et al. 2016). El Nino Southern Oscillation (ENSO) describes anomalously high SSTs in the Tropical Pacific Ocean driven by atmospheric changes, and it can cause many unusual and extreme weather events (Trenberth 1996).

A positive correlation has been found between AMO and tropical cyclone-associated rainfall in Florida and other parts of the southeastern United States. A negative correlation has been found between ENSO and tropical cyclone-associated rainfall in Texas (Nogueira et al. 2013a). PDO may be a driver of hurricane activity in the Atlantic Basin and it interacts heavily with ENSO (Lupo et al. 2008).

Description of the Emerald Coast

The study area for this project, The Emerald Coast, lies within the Florida Panhandle and the adjacent region of Alabama to the West. This area is generally considered to be comprised primarily of Escambia, Santa Rosa, Walton, Bay, and Okaloosa Counties, although some counties in Alabama, especially Baldwin County, can also be included, as well, as can be seen in Fig. 2. The Emerald Coast is urbanizing and undergoing ecosystem changes associated with urbanization, such as habitat loss problems related to the discharge of effluent from sewers. The region contains the outlets of many vital rivers that feed into estuaries due to their economic and recreational value. The surface geology is composed of sedimentary rock; it has a mild, subtropical climate stabilized by the Gulf of Mexico and large groundwater stores (Wolfe 1988). Being in southern Alabama and western Florida, it is also in a hurricane-prone region, and the subject of how hurricane trends are changing and are relevant to land use and risk in the area is worthy of research.

Knowledge Gaps

- Limited availability of gridded hurricane data, especially before the satellite era
- Global Drivers and local impact analysis for the Emerald Coast

My research addresses the non-availability of gridded hurricane data by creating a gridded hurricane dataset. This data is used to analyze hurricane-associated precipitation changes.

Objectives

This thesis aims to understand the changing risks that tropical cyclones pose to the Emerald Coast, encompassing southern Alabama and the Northwestern portion of Florida (box in Fig. 2). A larger goal of the study is to understand the impacts of climate change and land-use change on hurricane activity in the region. Hence, we have investigated long-term trends in hurricane frequency and overall hurricane activity (1900 to 2019) and their impact on extreme precipitation (1948 to 2019).

Specific objectives are:

(a) **Develop a high-resolution gridded hurricane dataset (GRID-HURDAT2)** – I developed GRID-HURDAT2 data to investigate hurricane trends over land and ocean, separately from 1900 to 2019. In addition, I investigated how hurricane frequency and overall intensity, determined by maximum wind speed, changed within that period.

(b) **Investigate hurricane-related heavy precipitation events:** The second phase of analysis investigates how precipitation along the hurricane path has changed from 1948 until 2019. The availability of high-resolution gridded precipitation data limits the precipitation analysis (1948 to 2019). In a review of what is available, I have not found precipitation data compatible with GRID-HURDAT2 before this period. Therefore, I overlayed the GRID-HURDAT2 data with the precipitation data and investigated the hurricane-related precipitation trends.

Justification for the Development of a Gridded Hurricane Dataset: GRID-HURDAT2

Another gridded hurricane dataset called HURSAT has been developed using satellite data (Kossin et al. 2020). Still, HURSAT has some drawbacks and insufficiencies compared to best-track data, which may be more accurate. The main advantage is that it is homogenous through time and space, whereas best-track datasets are not. The main disadvantage is that HURSAT only covers 1979-2017 (Kossin et al. 2020). Our gridded dataset, GRID-HURDAT2, has been generated using best-track data. Hence it goes back to the year 1900 and is suitable for long-term analysis. Some potential uses of GRID-HURDAT2 are analyses of land use along the tropical system path, analyses of precipitation along the tropical system path and analyses of tropical system trajectory.

Table 2: GRID-HURDAT2 and HURSAT Comparison. The dataset we developed, GRID-HURDAT2, is contrasted with another gridded hurricane dataset, HURSAT.

GRID-HURDAT2	HURSAT
Derived from HURDAT2 best-track data	**Derived from satellite data**
Heterogenous through space and time	**Homogenous through space and time**
Covers 1900-2019	**Covers 1979-2017**
Resolution of 0.25 degrees latitude by 0.25 degrees longitude	**Resolution of 8 kilometers**

Chapter 2

Data and Tools

HURDAT2

NOAA has maintained a hurricane database going back to 1851, recording minimum pressure, wind speed, maximum wind speed, location through time, and maximum wind radius, along the hurricane track. The original hurricane dataset maintained by NOAA (https://www.aoml.noaa.gov/hrd/hurdat/Data_Storm.html, accessed 2022) was called HURDAT, a portmanteau of hurricane and database. HURDAT2, which can be downloaded at the official NOAA website, is the revised version of HURDAT and is a continuation of it in many ways, but has been improved through the inclusion of landfall and intensity maxima, non-developing tropical depressions and best track wind radii (Landsea and Franklin 2013). Data from more recent years are more accurate than older data in HURDAT2 because the tropical systems in HURDAT2 go back to the 1800s. As one moves forward in time, superior methods are available to gather information about the tropical systems. The Best Tracking Change Committee with the NHC (National Hurricane Center) regularly revises HURDAT2 to align it with changes in tropical cyclone analysis.

HURDAT2 includes the following information in the heading for a tropical system:

Table 3: HURDAT2 Data Example.

Column1	Column2	Column3	Column4	Column5	Column6	Column7	Column8	Column9	Column10	Column11
Date	Time_Name	Number_of_	RecordIdent	Latitude	Longitude	Maximum_S	Minimum_P	34-kt_wind_	34-kt_wind_r	34-kt_wind_r
AL011851	UNNAMED	14								
18510625	0000		HU	28.0N	94.8W	80	-999	-999	-999	-999
18510625	0600		HU	28.0N	95.4W	80	-999	-999	-999	-999

Table 4: HURDAT2 Data Example Continued.

Column12	Column13	Column14	Column15	Column16	Column17	Column18	Column19	Column20	Column21
34-kt_wind_r	50-kt_wind_r	50-kt_wind_r	50-kt_wind_r	50-kt_wind_r	64-kt_wind_r	64-kt_wind_r	64-kt_wind_r	64-kt_wind_radii_maximum	
-999	-999	-999	-999	-999	-999	-999	-999	-999	
-999	-999	-999	-999	-999	-999	-999	-999	-999	

Table 5: Hurricane Michael Example Data.

AL142018	MICHAEL	38								
20181006	1800		LO	17.8N	86.6W	25	1006	0	0	0
20181007	0000		LO	18.1N	86.9W	25	1004	0	0	0
20181007	0600		TD	18.4N	86.8W	30	1004	0	0	0
20181007	1200		TS	18.8N	86.4W	35	1003	120	180	0
20181007	1800		TS	19.1N	85.7W	45	999	120	180	0

Column 1: Two characters for the basin, A.L. in the case of the Atlantic Basin, two characters for the storm's place in that year, and four characters for the year. After the heading for the storm, the year and day are recorded. For example, Hurricane Michael (AL142018) was the 14th storm in the Atlantic Basin (A.L.) in 2018.

Column 2: Name and time.

Column 3: Number of entries.

Column 4: Category.

Columns 5 and 6: Latitude and longitude.

Column 7: Maximum sustained wind speed in knots.

Column 8: Minimum pressure in millibars

Column 9-21: Wind radius in nautical miles.

Tropycal

Tropycal is a Python package to retrieve and analyze tropical cyclone data. The Tropycal package was developed by Sam Lillo at the University of Boulder in Colorado (Lillo 2022). It can work with different datasets to present information for different storms in different parts of the world, but for our purposes, we only used HURDAT2, since that is the dataset for tropical cyclones in the Atlantic Basin. We used the Tropycal package to convert HURDAT2 data into gridded data for all storms (1,523 from 1900 to 2019). A full description of the Tropycal implementation is given in Appendix A.

Atlantic Multidecadal Oscillation, Pacific Decadal Oscillation, and El Nino Southern Oscillation

Atlantic Multidecadal Oscillation (AMO) is a multidecadal pattern of warming and cooling in the Atlantic Ocean which may be one driver of some climatic phenomena (Enfield et al. 2001). We accessed data for Atlantic Multidecadal Oscillation (AMO) through the website of the Physical Sciences Laboratory of NOAA (National Oceanic & Atmospheric Administration Physical Sciences Laboratory 2023a)

Pacific Decadal Oscillation (PDO) and El Nino Southern Oscillation (ENSO) are patterns of sea surface temperature change in the Pacific Ocean that may also influence tropical cyclones in the Atlantic Basin. We accessed data for PDO through the National Centers for Environmental Information with NOAA (National Oceanic & Atmospheric Administration National Centers for Environmental Information 2023). We accessed data for ENSO through the Physical Sciences

Laboratory of NOAA (National Oceanic & Atmospheric Administration Physical Sciences Laboratory 2023b)

Precipitation Data

NOAA's Physical Science Laboratory Data: CPC Unified Gauge-Based Analysis of Daily Precipitation over CONUS: NOAA Physical Sciences Laboratory has developed daily gridded

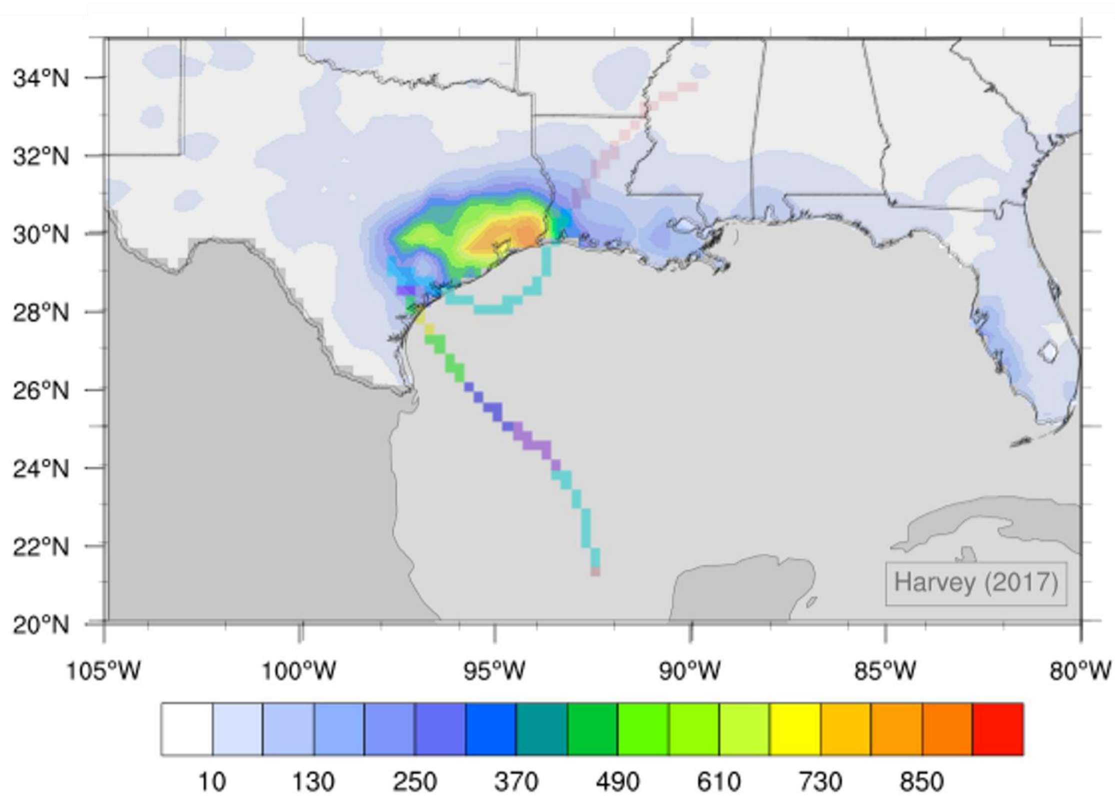

Fig. 3: Five Days Total Precipitation, Ending on August 30th, 2017. During Hurricane Harvey in CPC Unified Gauge-Based Precipitation Analysis gridded dataset. Unit: mm of precipitation in five days.

precipitation data using station-based observations (Xie et al., 2007). These precipitation data go back to 1948 until the present. The spatial resolution is 0.25 - degree latitude x 0.25 - degree longitude U.S. grid (300x120), and the spatial extent is 20.125N-49.875N, 230.125E-304.875E. An example of the data showing Hurricane Harvey is provided in Fig. 3.

Summary of Chapter 2

I used HURDAT2 as the raw input and Tropycal software. Additionally, I used gridded precipitation data from the Climate Prediction Center and data for AMO, PDO, and ENSO from the Physical Sciences Laboratory of the National Oceanic and Atmospheric Administration. Additionally, HURDAT2 data were used to find dates of landfall and create tropical storm frequency analysis. We used GRID-HURDAT2 for the ACE analysis over land and ocean. The gridded precipitation data were used to assess precipitation along the storm paths. We used data for AMO, PDO, and ENSO to investigate their influence on hurricane activity.

Chapter 3

Tropical System Frequency Through Time in the Atlantic Basin

3.1 Introduction

The first phase of our analysis was to investigate how the frequency of tropical systems has changed since 1900. Multiple measures can be used to determine how hurricane trends have changed through time. The frequency of tropical systems is relevant to society because if more hurricanes strike the United States, they could cause more damage and drop more precipitation.

3.2 Methods

For this phase of our analysis, we sorted through the dataset HURDAT2, to find how many tropical systems of all categories were identified in the Atlantic Basin in each year. Then, we analyzed the data graphically and performed trend analysis (linear regression) to see if frequency has changed over time. We separated it into different periods, 1900 forward, 1950 forward, and 1970 forward, to see if different trends would be present in those periods and analysis would be less subject to underreporting in the pre-1950s period.

3.3 Results

Storm frequency analysis – We analyzed all storms recorded in HURDAT2 database, including tropical depressions, tropical storms, and H1 to H5 in terms of their number of occurrences per year. Then I fit a linear trend line and assessed its significance, as can be seen in Fig. 4. For the period 1900 to 2019, we found a statistically significant increasing trend with a *p*-value of < 0.001; for the period 1950 to 2019, we found a statistically insignificant increasing trend with a p-value of 0.08, and for the period 1970 to 2019 we found a statistically insignificant decreasing trend with a p-value of 0.81.

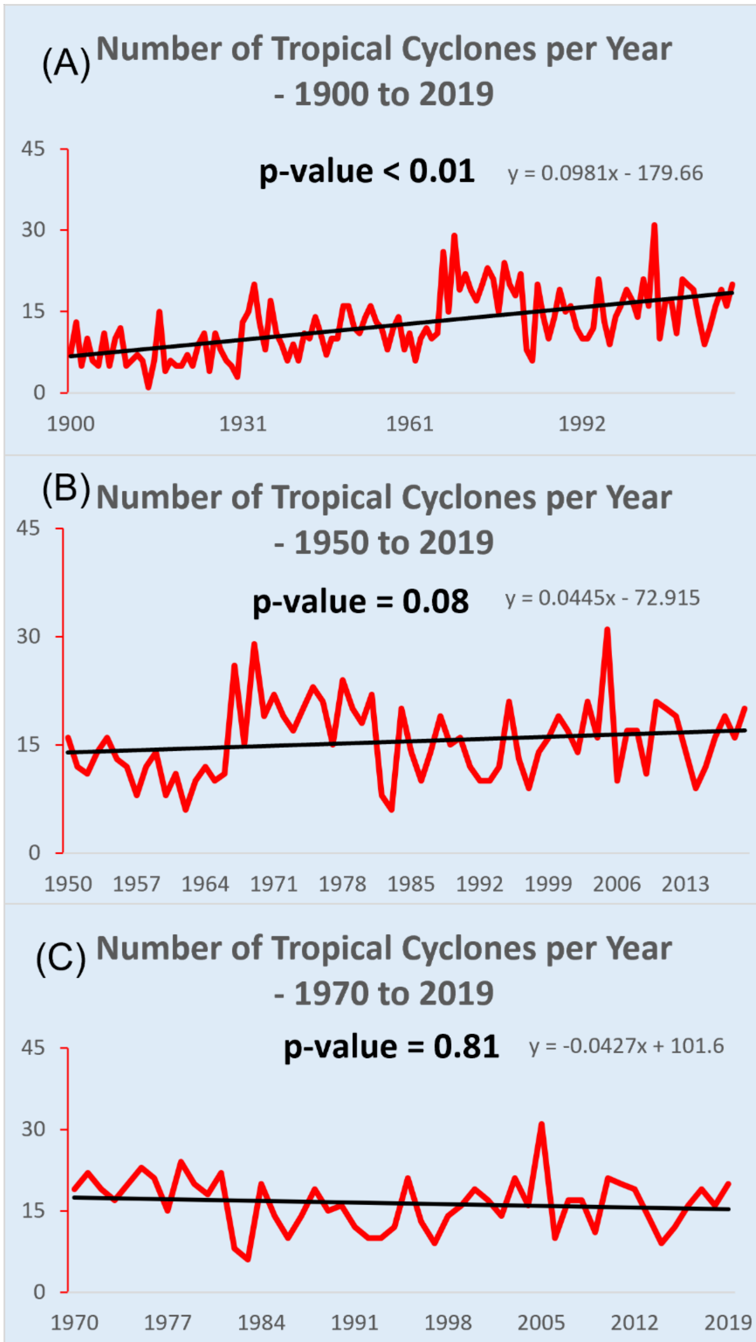

Fig. 4: Hurricane Frequency in Different Time Periods. (A) is 1900 onward, which shows a significant increase of 0.98 tropical cyclones per decade; (B) is 1950 onward, which shows a statistically insignificant increase of 0.45 tropical cyclones per decade (p-value: 0.08); and (C) is 1970 onward which does not show an increasing trend in hurricane frequency. The significance of the trends varies greatly between different periods, possibly due to data quality improving over time; and / or multi-decadal variability (discussed later)

3.4 Discussion

According to the background information that goes along with the HURDAT2 dataset, many tropical systems of lower intensity were not adequately identified in the Atlantic Basin before the 1950s, but after that, especially in the satellite era, many more were adequately identified (Nhc.noaa.gov. 2022). The trend for 1900 to 2019 is statistically significant compared to those for 1950 to 2019 and 1970 to 2019, which are not. Caution is needed to interpret the hurricane trends from 1900 to 2019 due to underreporting of hurricane activity in the pre-1950s period.

Chapter 4

Validation of GRID-HURDAT2 and Accumulated Cyclone Energy Analysis

4.1 Introduction

This phase of the analysis aimed to produce aggregated cyclone activity measures in different geographic areas. It served two purposes: (1) to create and validate the gridded dataset, GRID-HURDAT2, and (2) to better understand if tropical cyclone activity has changed over time in the areas mentioned, taking into consideration AMO, PDO, and ENSO. The measure I used was ACE, a widespread measure of tropical cyclone activity (Yu, 2009)

ACE is calculated by taking the maximum wind speed for a cyclone every six hours and summing them together along with the life of the storm (Eq. 1). A complete season's ACE can then be calculated by summing the ACE of all the storms together.

$$ACE = 10^{-4}\sum v^{2}{}_{max}$$

Equation 1: ACE Equation. ACE equals the summation of the maximum wind speed of a tropical cyclone at 6-hour intervals. Vmax represents the maximum wind speed (unit: 10^4 kt^2).

4.2 Methods

4.2.1 Creation of GRID-HURDAT2

The first step in this phase of analysis was to create a gridded hurricane dataset named GRID-HURDAT2. It was necessary to further develop an analysis of ACE, a metric of tropical cyclone intensity, in the southeastern United States, and it was used in conjunction with another precipitation dataset for a hurricane-associated precipitation analysis in the eastern United States.

To create our high-resolution gridded dataset, we used a python package called Tropycal. This python package can work with different storm-related datasets. The HURDAT2 data (csv files) was used as input to the Tropycal, because HURDAT2 is the most commonly used dataset for hurricane paths in the Atlantic, and it is already what we are using in other parts of our analysis. The following is a description of how the gridded dataset was produced within Jupyterlab, using the TroPYcal python package.

Step 1: tropycal.tracks was imported as tracks and datetime was imported as dt.

Step 2: Load in the HURDAT2 dataset as hurdat_atl, using hurdat_atl = tracks.TrackDataset(basin='north_atlantic',source='hurdat',include_btk=False).

Step 3: Got a key for each of the hurricanes to use in a loop. The key is a unique identifier for each storm including the basin it is in, which is the Atlantic Basin for all the storms in our study, the year of the storm, and the storm's place during that year. keys = hurdat_atl.filter_storms(year_range=(1990,2020),return_keys=True).

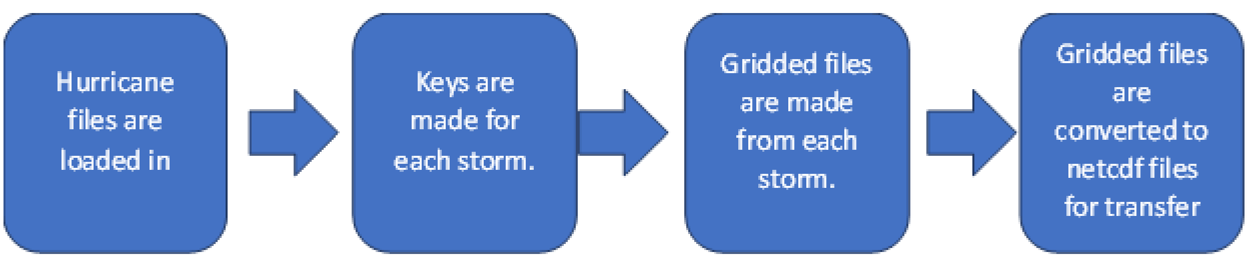

Fig. 5: Flowchart to Describe Creation of GRID-HURDAT2

Step 4: The main function used to generate the high-resolution gridded dataset was gridded_stats, but it could not plot out individual storms, so a script was written for that. The gridded_stats function was then used together with the simple script we wrote to plot out individual storms, which were converted to netcdf files using the storm.to_netcdf function, "storm.to_netcdf(str(key) = '.nc').

The steps described in Fig. 5 produced a dataset with one netcdf file for each storm in the HURDAT2 dataset. The format for the file names is A.L. for Atlantic since they are in the Atlantic Basin, followed by two digits for the storm's place within the year it occurred, followed by four

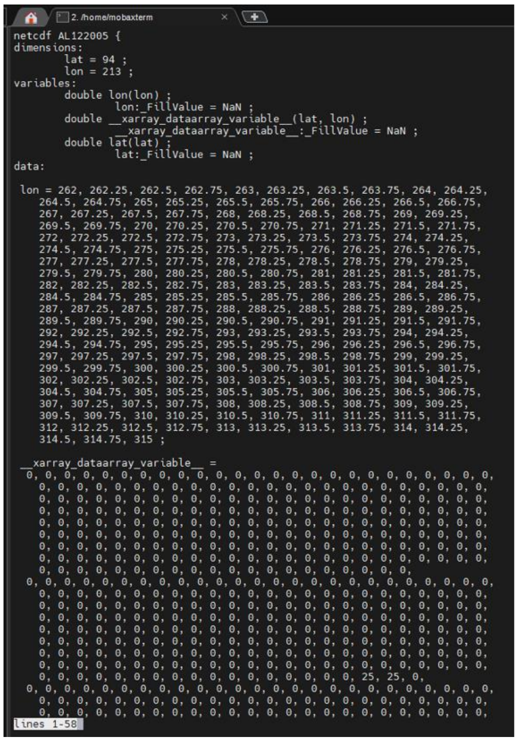

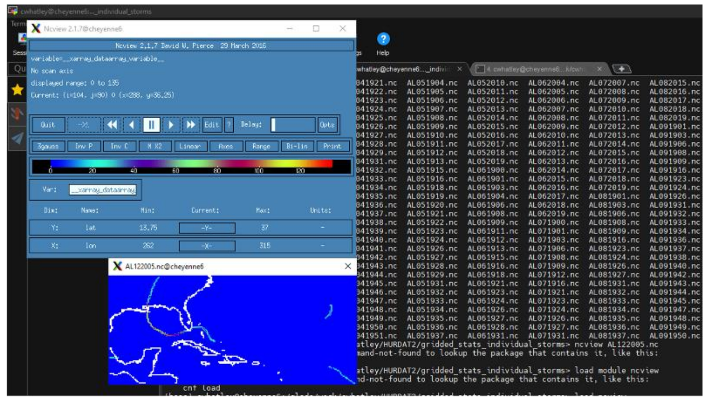

Fig. 6: Storm Path Data. The image to the right shows each storm file with an example of Hurricane Katrina. The image to the left shows each file's lat, lon, time, and wind speed.

digits for the year. The files contained four variables, latitude, longitude, time, and wind speed, at a resolution of 0.25 degrees. Fig. 6 shows all the tropical cyclone files together with Hurricane Katrina open as a graphic example along with the data contained within each file.

This dataset has been helpful in the phases of our analysis that are dealt with in other analyses in the following chapters. As a result of the fact that it has wind speed, hurricane category, and ACE can both be determined with it alone, and it can be used in conjunction with compatible datasets of the same resolution to perform other forms of analysis, as we did for our precipitation analysis.

Finally, I developed an animation to visualize hurricanes from 1900 to 2019. For each year, I plotted the hurricanes using NCAR Command Language (NCL) as a 'png' file. Then, I used MATLAB's VideoWriter function to read each 120 png files (1900 to 2019) and make a movie. This animation has been uploaded as video data along with my thesis. A sample program is shown in the appendix.

4.2.2 Accumulated Cyclone Energy Analysis

The primary dataset we used for this analysis was the gridded dataset we created, GRID-HURDAT2. It has location through time for the duration of each storm and wind speed in knots, which are both necessary for our ACE analysis. The wind speed was essential for the calculation of ACE, time was required to determine in what year each storm's ACE belonged, and position was necessary for masking, i.e., subsetting by region to determine what spatial domain the ACE would be for. We used a mask to separate our analysis into three different regions: the entire Atlantic Basin and eastern United States, which includes the tropical and midlatitude regions of the Atlantic Basin; the eastern United States, which includes the continental United States east of the states of North Dakota, South Dakota, Nebraska, Kansas along with the coastline; and the southeastern United States, which is Texas, Oklahoma, Arkansas, Louisiana, Mississippi, Tennessee, Alabama, Georgia, North Carolina, South Carolina, and Florida, along with the coastline (Fig. 7). We did this as we expected, we could find different trends in these regions. We included the entire southeastern United States instead of only the coast along the Gulf of Mexico because we wanted to understand large-scale drivers of tropical cyclone changes.

Apart from separating ACE spatially by region, we also divided it temporally into two periods: 1900 forward and 1950 forward. We did this to isolate different trends in these periods in general, and, more particularly, because more recent data are more reliable due to better data collection methods, especially those employing satellite technology after the beginning of the satellite era in 1979. In addition to dividing tropical cyclones by region and time, we also divided them by category: tropical depression, tropical storm, and hurricanes of category 1 through 5, all based on maximum wind speed.

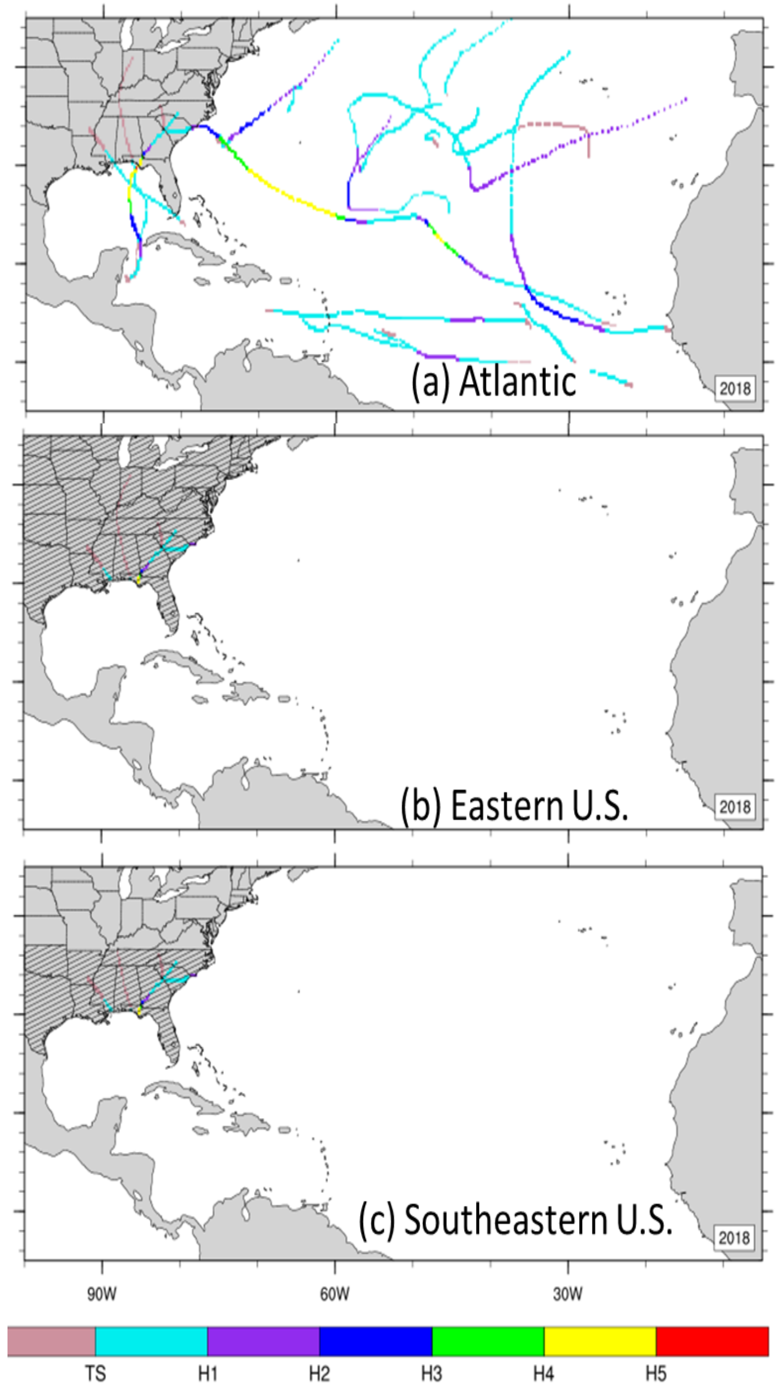

Fig. 7: Three Regional Domains for Hurricane Analysis. (a) Atlantic domain including the Eastern U.S., (b) Eastern U. S. only domain, (c) Southeastern U.S. only domain. Hurricane season 2018 is overlaid on each map.

For the script that was used to develop ACE, the necessary files, the hurricane paths and mask files, were first opened. The variables that were taken from the gridded_stats, ncl files were wind speed, latitude and longitude, represented by, "ws," "lat," and "lot," in the script. ACE was then calculated using wind speed according to time and region.

"hurdat_ana_amv_ana2_ind_storm_rev2_south.ncl" is the script that was used to produce that ACE dataset. The reader can find it in the appendix.

4.3 Results

Validation of GRID-HURDAT2

GRID-HURDAT2 compares well with NOAA's ACE estimate. The official ACE released by NOAA was used as a benchmark to compare our measures to as a way of validating the dataset we made, GRID-HURDAT2, and our methods. Our results are largely in alignment with those of NOAA, with a correlation coefficient of 0.94, as seen in Fig. 8, which we interpret to mean that our dataset, GRID-HURDAT2, is valid. Other statistical metrics were unable to be used to verify it because the two calculations are at different scales.

The ACE index produced using GRID-HURDAT2 calculates ACE using the wind speed estimate at each grid point along the path of each tropical cyclone, whereas NOAA's ACE estimate was calculated using wind speed estimates every six hours. Hence the GRID-HURDAT2 ACE estimate is one order larger than NOAA's ACE estimate. For example, in the year 2017, the ACE calculated by NOAA was 239.4 (unit: 10^4 kt^2) and the ACE we calculated using GRID-HURDAT2 was 2237.1. However, their interannual variability is similar ($r = 0.94$).

Long-term Hurricane Trends

Hurricane activity has increased over the ocean but not over land. I found that ACE has increased over land and ocean together, though not over the southeastern United States or the eastern United States (Figs. 9-10). The trend is consistent when accounting for different categories of tropical cyclones and when observing a more recent study period (Figs. 11-14).

When all categories of tropical cyclones are used in calculating ACE, the trend is highly statistically significant over land and ocean from the period 1900 to 2019 (Fig. 9, $p < 0.01$). However, when the temporal period of the analysis is confined to 1950 to 2019, the trend is less significant (Fig. 10, $p = 0.05$)

As trends in ACE could vary between tropical cyclones of lesser intensity compared to tropical cyclones of greater intensity, I produced additional ACE calculations that exclude tropical cyclones of lesser intensity. When tropical storms are excluded from the analysis, the trend is still statistically significant over land and ocean in the period 1900 to 2019 (Fig. 11, $p < 0.01$). However, for the period 1950 to 2019 over land and ocean, the trend does not meet the threshold for statistical significance, although it does approach it (Fig. 12, $p = 0.10$).

Excluding both tropical cyclones and hurricanes of category 1 from the analysis still makes apparent an increasing trend in ACE over land and ocean (Fig. 13, $p < 0.01$), which is less significant over a shorter temporal period (Fig. 14, $p = 0.05$).

AMO, PDO and ENSO

ACE, PDO, and ENSO, all internal modes of sea surface temperature variability, appear to be potential drivers of hurricane activity in the Atlantic Basin.

Of the three, AMO is the only one that has a positive correlation with ACE and has the greatest correlation coefficient of the three (Fig. 15, $r = 0.45$, $p < 0.01$). This intuitively makes sense, as AMO occurs in the Atlantic Basin where hurricanes form and move, whereas the other two modes occur in other parts of the world. Confining the analysis to a shorter period does not have an appreciable effect on how well they correlate (Fig. 16, $r = 0.46$, $p < 0.01$).

In contrast to AMO, PDO has a weak negative correlation with ACE (Fig. 15, $r = -0.23$, $p < 0.01$). In the 1900 – 2019 period and 1950 – 2019 period we found similar correlations between PDO and ACE (Fig. 16, $r = -0.22$, $p < 0.01$).

The results for ENSO are quite similar to those for PDO. ENSO also shows a negative correlation with ACE (Fig. 15, $r = -0.24$, $p < 0.01$), though it is notable that in this case, it varies more between the two temporal periods (Fig. 16, $r = -0.29$, $p < 0.01$).

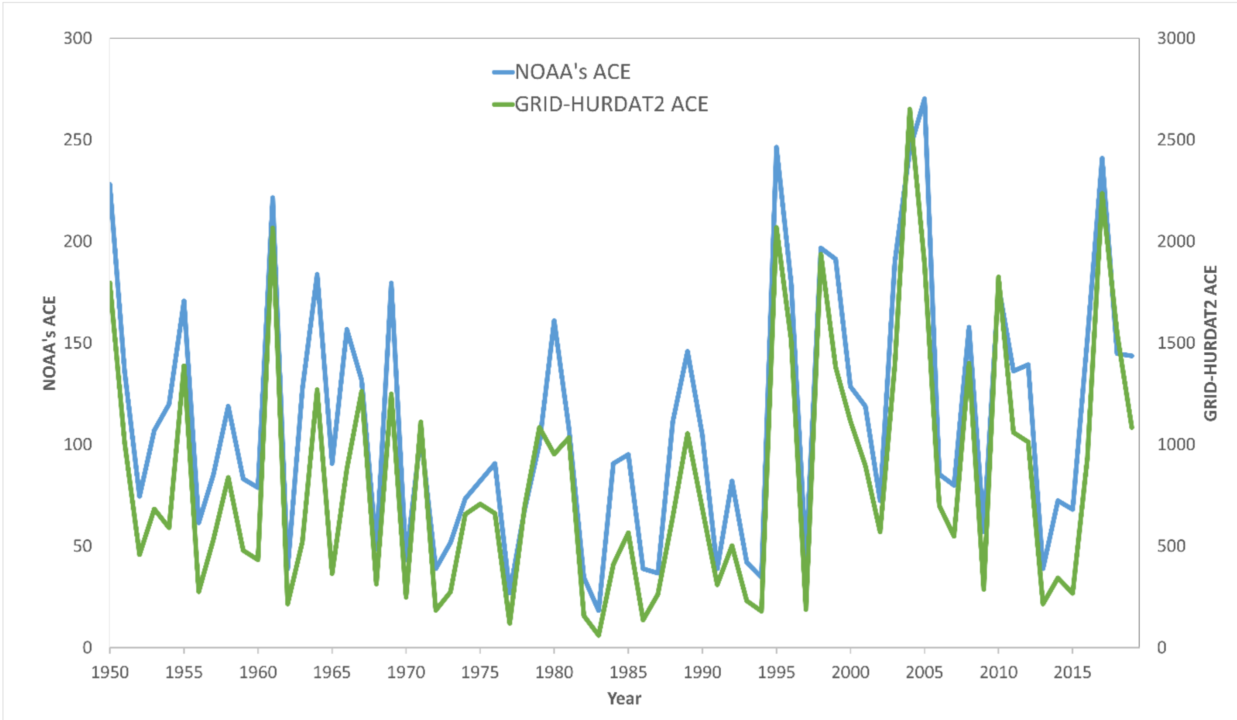

Fig. 8: NOAA's Official ACE Compared with the ACE Calculated Using GRID-HURDAT2.

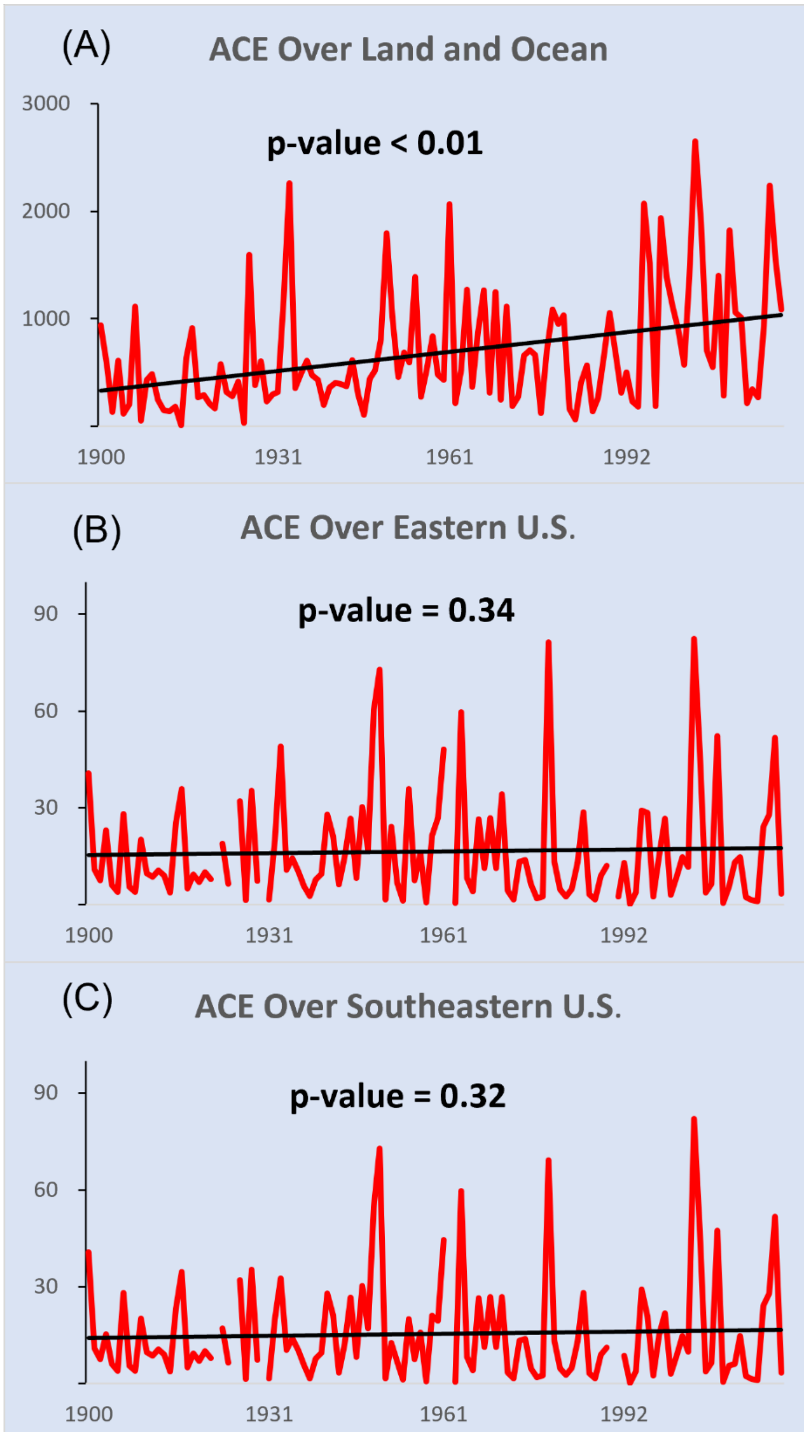

Fig. 9: Tropical Storms and Above ACE – 1900 to 2019 in Three Regional Domains. Depicted is ACE in different regions for 1900 to present: (A) the Atlantic Basin, (B) the eastern U.S., and (C) the southeastern U.S.

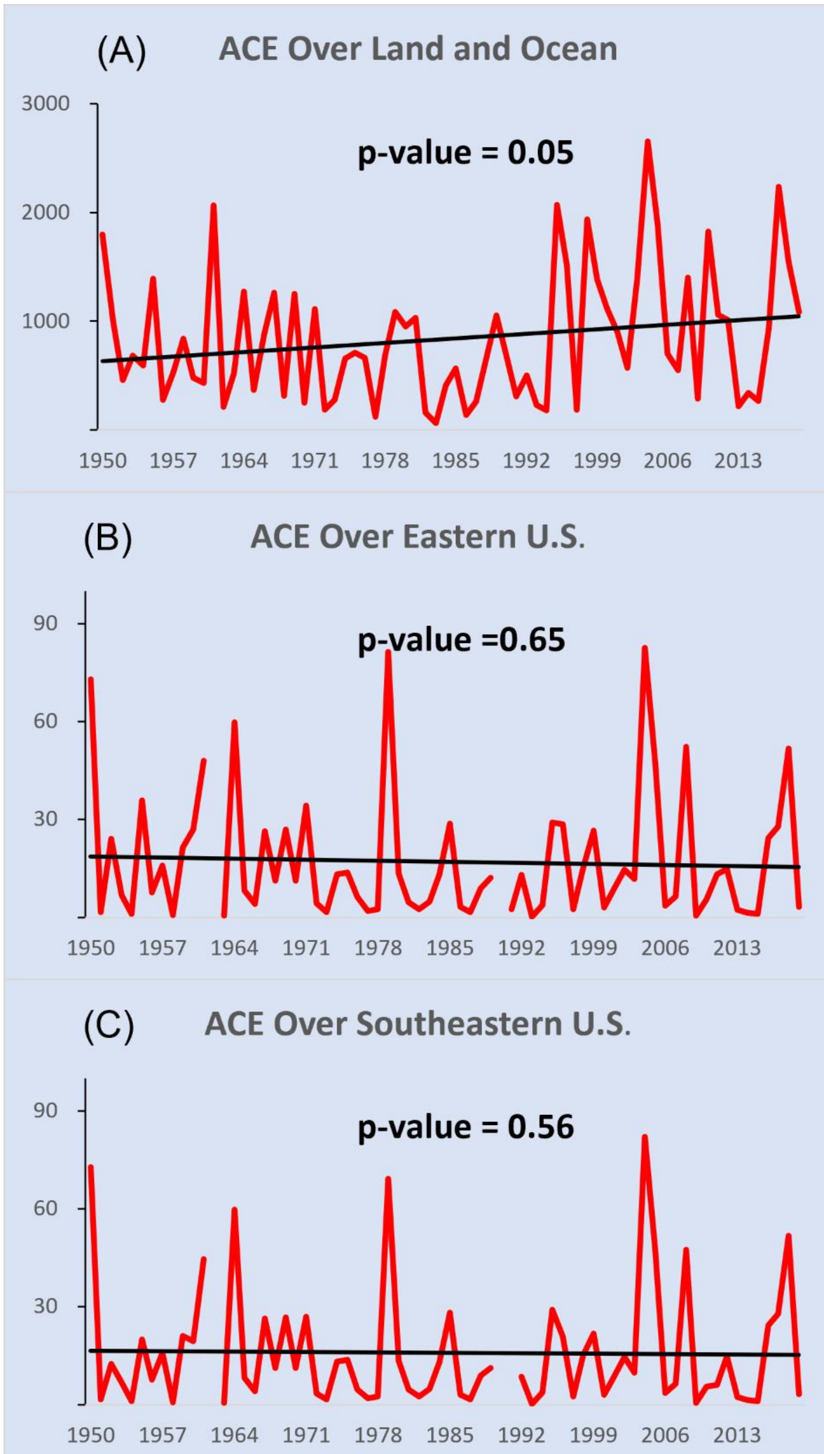

Fig. 10: Tropical Storms and Above ACE – 1950 to 2019 in Three Regional Domains. Depicted are ACE in different regions: (A) the Atlantic Basin, (B) the Eastern U.S., and (C) the Southeastern U.S.

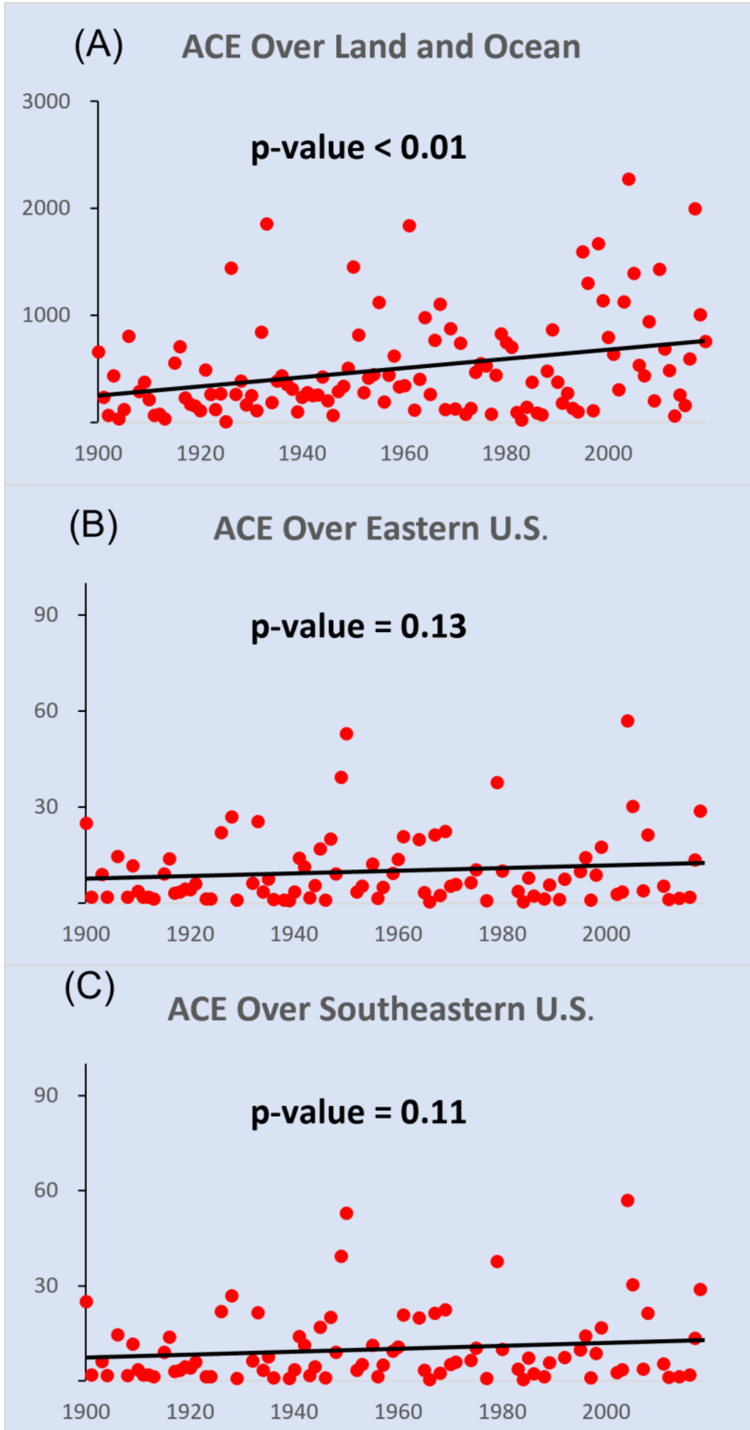

Fig. 11: Hurricane Category 1 and Above ACE – 1900 to 2019 in Three Regional Domains. Depicted are ACE in different regions: (A) the Atlantic Basin, (B) the Eastern U.S., and (C) the Southeastern U.S.

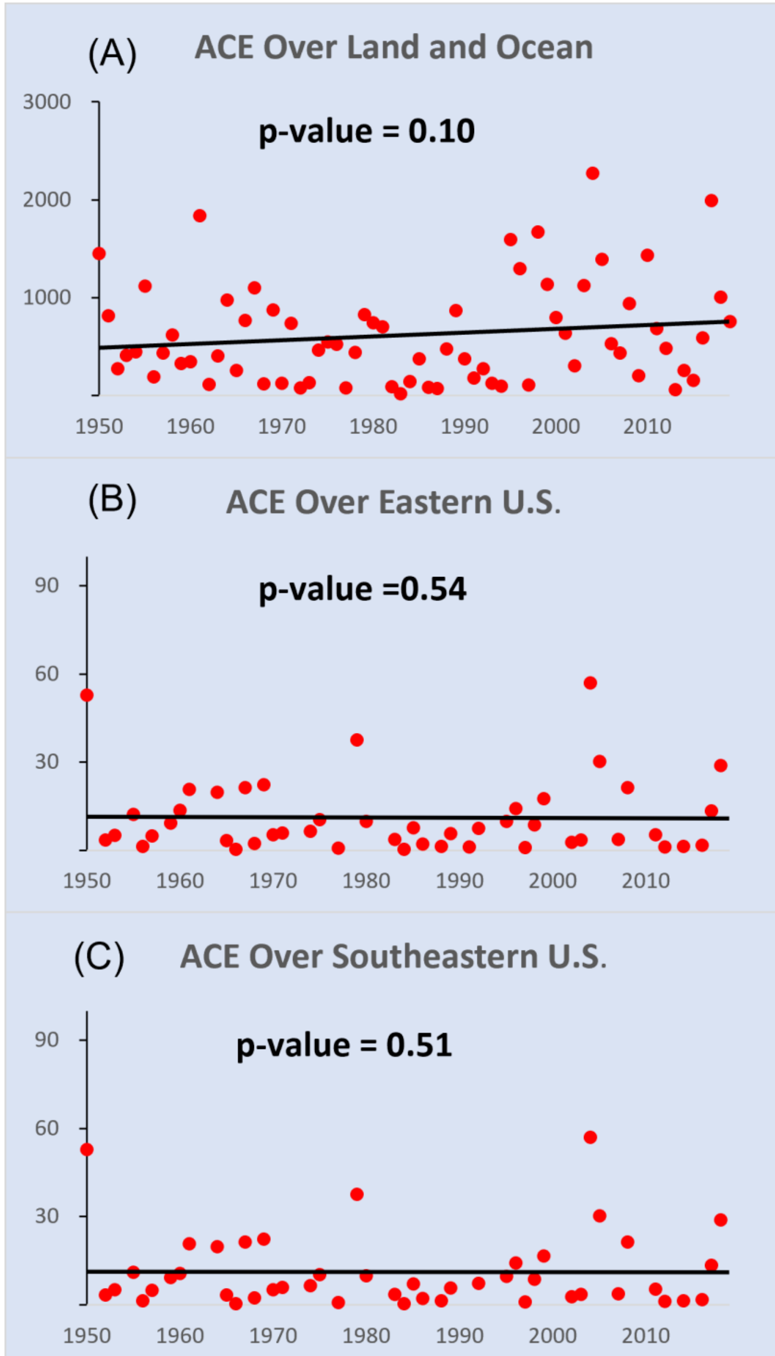

Fig. 12: Hurricane Category 1 and Above ACE – 1950 to 2019 in Three Regional Domains. Depicted are ACE in different regions: (A) the Atlantic Basin, (b) the Eastern U.S., and (c) the Southeastern U.S.

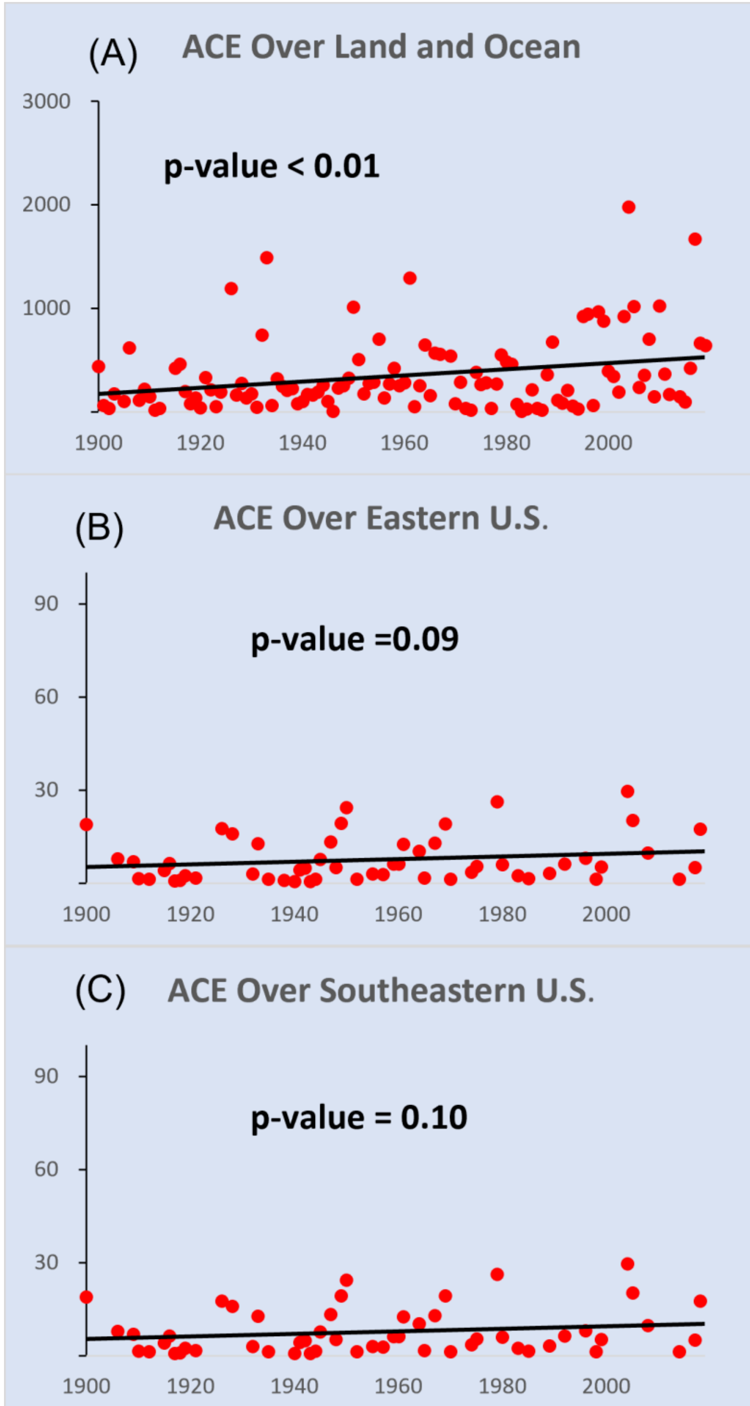

Fig. 13: Hurricane Category 2 and Above ACE – 1900 to 2019 in Three Regional Domains. Depicted are ACE in different regions: (A) the Atlantic Basin, (B) the Eastern U.S., and (C) the Southeastern U.S.

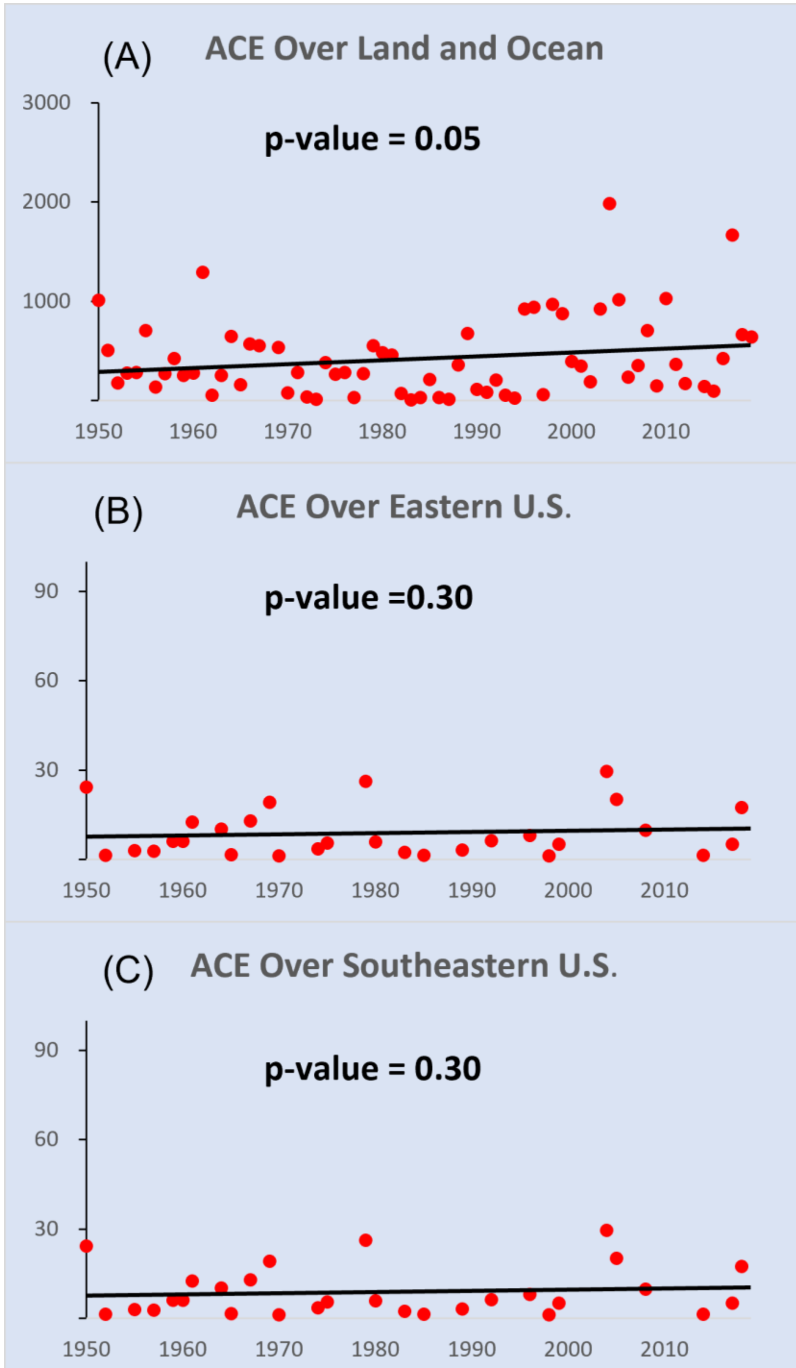

Fig. 14: Hurricane Category 2 and Above ACE – 1950 to 2019 in Three Regional Domains. Depicted are ACE in different regions: (A) the Atlantic Basin, (B) the Eastern U.S., and (C) the Southeastern U.S.

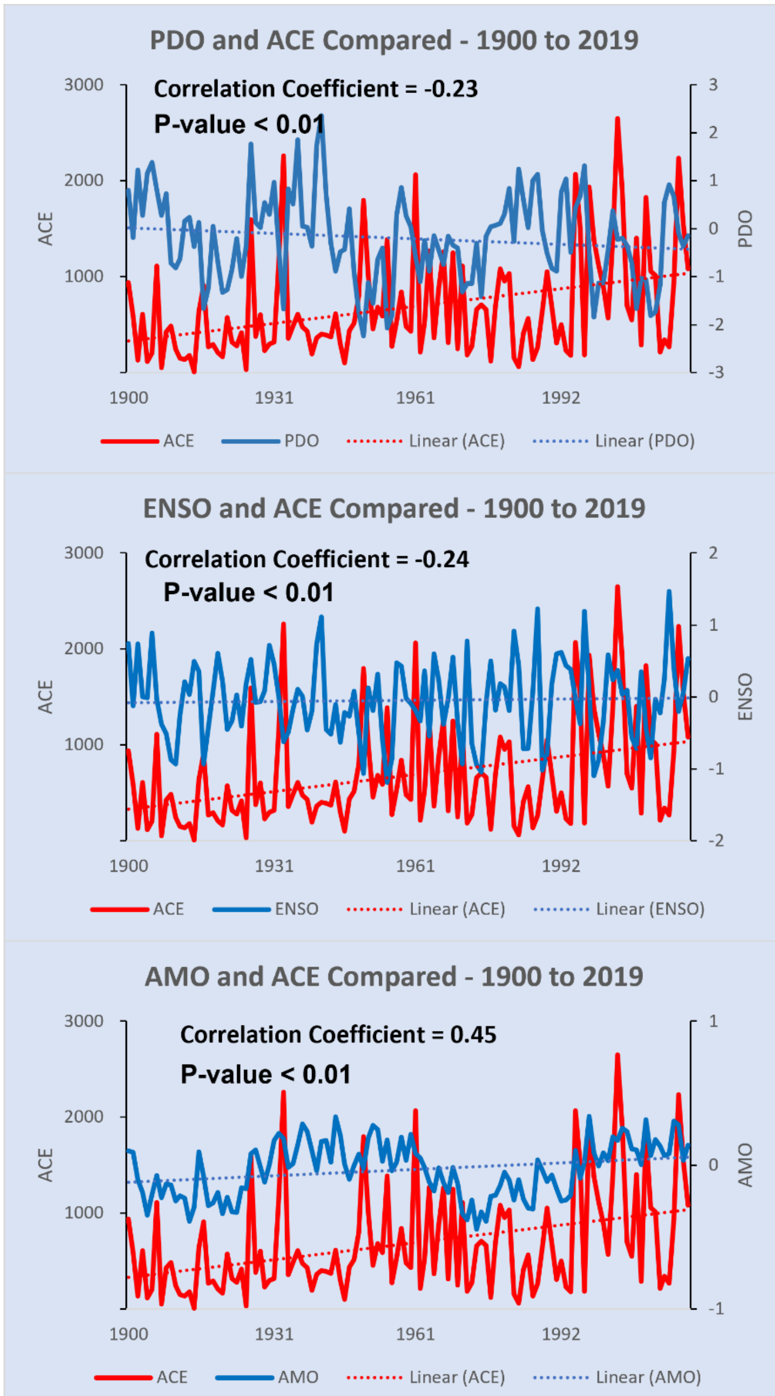

Fig. 15: SST Anomalies Compared to ACE – 1900 to 2019. Multiple SST anomalies are plotted against ACE within the entire Atlantic Basin from 1900 to present, including PDO, ENSO and AMO.

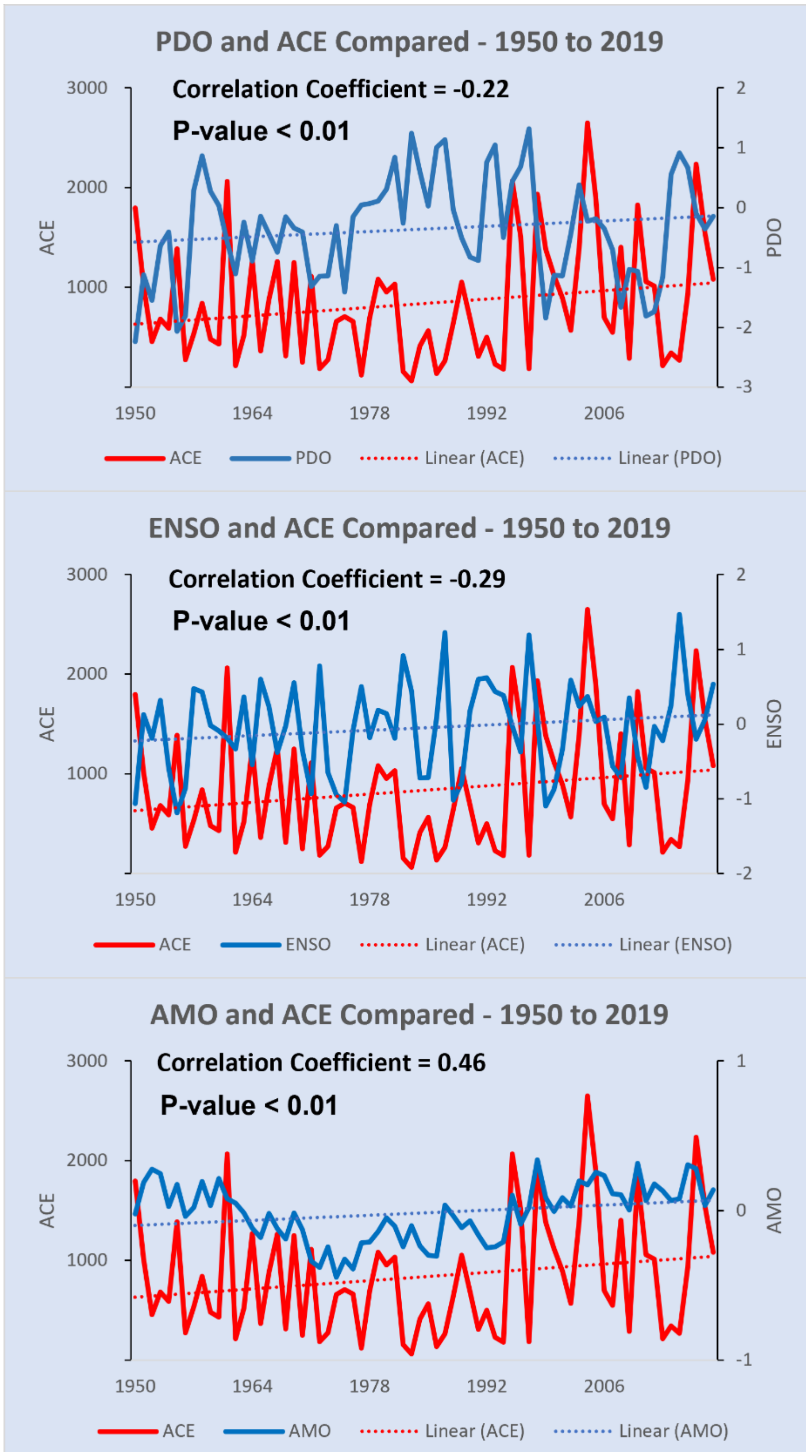

Fig. 16: SST Anomalies Compared to ACE – 1950 to 2019. Multiple SST anomalies are plotted against ACE within the entire Atlantic Basin from 1950 to present, including PDO, ENSO and AMO, and their correlation coefficients are shown, as well.

4.4 Discussion

We found that in the eastern United States and the southeastern United States, none of our results were statistically significant for any hurricane category. For ACE over land and ocean, we found the increasing trend was statistically significant for multiple hurricane categories and periods, and it did not seem to vary notably across categories. However, that could be because of better tracking in the ocean going forward through time.

We interpret the results to mean that hurricane activity has increased within the Atlantic Basin but not over the continental United States. Although many other studies have dealt with ACE in various ways (Murakami et al. 2014; Villarini and Vecchi 2012, 2013; Yu et al. 2009), none have divided the study area into spatial domains as this study does. This highlights the usefulness of the dataset we developed, GRID-HURDAT2, as it was indispensable in performing our analysis across the three spatial domains.

As to the reason ACE seems to have increased over the ocean, we speculate that the results could be reflective of reality, or it could be because of data heterogeneity, given that in the past, some of the weaker cyclones were not identified over the ocean, and in more recent decades weaker storms were. In contrast, over land, they may have been easier to identify further back in the past. Assuming the results reflect actual increasing trends in hurricane activity over the ocean, another line of speculation is that increased SSTs could play a role (Trenberth 2005).

Regarding the connections that AMO, PDO, and ENSO have with ACE, our interpretation of our results is that all three are drivers of tropical cyclone activity within the Atlantic Basin. Still, AMO seems to be the greatest of the three, given that the coefficient of correlation is the highest, which makes sense intuitively because AMO is a SST pattern within the Atlantic Basin where hurricanes occur. In contrast, the other two SST patterns occur in the Pacific basin. That ENSO has an inverse relationship with hurricane activity in the Atlantic Basin is supported by the work of Lupo et al. (2008), particularly during PDO's warm phases. Additionally, others have found evidence that AMO contributes directly to hurricane activity in the Atlantic Basin (Zhang and Delworth 2006).

Chapter 5

Hurricane Impacts on Precipitation

5.1 Introduction

Tropical storms drop tremendous amounts of precipitation along their paths. Evidence suggests that tropical storm translation speeds, i.e. the speeds at which the whole systems move, may be decreasing, which could allow larger amounts of precipitation to fall along their paths (Kossin 2018). The aim of this phase of analysis is to investigate if this holds within the eastern United States. Using the gridded hurricane files generated through Tropycal, along with gauged-based, gridded precipitation data, this phase of analysis estimates how much precipitation is dropped along the tropical cyclone path for the greatest amount of precipitation in each year, then plots them all as a time series for 1948-2019.

ERM is then used as another metric to compare and validate our results (Bosma et al. 2020).

$$ERM_{s,x,t} = \frac{R_{s,x,t}}{R_{x,t}^{2-yr}}$$

Equation 2: ERM Equation. S represents the storm, t is the duration, x is the location, and R is the rainfall depth. $R_{x,t}^{2-yr}$ represents the rainfall depth for the 2-yr average recurrence interval for the same duration and location.

Once we had our hurricane path files generated through Tropycal, we took our precipitation data from the Physical Sciences Laboratory at NOAA. PSL Data: CPC Unified Gauge-Based Analysis of Daily Precipitation over CONUS: NOAA Physical Sciences Laboratory These precipitation data go back to 1948 and up until the present. The spatial extent is 0.25 - degree latitude x 0.25 - degree longitude U.S. grid (300x120), 20.125N-49.875N, 230.125E-304.875E.

5.2 Methods

The data files used come from GRID-HURDAT2 and CPC Daily Precipitation data. The HURDAT2 dataset doesn't include precipitation, so for that we took data from the Climate Prediction Center (CPC) and selected precipitation files with gridding matching those in GRID-HURDAT2.

The tropical storm path files were concatenated into a larger file to make them easier to work with. The HURDAT2 dataset was filtered so that the date of landfall date on the continental United States was recorded and matched with each storm, and the script would only record precipitation for the five-day period after landfall. Because some storms can release significant amounts of precipitation over more than a day, I used the five-day total after the date of landfall in the continental United States to derive the final precipitation value for the storm. This was to account for storms lasting more than a day. I also filtered the landfall data according to latitude since some storms originally made landfall on Caribbean islands or Central America, rather than the United States.

A stepwise description of the precipitation analysis is shown in Figs. 17 to 20. The original tropical storm path files also only include one grid point along the path of the storm, so the analysis script was written to include adjacent cells: 100km X 100km window around the T.C. grid-cell; and select the maximum precipitation grid cell. I decided to use Hurricane Harvey to verify my results and found a value of 877.58 mm of precipitation, which aligns with what others have reported (Emanuel 2017; Van Oldenborgh et al. 2017).

Step 1: Select a hurricane (GRID-HURDAT2).

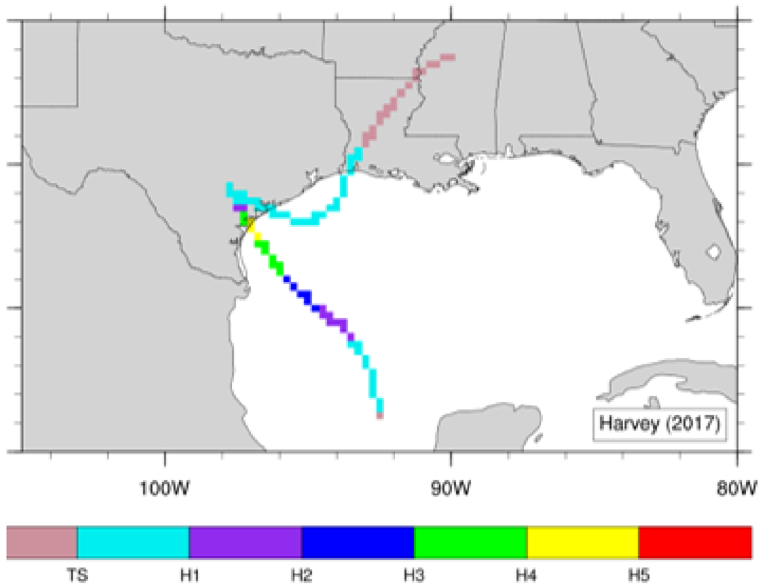

Figure 17: Precipitation Analysis Step 1

Step 2: Select five-day total precipitation (CPC Gauge—based Precipitation), where day 1 is the landfall date on the conterminous United States.

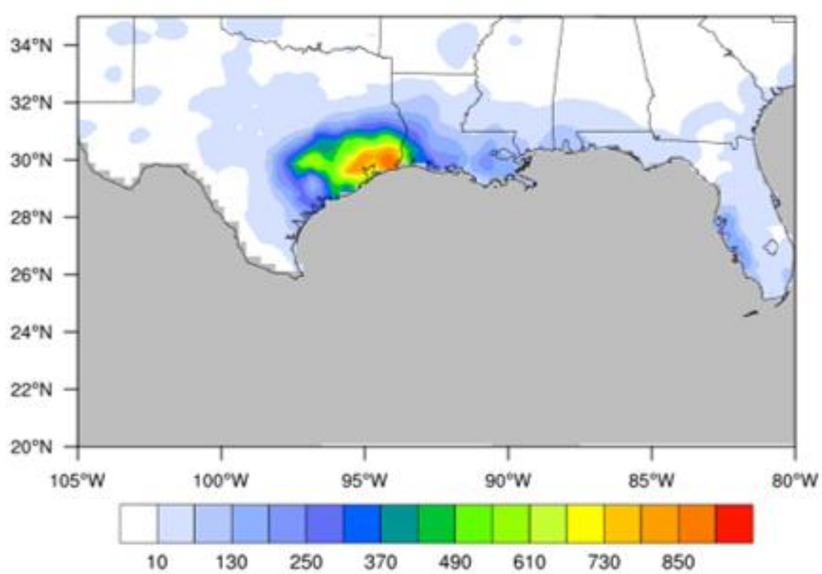

Figure 18: Precipitation Analysis Step 2

Step 3: Overlay these two maps.

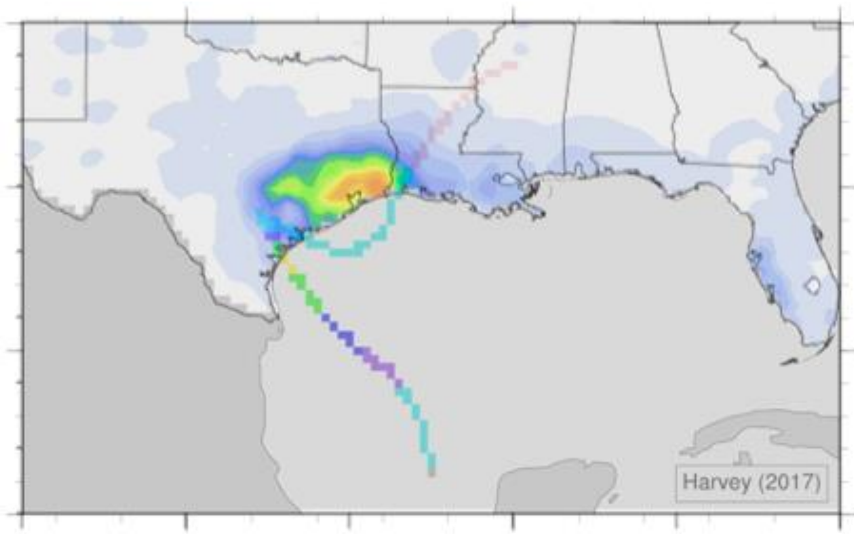

Figure 19: Precipitation Analysis Step 3

Step 4: Go through the hurricane path, <u>one grid cell at a time</u>, and identify the maximum precipitation by expanding the grid to a 100 km X 100 km spatial box and select the maximum precipitation grid cell (25 km X 25 km).

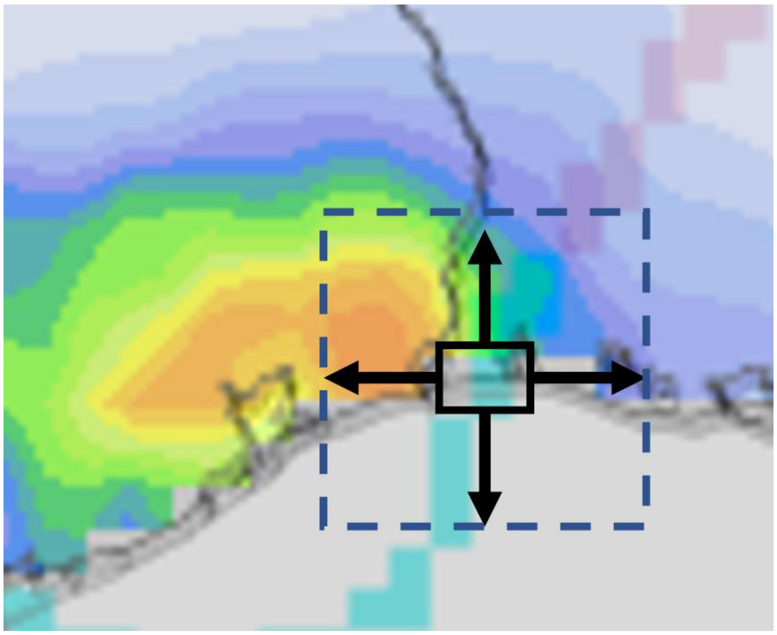

Figure 20: Precipitation Analysis Step 4

Step 5: Repeat Step 4 for all the grid cells in the hurricane path, creating an array of maximum precipitation along the hurricane path.

Step 6: Select the maximum value for the maximum precipitation array in Step 5

5.3 Results

Annual, Maximum Hurricane-Associated Precipitation

Annual maximum hurricane-associated precipitation has increased in the continental United States. I found that within the continental United States, the precipitation associated with the greatest rainfall events produced by hurricanes has increased from 1948 to 2019 (Fig. 21). However, this trend is highly dependent on the most recent years of data due to severe storms such as Hurricane Harvey and Hurricane Florence, and when the analysis excludes the years 2017, 2018 and 2019 the trend is less significant (Fig. 22). After calculating ERM, I found that it supported those results in both temporal periods (Figs. 23-24).

Figs. 21 and 22 show annual maximum hurricane-associated precipitation trends, for different time periods, and excluding various categories of tropical cyclone. The results are statistically significant when the years 2017, 2018 and 2019 are included, but when those years are excluded, the trend is less significant and more dependent on tropical cyclone category. In the period 1948 – 2016, when accounting for different categories of tropical cyclone, the increasing trend becomes gradually more pronounced as the lower categories are excluded (Fig. 22 d, $p = 0.03$).

ERM was used to validate our results, and the ERM we calculated is largely in line with the previous results, particularly in the period 1948 – 2019 (Fig. 23). However, in the period 1948 – 2016 the results of the ERM calculation do not align quite as well with the previous results. As with the precipitation analysis, the trend does become more significant as lower categories of tropical cyclones are excluded, though not to the same degree (Fig. 24). In particular, the trend for Fig. 24 (d) is not statistically significant.

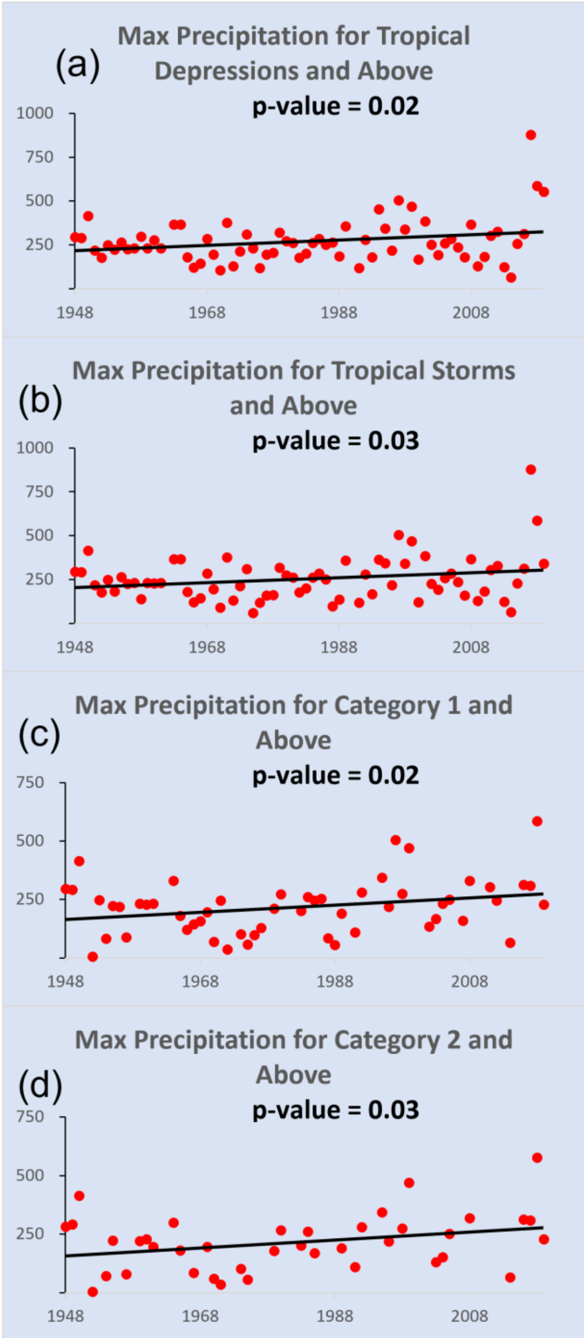

Fig. 21: Annual, maximum, tropical cyclone-associated precipitation events – 1948 to 2019. Depicted are trends over time of the greatest tropical cyclone-associated precipitation events of each year separated by category. (a) includes all tropical cyclones, (b) includes tropical storms and above, (c) includes all hurricanes category 1 and above, and (d) includes hurricanes category 2 and above.

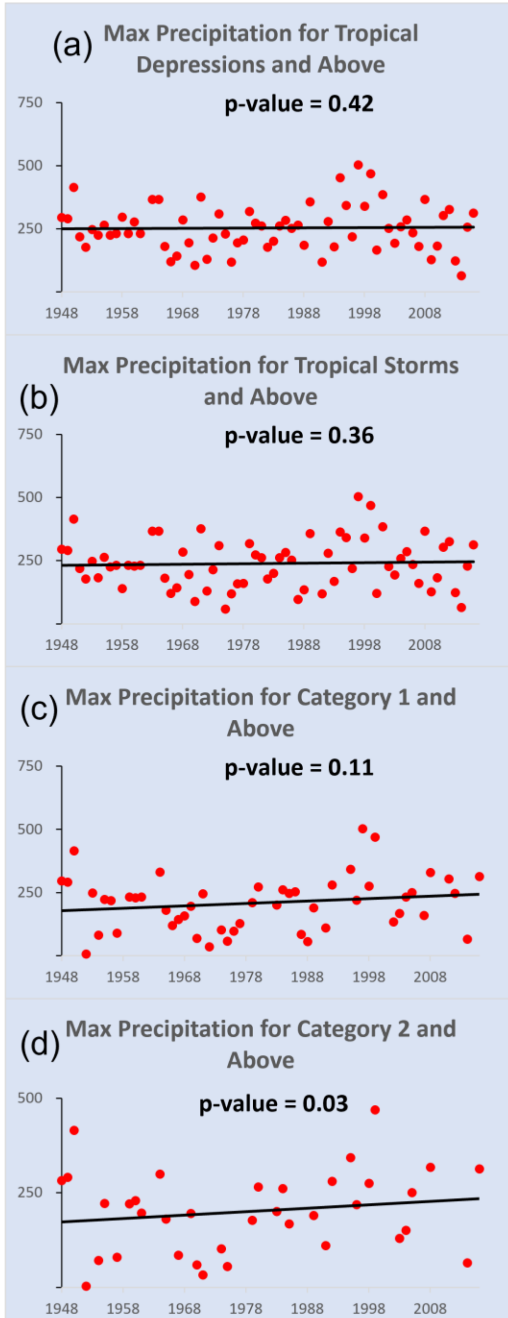

Fig. 22: Annual, maximum, tropical cyclone-associated precipitation events: 1948 - 2016. Depicted are trends over time of the greatest tropical cyclone-associated precipitation events of each year separated by category. (a) includes all tropical cyclones, (b) includes tropical storms and above, (c) includes all hurricanes category 1 and above, and (d) includes hurricanes category 2 and above.

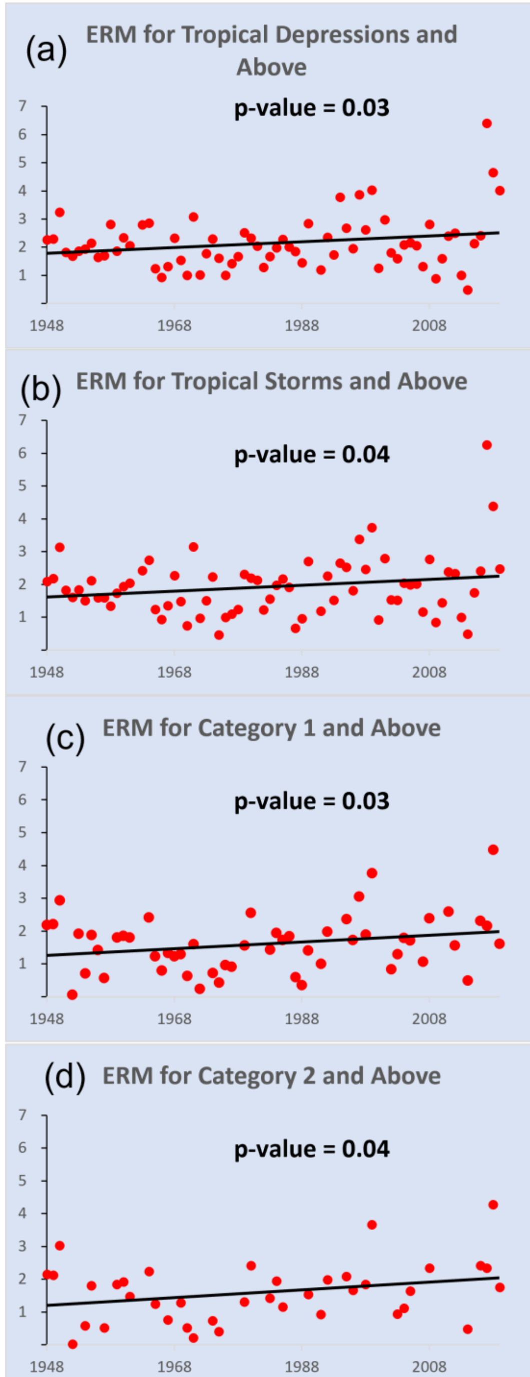

Fig. 23: ERM from Tropical Depression to Category 2: 1948 – 2019. Depicted are trends over time of the ERM of each year separated by category. (a) includes all tropical cyclones, (b) includes tropical storms and above, (c) includes all hurricanes category 1 and above, and (d) includes hurricanes category 2 and above.

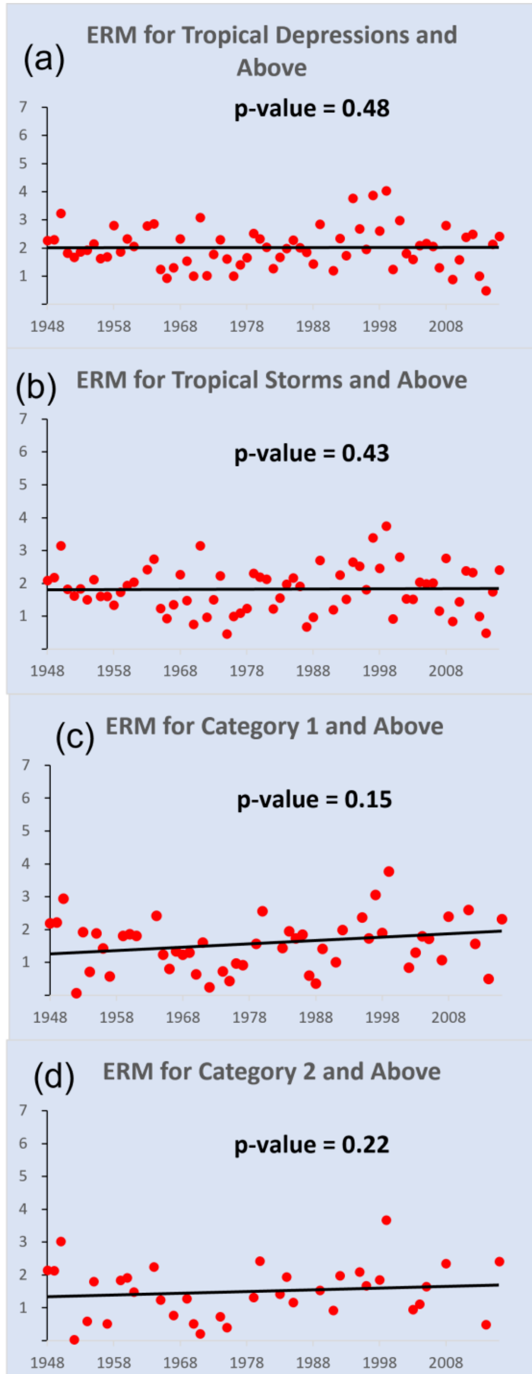

Fig. 24: ERM from Tropical Depression to Category 2: 1948 – 2016. Depicted are trends over time of the ERM of each year separated by category. (a) includes all tropical cyclones, (b) includes tropical storms and above, (c) includes all hurricanes category 1 and above, and (d) includes hurricanes category 2 and above.

5.4 Discussion

We found that there has been a statistically significant increasing trend in precipitation along the storm path. The ERM results are in line with that. The results for Figs. 21 and 23 are statistically significant. They all show that tropical cyclone-associated precipitation along the storm path for the maximum rainfall events of each year. ERM increased from 1948-2019, and the trend was still present when excluding tropical cyclones of lower intensity. When the years 2017, 2018, and 2019 are removed, the hurricane category becomes a more relevant factor in determining the significance of the trend. The maximum precipitation trend is statistically significant in Fig. 22 (d), whereas they are not significant for ERM analysis (Fig. 24).

The discrepancy between the results for the annual maximum hurricane-associated precipitation results and the ERM results is likely because ERM takes into account the effect of the global warming effect that may have increased the annual maximum precipitation (Shearer et al. 2022); so the denominator in ERM equation (Eq. 2) has also increased.

We interpret the results to mean that the precipitation along the storm path associated with the maximum rainfall events of each year has increased over time due to decreasing tropical cyclone translation speeds, although this result is heavily dependent on the data from the years 2017-2019. The hurricane associated increasing precipitation trend is partly attributable to hurricane stalling events, which are when the system spends hours in a confined area as Hurricane Harvey did (Van Oldenborgh et al. 2017). An increasing trend in hurricane stalling events has been found by Hall and Kossin (2019) from 1948-2017, attributed both to decreasing translation speeds and to an increase in abrupt changes in trajectory, though it is not clear that AMO is a contributing factor (Hall and Kossin 2019). Another study has found that AMO appears to be a contributing factor to tropical cyclone rainfall, although this study does not focus on the most extreme events as ours does (Nogueira et al. 2013b). Our finding that the most extreme annual rainfall events caused by tropical cyclones are in line with what others have found (Gori et al. 2022; Knight and Davis 2009; Lau et al. 2008).

Chapter 6

Summary and Discussions

6.1 Main Findings

For trends in general hurricane activity measured through ACE, we found that there has not been a significant increasing or decreasing trend over land. There appears to be an increasing trend over the ocean, but that is likely because of better tracking in more recent decades and better data more recently in the dataset. For trends in precipitation along the hurricane path, I found that there is an increasing trend in precipitation associated with the storms dropping the most precipitation in each year. It was also found that AMO, PDO, and ENSO are all likely contributing factors to the formation of tropical cyclones in the Atlantic Basin, and AMO is the most significant among them.

6.2 Unique Contributions

ACE has already been developed in other studies, but the unique contribution of this work is that we did it using the GRID-HURDAT2 developed with Tropycal, and then isolated the calculation to the southeastern United States, which other studies have not done.

The precipitation analysis is also unique in that it makes use of GRID-HURDAT2, is limited spatially to the eastern United States, and estimates precipitation associated with tropical cyclones.

Appendix - A

Script Used to Produce GRID-HURDAT2

1. tropical.track and datetime are imported.

```
import tropycal.tracks as tracks

import datetime as dt
```

2. The dataset is loaded.

```
hurdat_atl = tracks.TrackDataset(basin='north_atlantic',source='hurdat',include_btk=False)
```

3. We get a key for each of the hurricanes to use in a loop. The key is a unique identifier for each storm including the basin it's in, which is the Atlantic Basin for all the storms in our study, the year of the storm, and the storm's place during that year.

```
keys = hurdat_atl.filter_storms(year_range=(1990,2020),return_keys=True)
```

4. This part is used to take each individual storm and collect data from it to pass onto the next function, which plots out the storms that were present in the Atlantic Basin. This was done because the gridded_stats function can plot out time periods but not individual storms.

```
for key in keys:

    a = hurdat_atl.get_storm(key)
    b = a.to_dataframe()
    c = b["date"]
    d = c[0]
    e = c[len(c)-1]
    f = str(d)
    g = f[5:7]
    h = f[8:10]
    i = str(e)
    j = i[5:7]
    k = i[8:10]
```

```
l = f[0:4]
m = i[0:4]
n = g + '/' + h
o = j + '/' + k
```

Hurricane Michael from the year 2018 is featured in Fig. 2 (main text) striking the southeastern United States. It's cutoff at North Carolina because that's the point where it becomes an extratropical cyclone. It made landfall at 17:30 at 30.0N, 85.5W.

5. This is where the gridded_stats method is used. It plots the tropical storms out on a grid. We chose resolution 0.25 where it mentions binsize, determining resolution. Maximum wind is used as the request for what to plot because we need it to compute ACE. The lat and lon coordinates are mapped according to binsize.

```
storm = hurdat_atl.gridded_stats(request="maximum wind",
year_range=(int(l),int(m)),date_range=(n,o),binsize=0.25, return_ax=True, return_array=True)
```

6. The file is converted into a netcdf file for analysis using Cheyenne.

In the program we used to calculate ACE it uses the maximum wind speed data from the files generated using gridded_stats and calculates ACE using the maximum wind speed squared at intervals and summed together.

```
storm.to_netcdf(str(key) + '.nc')
```

Script Used to Calculate ACE from GRID-HURDAT2 Data

```
 inDir = "/glade/work/kumar34/HURDAT2"
f1 = addfile(inDir+"/HURDAT2_IND_STORM_1900_2019_rev1.nc", "r")
f2 = addfile(inDir+"/HURDAT2_1900_2018.nc", "r")
print(f1)
lat = f2->lat
lon = f2->lon
print(lon(0:10))
nlat = dimsizes(lat)
nlon = dimsizes(lon)
fe = addfile(inDir+"/hurdat2_east_us_mask.nc", "r")
fs = addfile(inDir+"/hurdat2_south_us_mask.nc", "r")
ws_yr = f1->hurdat2_ws    ; 1 knots  =  1.151 miles per hour = 1.852 km per hour
ws_yr = mask(ws_yr, ws_yr.ge.137.0, True)
time = ispan(1900, 2019, 1)
east_mask = fe->east_mask
south_mask = fs->south_mask
ntime = dimsizes(time)
P1 = new((/ntime, 3/), "double", -9999.0)
do i = 0, ntime-1
  ws = ws_yr(i, :, :, :)
  ws = mask(ws, ws.lt.35.0, False)
  temp1 = ((10.0^-4)*ws^2)   ; eq1 from Chylck and Lesins 2008
  P1(i, 0) = sum(temp1)
end do
do i = 0, ntime-1
  ws = ws_yr(i, :, :, :)
  ws = mask(ws, ws.lt.35.0, False)
```

```
  ws = mask(ws, east_mask.eq.1.0, True)
  temp1 = ((10.0^-4)*ws^2)   ; eq1 from Chylck and Lesins 2008
    P1(i, 1) = sum(temp1)
end do
do i = 0, ntime-1
  ws = ws_yr(i, :, :, :)
  ws = mask(ws, ws.lt.35.0, False)
  ws = mask(ws, south_mask.eq.1.0, True)


  temp1 = ((10.0^-4)*ws^2)   ; eq1 from Chylck and Lesins 2008
  P1(i, 2) = sum(temp1)
end do
;************************

opt1 = True
opt1@fout = "ACE_1900_2019_ATL_EAST_SOUTH_ind_storm_rev5.txt"
fmtx = "3f15.8"
write_matrix(P1, fmtx, opt1)
```

Appendix – B

Matlab Program to Create the Hurricane Movie

```
writerObj = VideoWriter('Hurricane_1900_2019_GRID-HURDAT2.avi');
open(writerObj);
for K = 1 : 120
   filename = sprintf('hurricane_%d_graph_rev1.png', 1900+K-1);
   thisimage = imread(filename);
   writeVideo(writerObj, thisimage);
end
close(writerObj);
```

Appendix - C

Supplemental Figs. for ACE Analysis

Category 3 and above – 1900 Forward

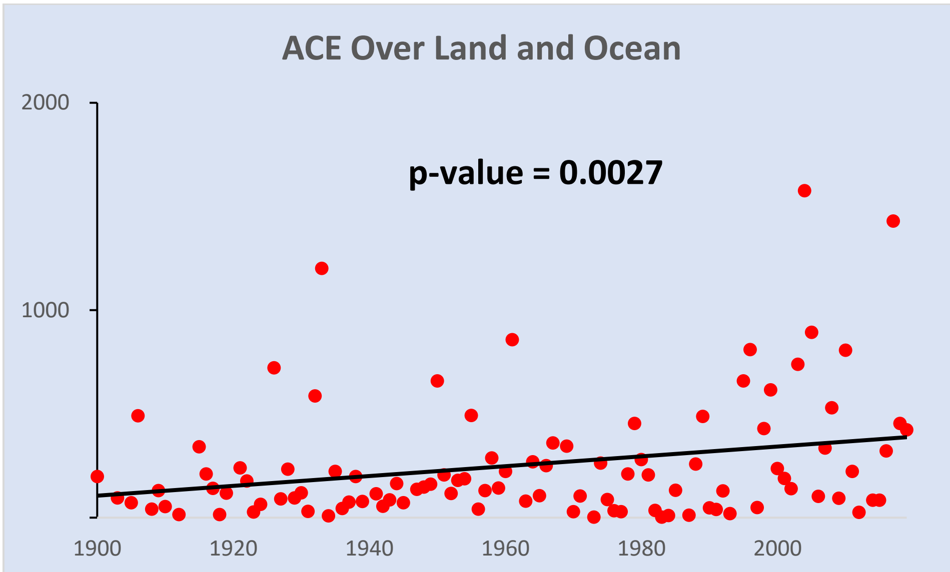

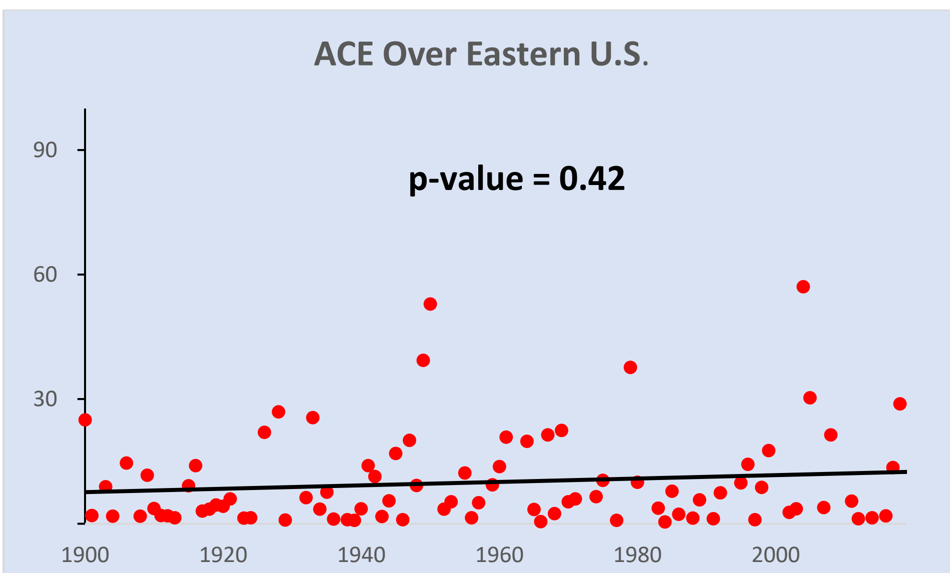

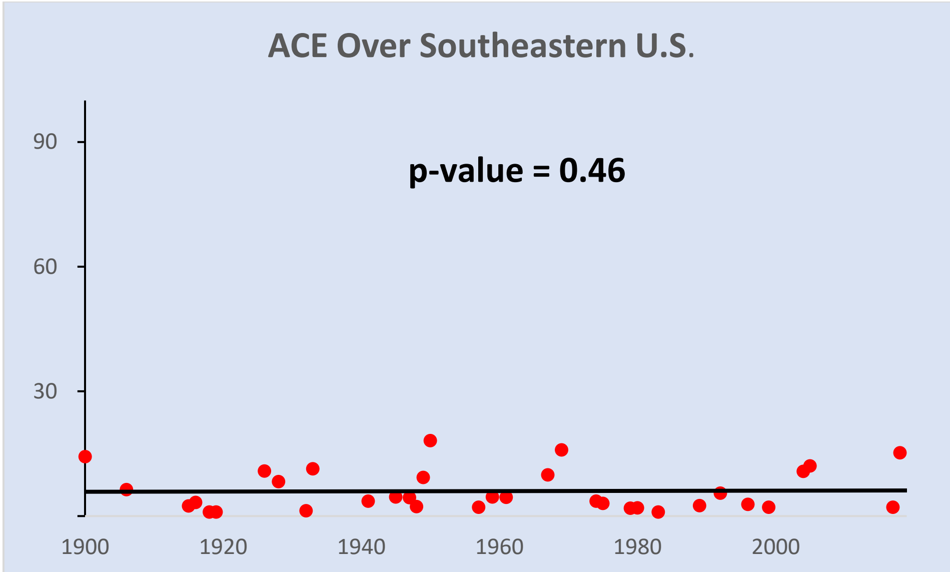

ACE Over Southeastern U.S.
p-value = 0.46
90
60
30
1900
1920
1940
1960
1980
2000

Category 3 and Above -1950 Forward

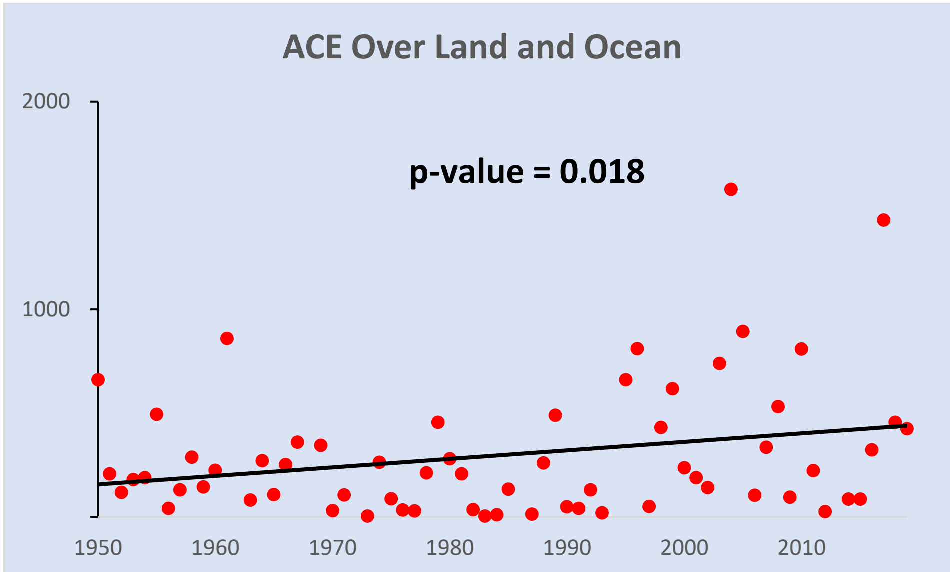

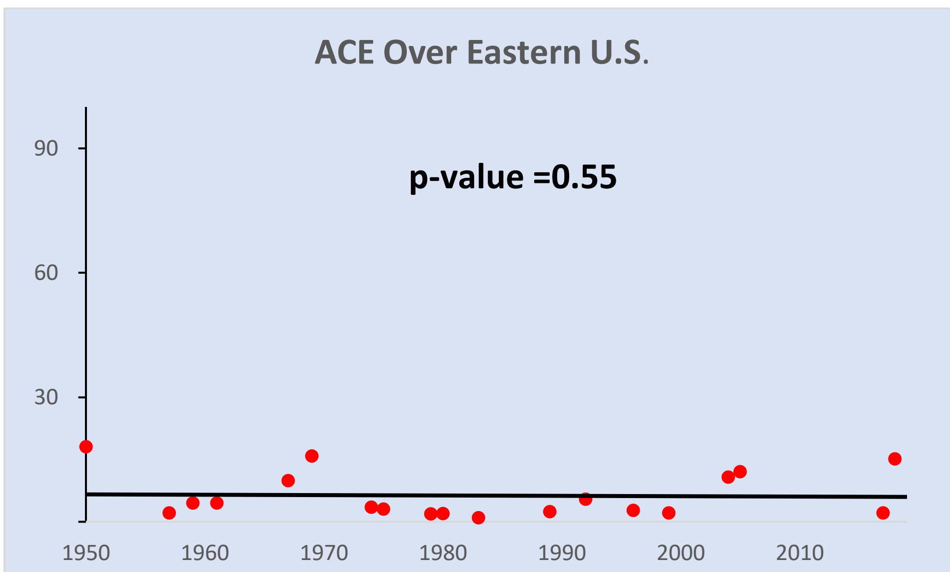

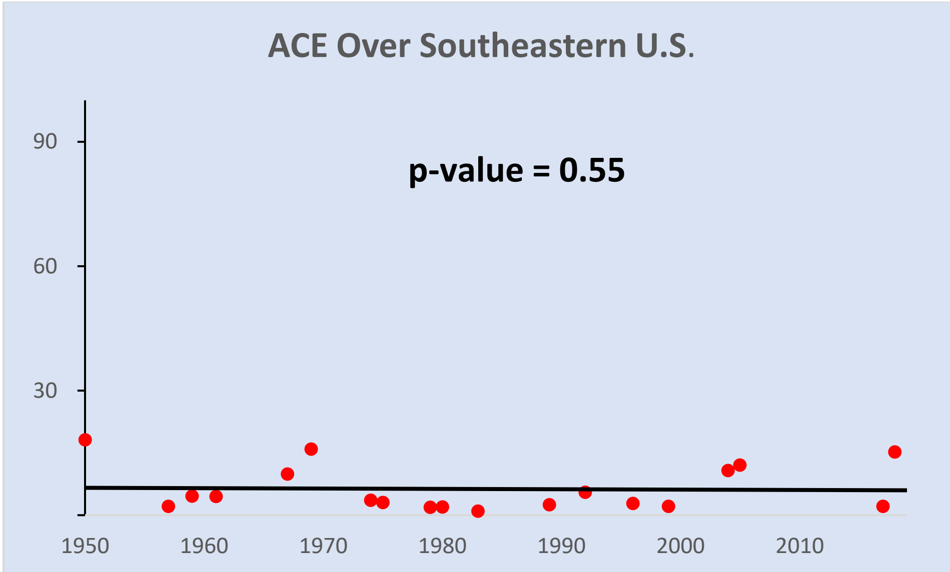
ACE Over Southeastern U.S.
p-value = 0.55
90
60
30
1950
1960
1970
1980
1990
2000
2010

Category 4 and Above -1950 Forward

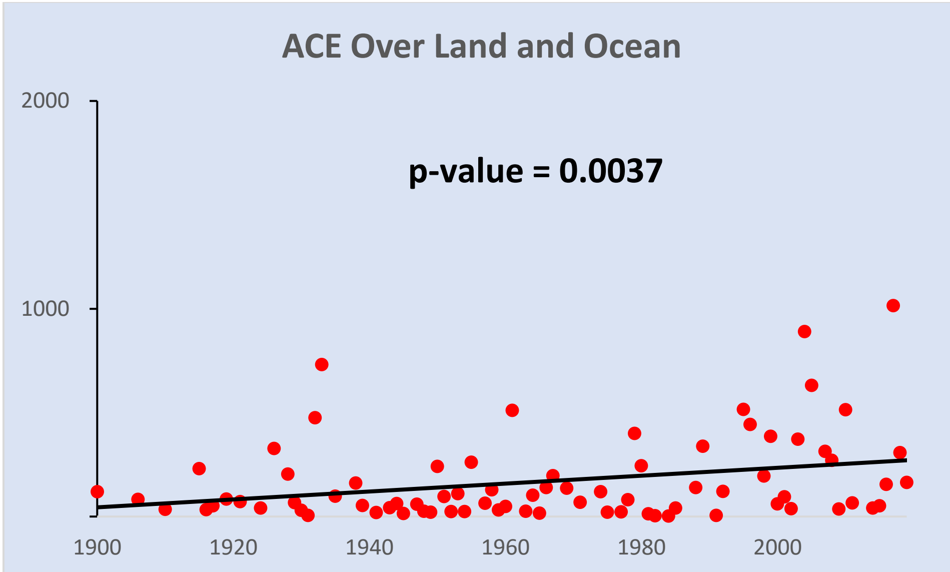

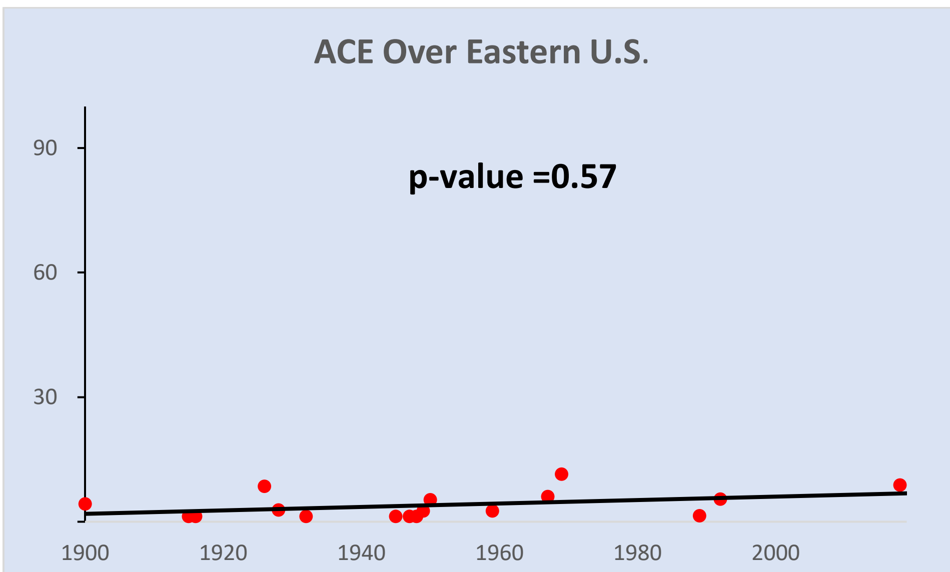

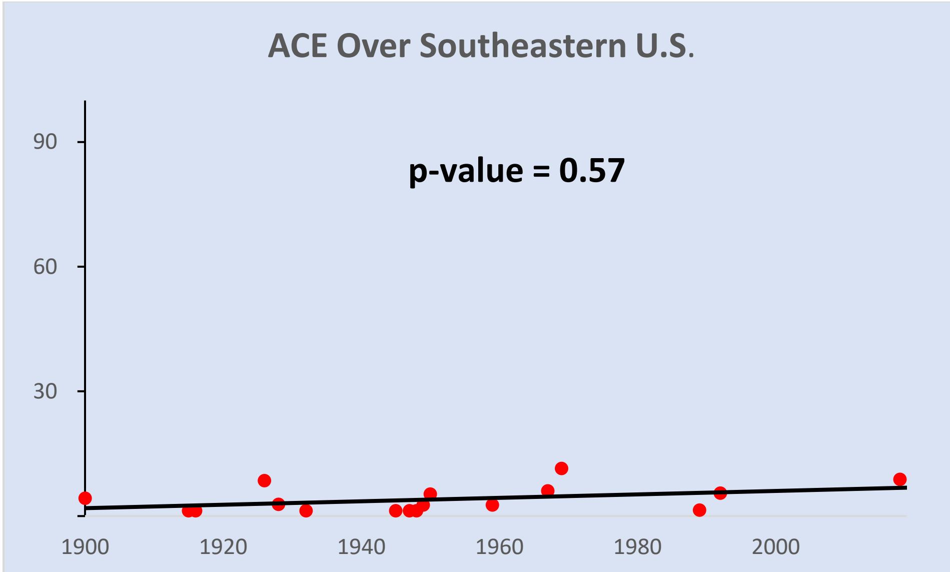

ACE Over Southeastern U.S.
p-value = 0.57
90
60
30
1900
1920
1940
1960
1980
2000

Category 4 and Above -1950 Forward

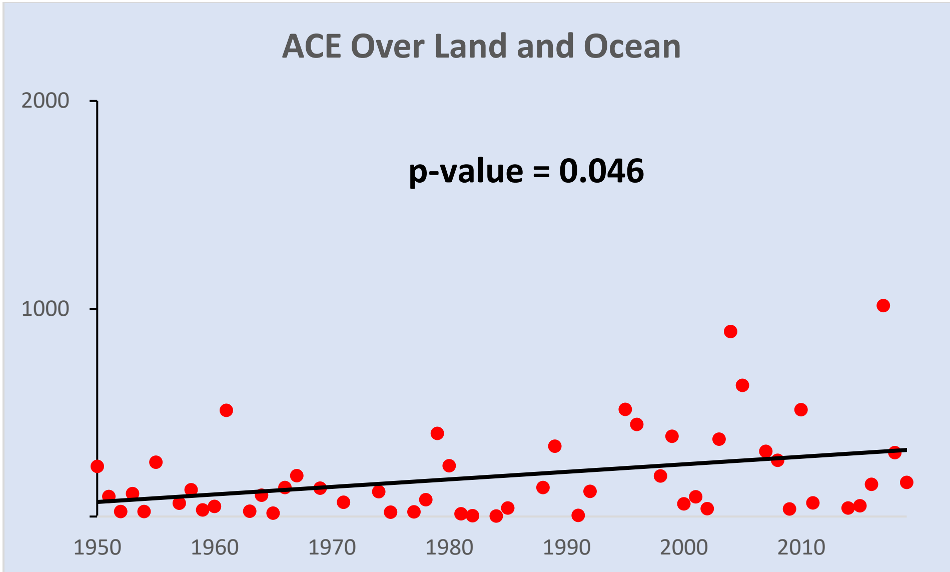

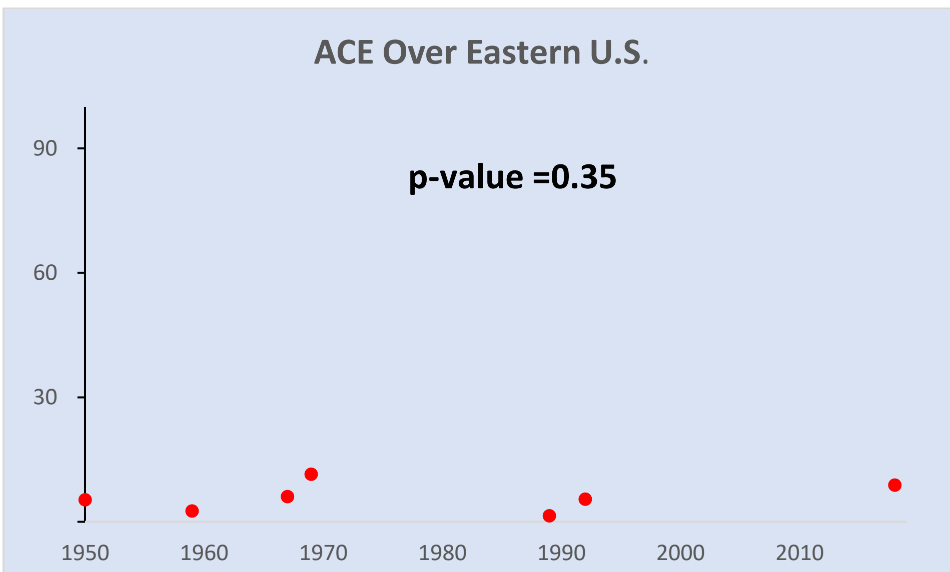

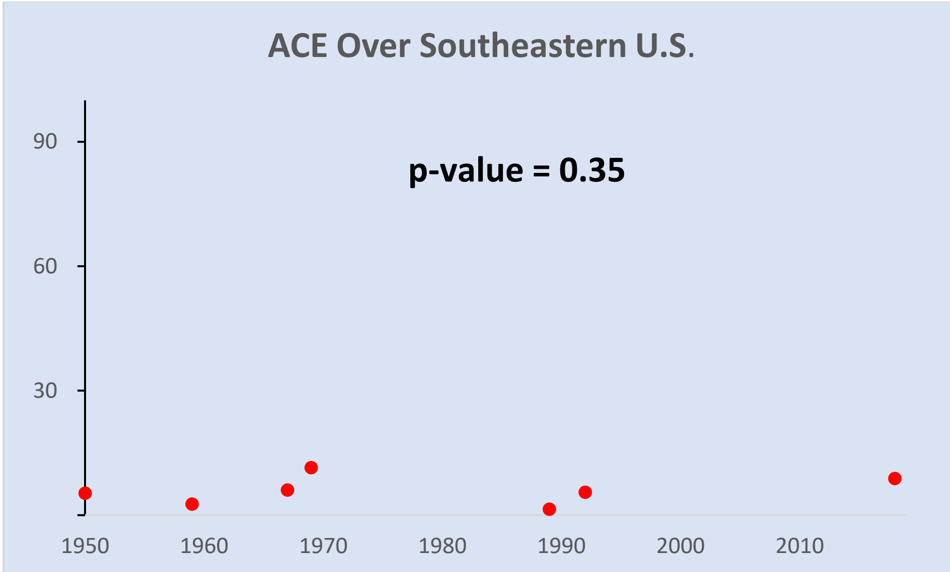
ACE Over Southeastern U.S.
p-value = 0.35
90
60
30
1950
1960
1970
1980
1990
2000
2010

Category 5 and Above -1950 Forward

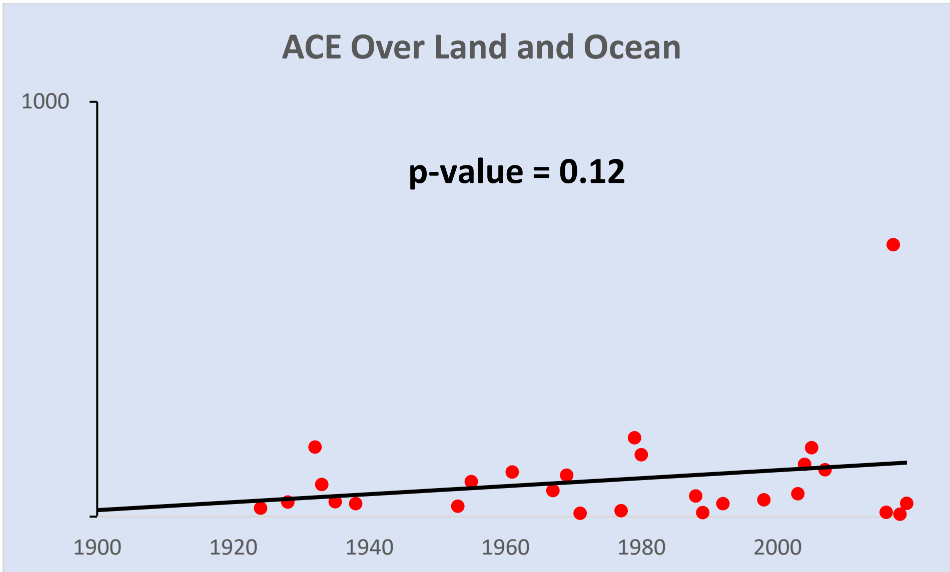

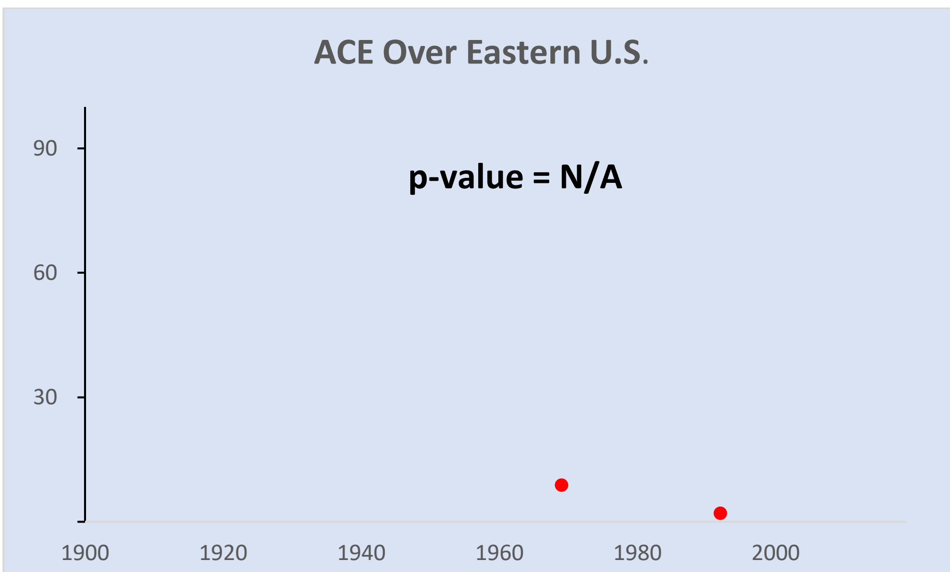

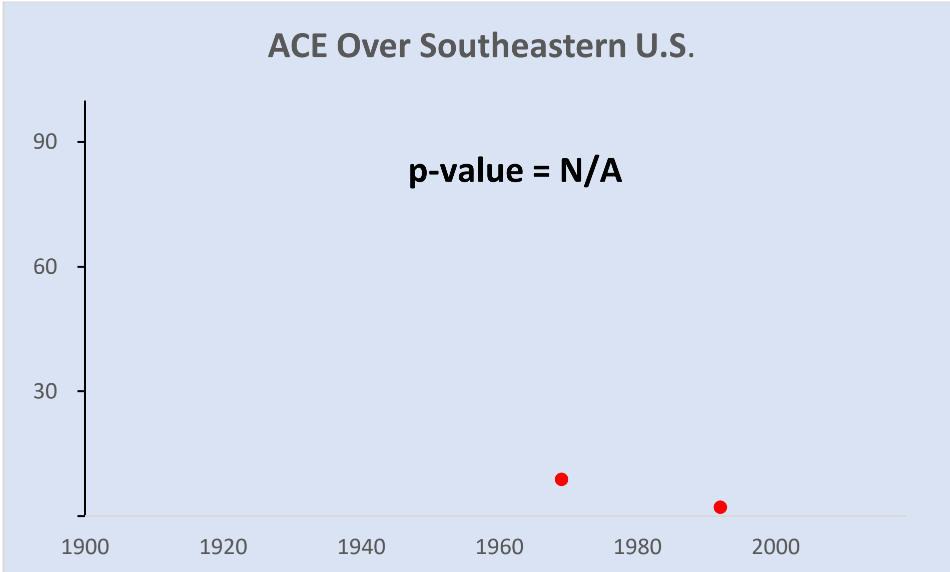
ACE Over Southeastern U.S.
p-value = N/A
90
60
30
1900
1920
1940
1960
1980
2000

Category 5 and Above -1950 Forward

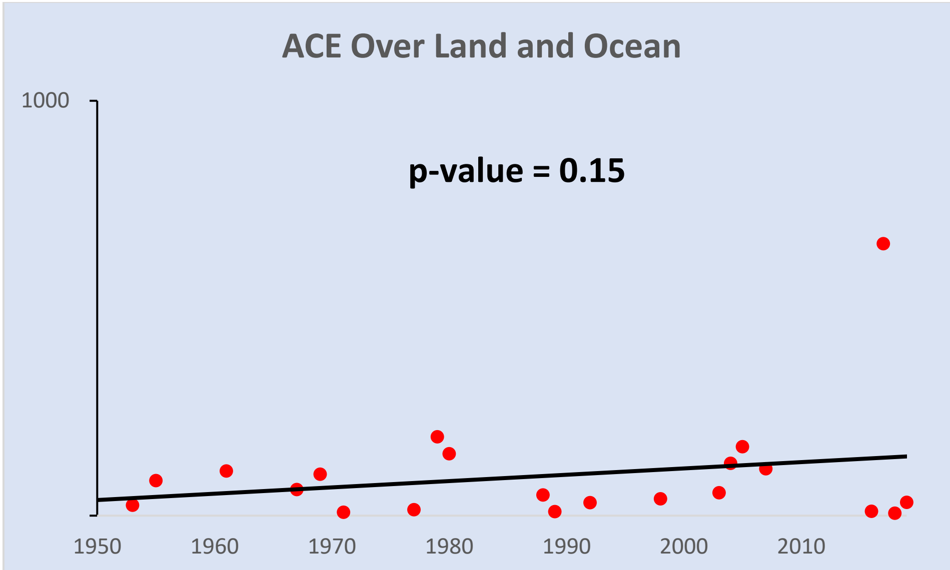

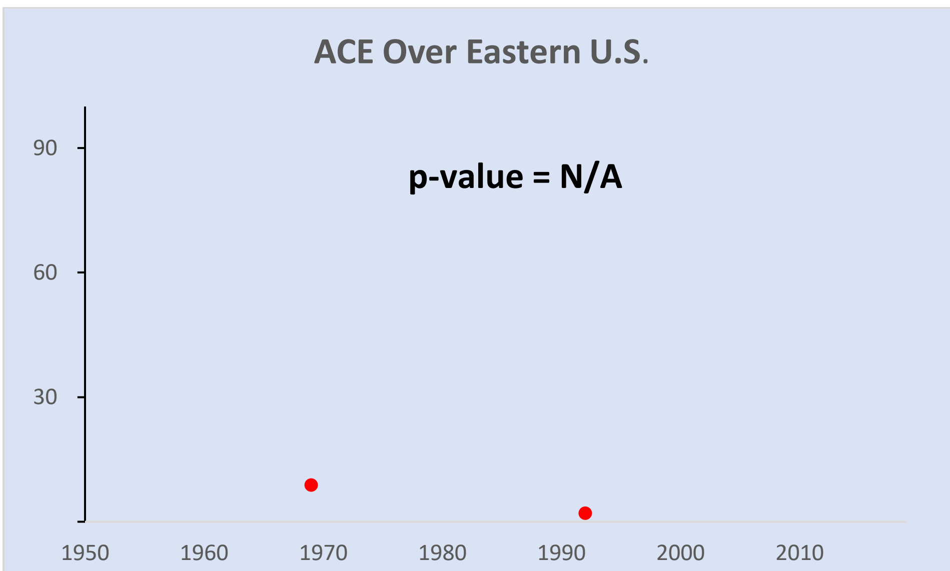

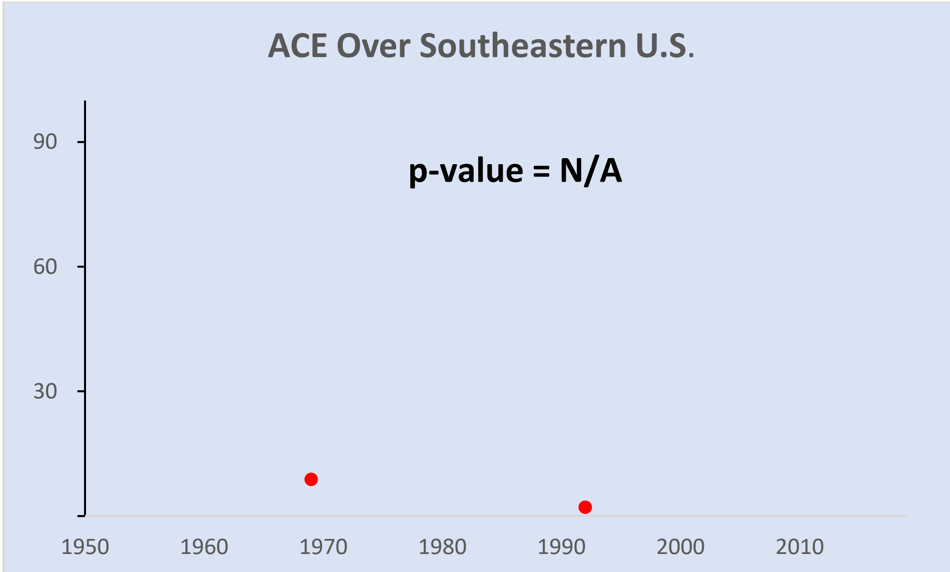
ACE Over Southeastern U.S.
p-value = N/A
90
60
30
1950
1960
1970
1980
1990
2000
2010

Appendix - D

Supplemental Figs. for Precipitation Analysis

Five Day Running Mean

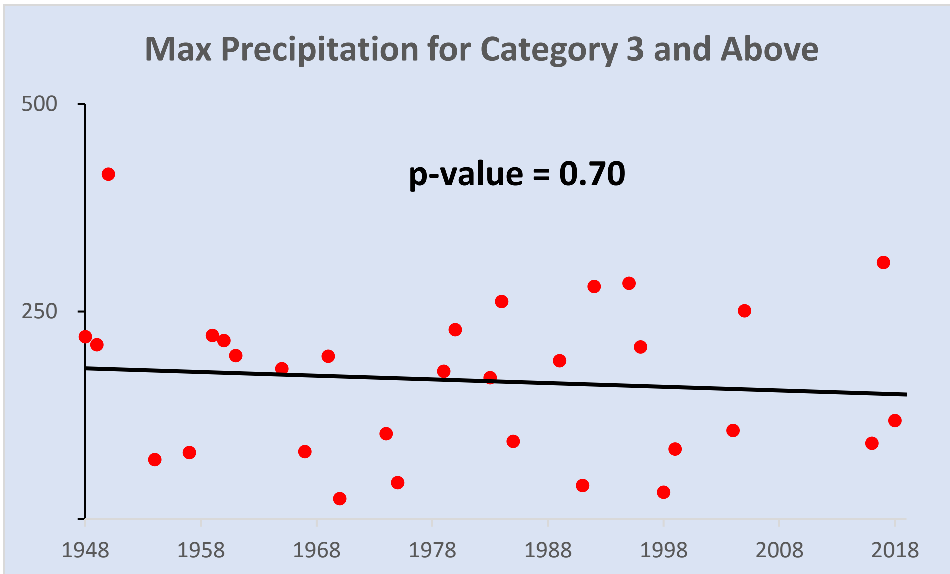

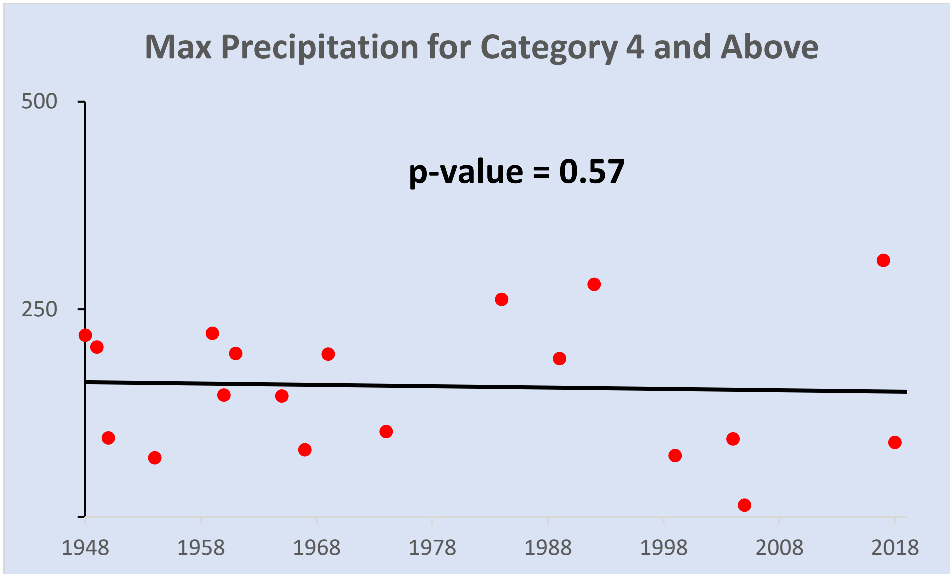
Max Precipitation for Category 4 and Above
500
250
p-value = 0.57
1948
1958
1968
1978
1988
1998
2008
2018

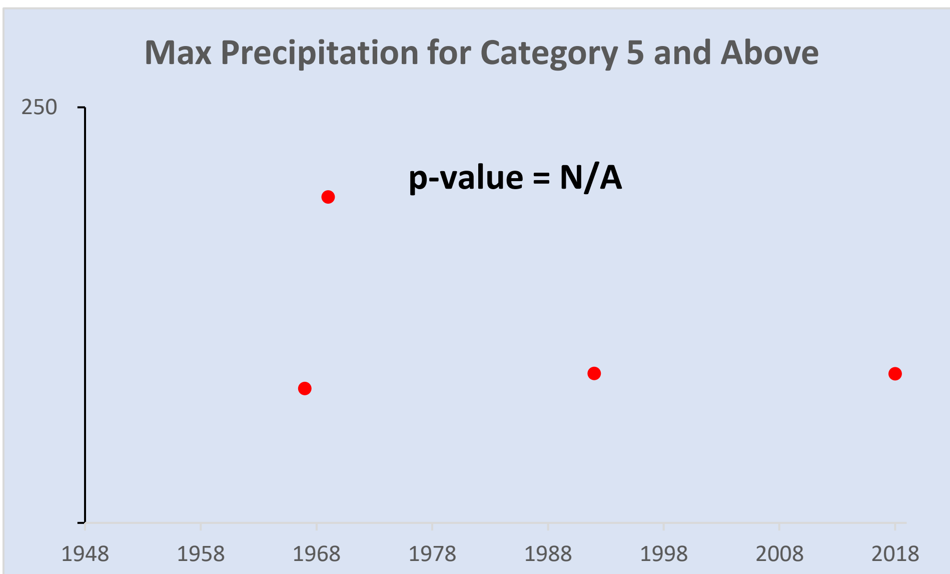
Max Precipitation for Category 5 and Above
250
p-value = N/A
1948
1958
1968
1978
1988
1998
2008
2018

Three Day Running Mean

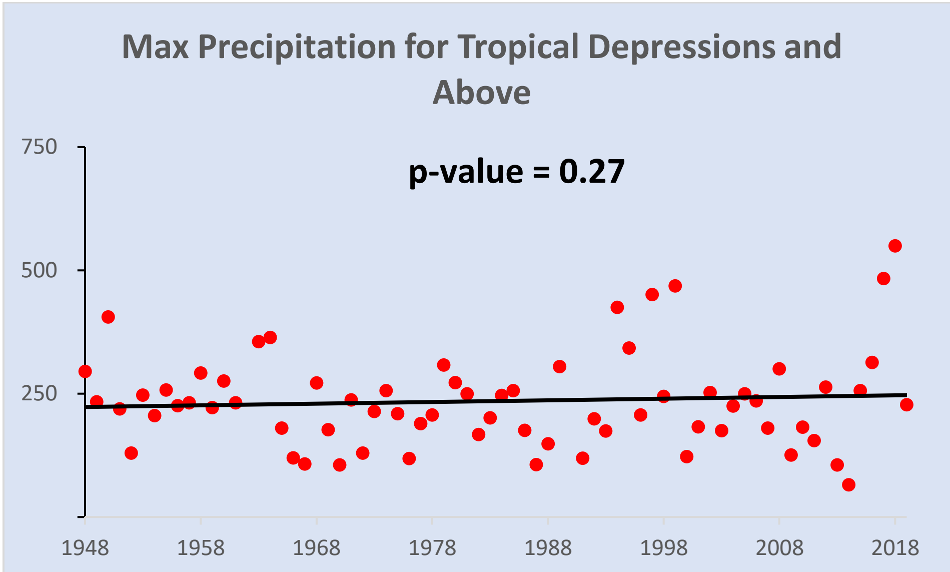

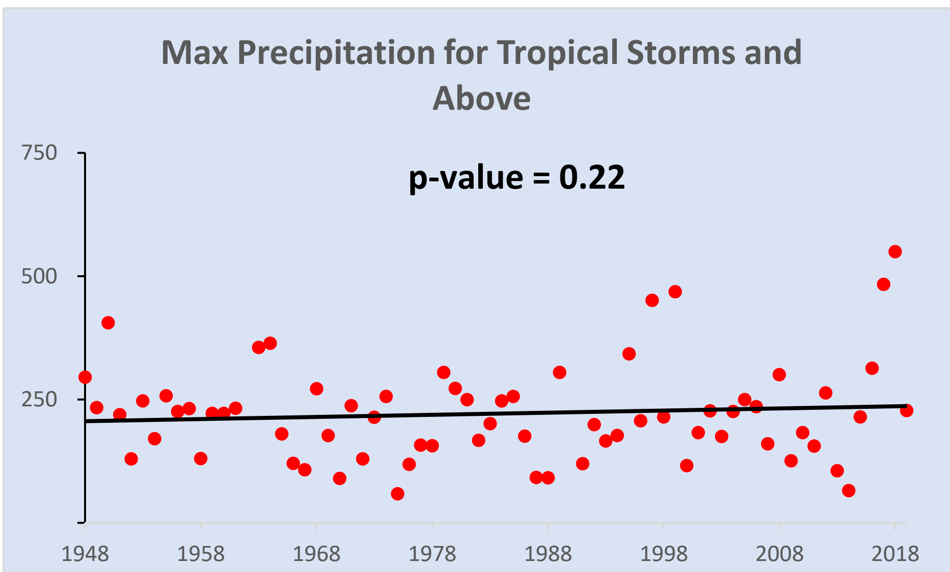

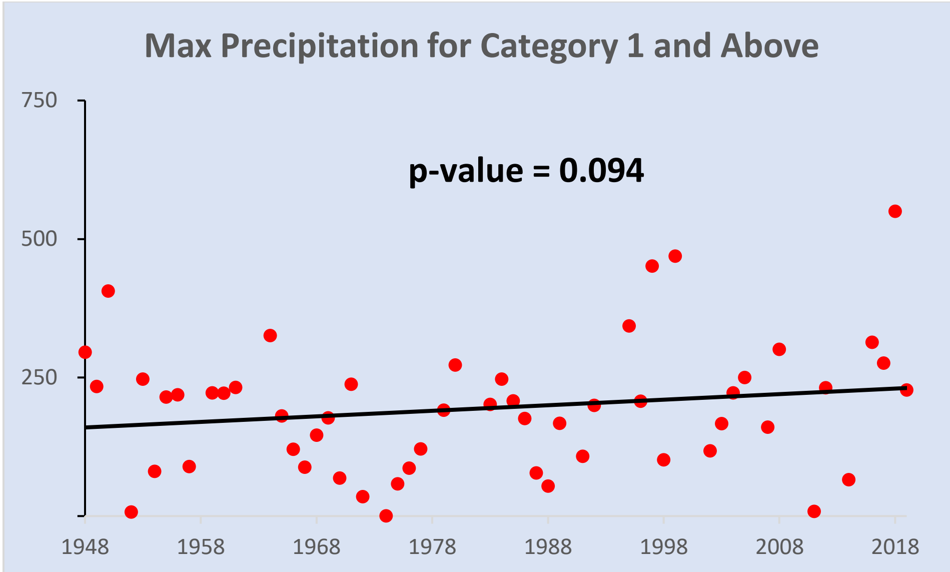
Max Precipitation for Category 1 and Above
750
500
250
p-value = 0.094
1948
1958
1968
1978
1988
1998
2008
2018

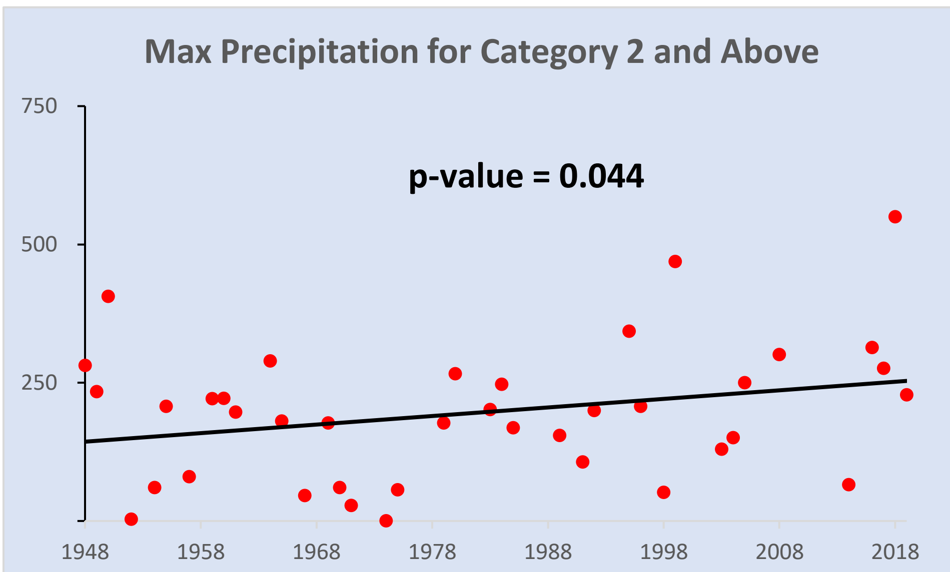
Max Precipitation for Category 2 and Above
750
500
250
p-value = 0.044
1948
1958
1968
1978
1988
1998
2008
2018

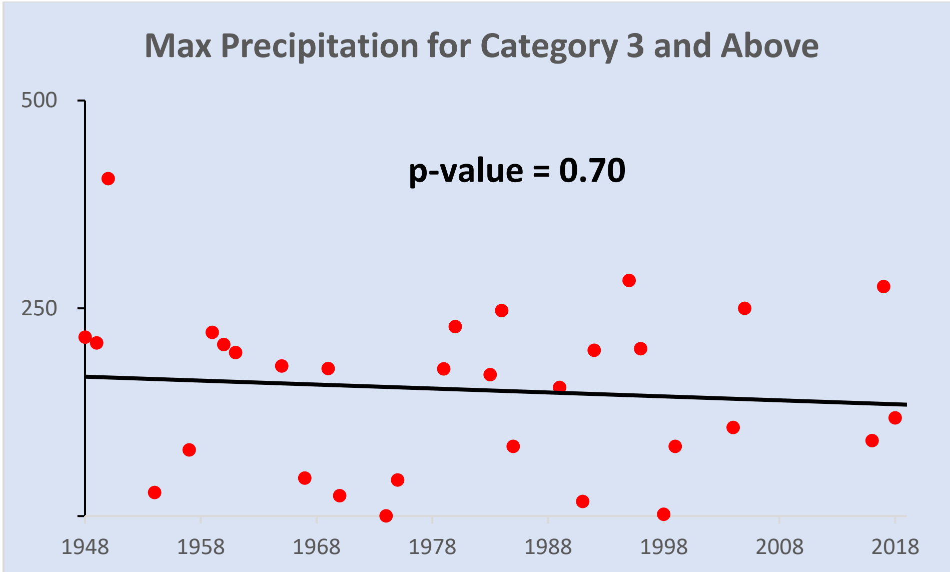
Max Precipitation for Category 3 and Above
p-value = 0.70
500
250
1948
1958
1968
1978
1988
1998
2008
2018

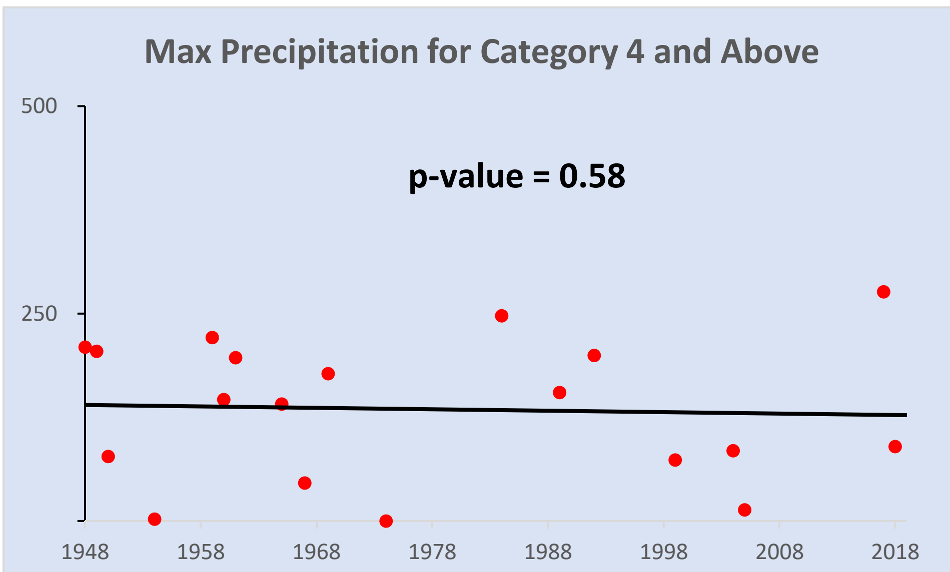
Max Precipitation for Category 4 and Above
p-value = 0.58
500
250
1948
1958
1968
1978
1988
1998
2008
2018

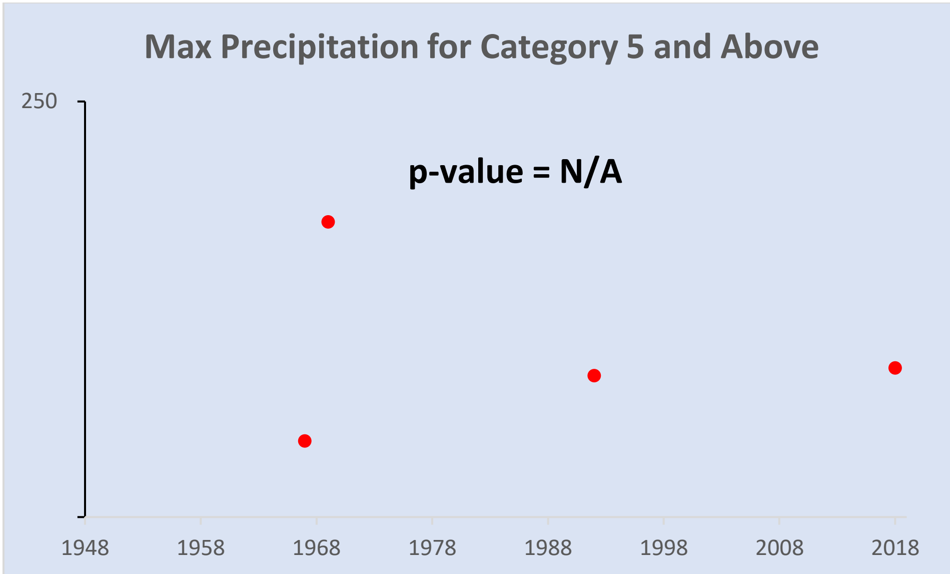
Max Precipitation for Category 5 and Above
250
p-value = N/A
1948
1958
1968
1978
1988
1998
2008
2018

ERM Five Day Running Mean

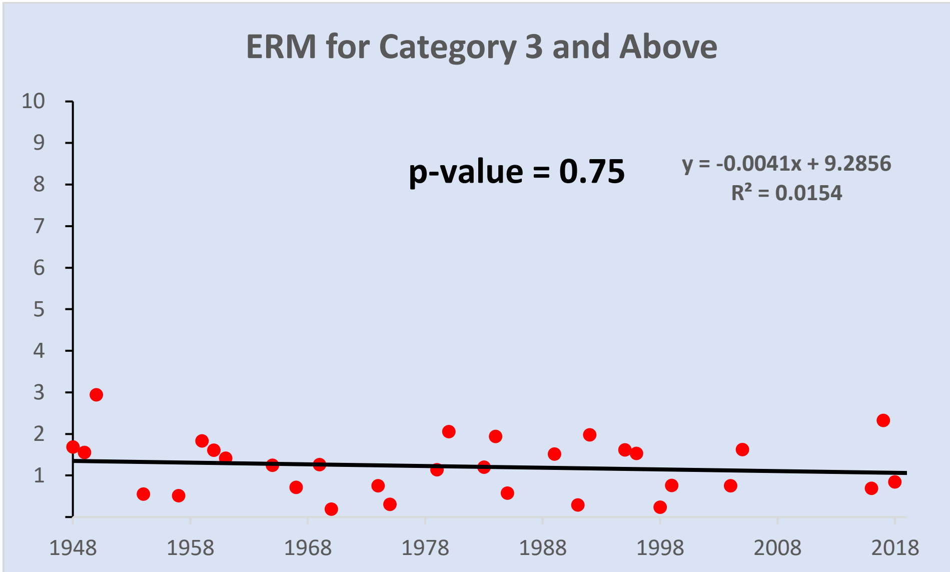

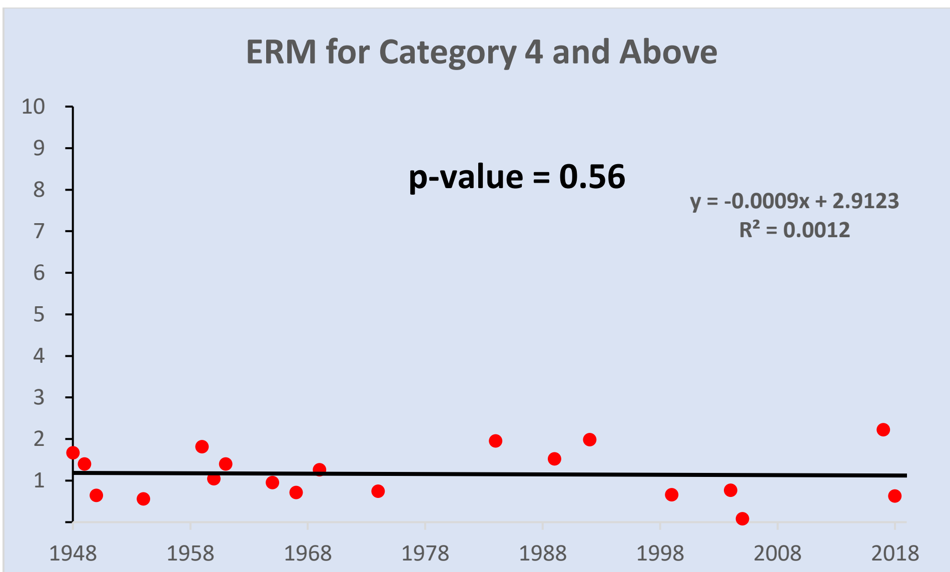

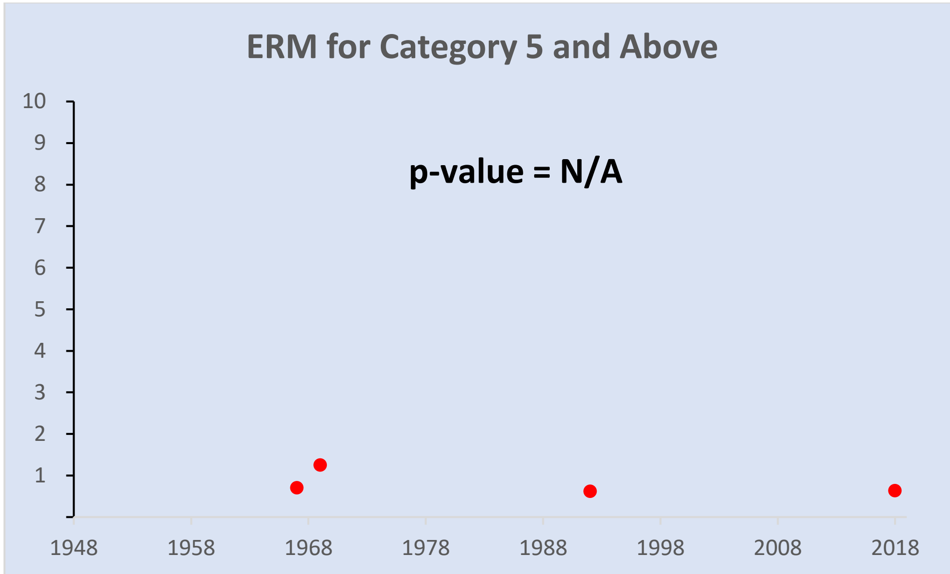
ERM for Category 5 and Above
p-value = N/A
10
9
8
7
6
5
4
3
2
1
1948
1958
1968
1978
1988
1998
2008
2018

Appendix – E

Hurricane Atlas

The following hurricane atlas contains images of all the tropical cyclones in each hurricane season.

Hurricane Season 1900

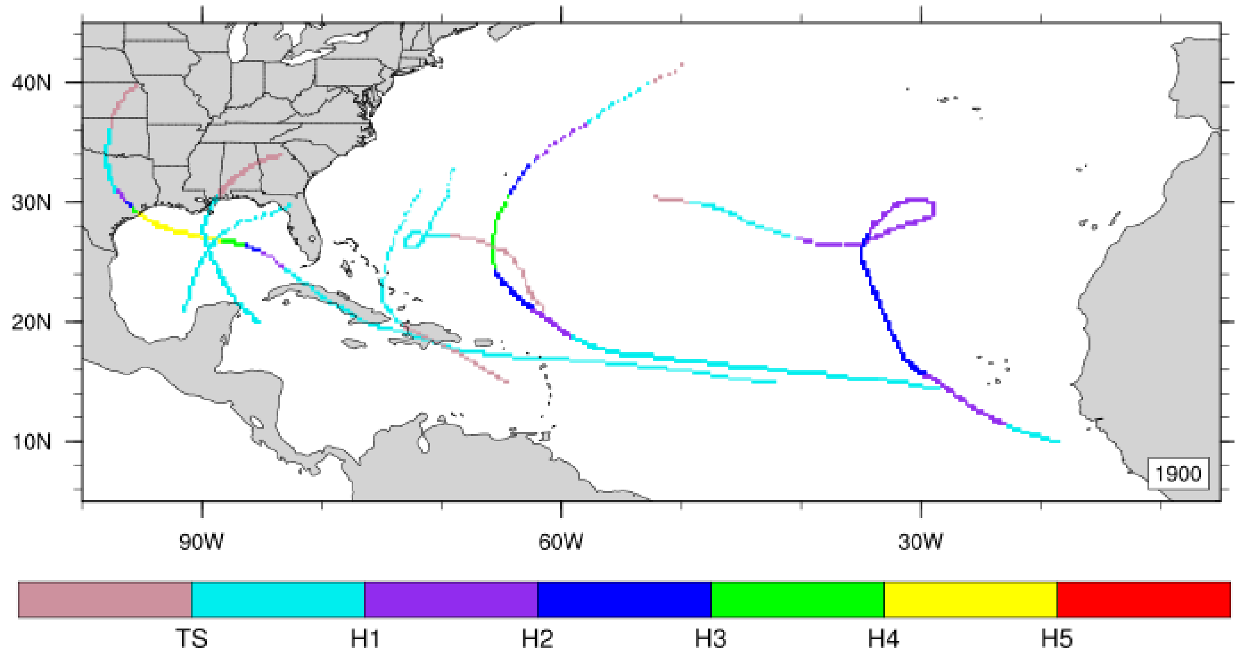

Hurricane Season 1901

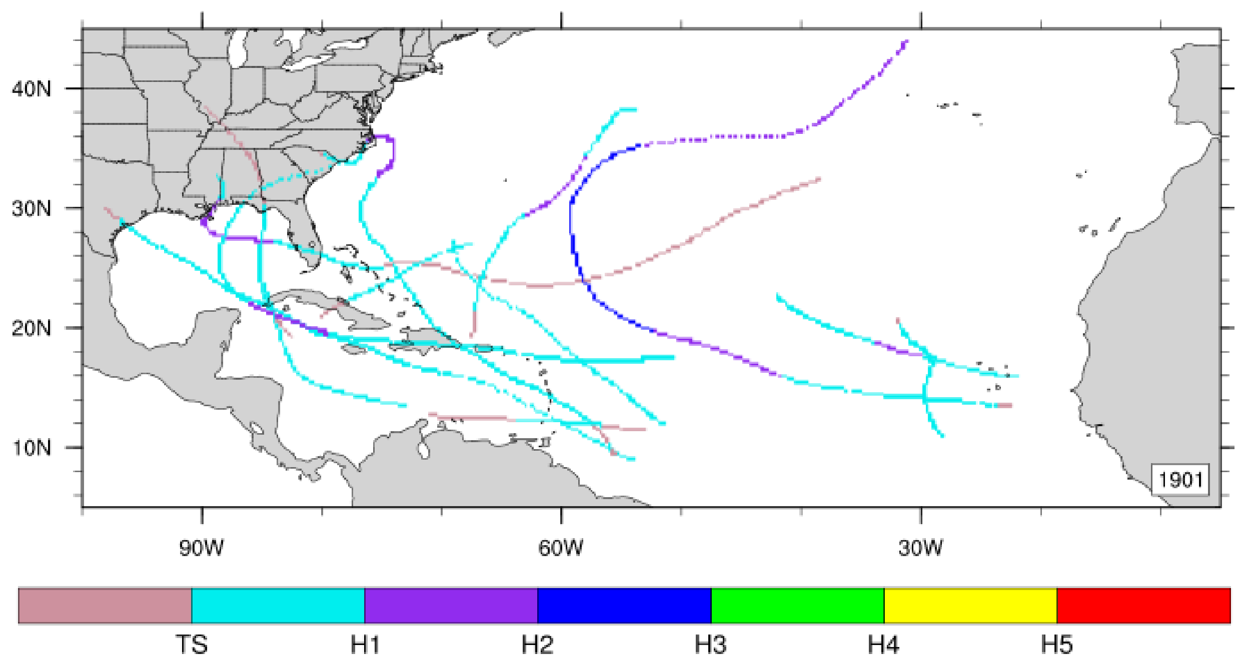

Hurricane Season 1902

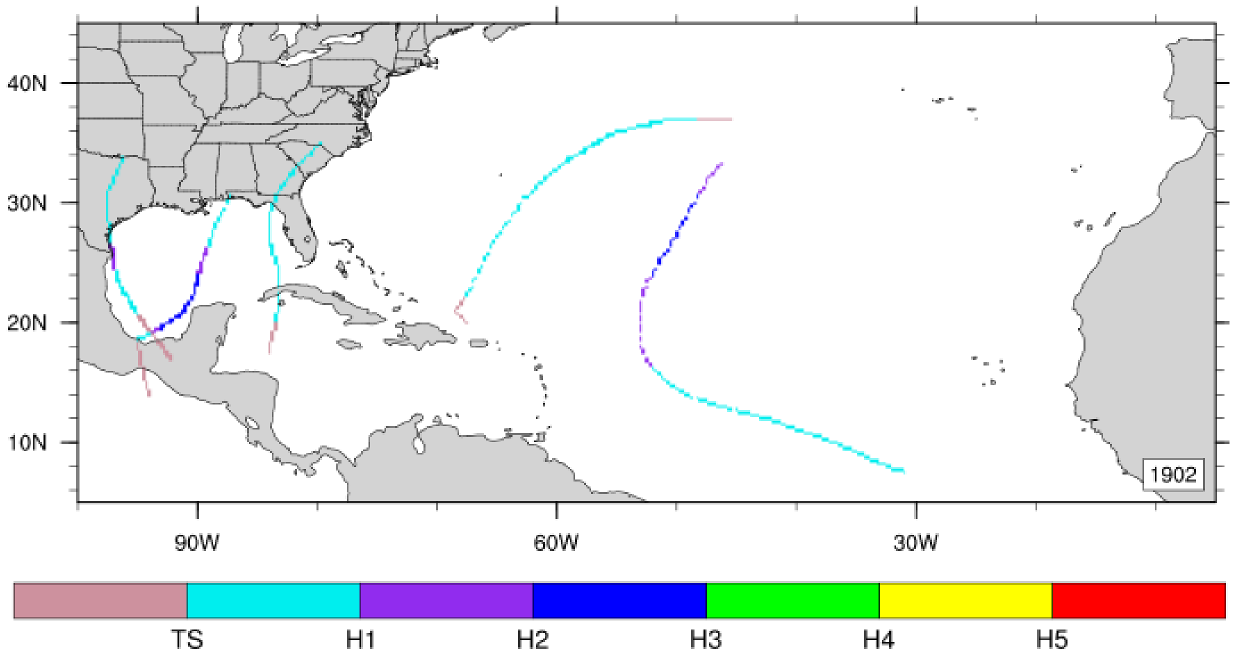

Hurricane Season 1903

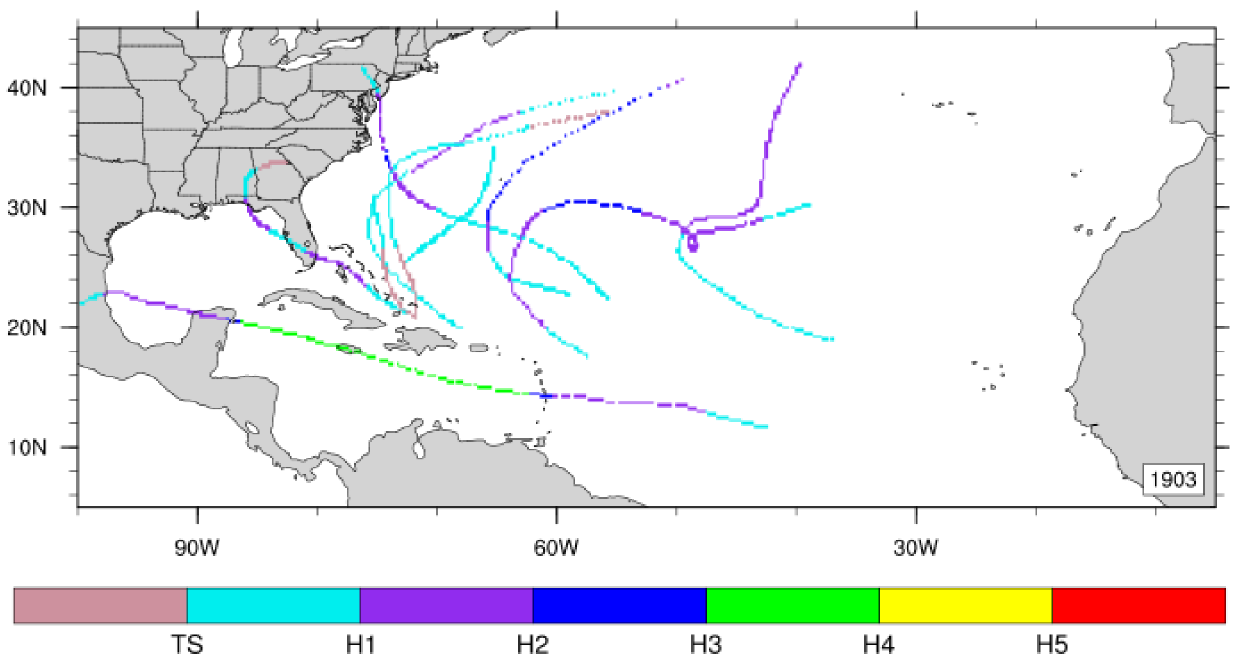

Hurricane Season 1904

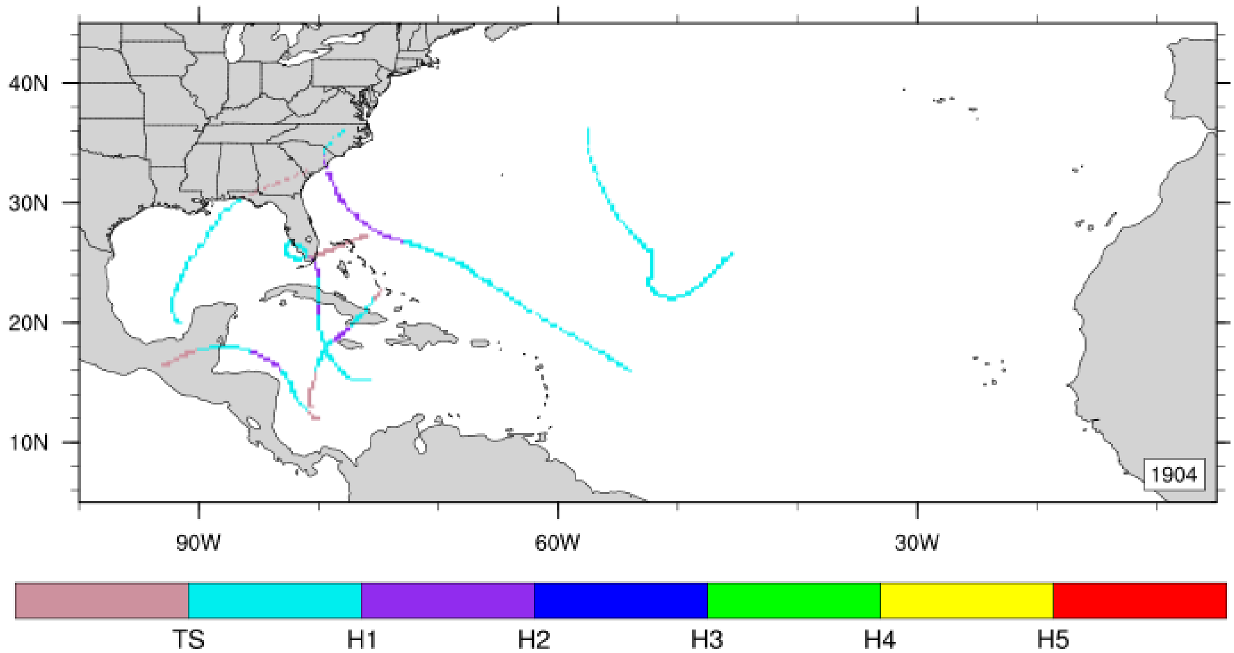

Hurricane Season 1905

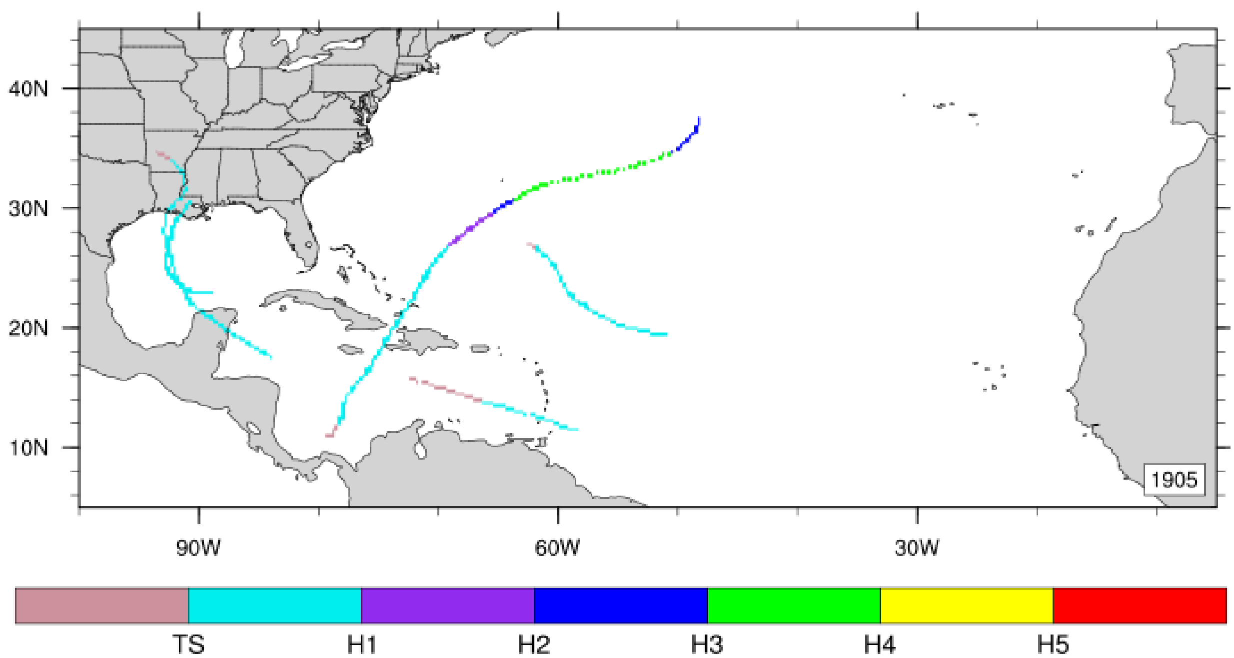

Hurricane Season 1906

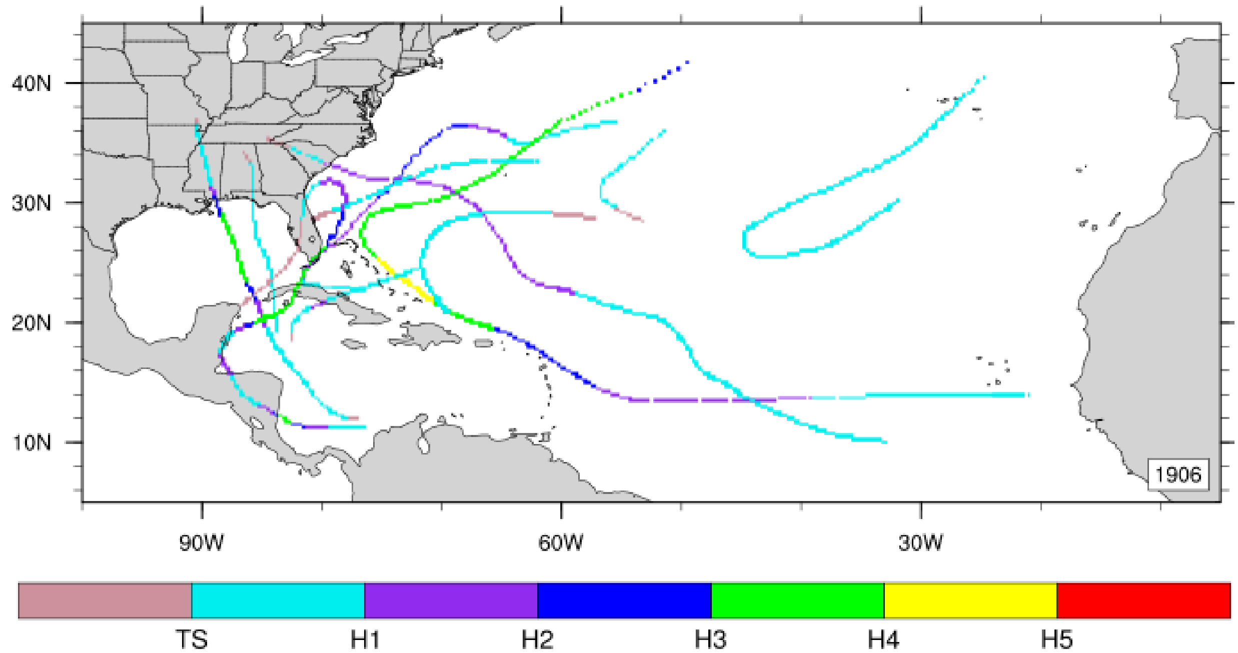

Hurricane Season 1907

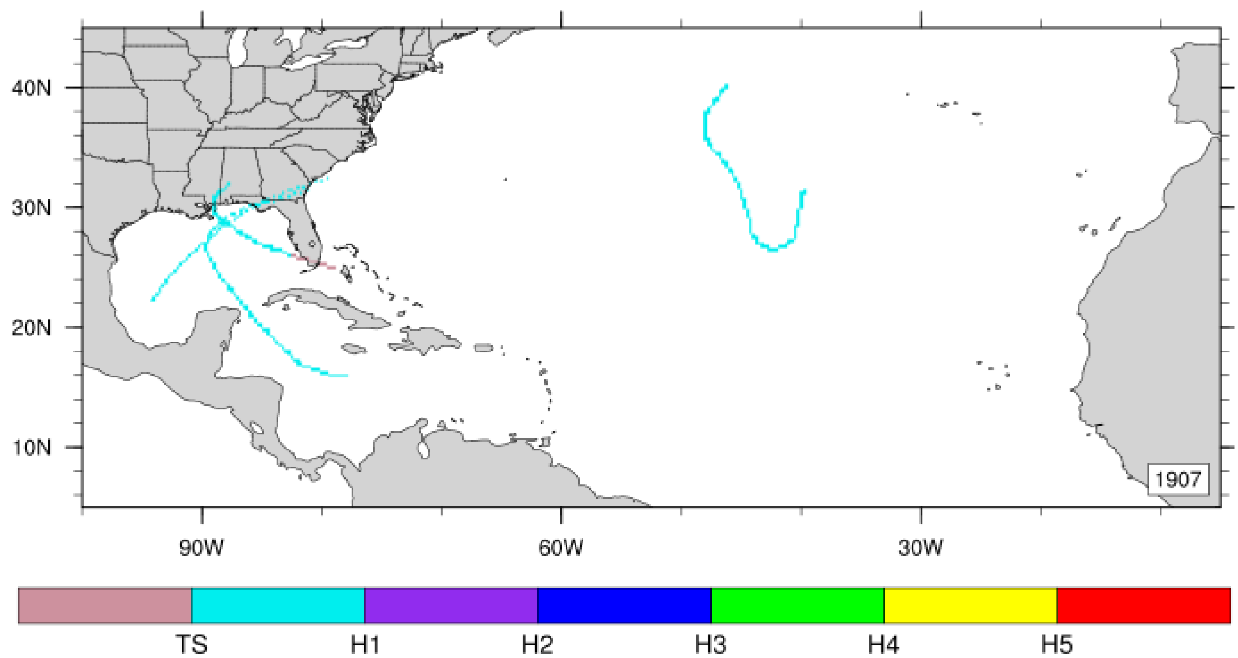

Hurricane Season 1908

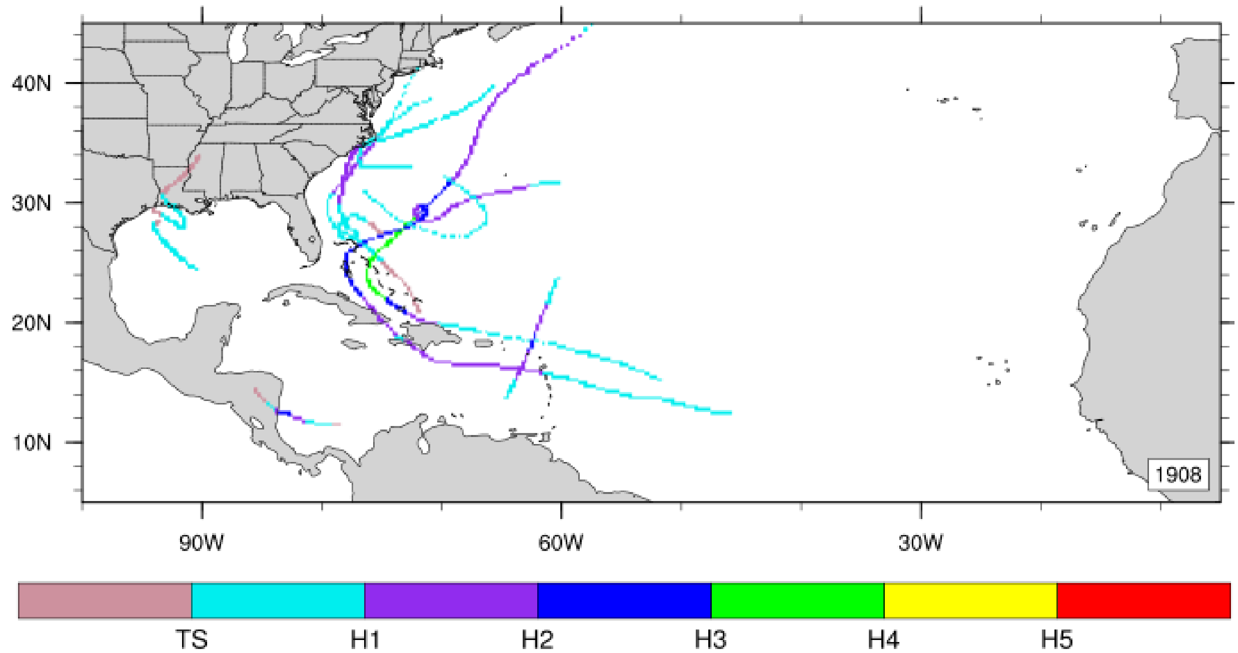

Hurricane Season 1909

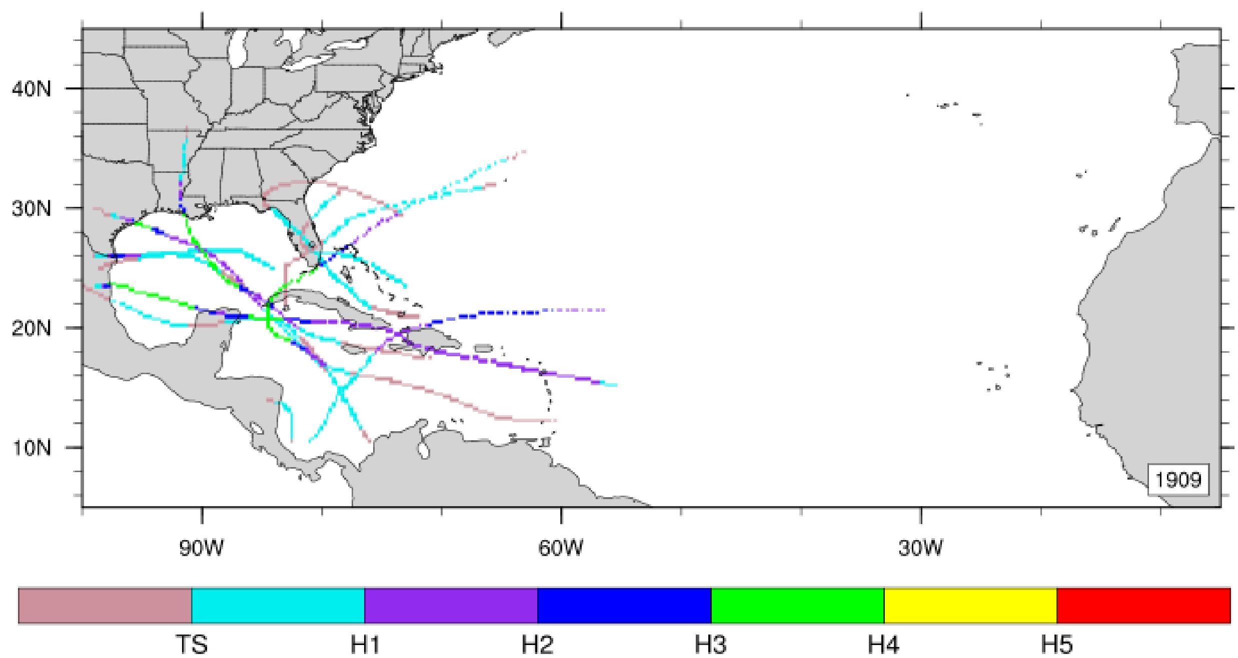

Hurricane Season 1910

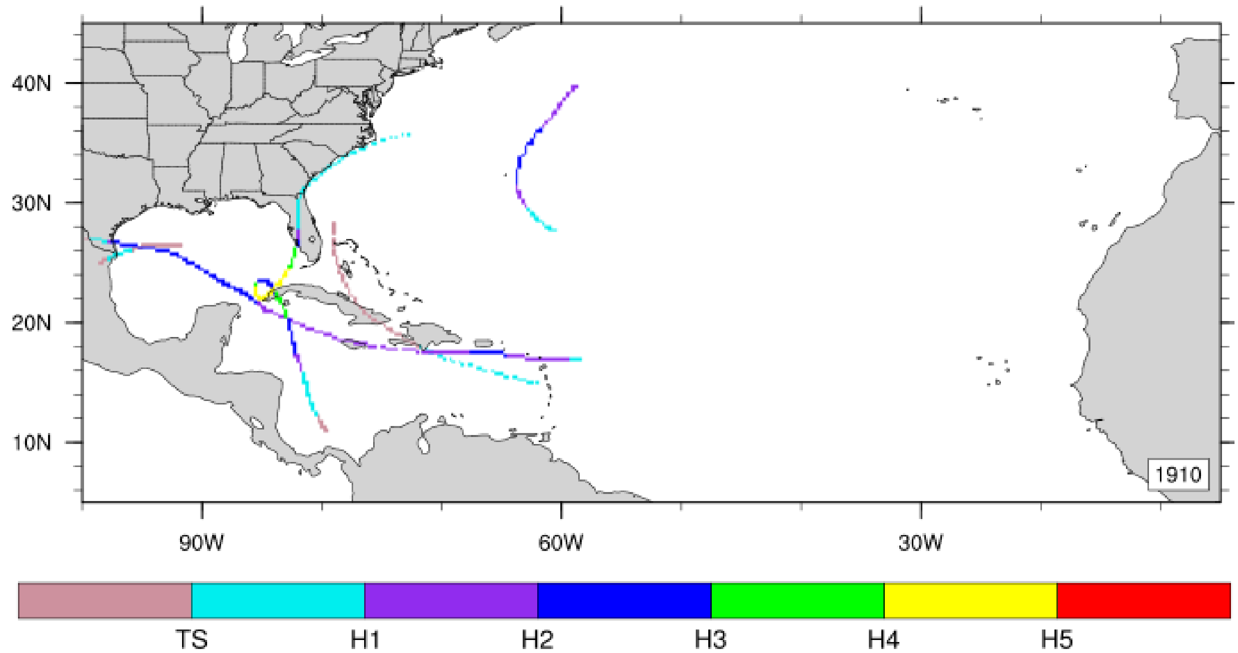

Hurricane Season 1911

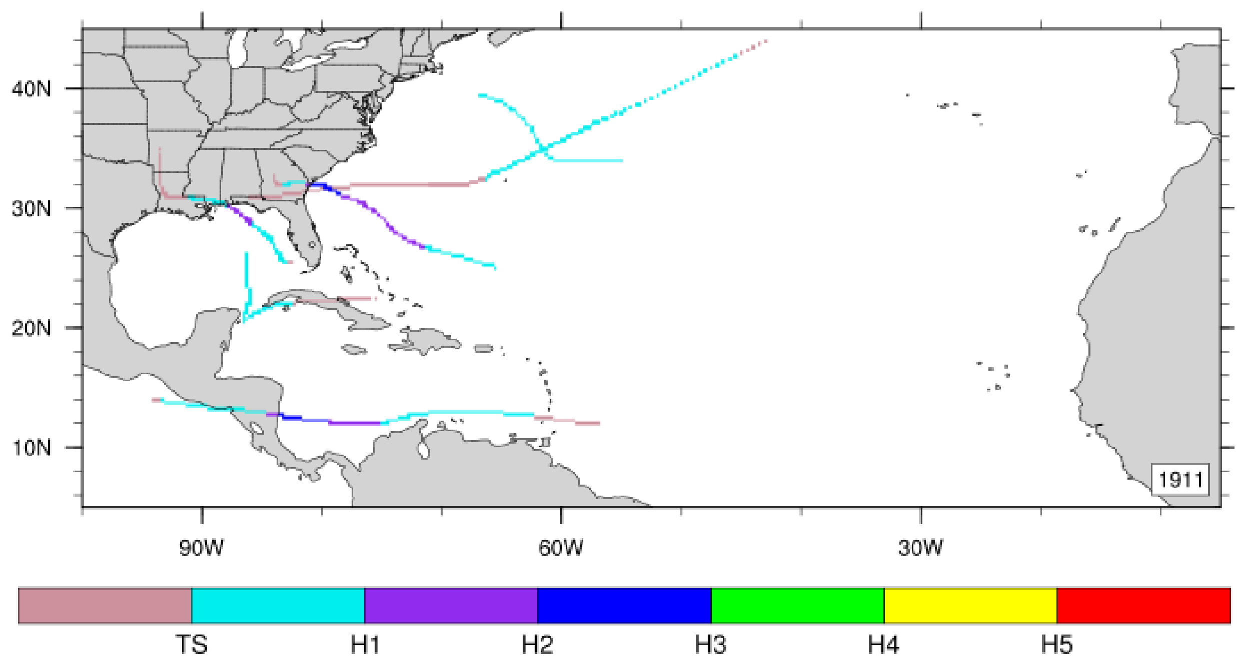

Hurricane Season 1912

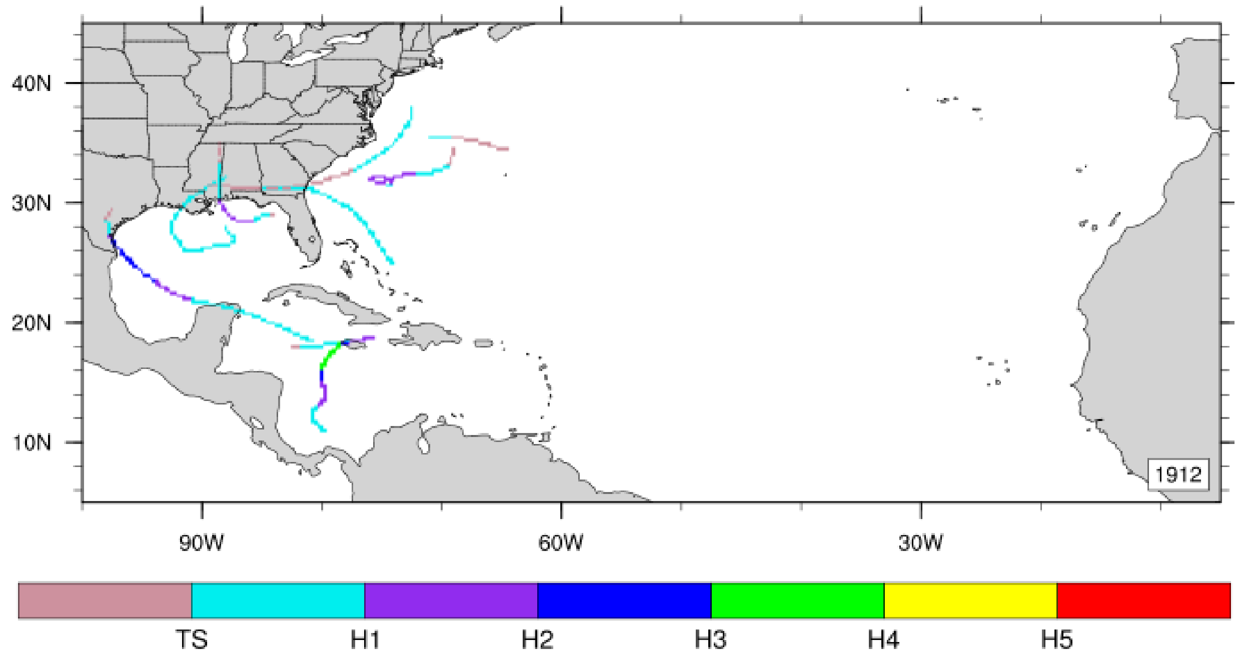

Hurricane Season 1913

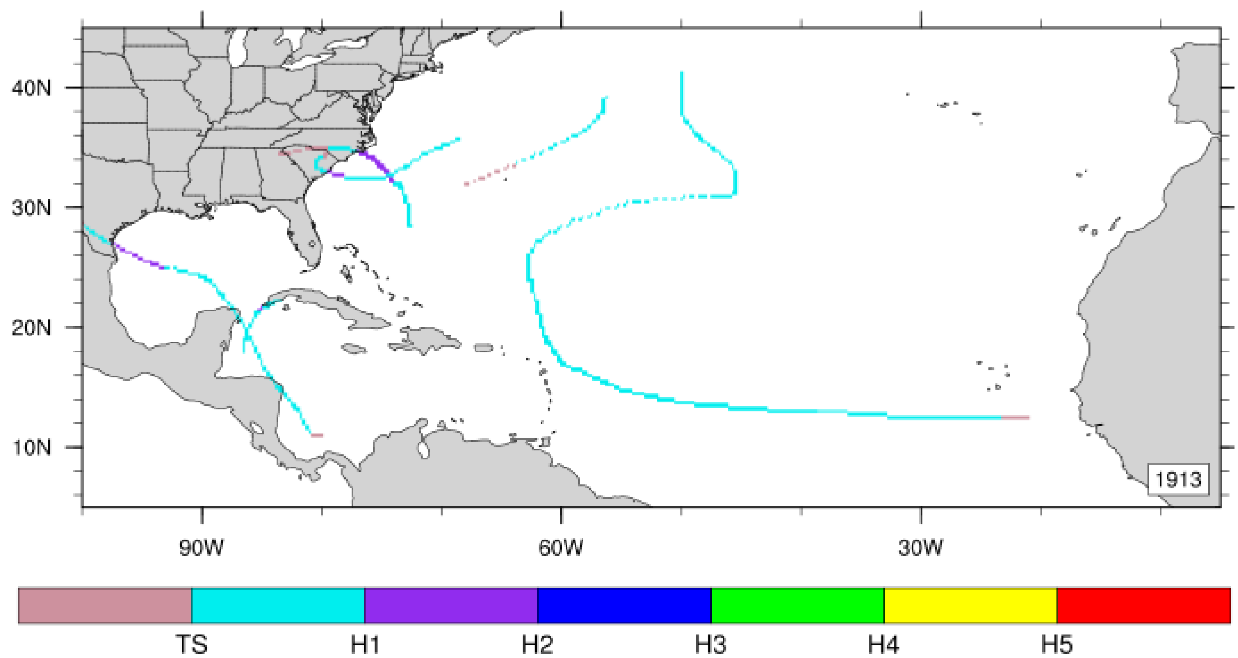

Hurricane Season 1914

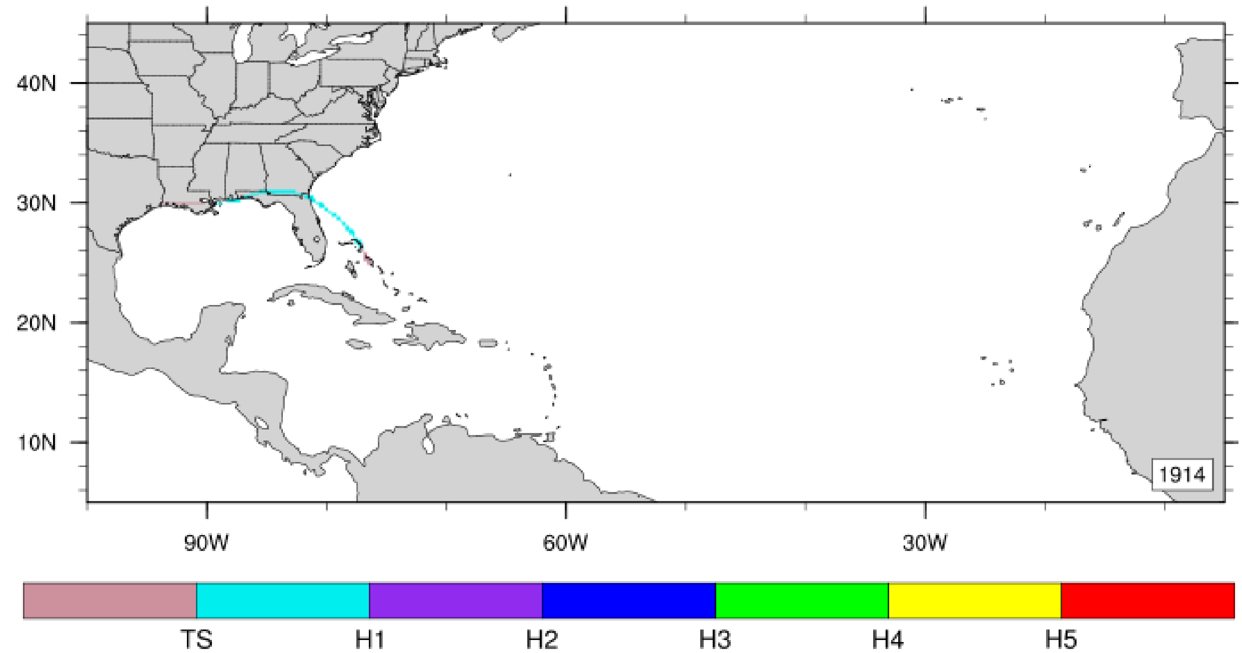

Hurricane Season 1915

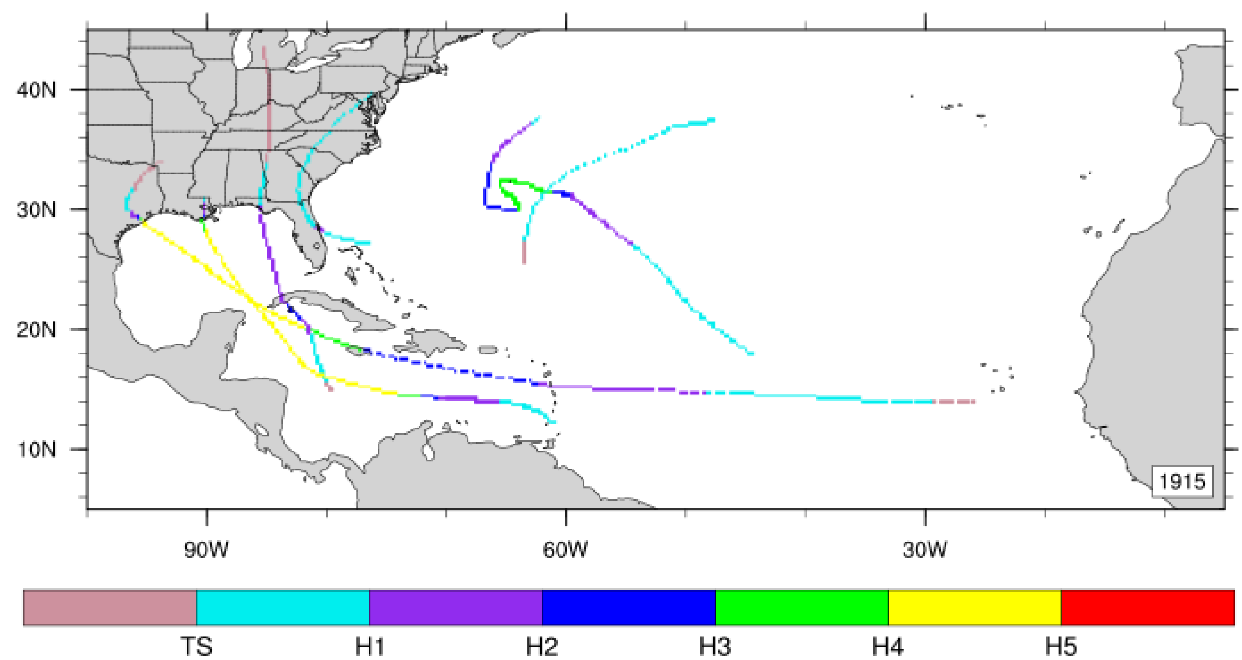

Hurricane Season 1916

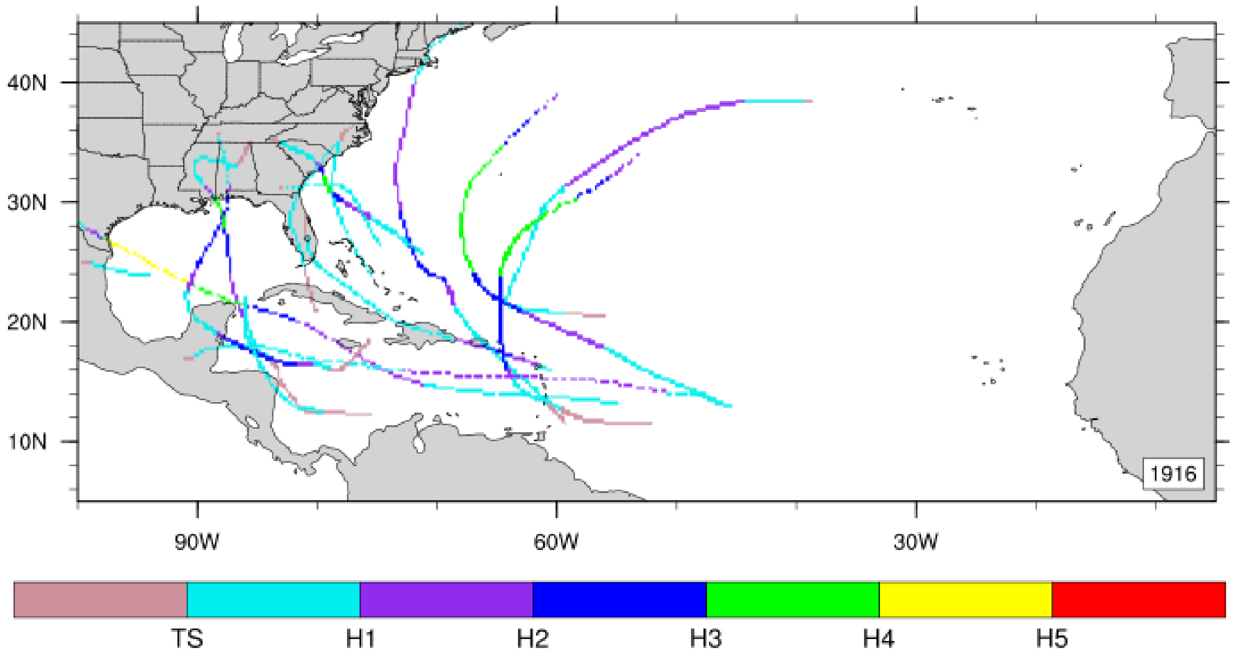

Hurricane Season 1917

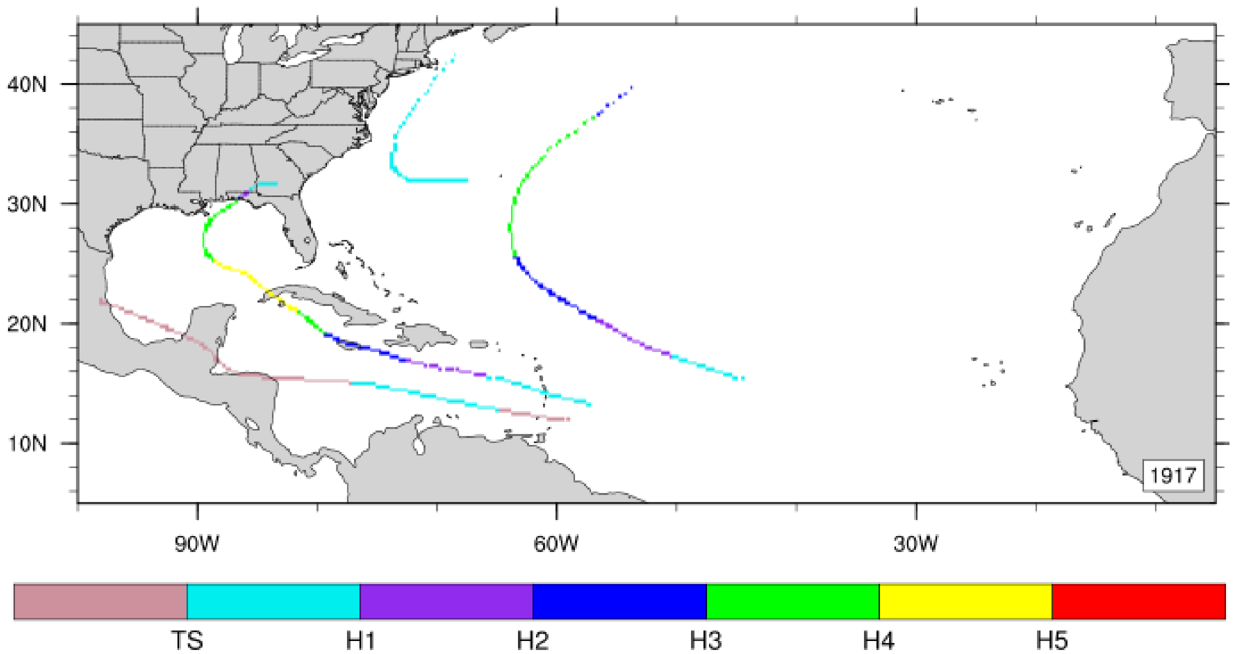

Hurricane Season 1918

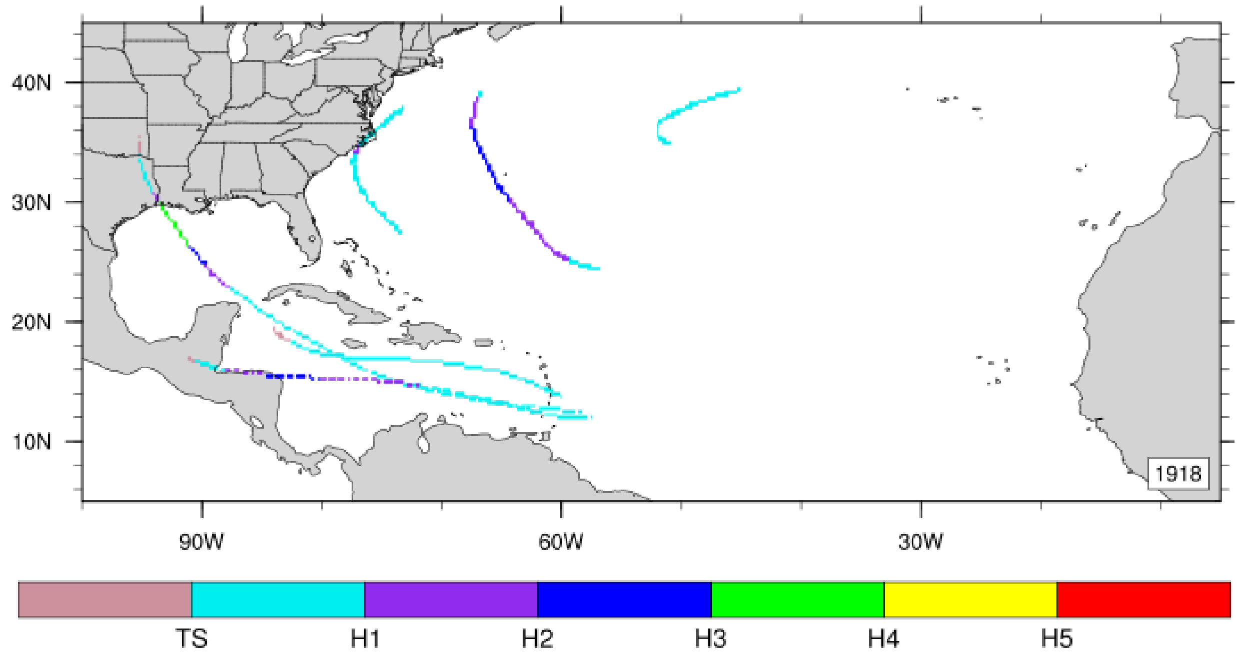

Hurricane Season 1919

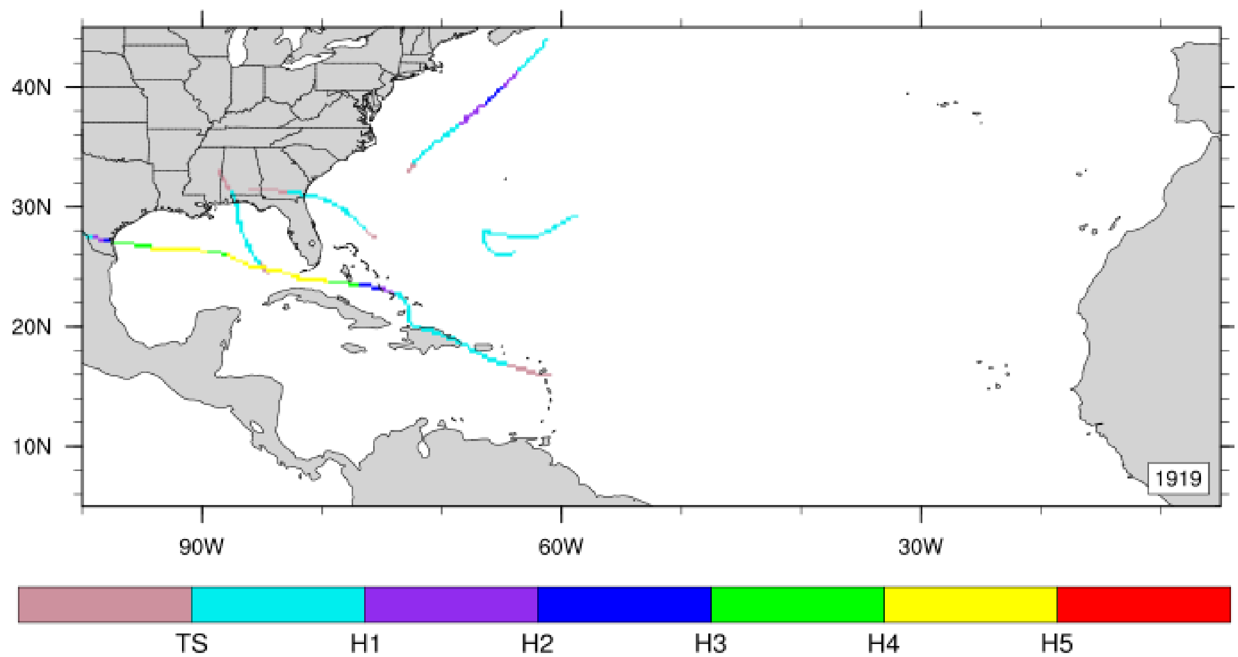

Hurricane Season 1920

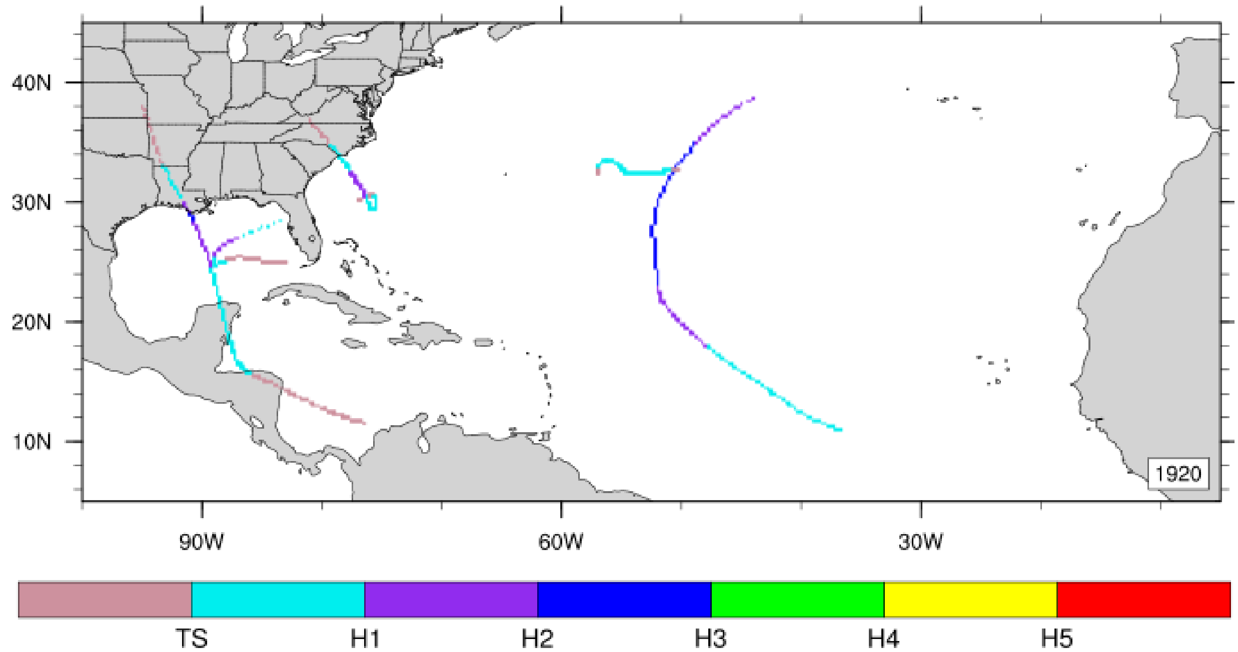

Hurricane Season 1921

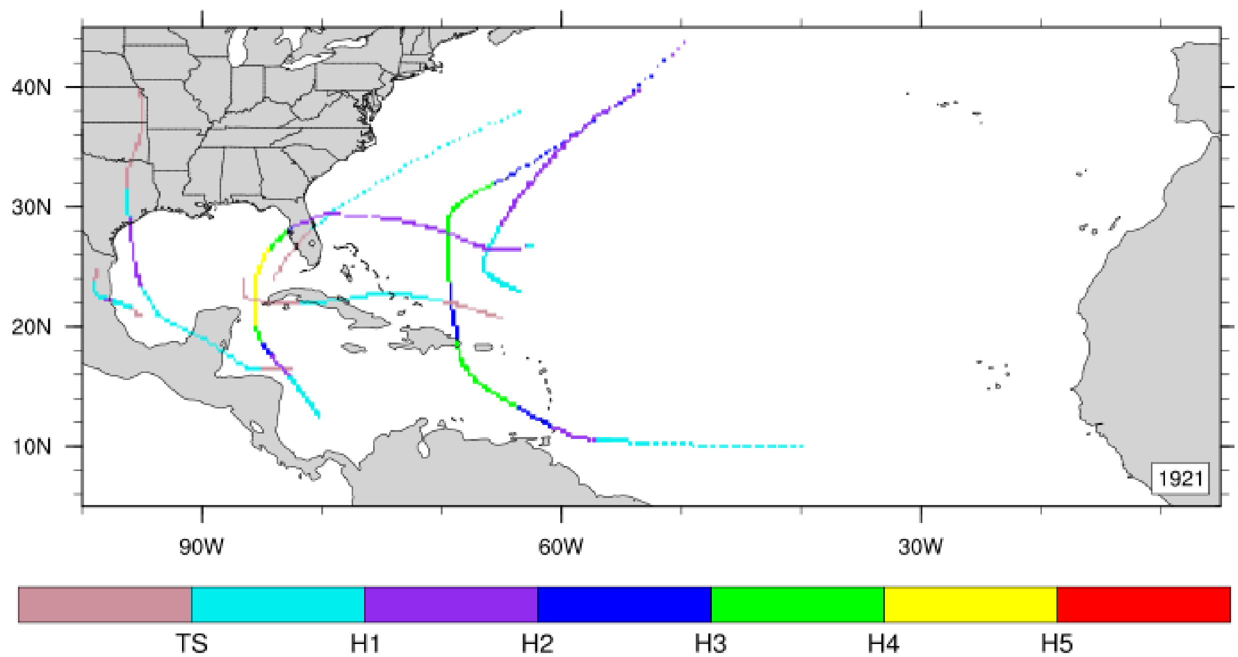

Hurricane Season 1922

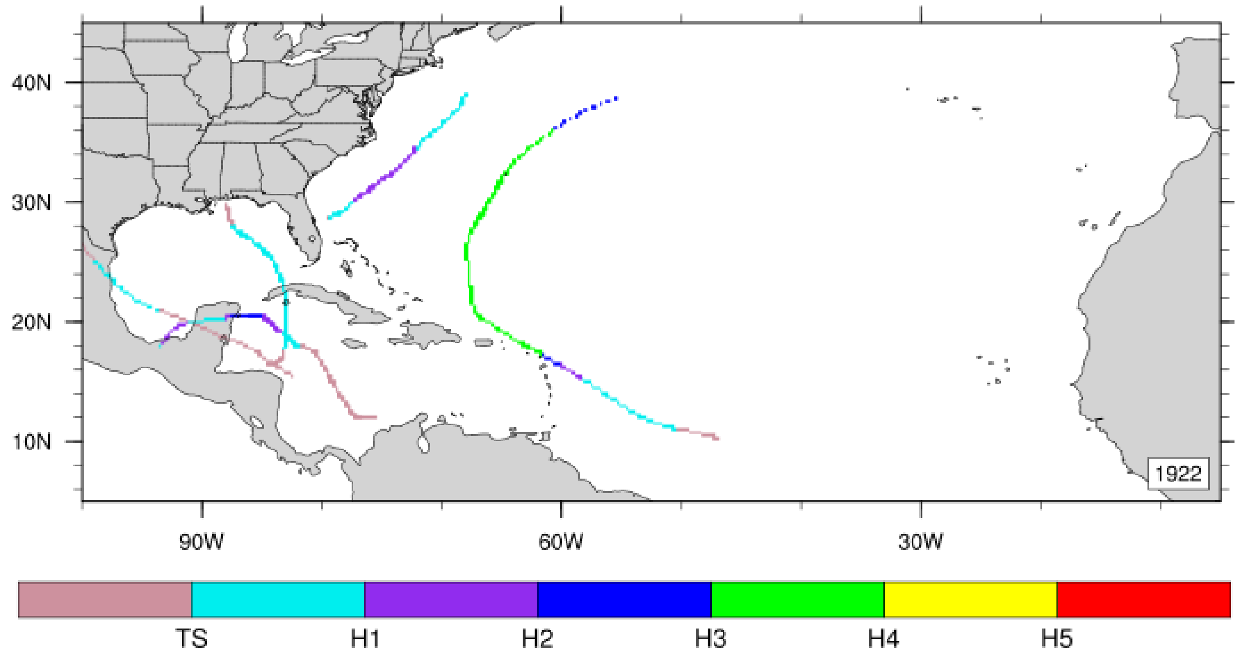

Hurricane Season 1923

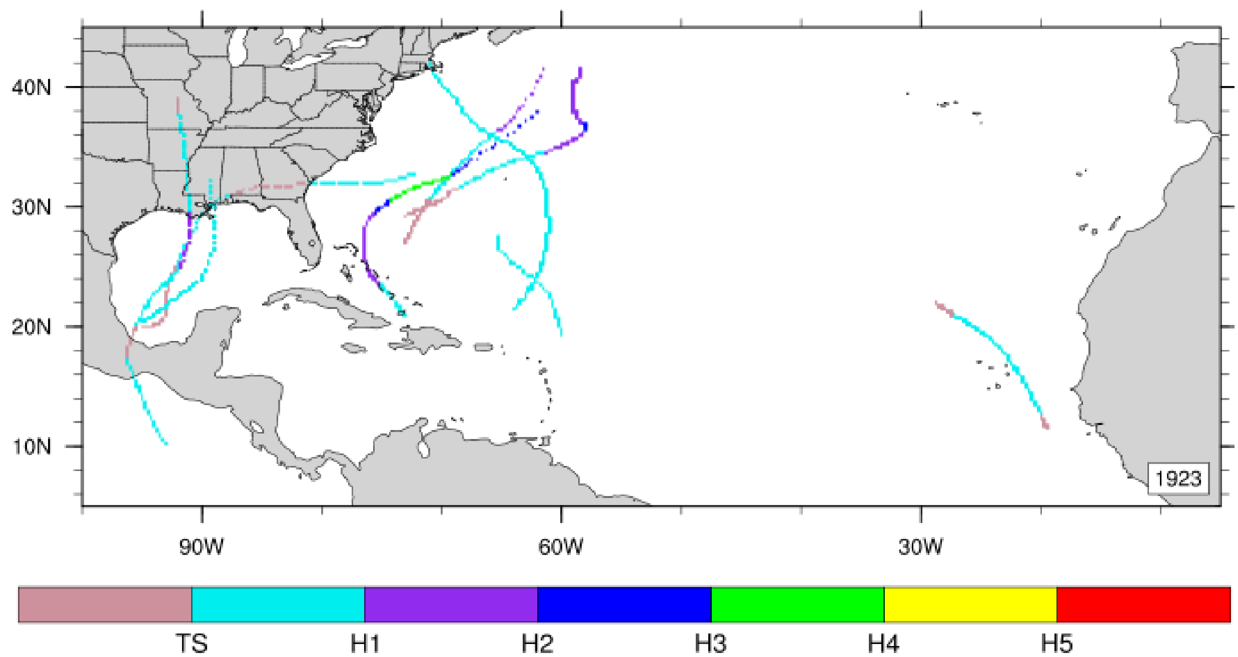

Hurricane Season 1924

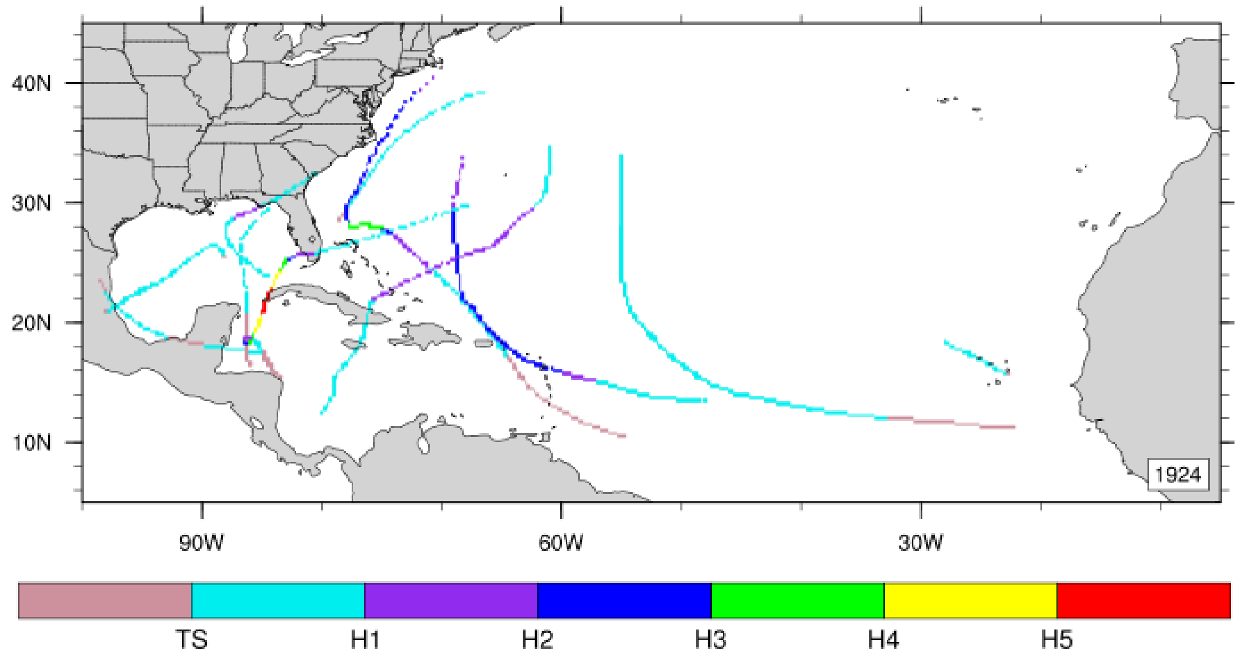

Hurricane Season 1925

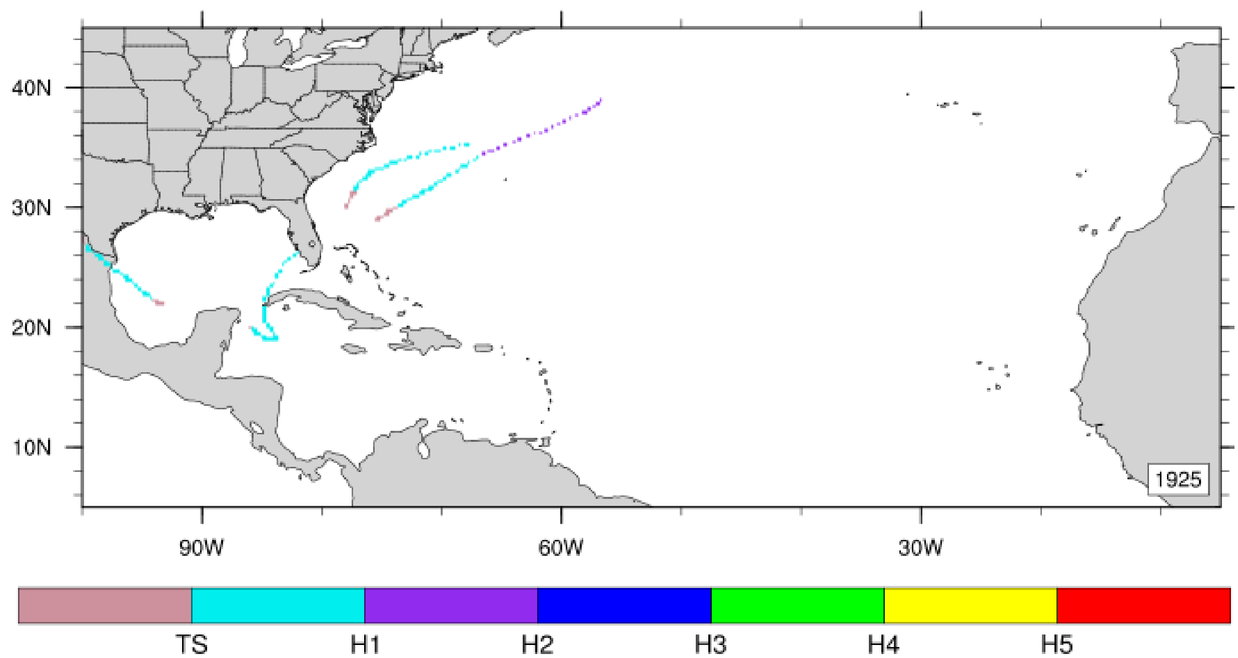

Hurricane Season 1926

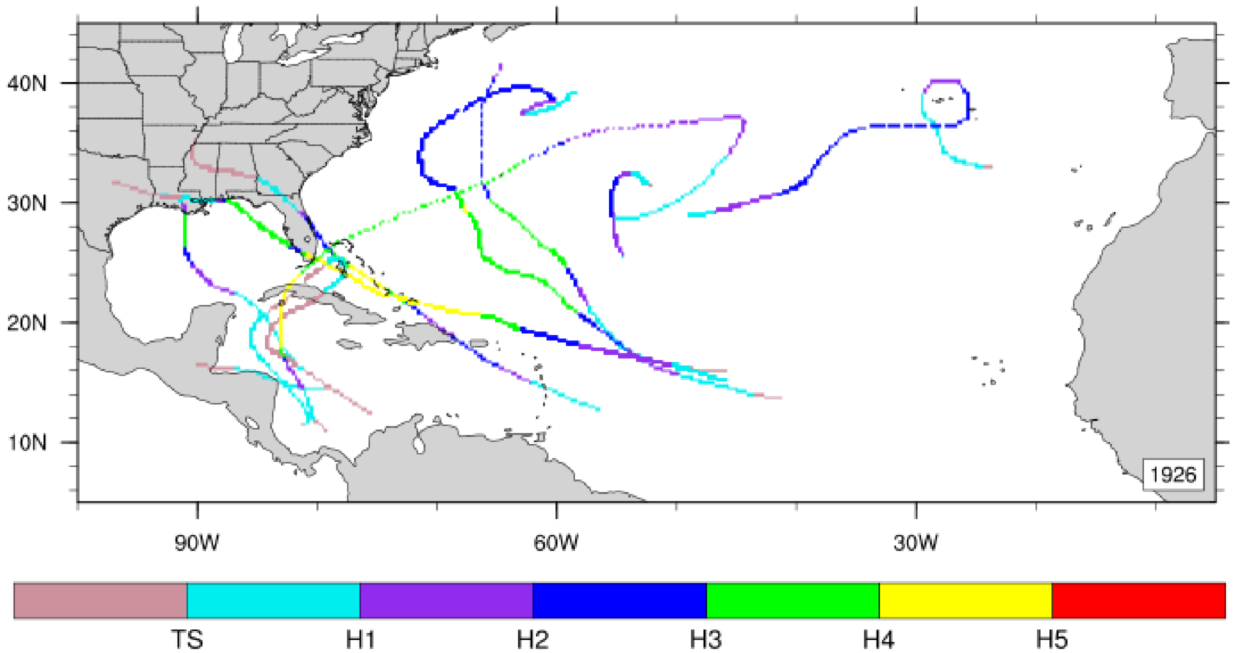

Hurricane Season 1927

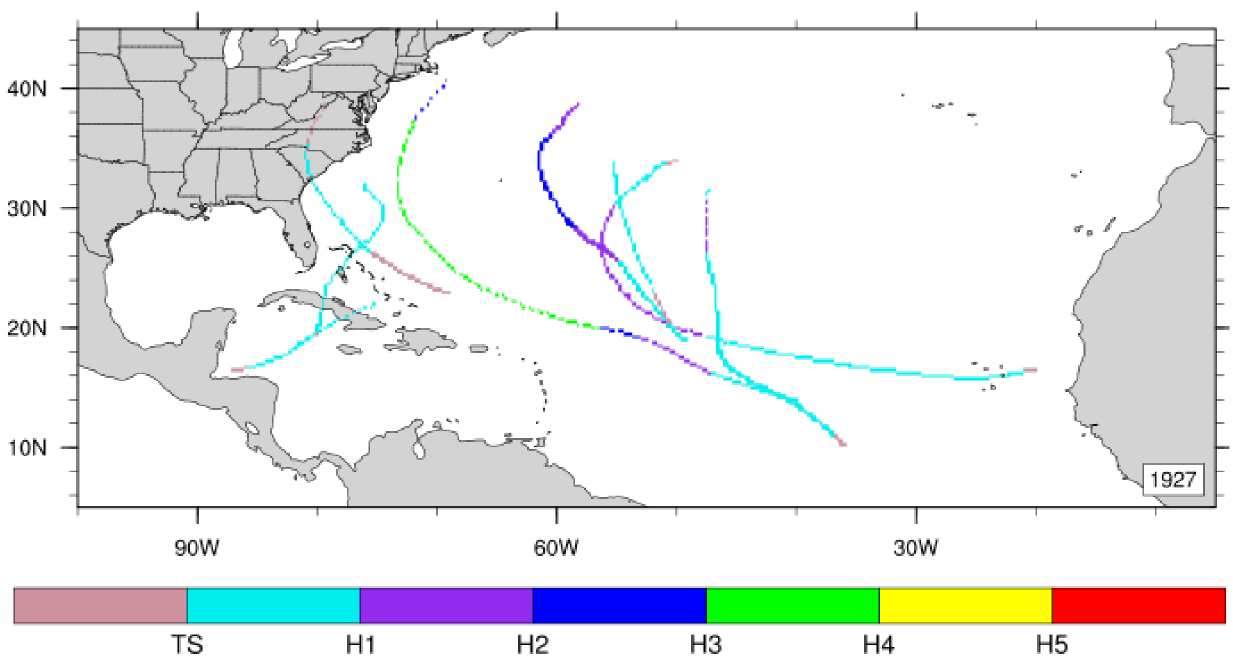

Hurricane Season 1928

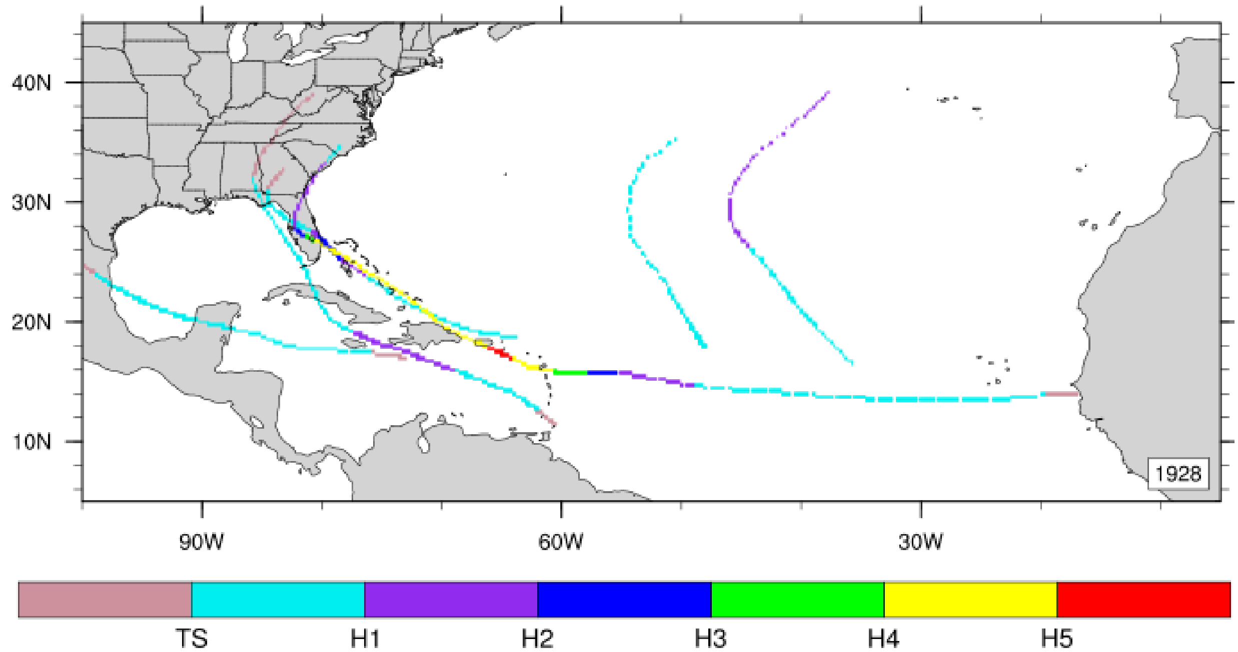

Hurricane Season 1929

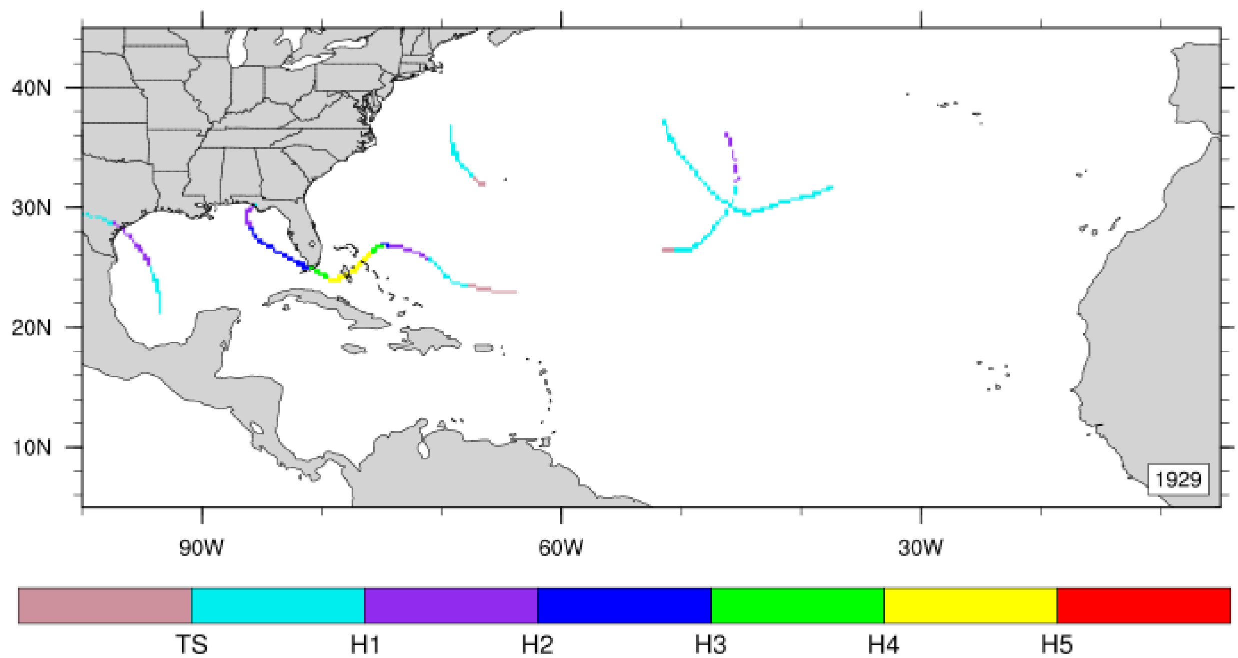

Hurricane Season 1930

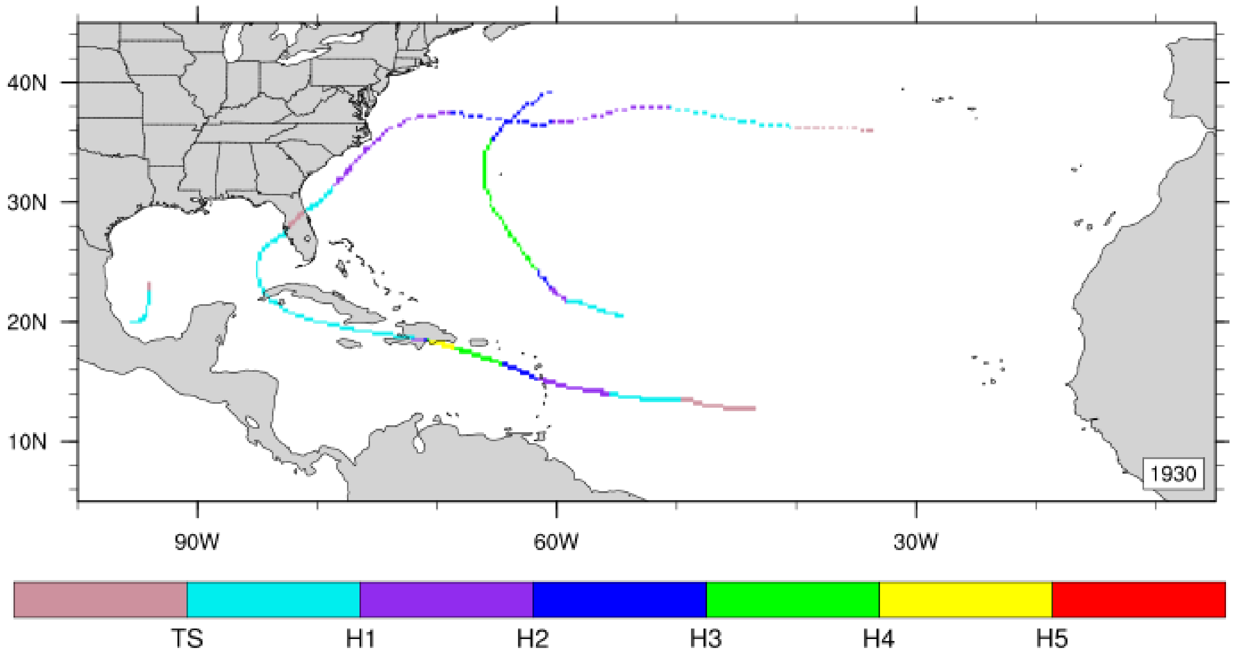

Hurricane Season 1931

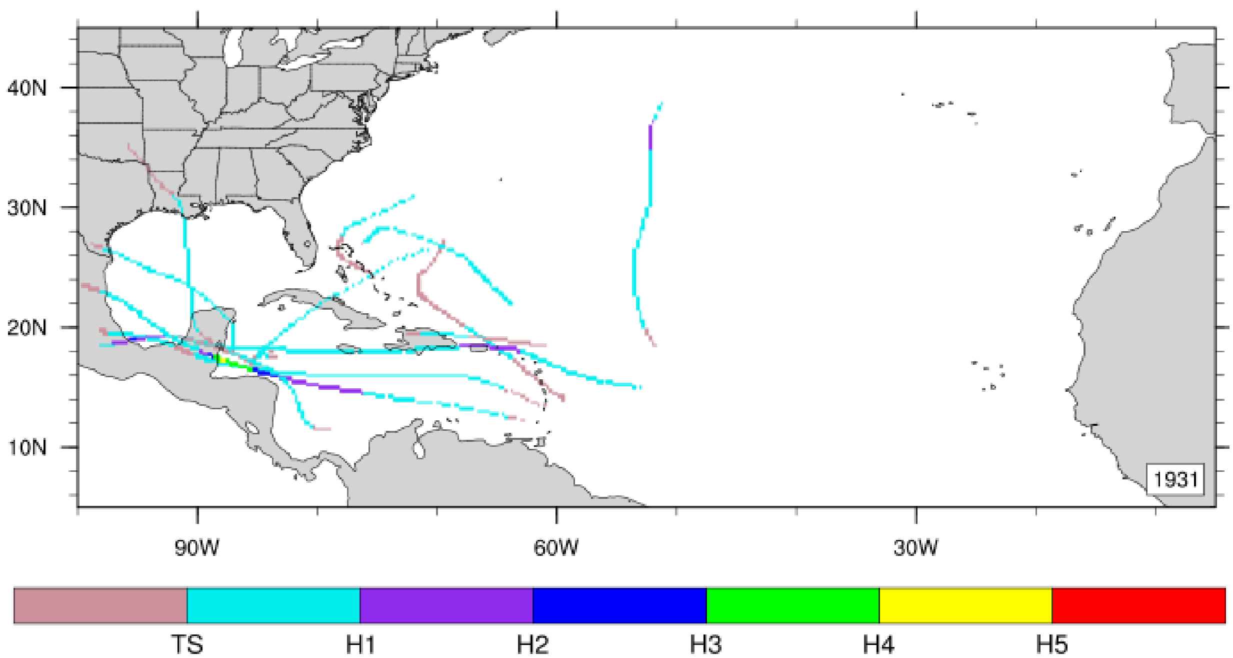

Hurricane Season 1932

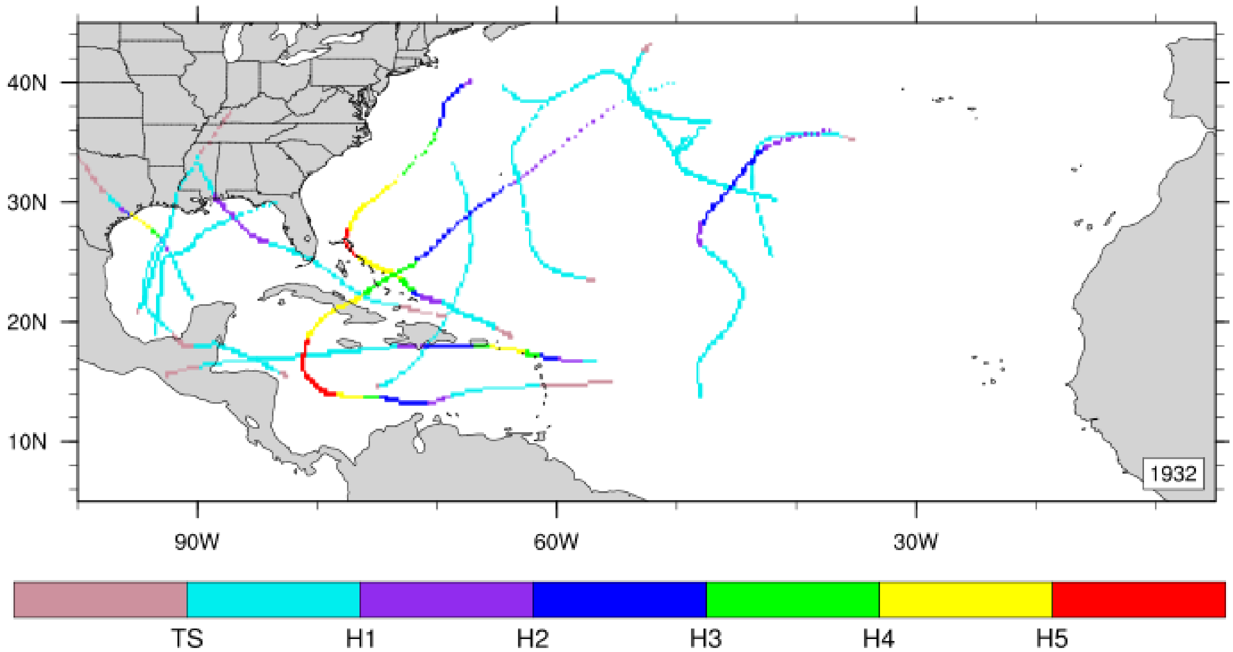

Hurricane Season 1933

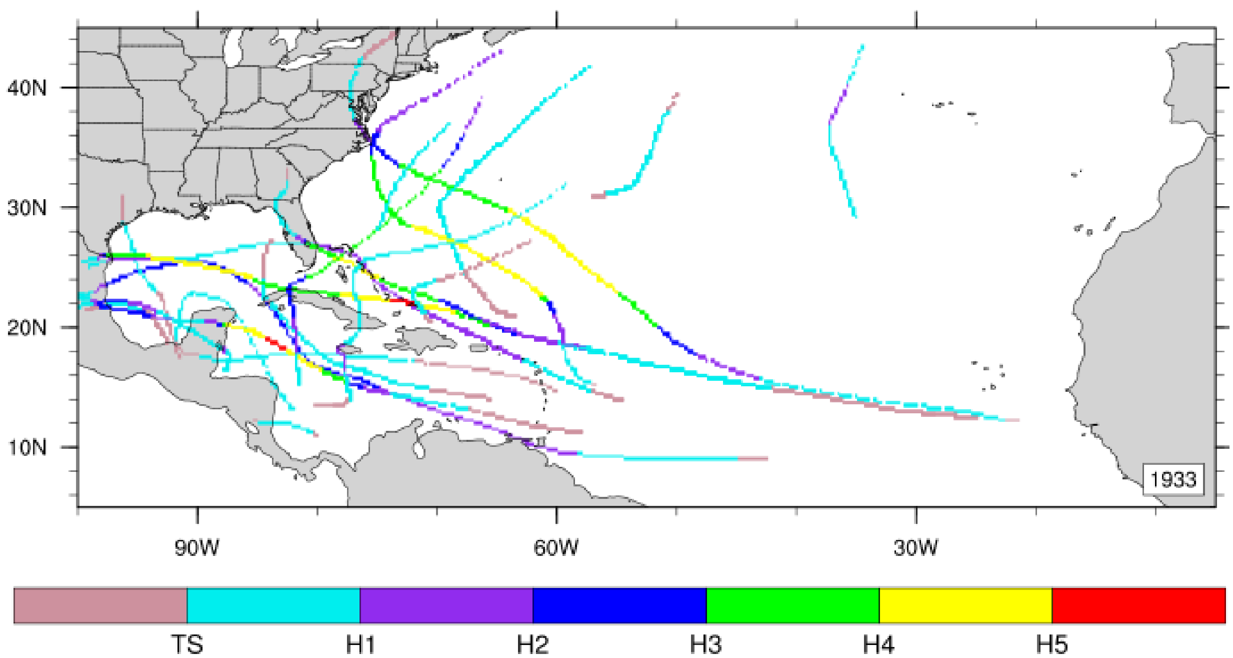

Hurricane Season 1934

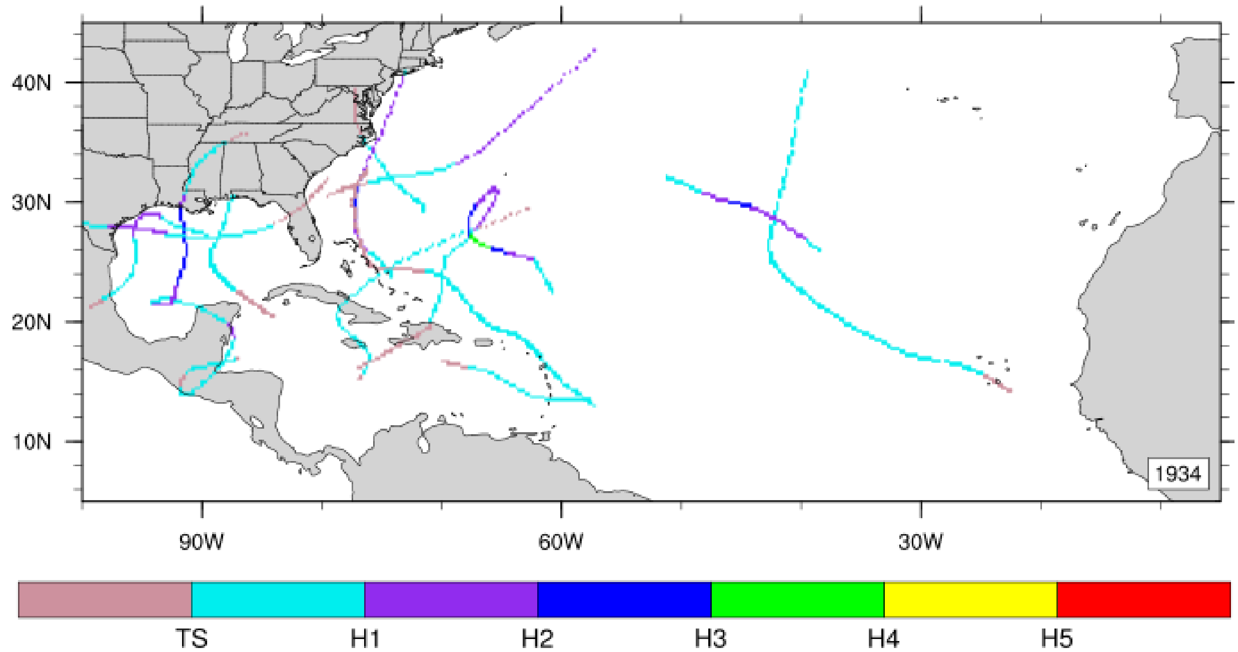

Hurricane Season 1935

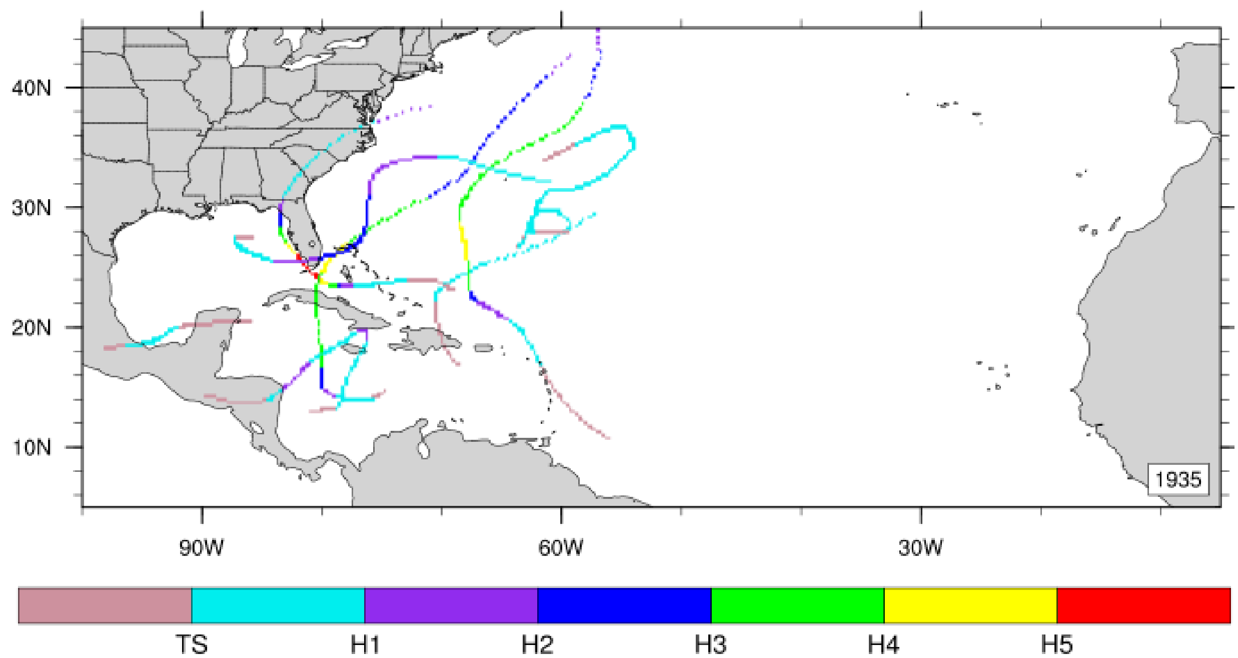

Hurricane Season 1936

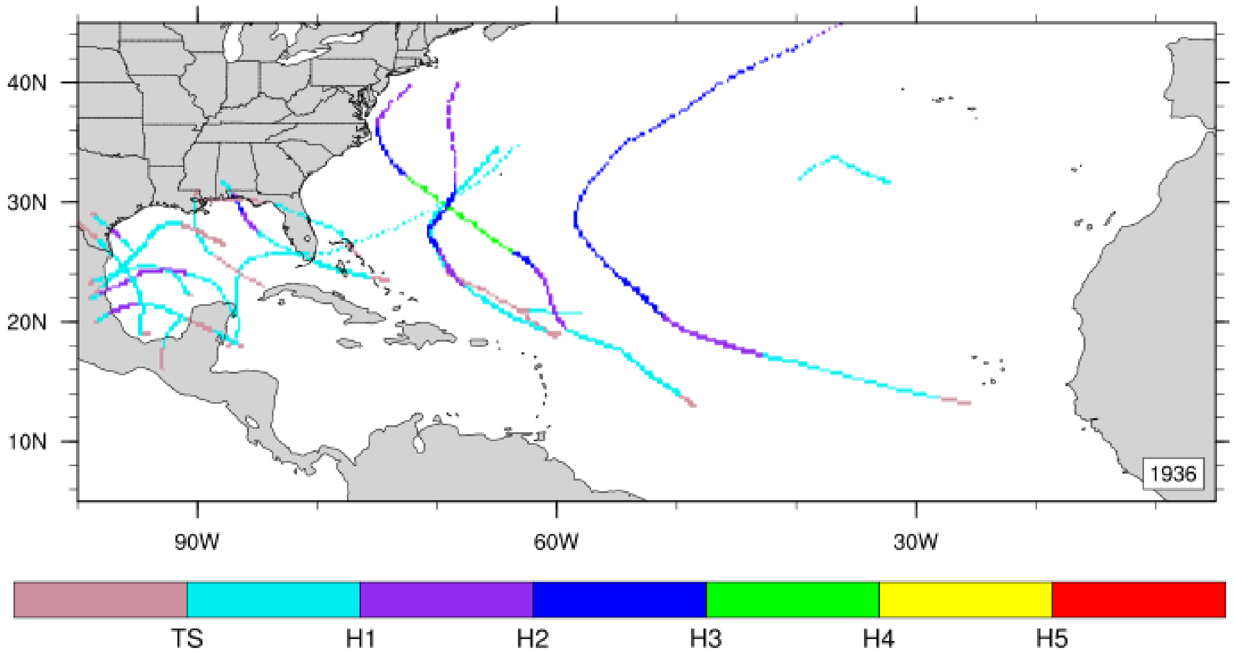

Hurricane Season 1937

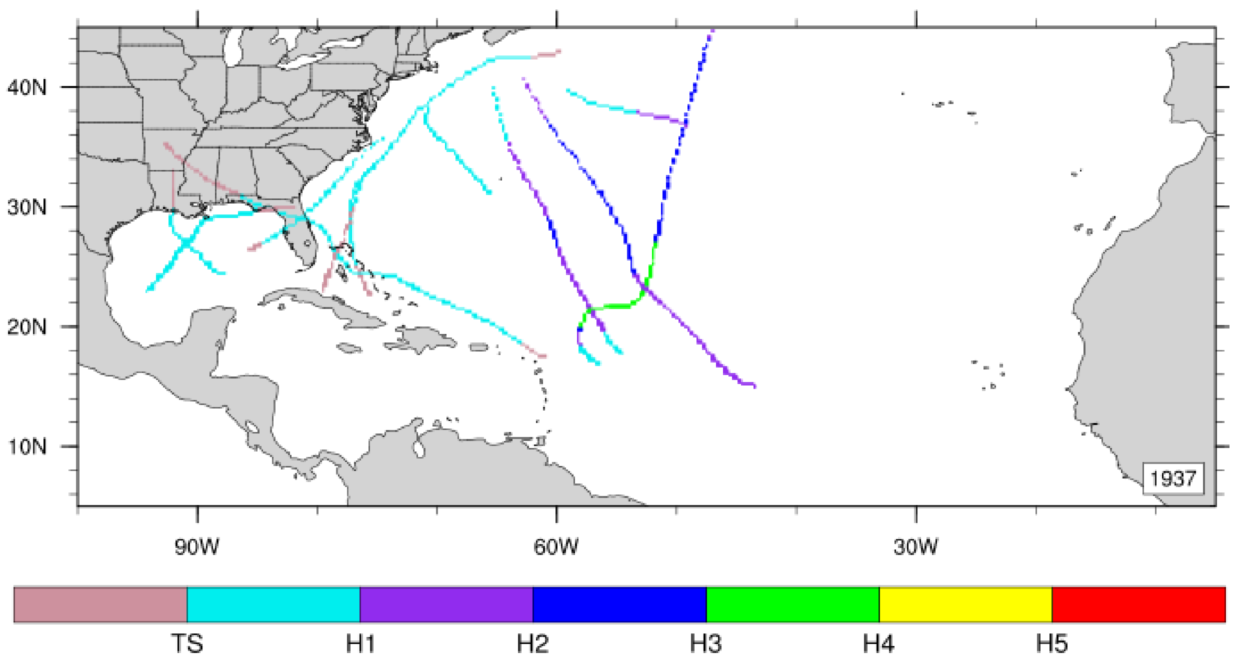

Hurricane Season 1938

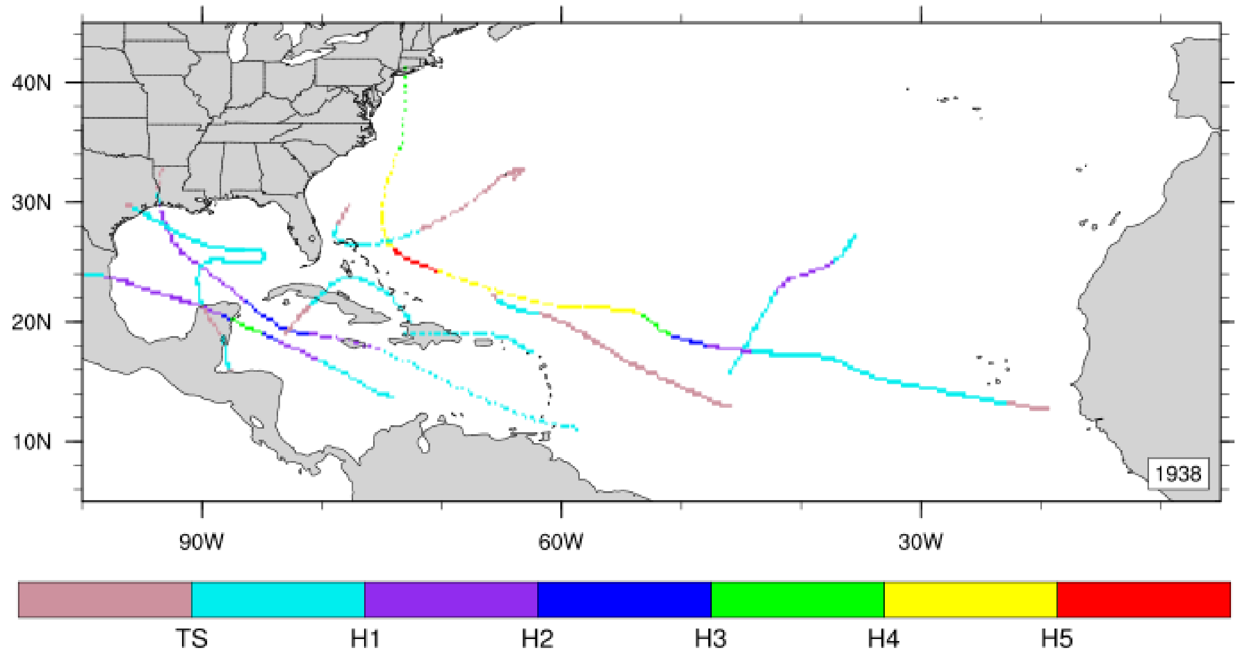

Hurricane Season 1939

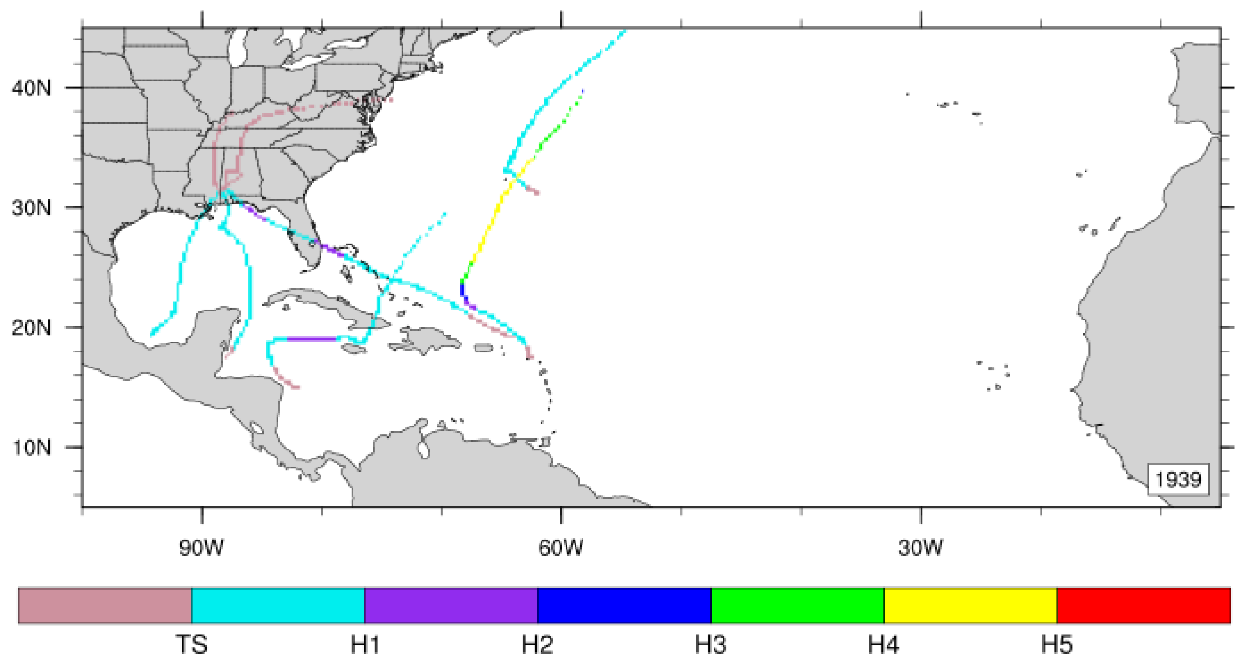

Hurricane Season 1940

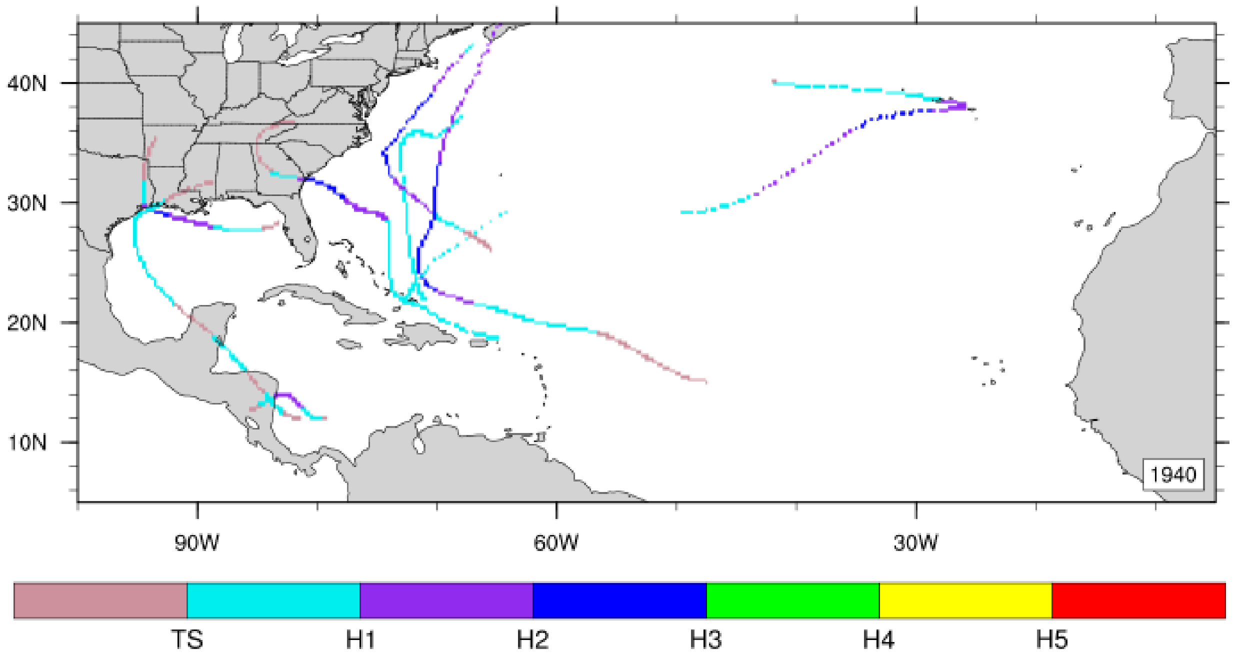

Hurricane Season 1941

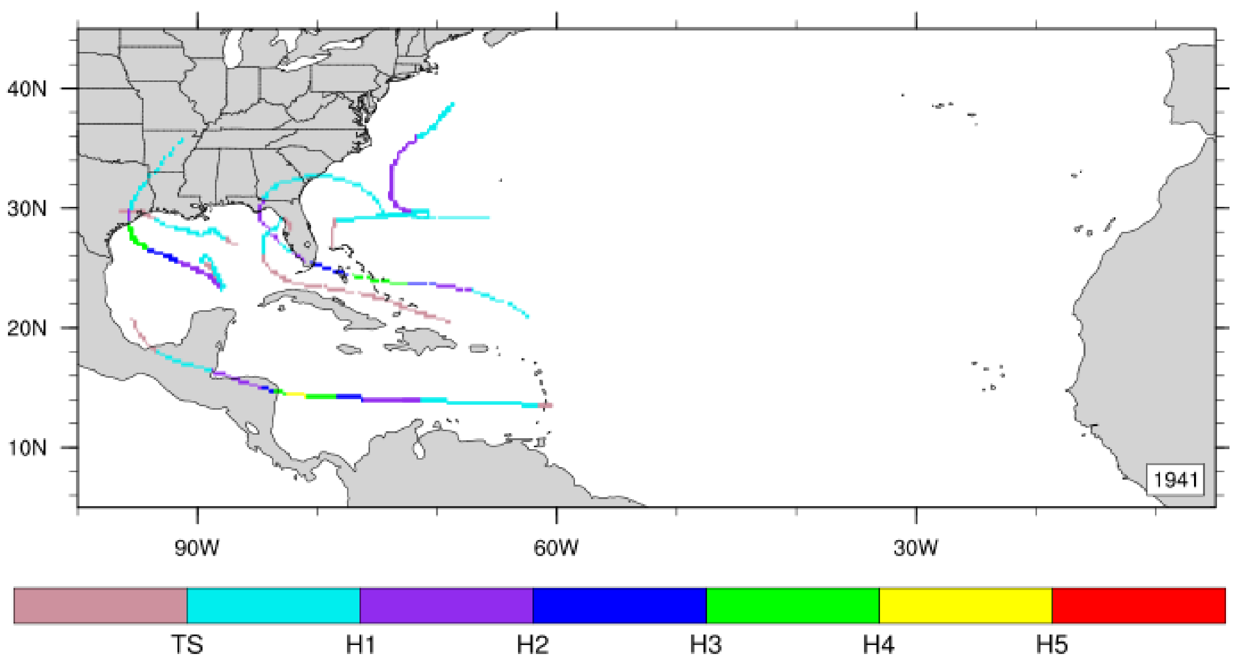

Hurricane Season 1942

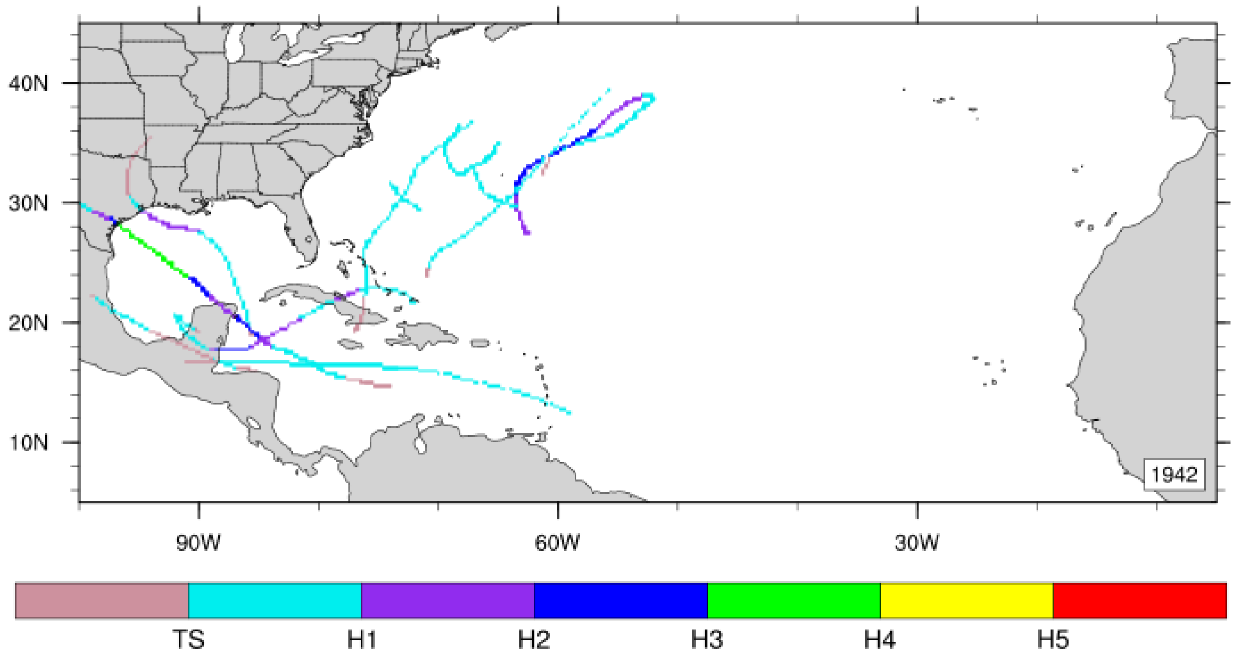

Hurricane Season 1943

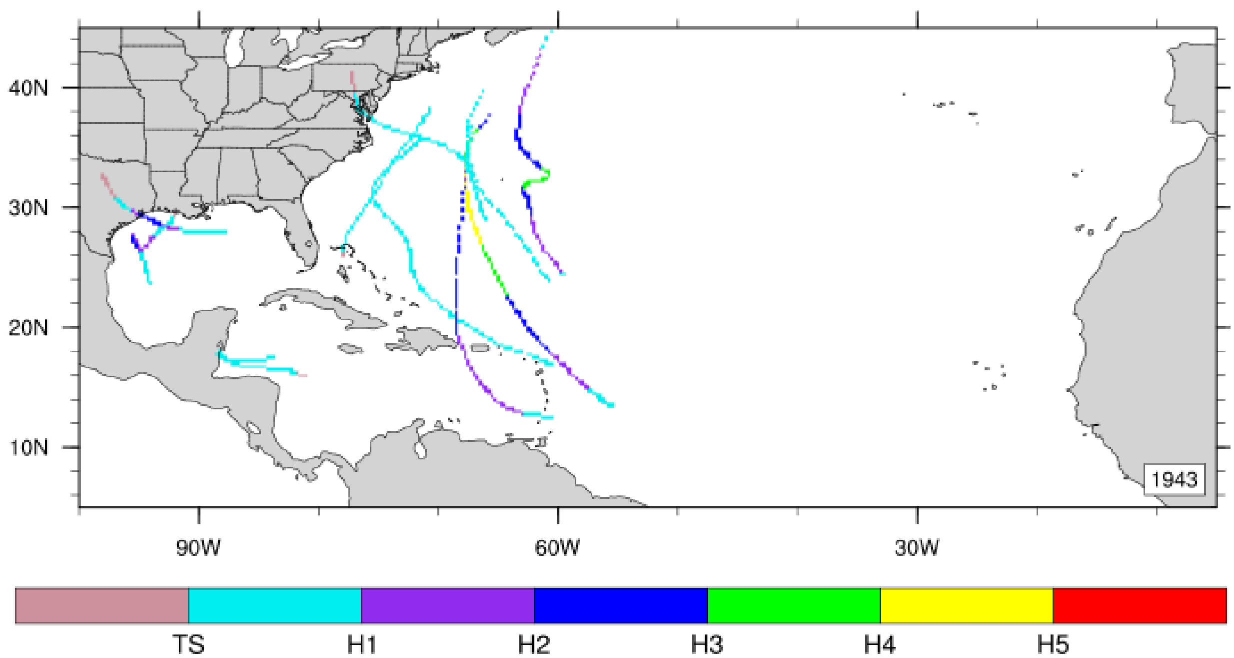

Hurricane Season 1944

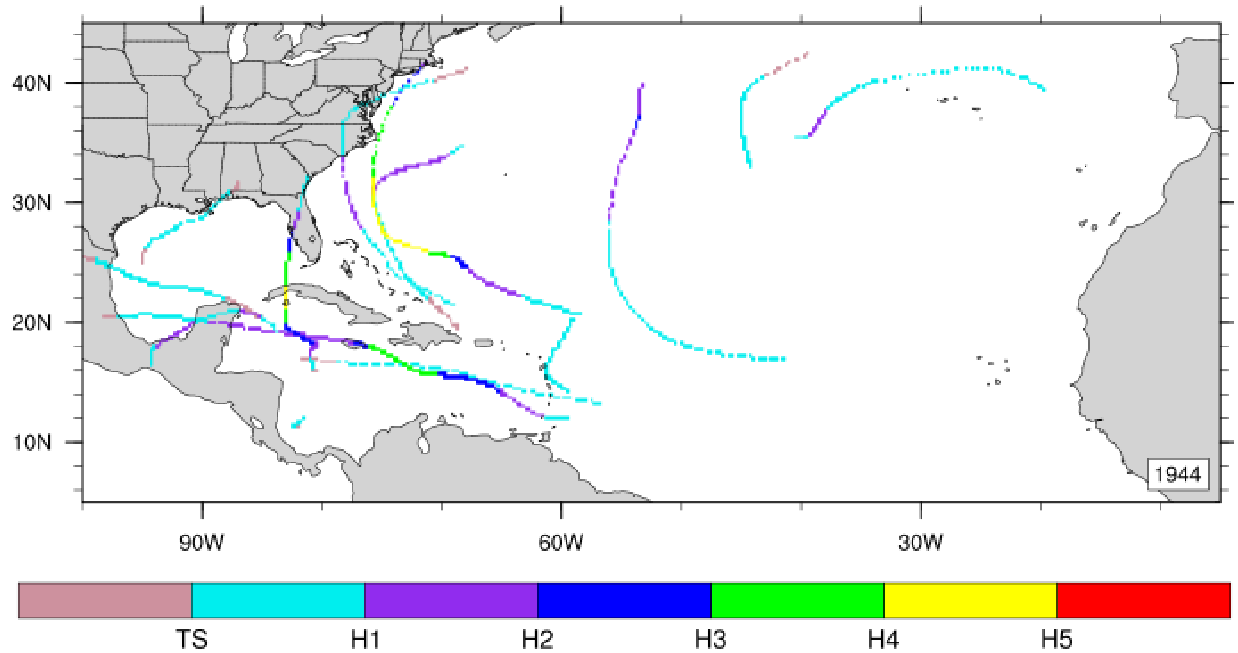

Hurricane Season 1945

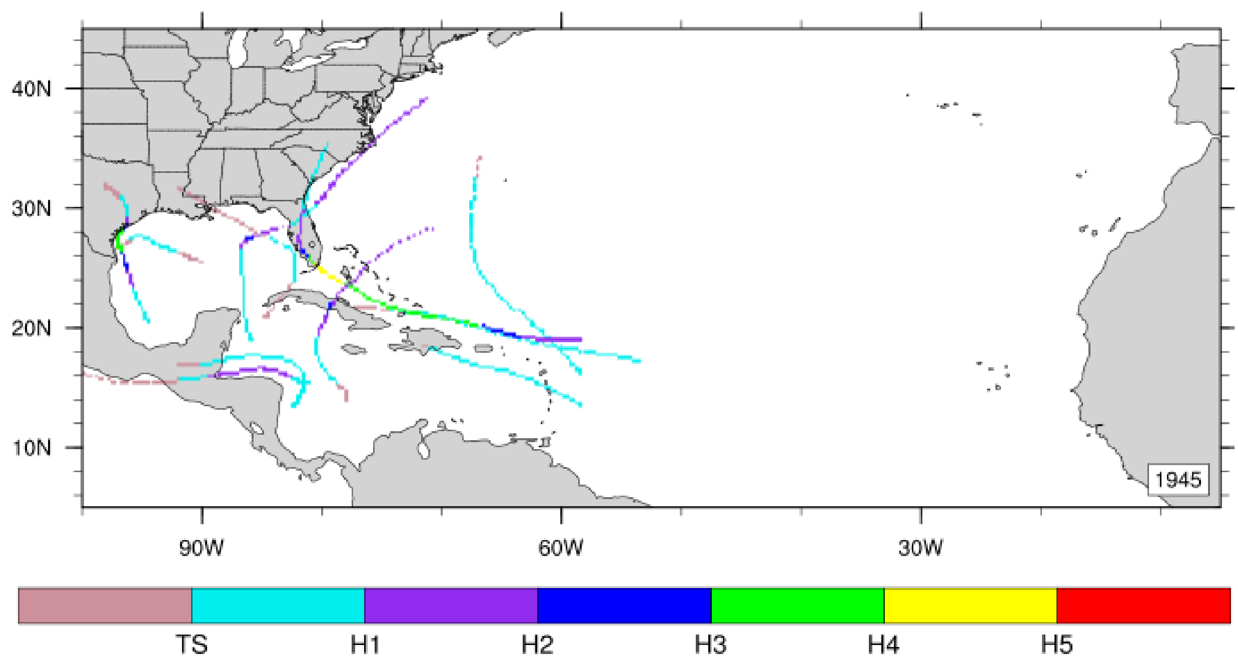

Hurricane Season 1946

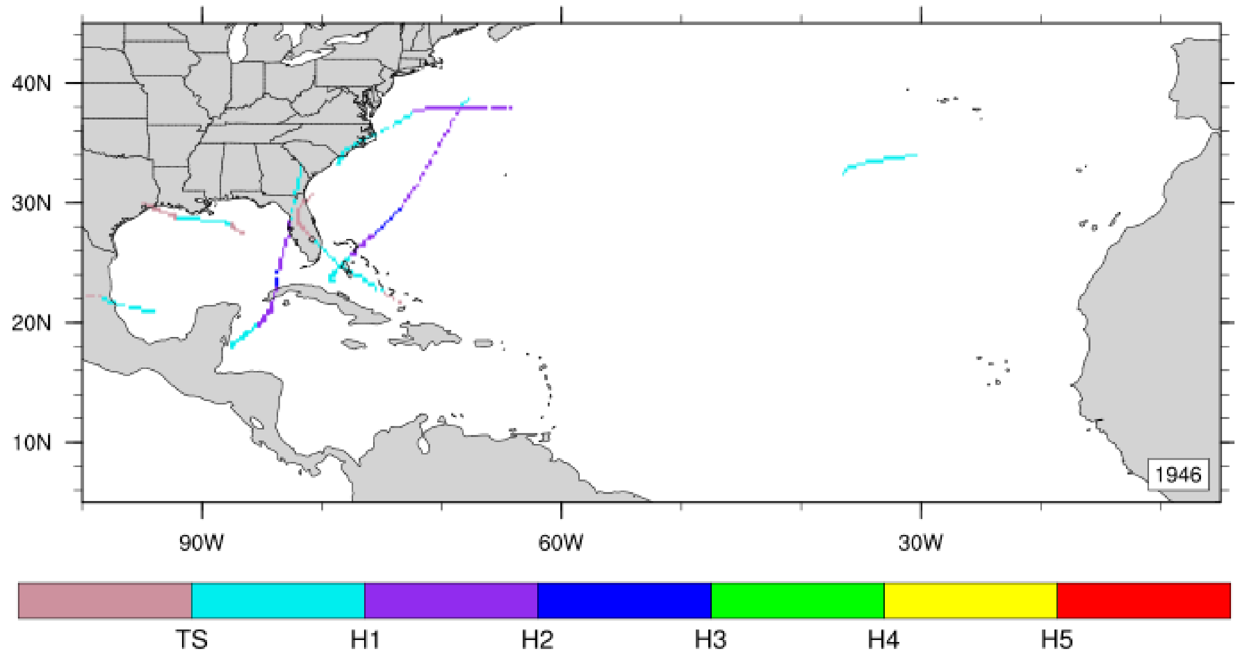

Hurricane Season 1947

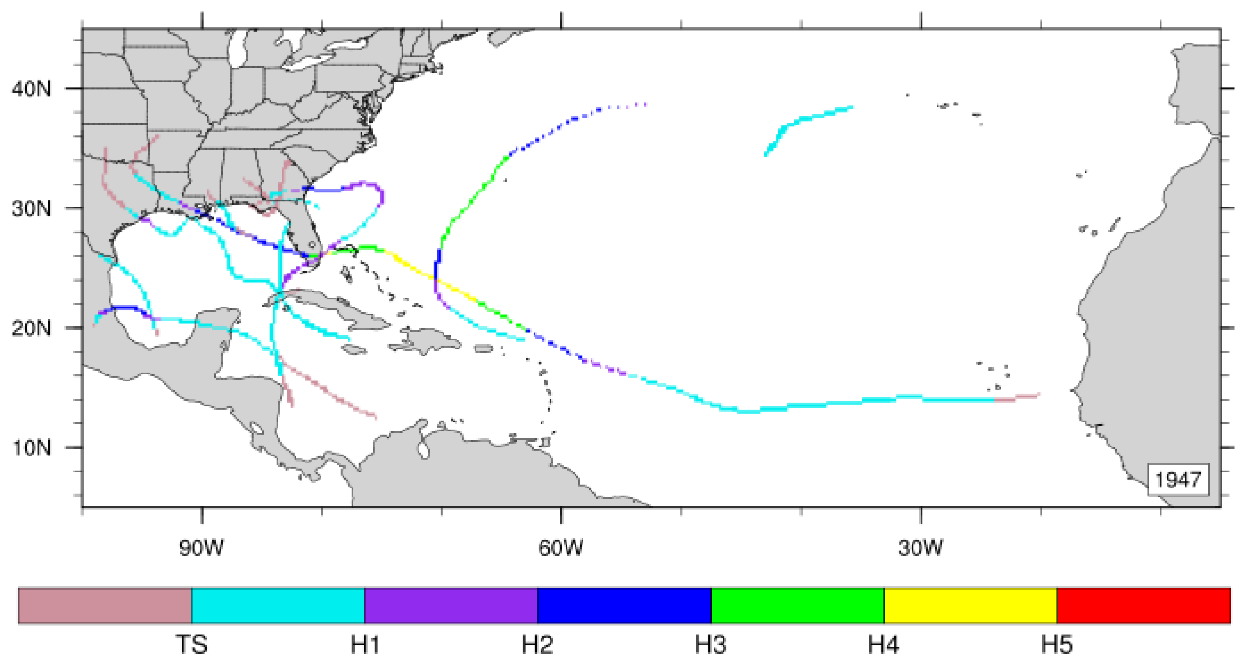

Hurricane Season 1948

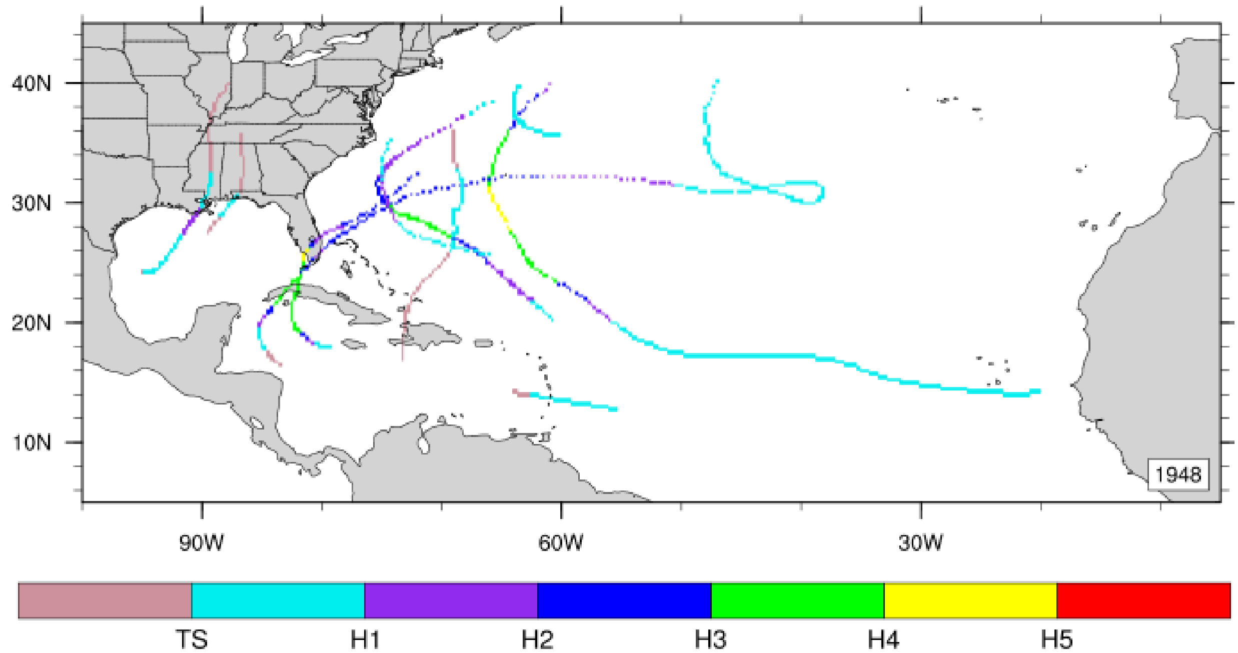

Hurricane Season 1949

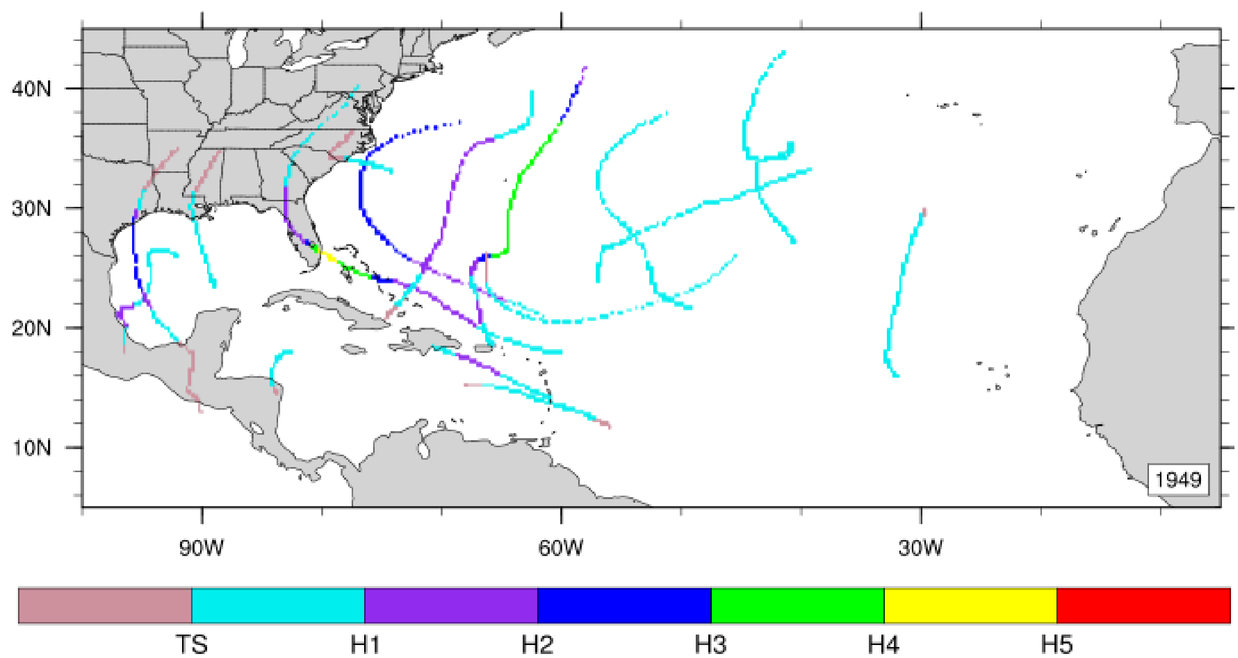

Hurricane Season 1950

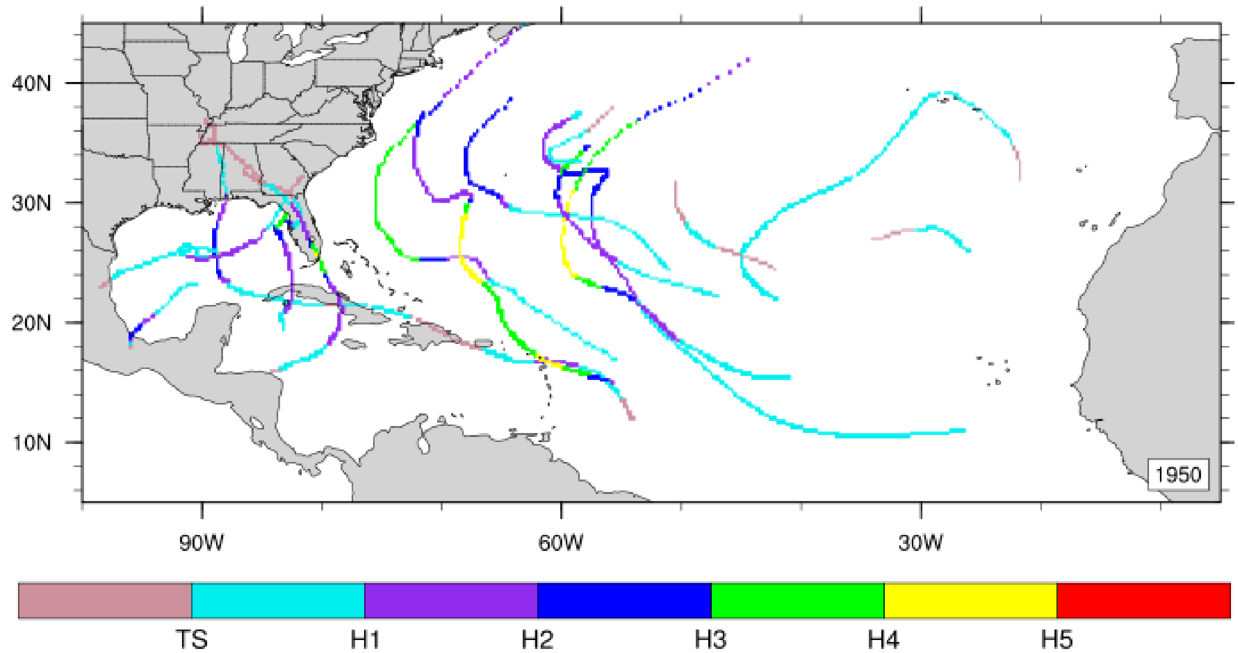

Hurricane Season 1951

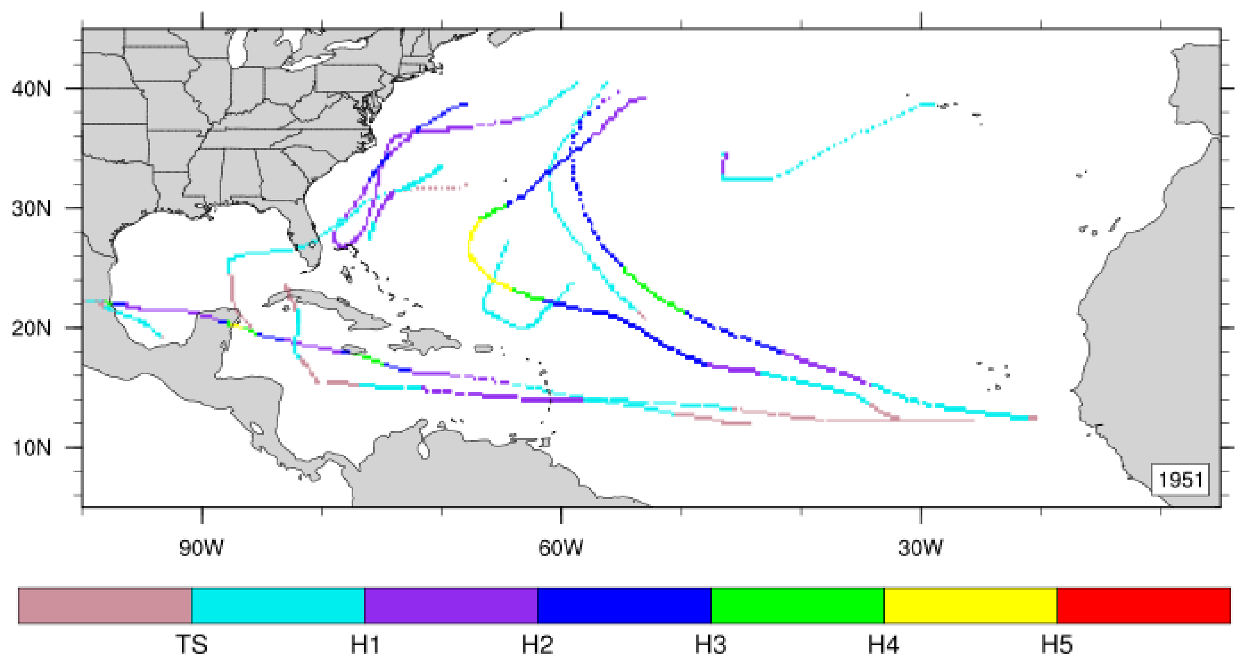

Hurricane Season 1952

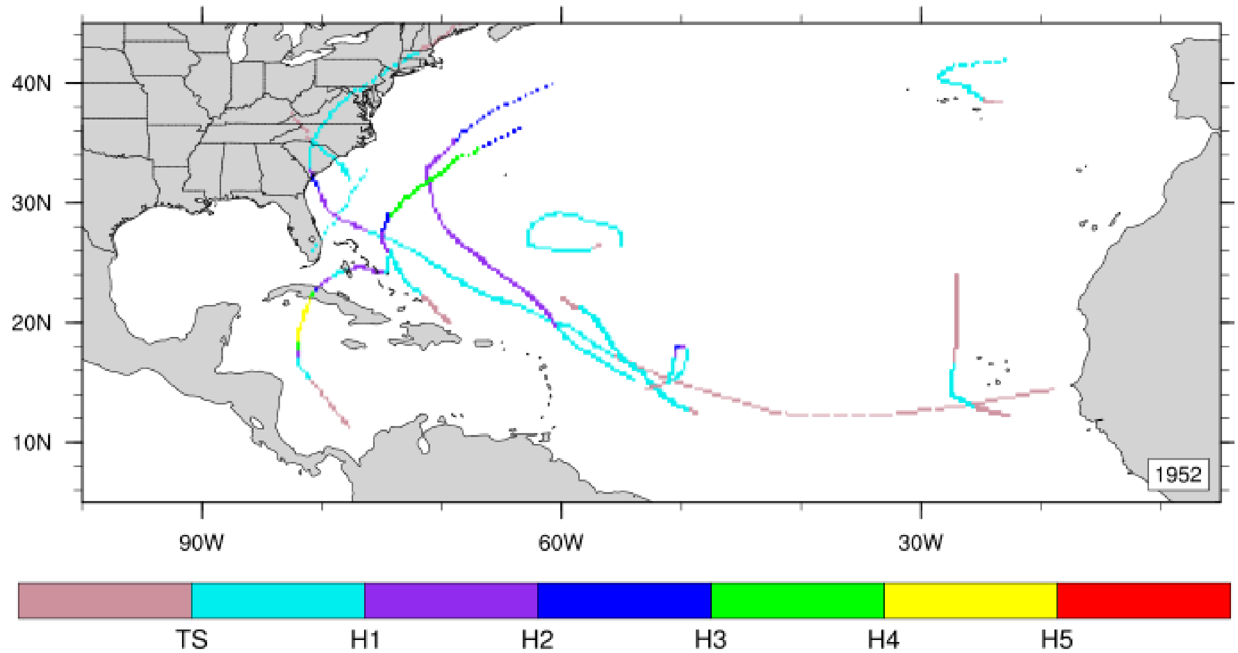

Hurricane Season 1953

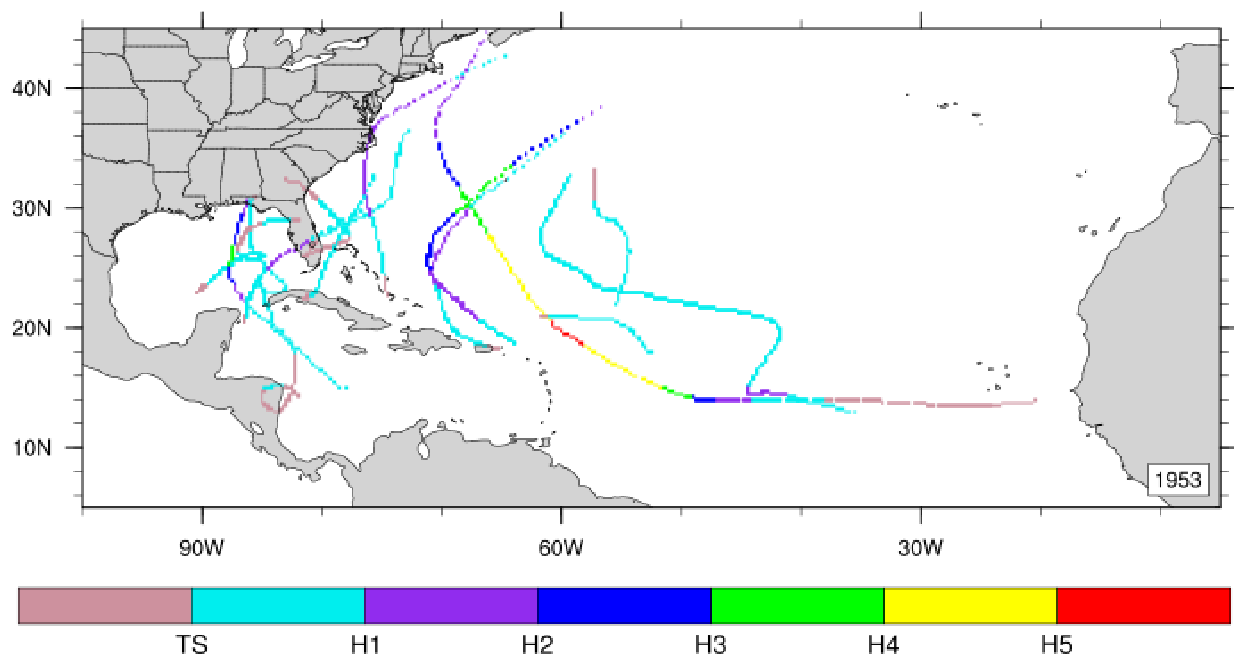

Hurricane Season 1954

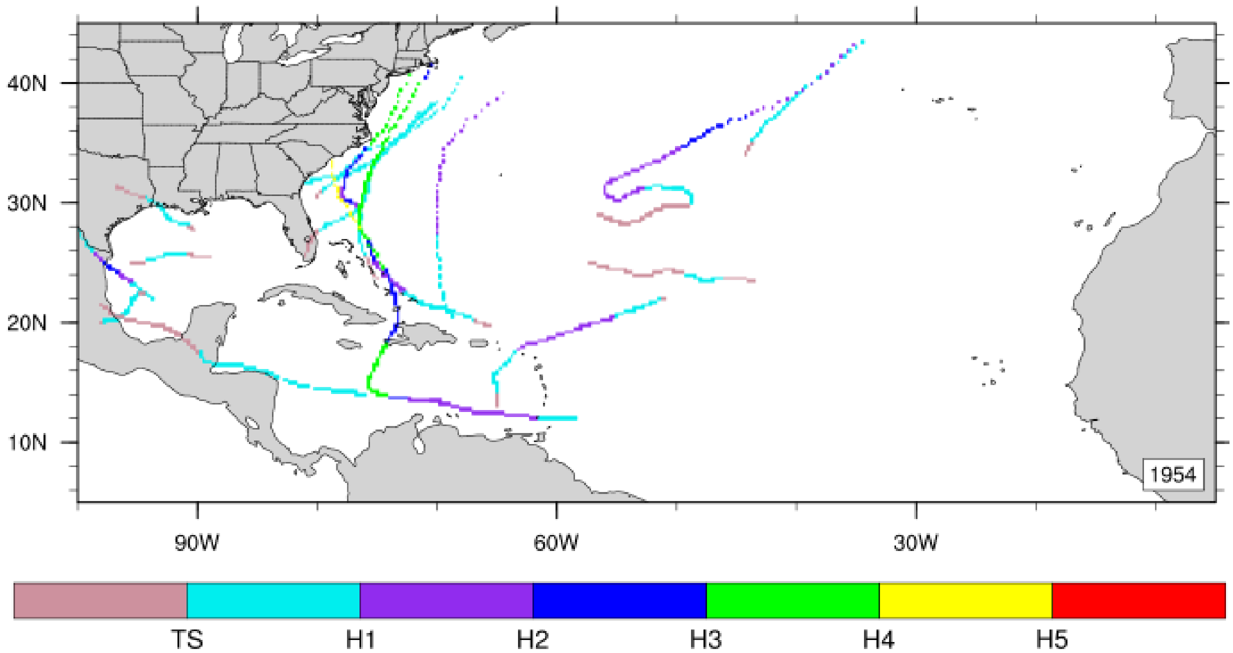

Hurricane Season 1955

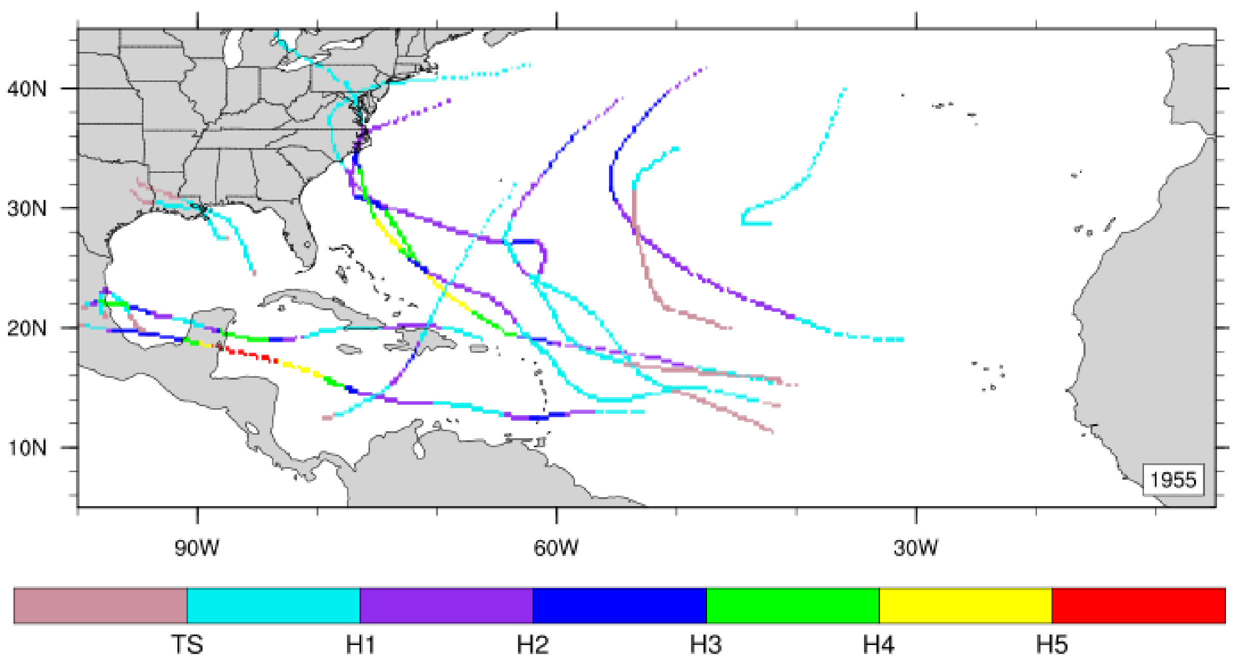

Hurricane Season 1956

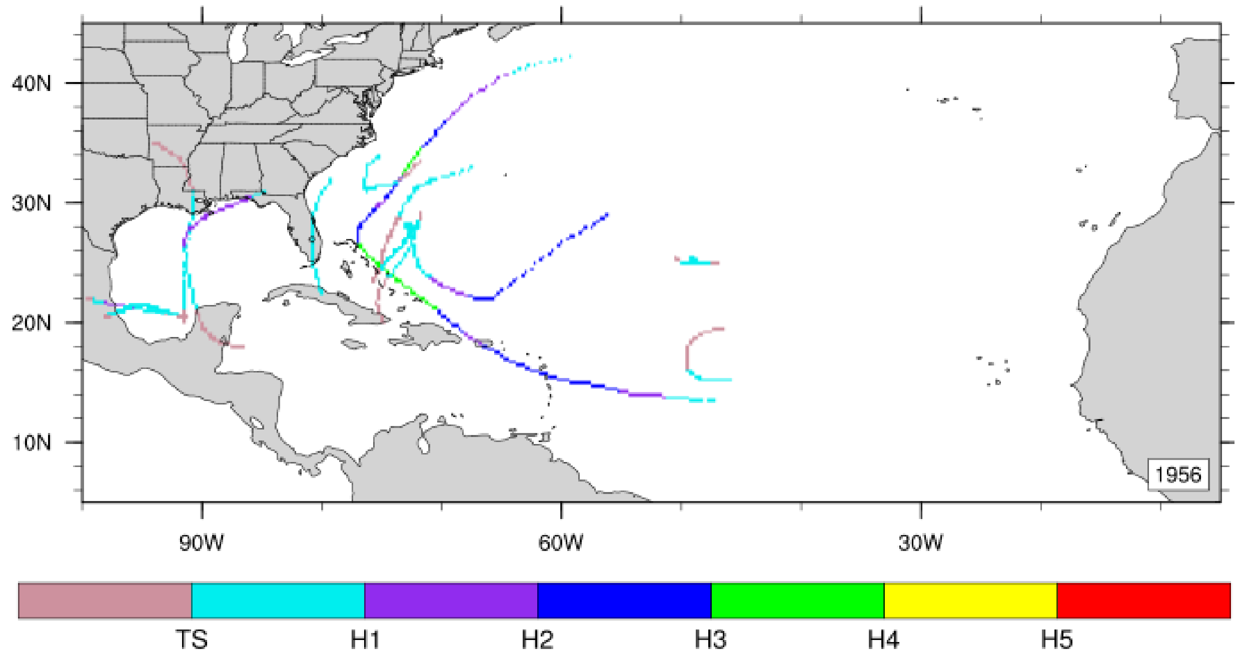

Hurricane Season 1957

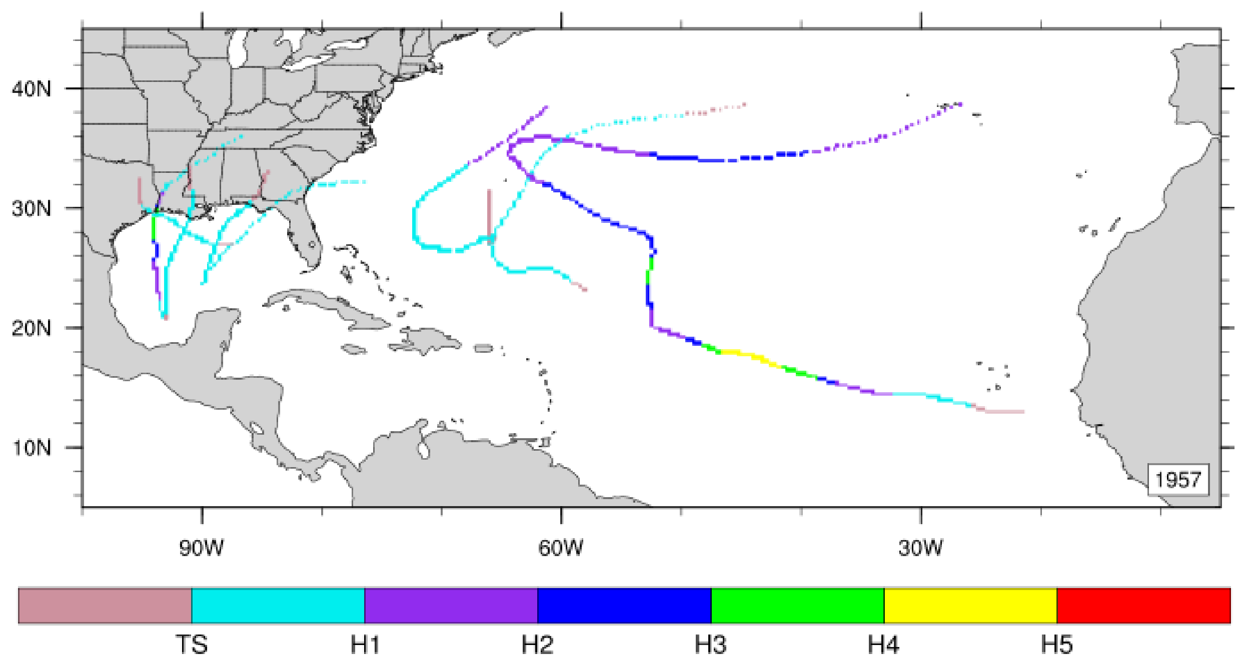

Hurricane Season 1958

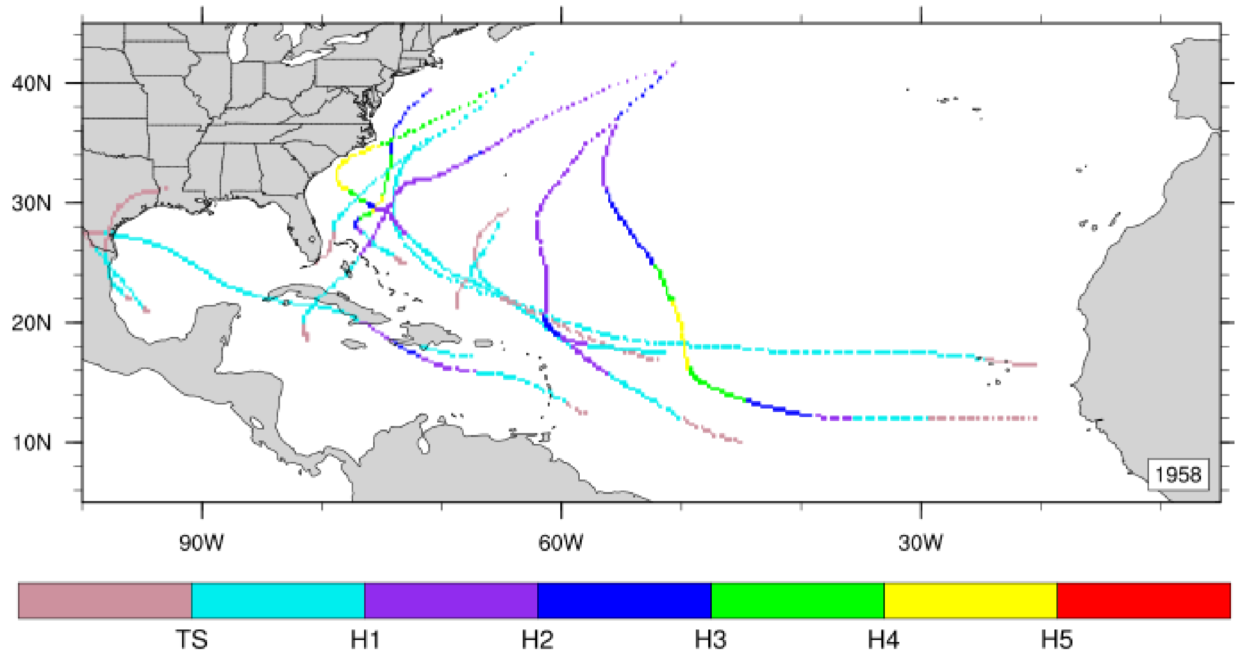

Hurricane Season 1959

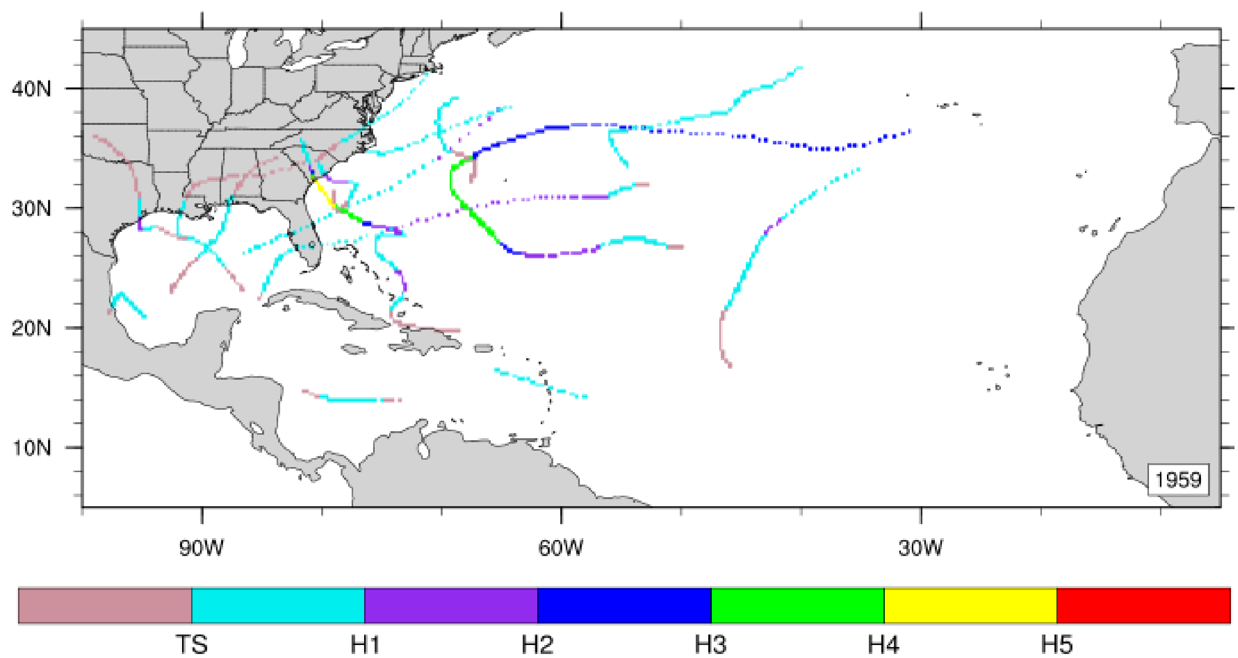

Hurricane Season 1960

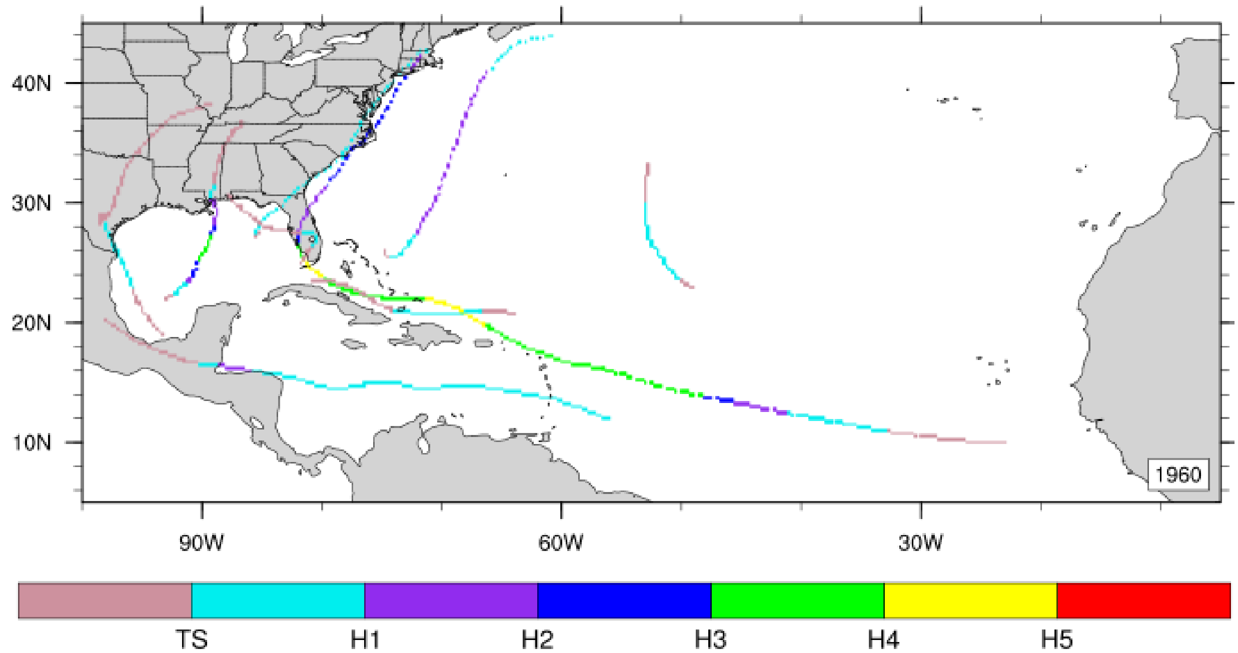

Hurricane Season 1961

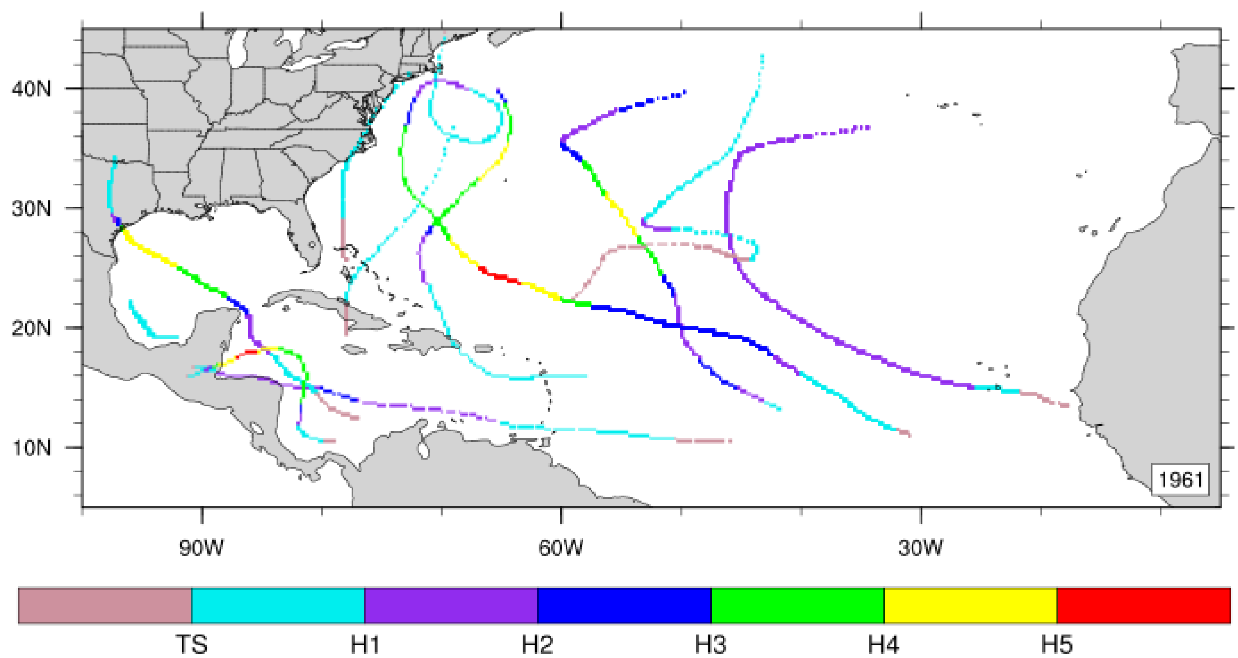

Hurricane Season 1962

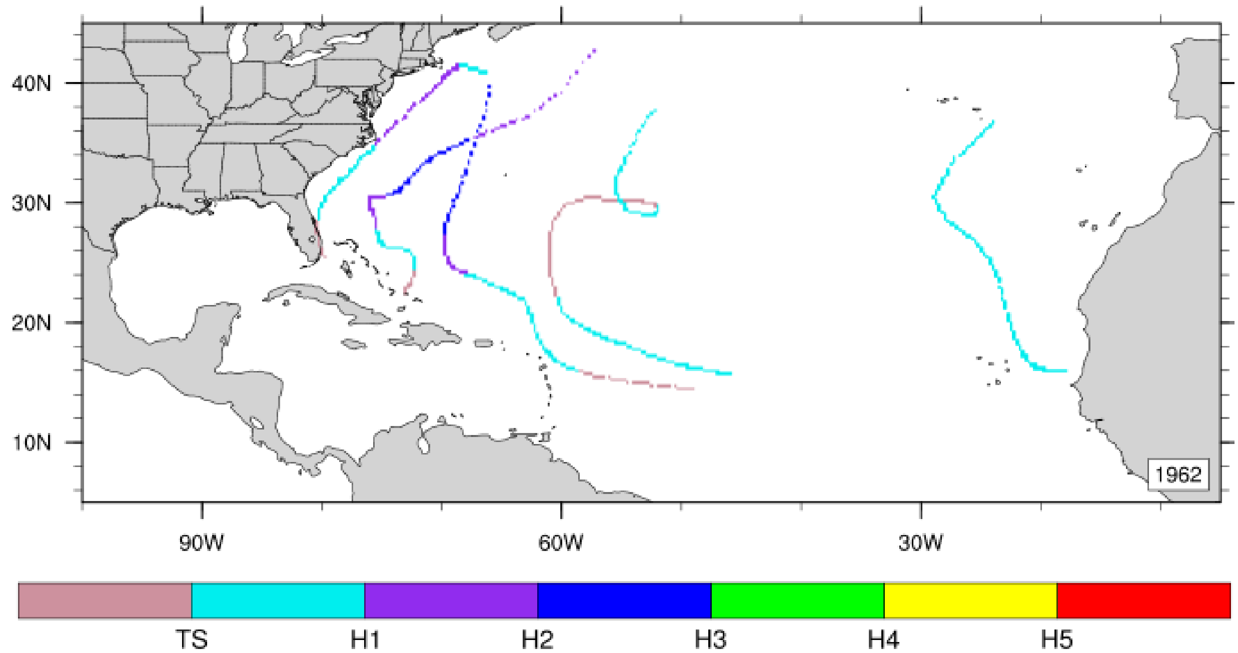

Hurricane Season 1963

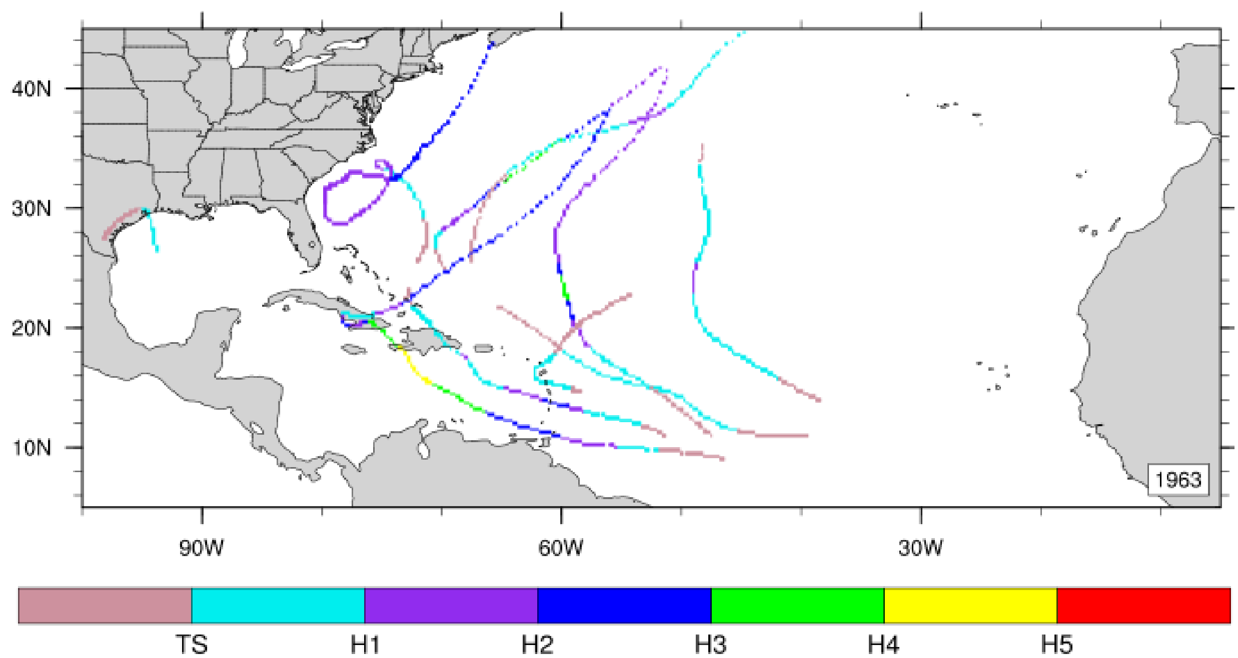

Hurricane Season 1964

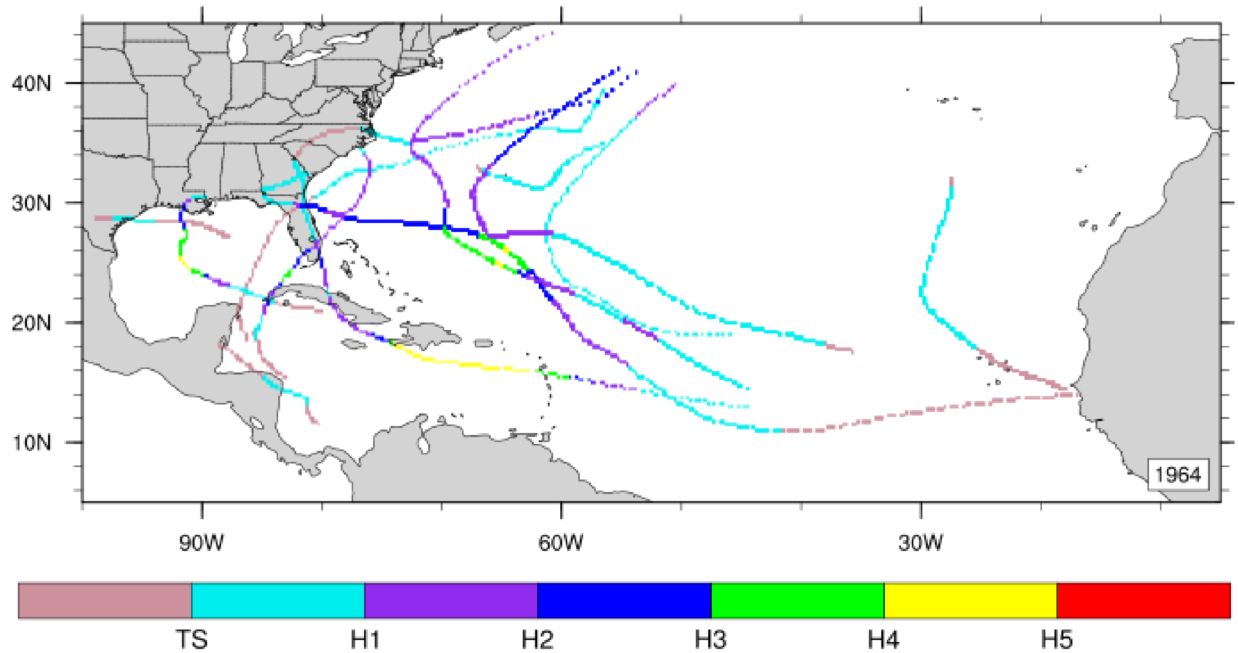

Hurricane Season 1965

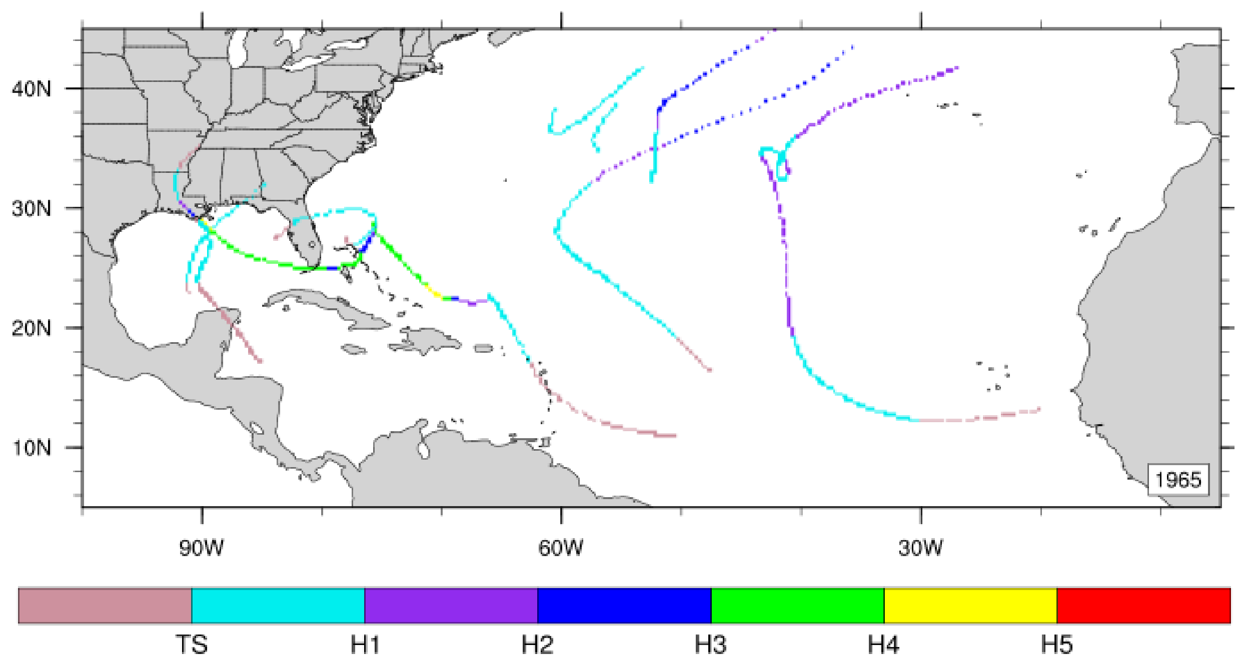

Hurricane Season 1966

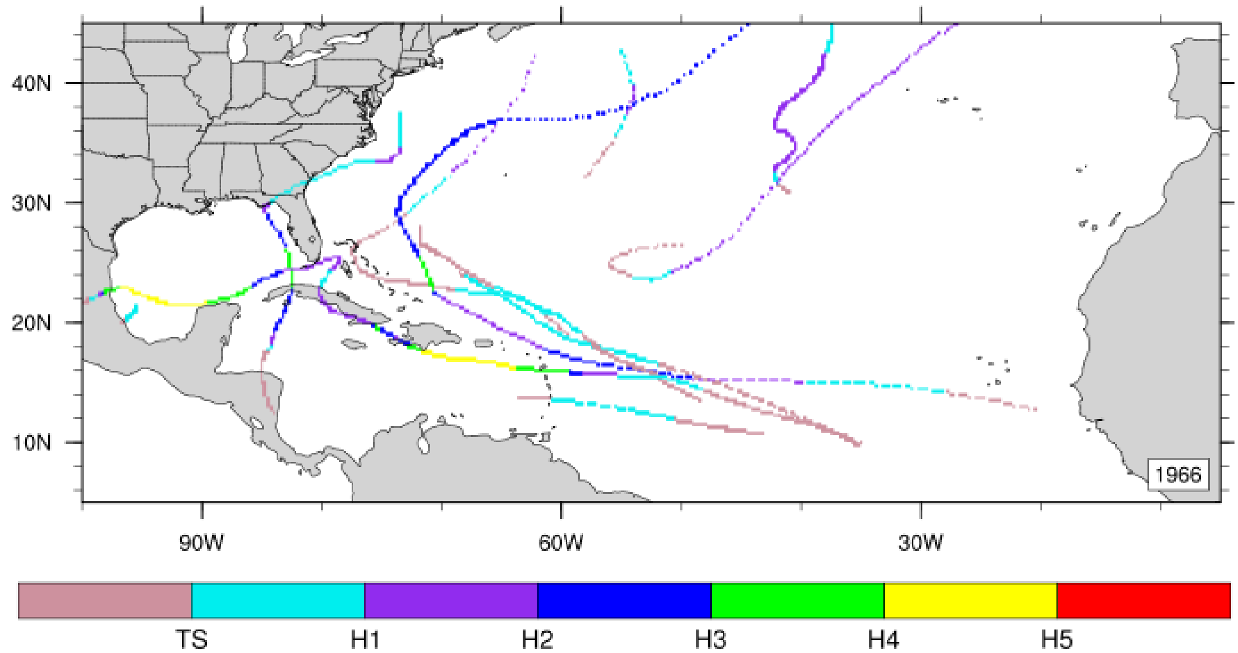

Hurricane Season 1967

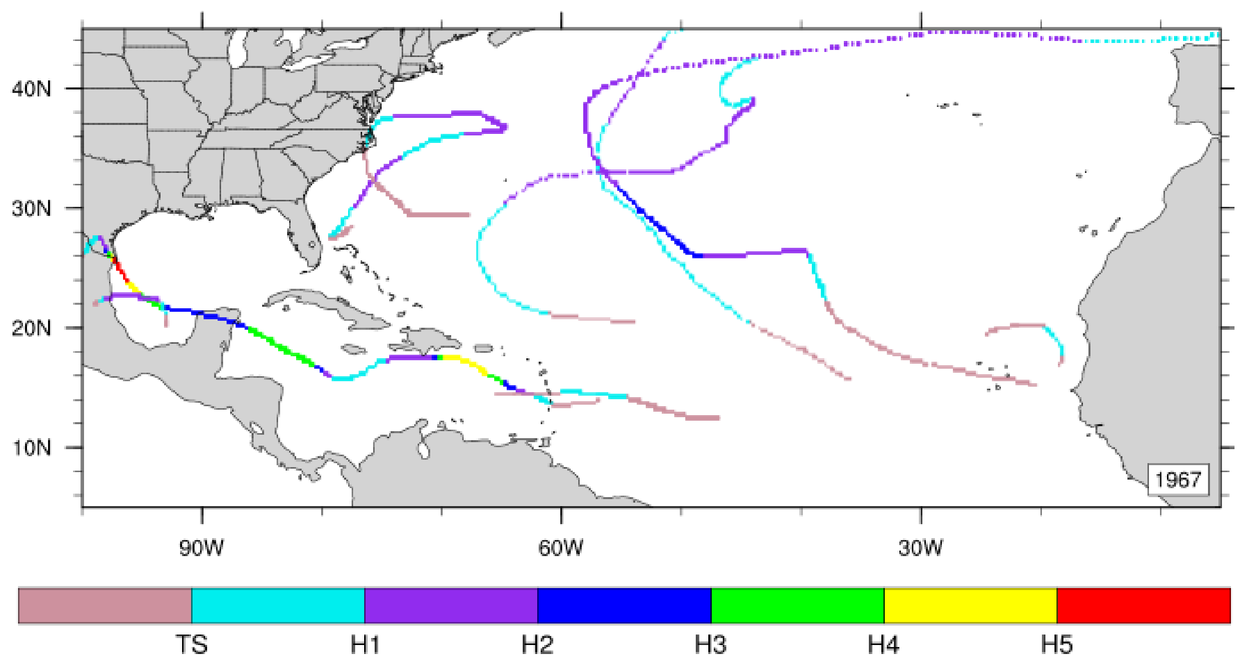

Hurricane Season 1968

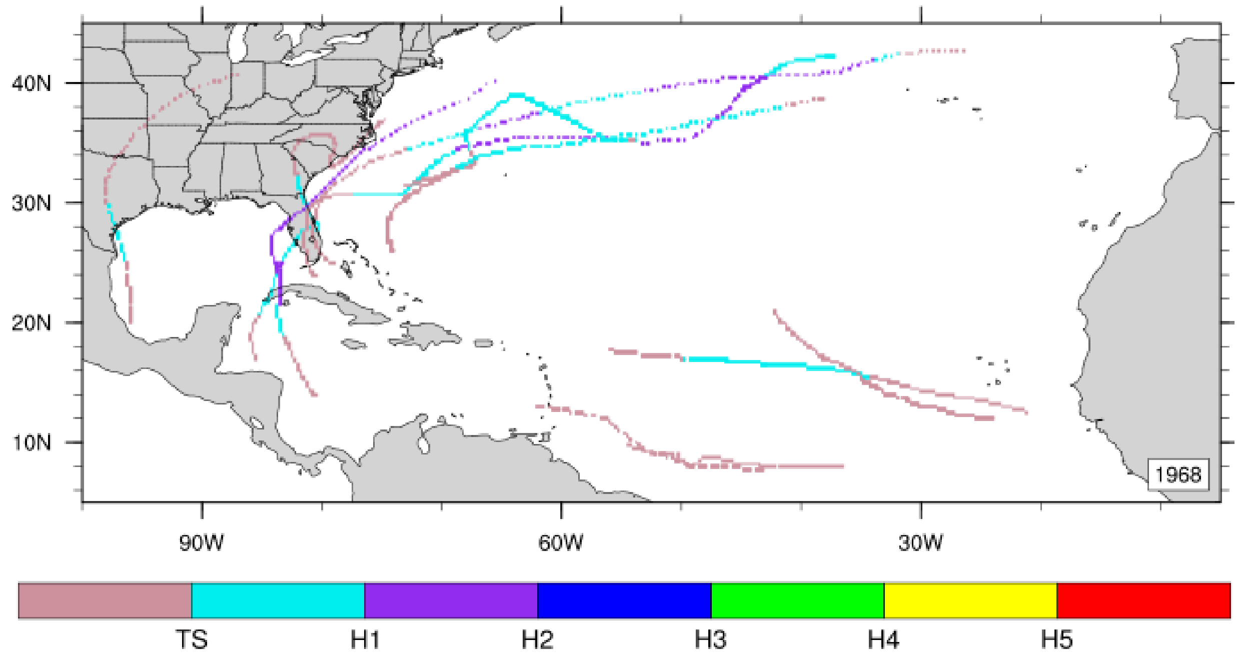

Hurricane Season 1969

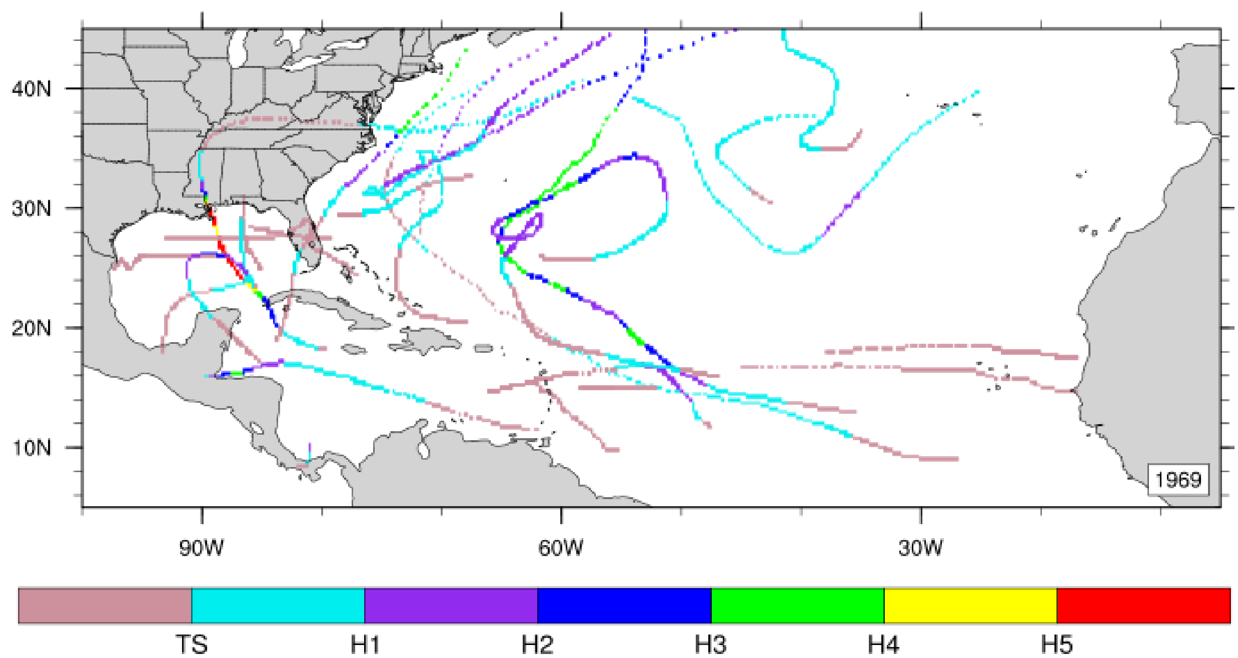

Hurricane Season 1970

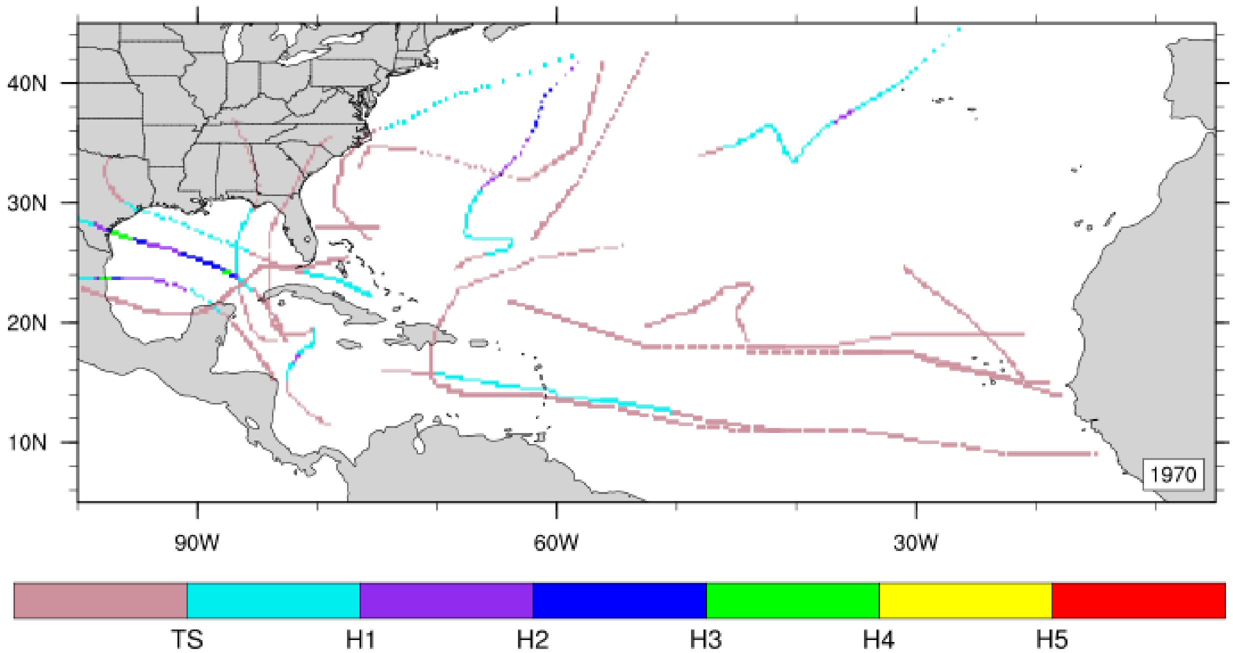

Hurricane Season 1971

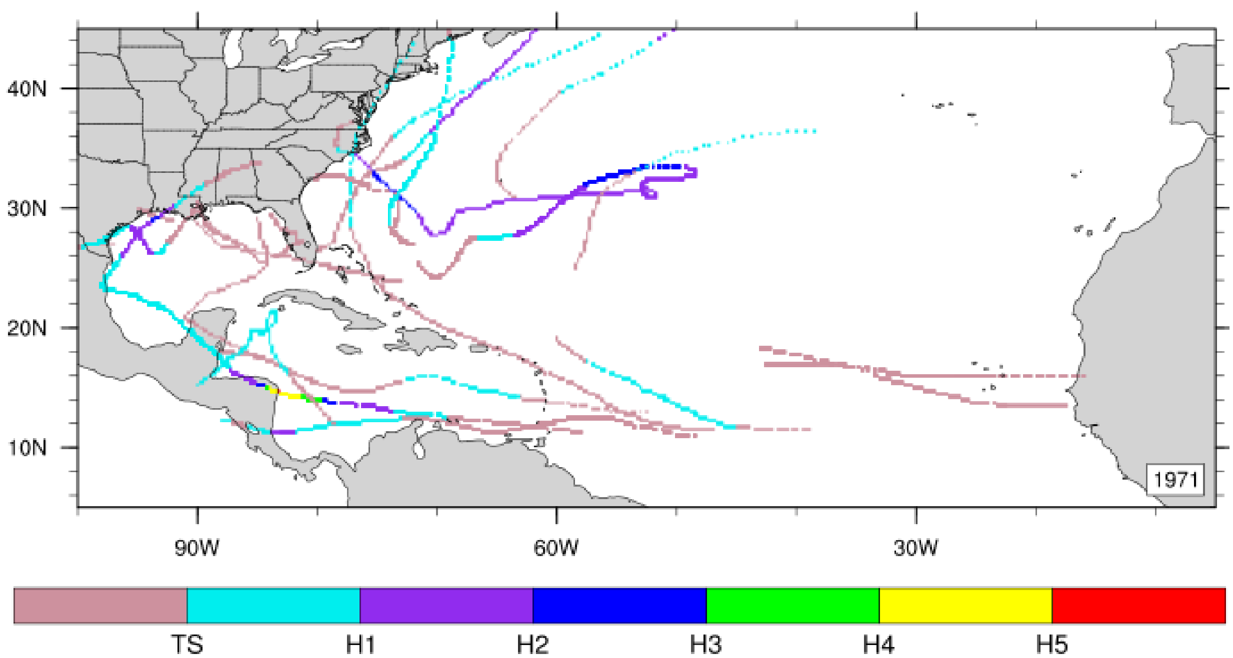

Hurricane Season 1972

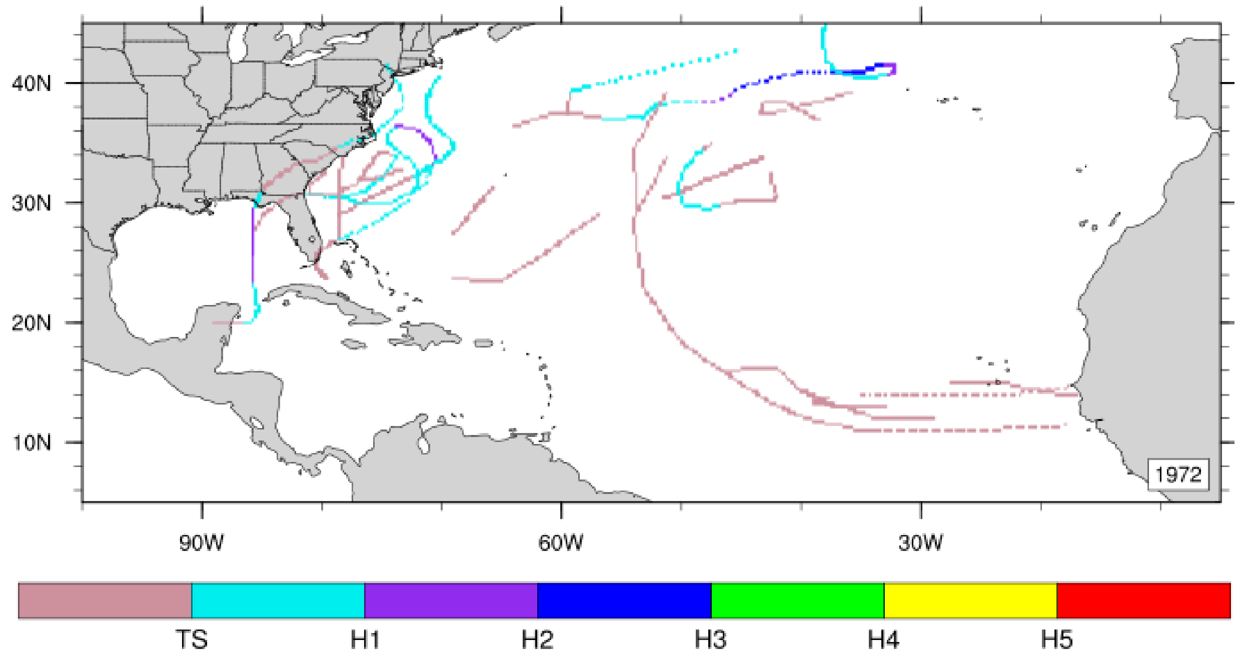

Hurricane Season 1973

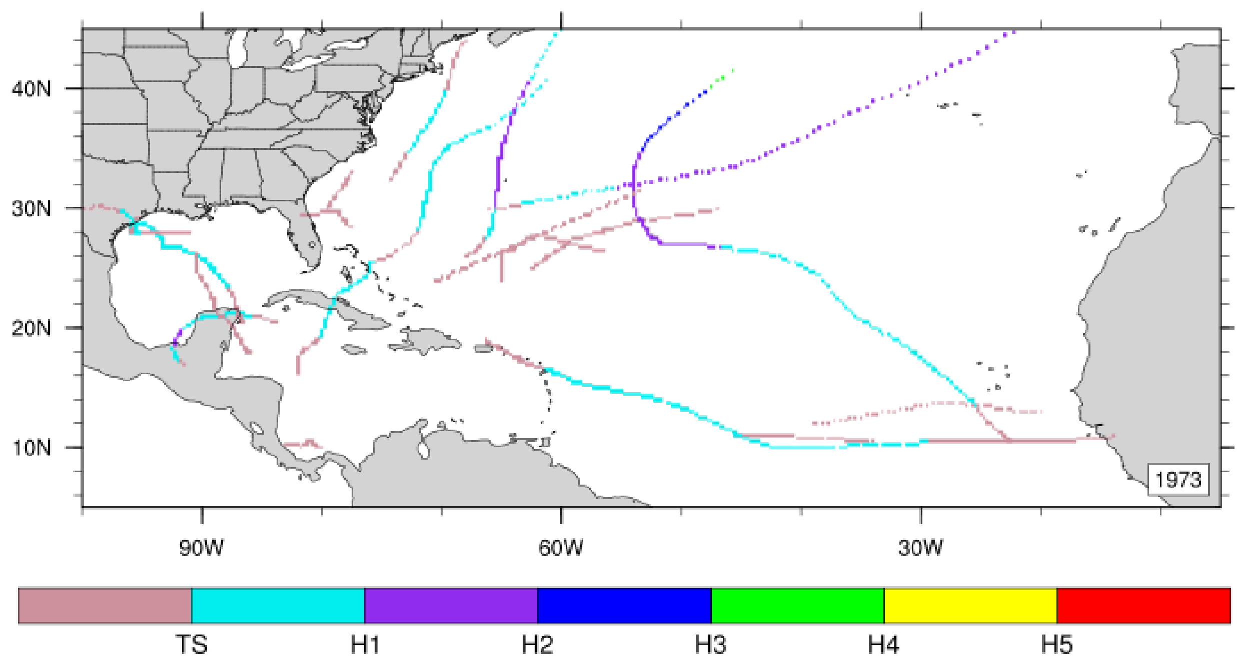

Hurricane Season 1974

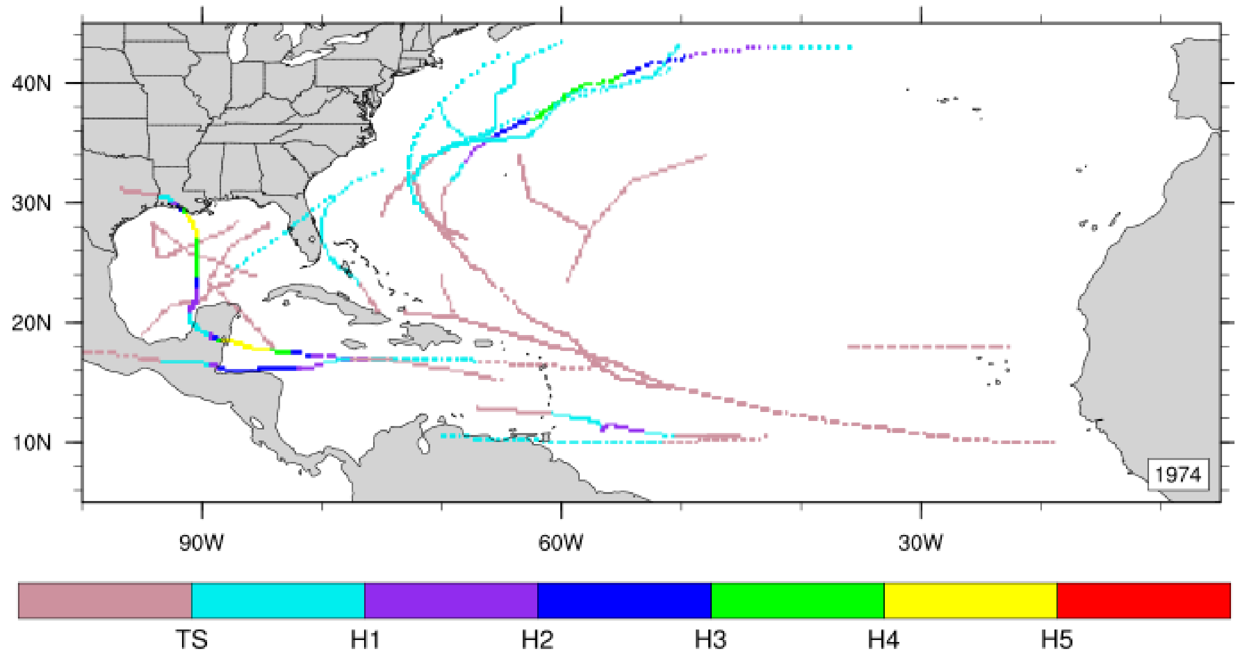

Hurricane Season 1975

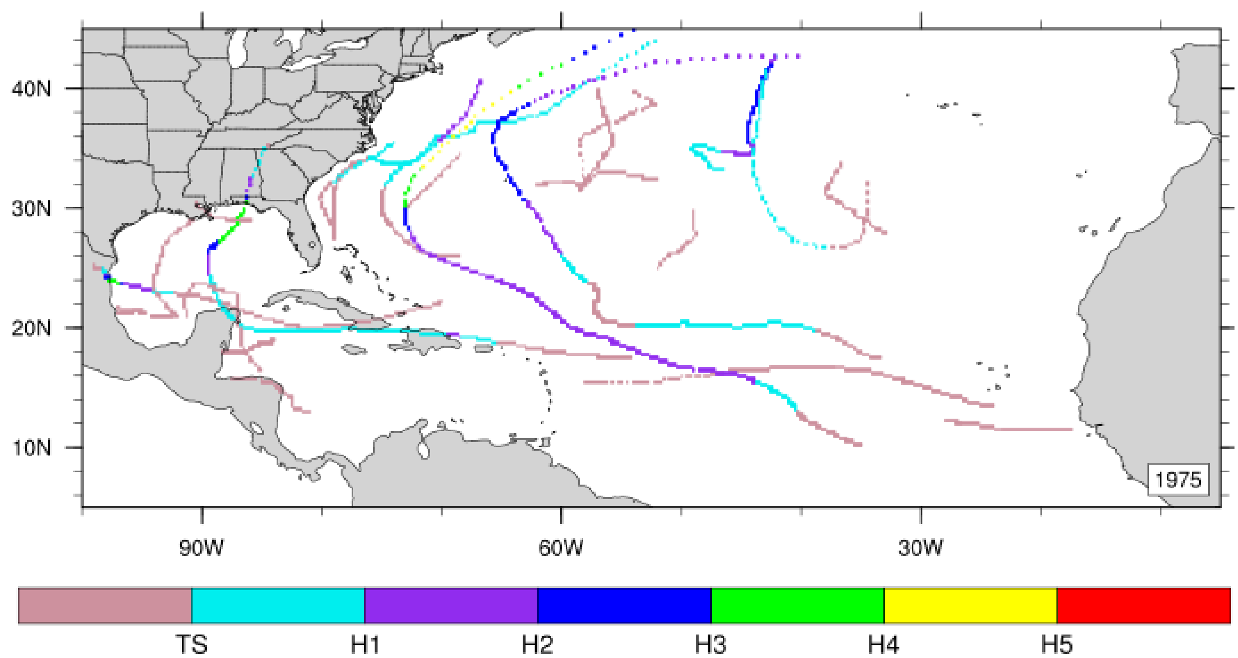

Hurricane Season 1976

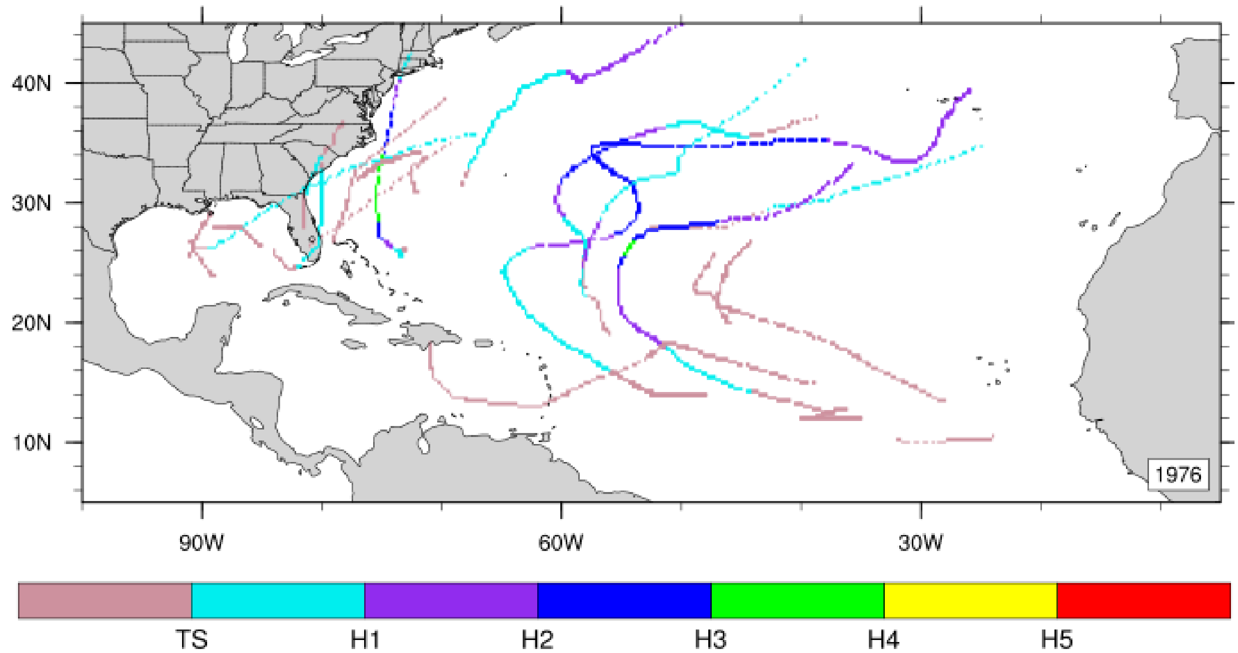

Hurricane Season 1977

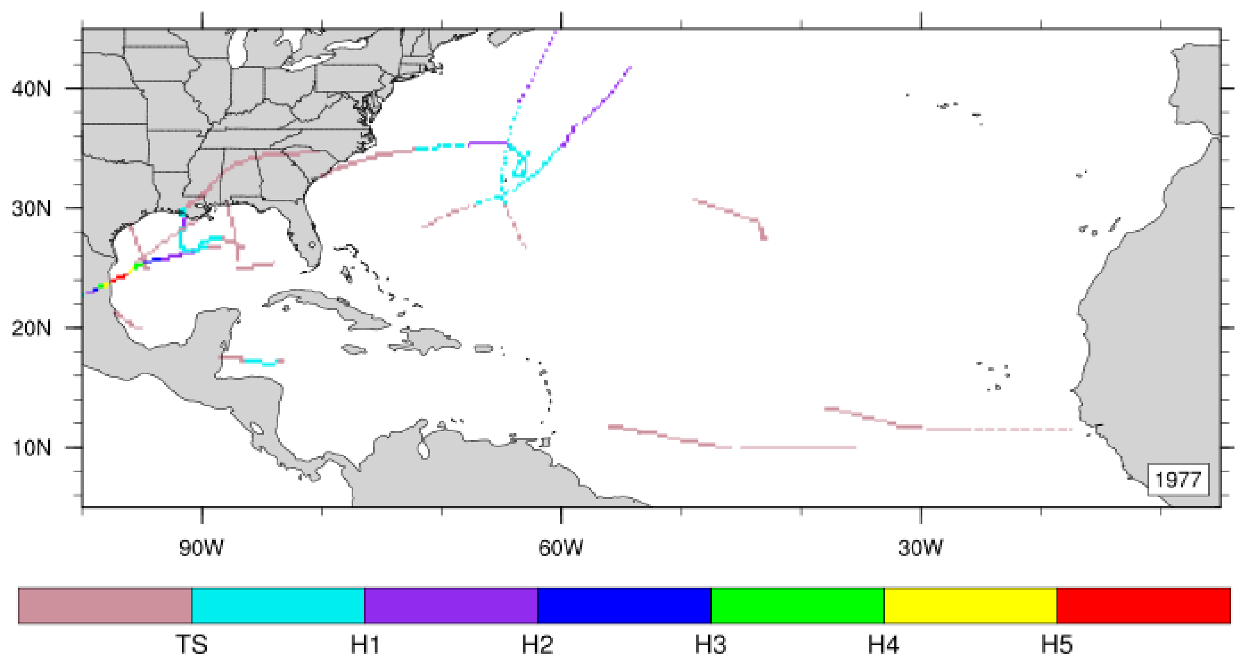

Hurricane Season 1978

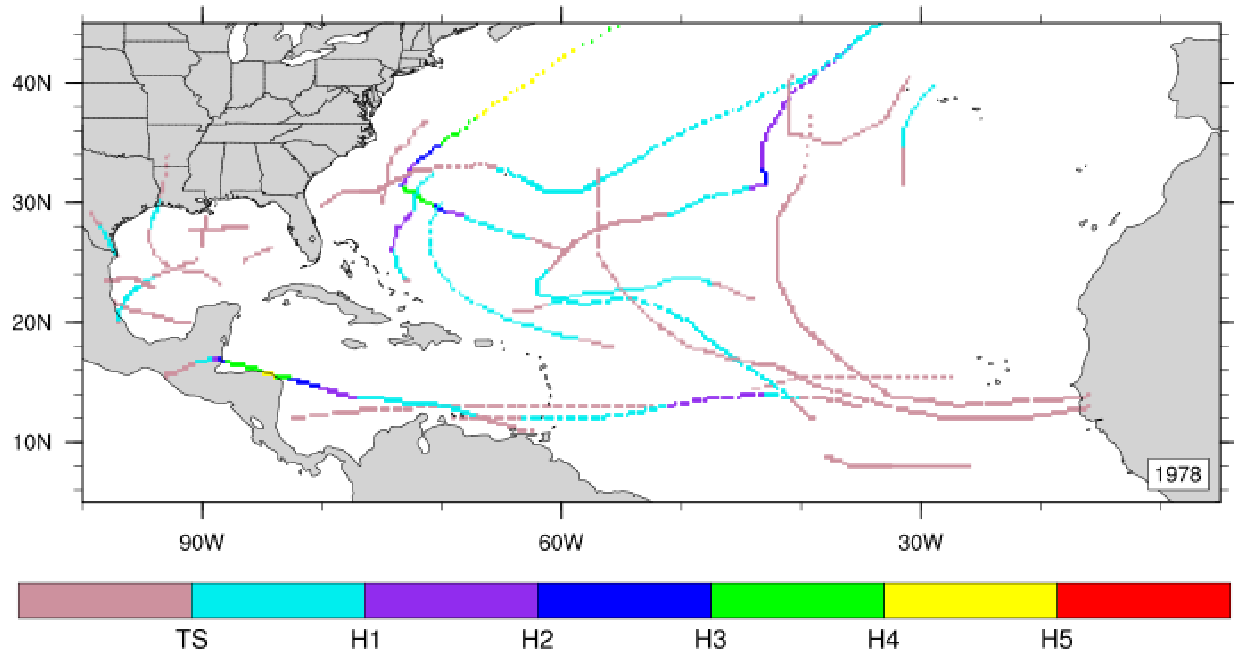

Hurricane Season 1979

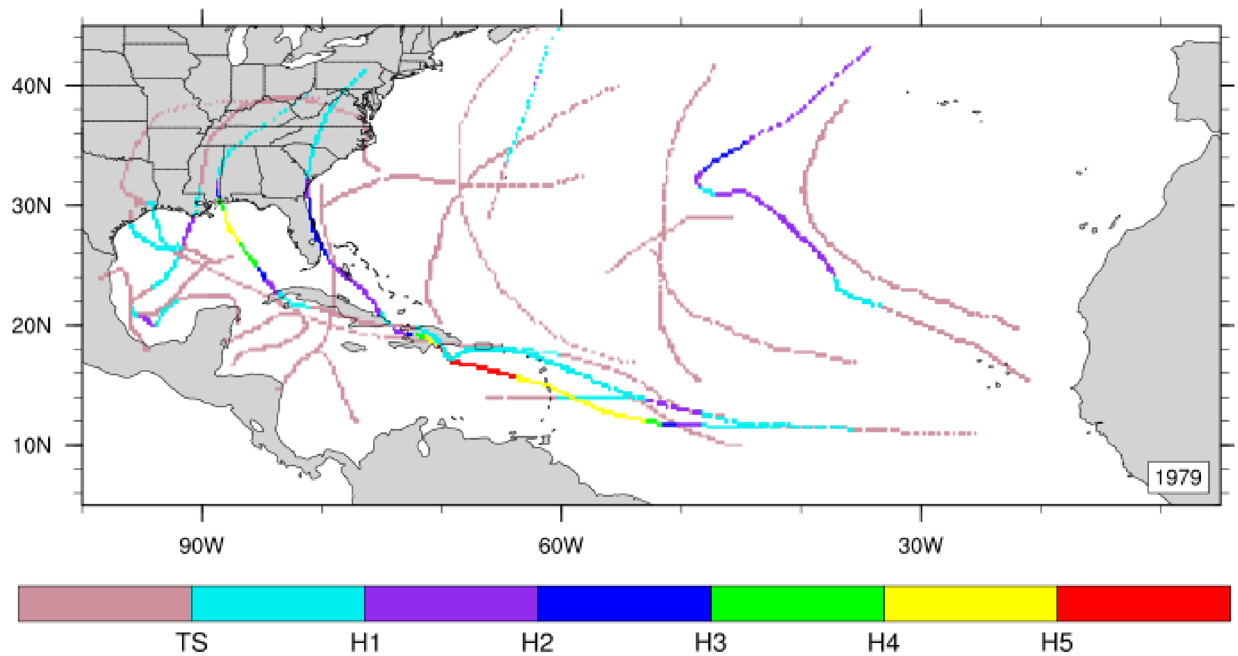

Hurricane Season 1980

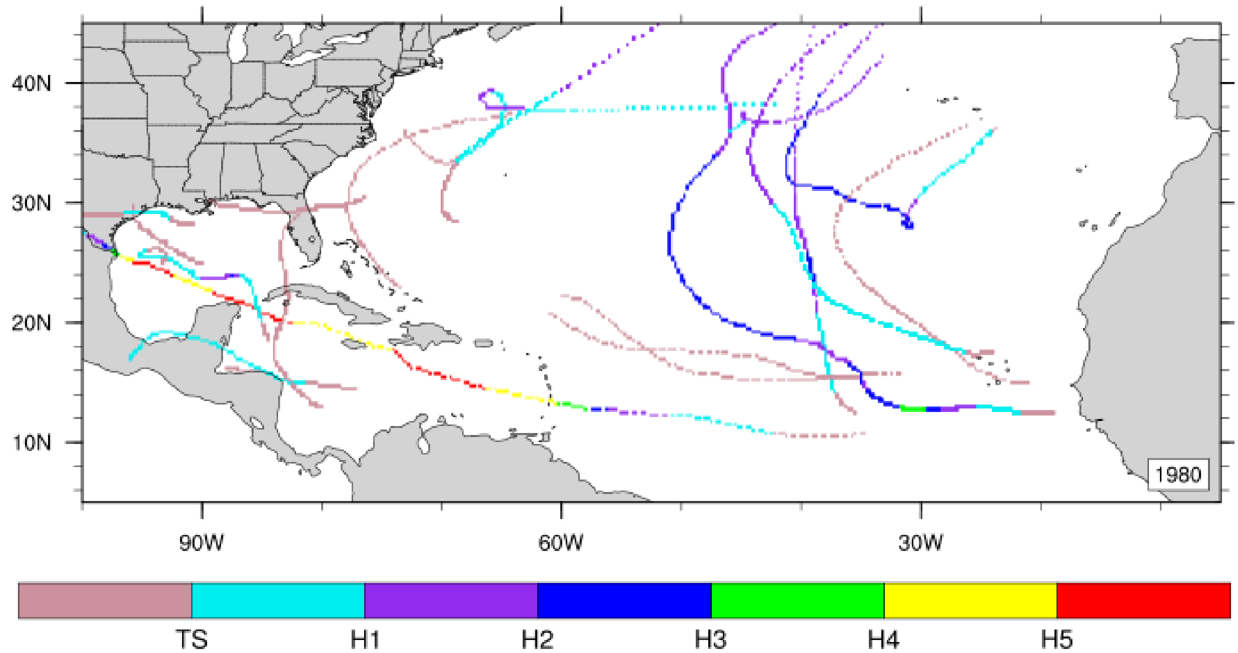

Hurricane Season 1981

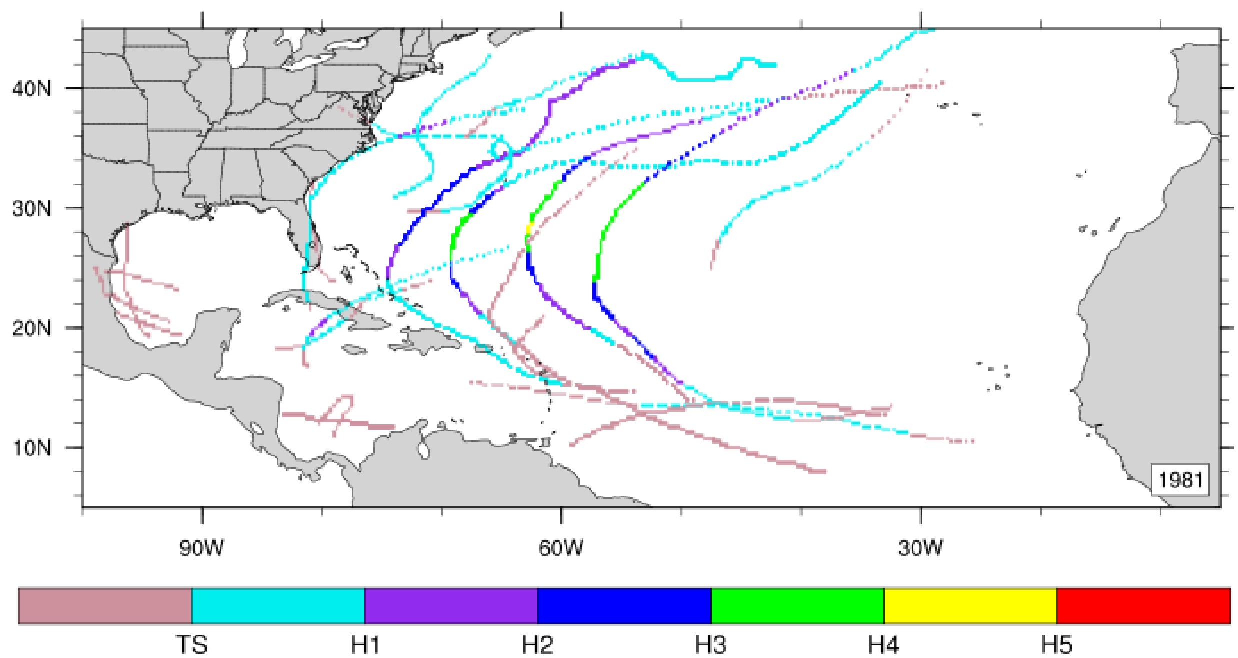

Hurricane Season 1982

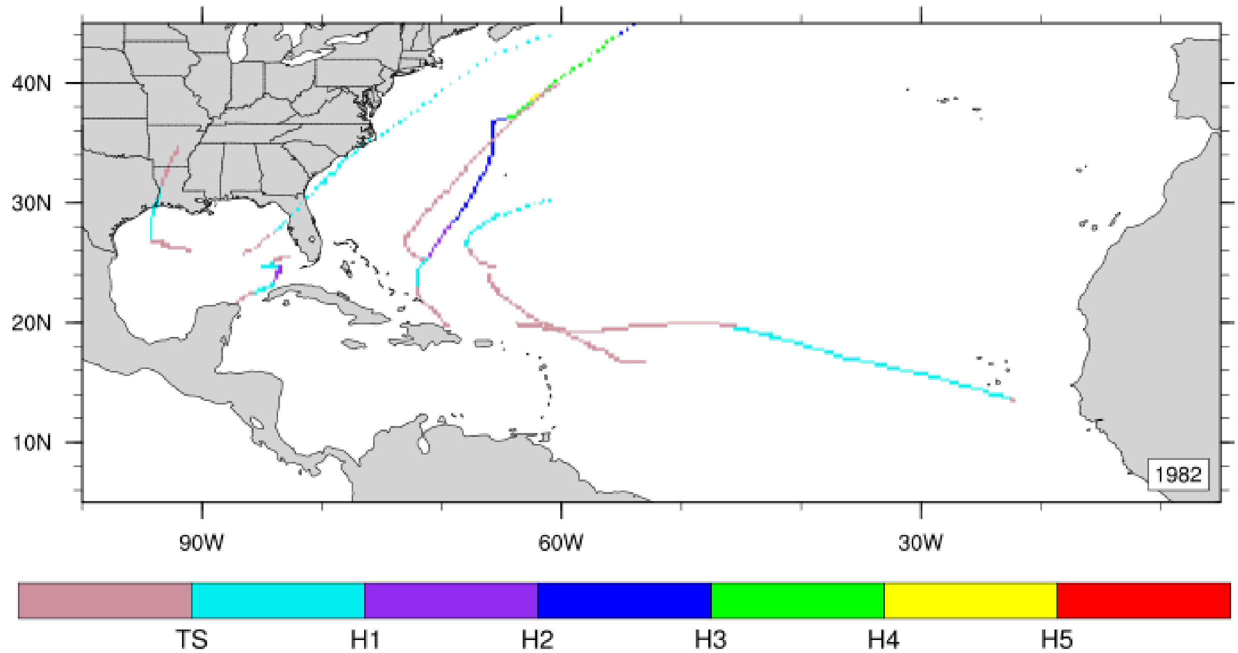

Hurricane Season 1983

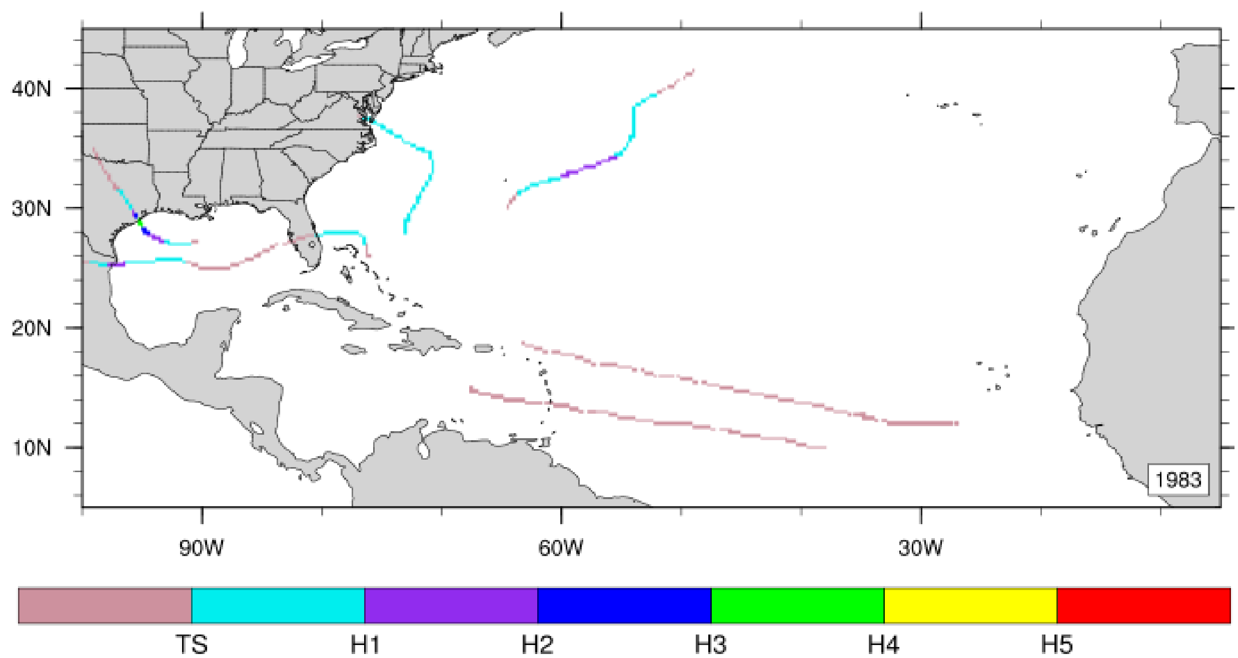

Hurricane Season 1984

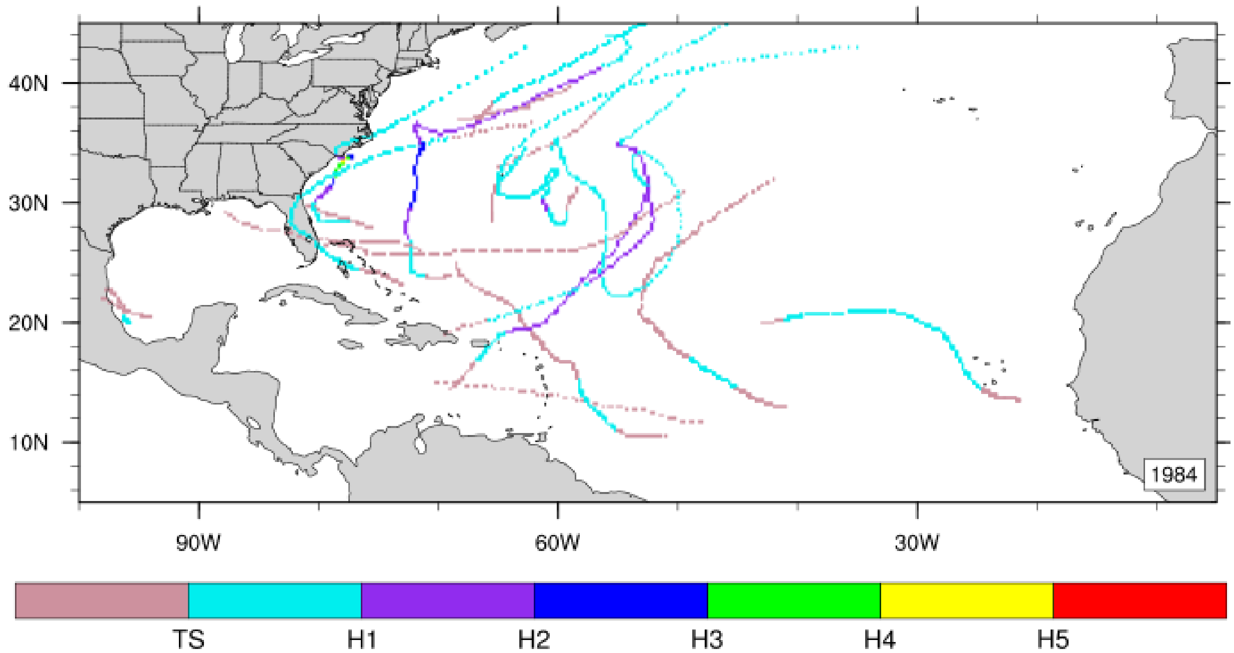

Hurricane Season 1985

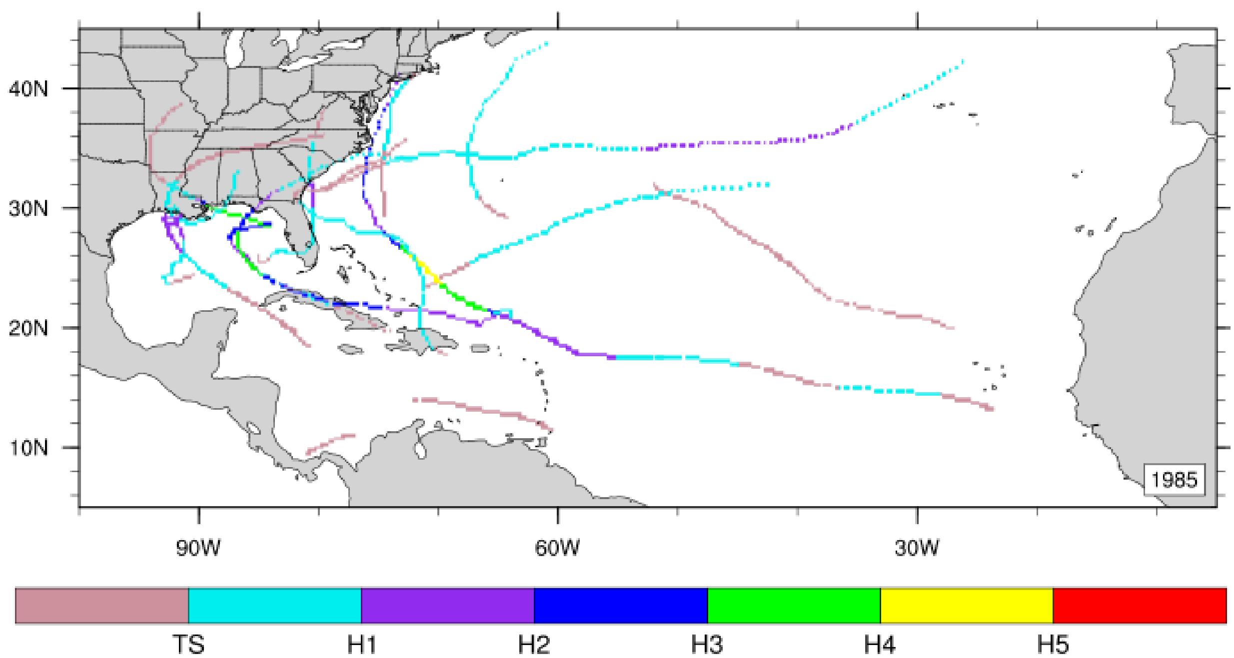

Hurricane Season 1986

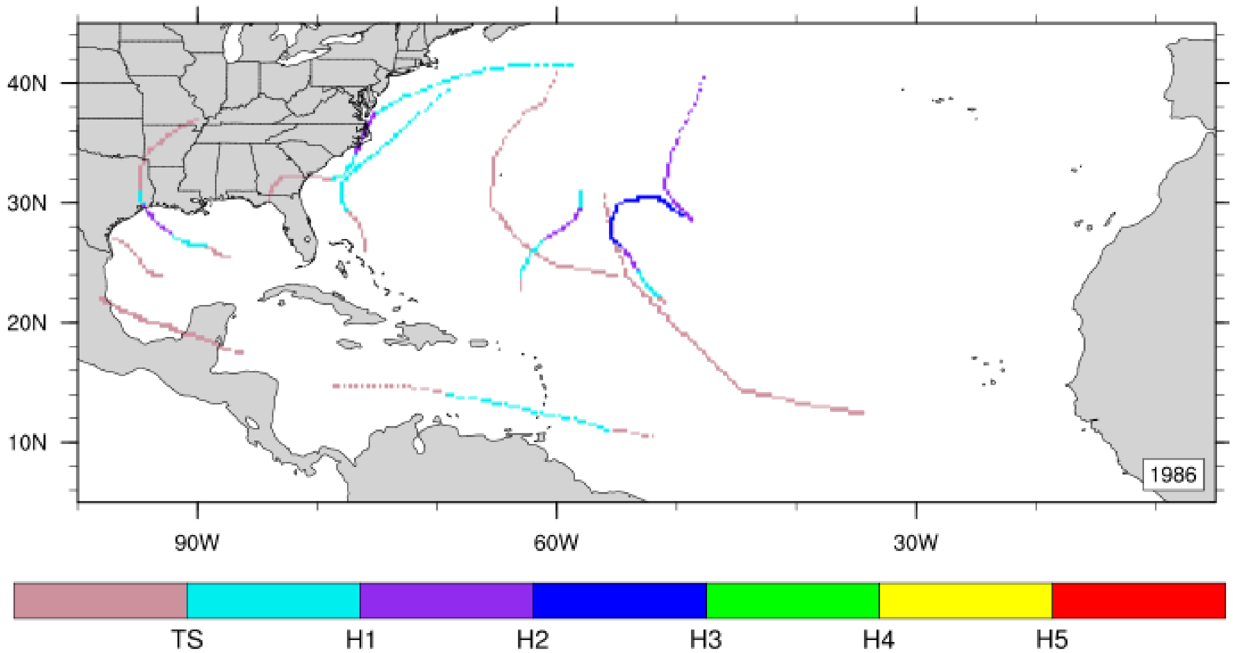

Hurricane Season 1987

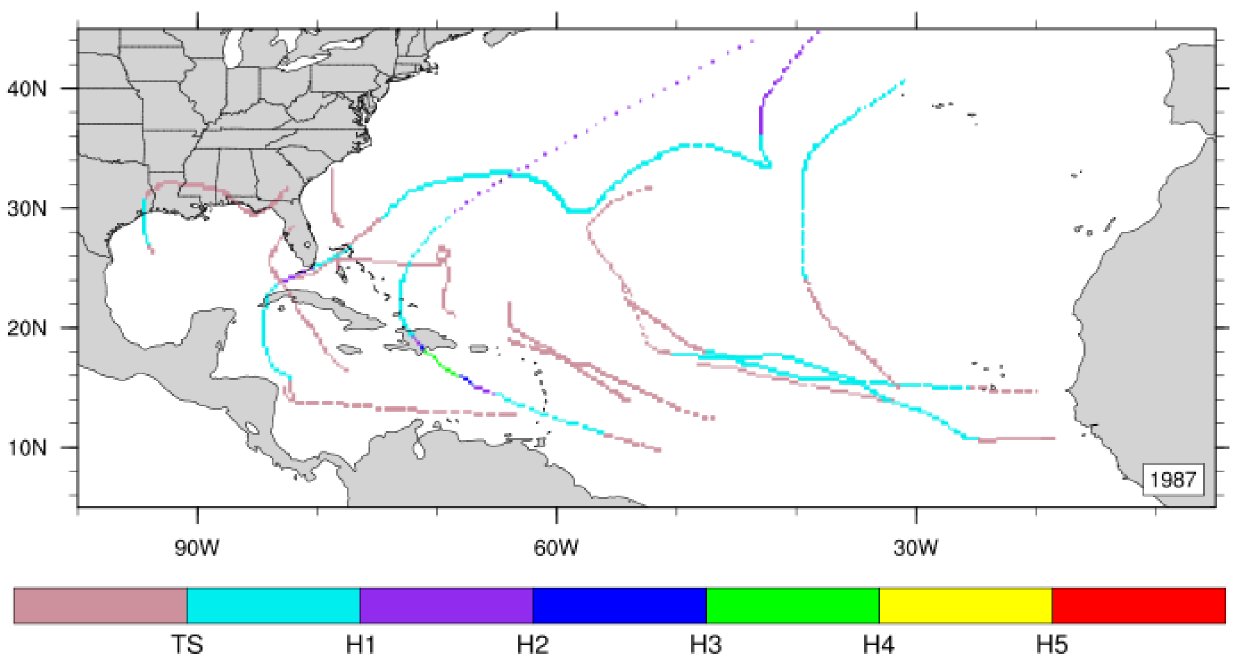

Hurricane Season 1988

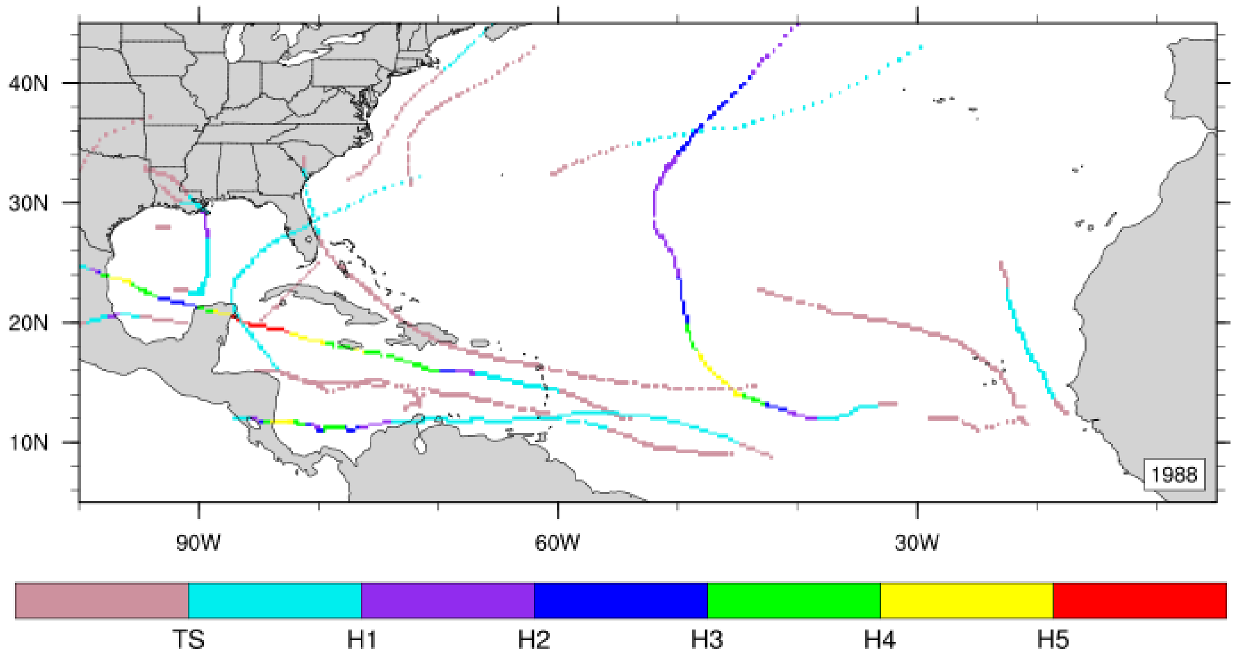

Hurricane Season 1989

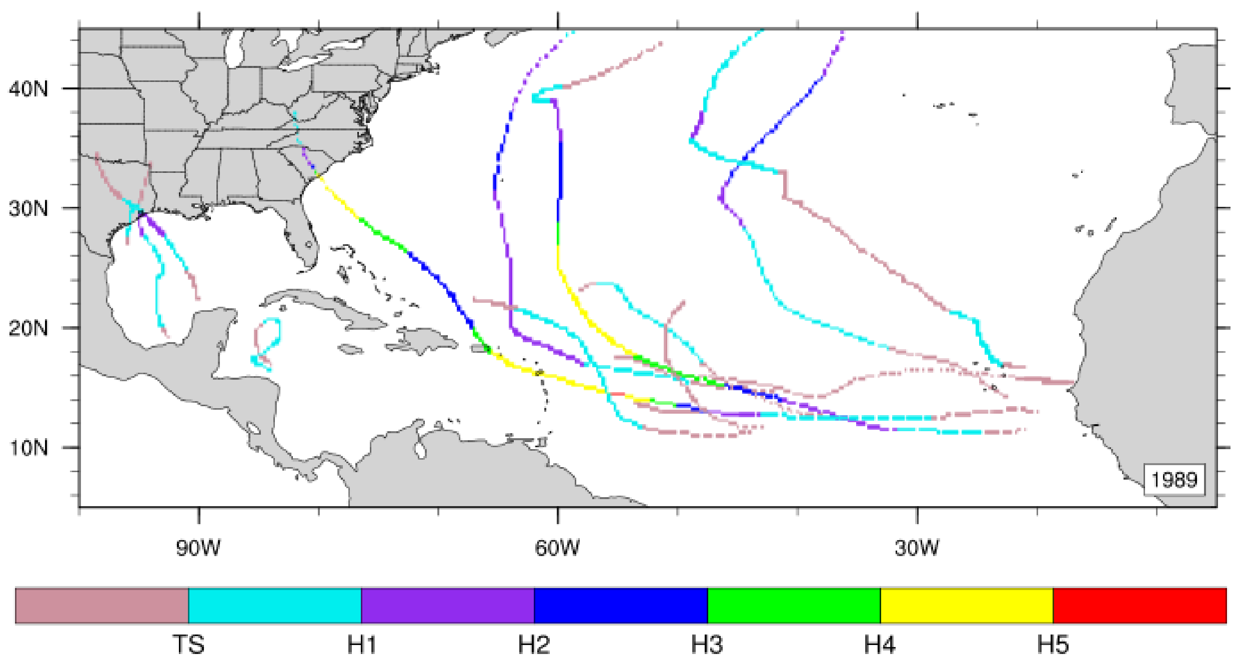

Hurricane Season 1990

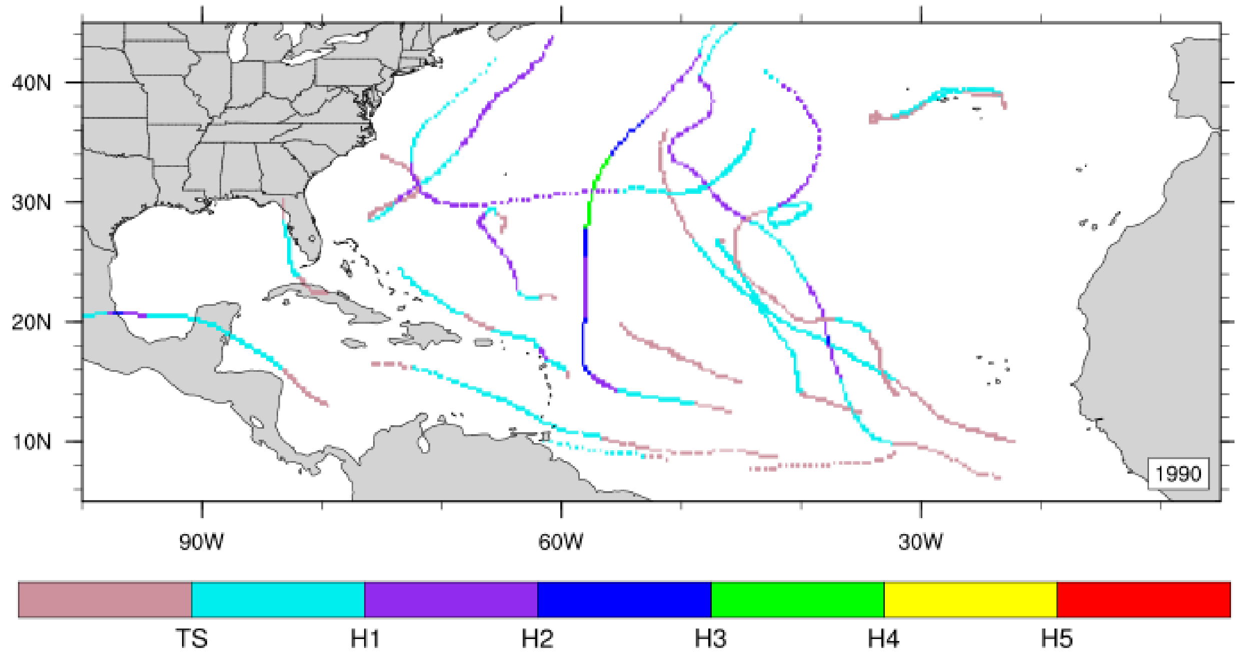

Hurricane Season 1991

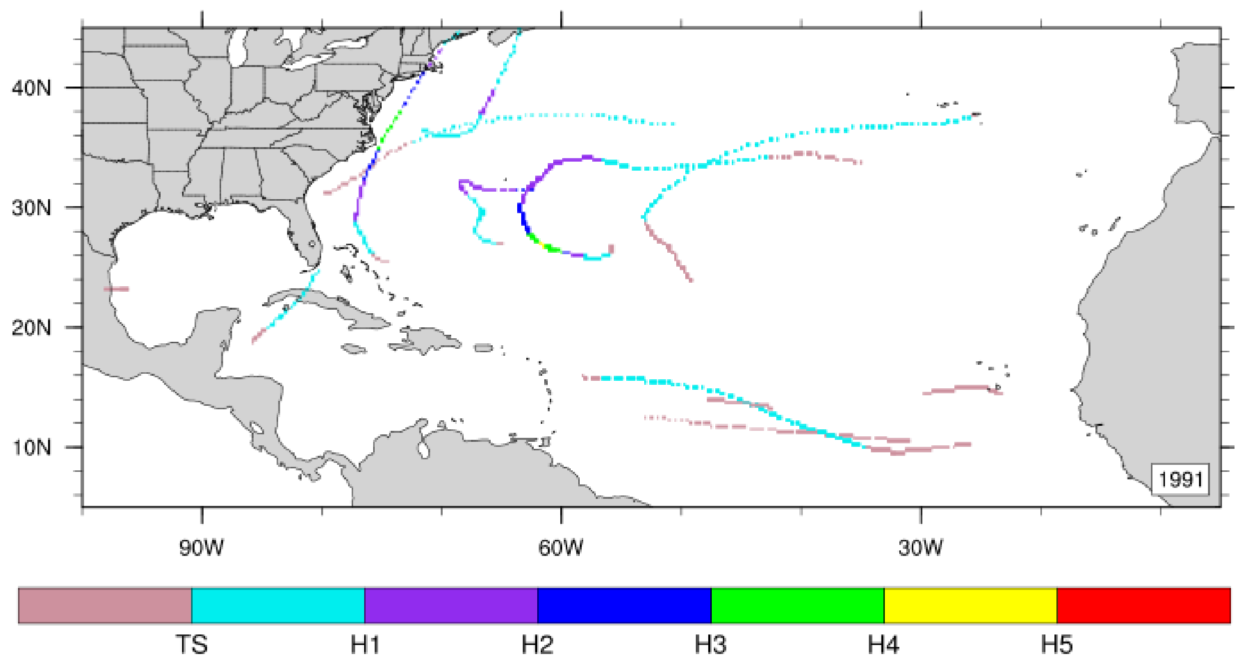

Hurricane Season 1992

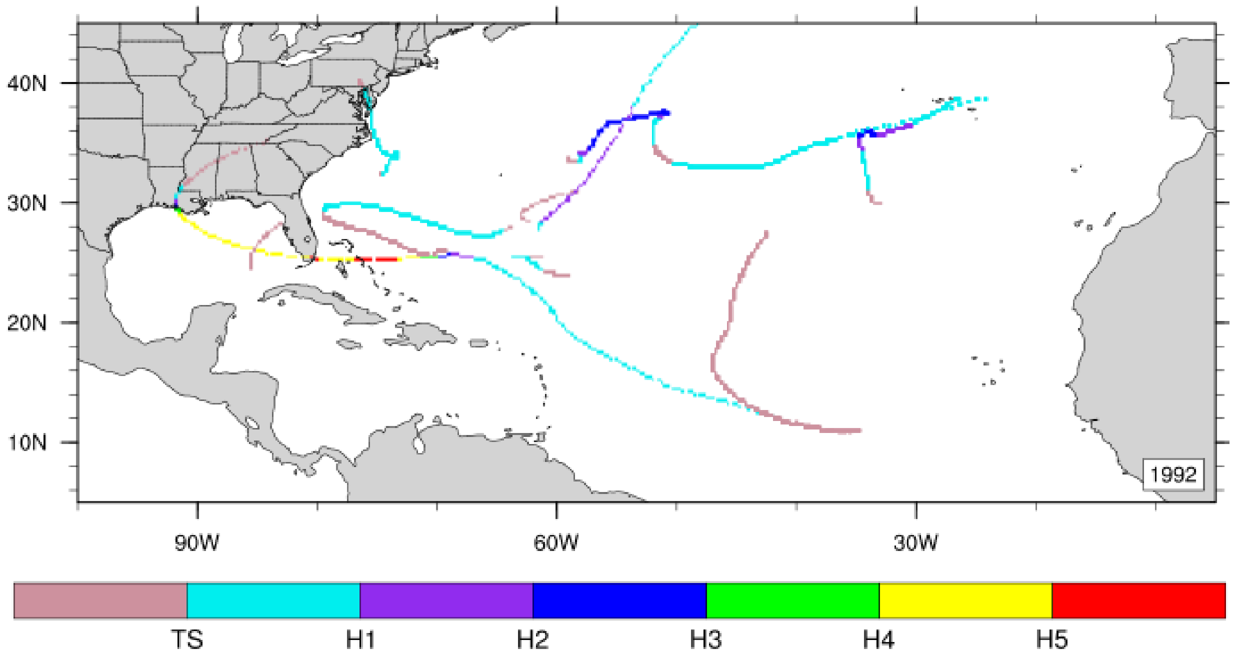

Hurricane Season 1993

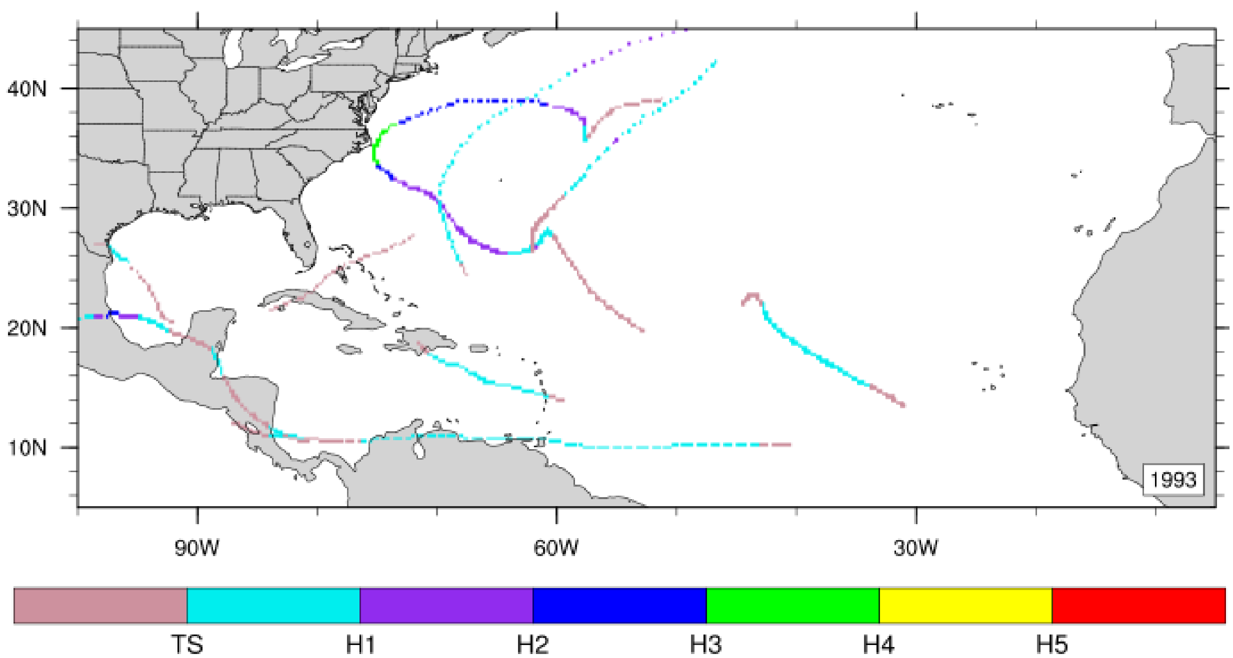

Hurricane Season 1994

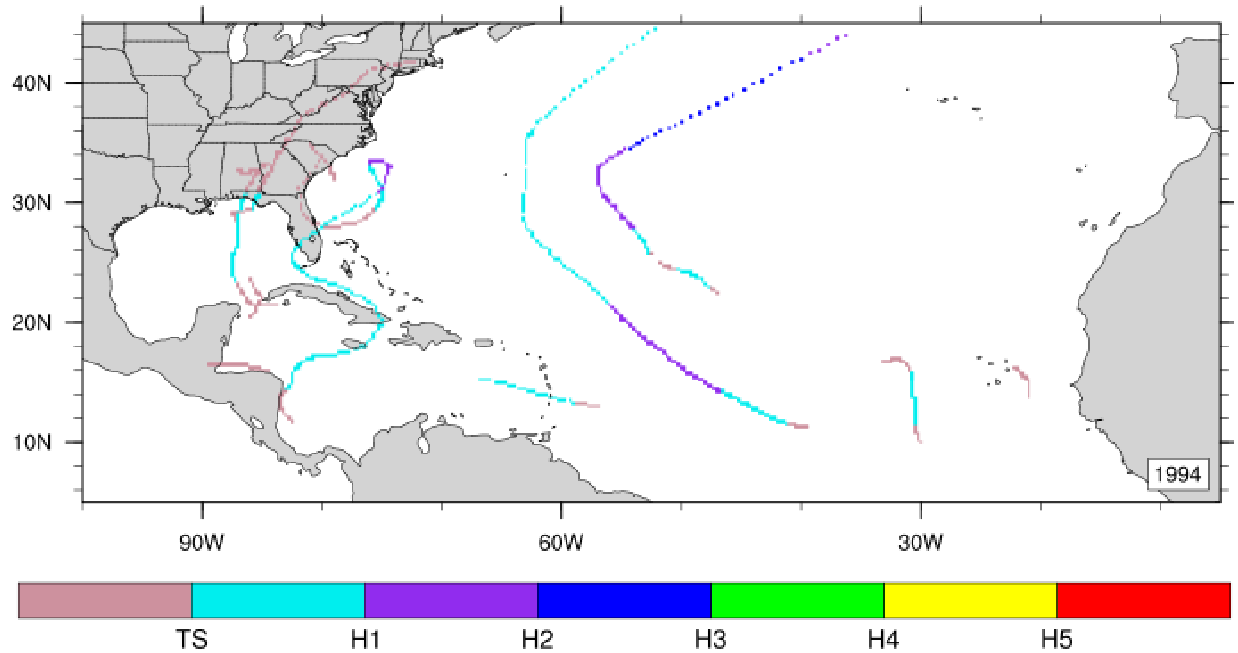

Hurricane Season 1995

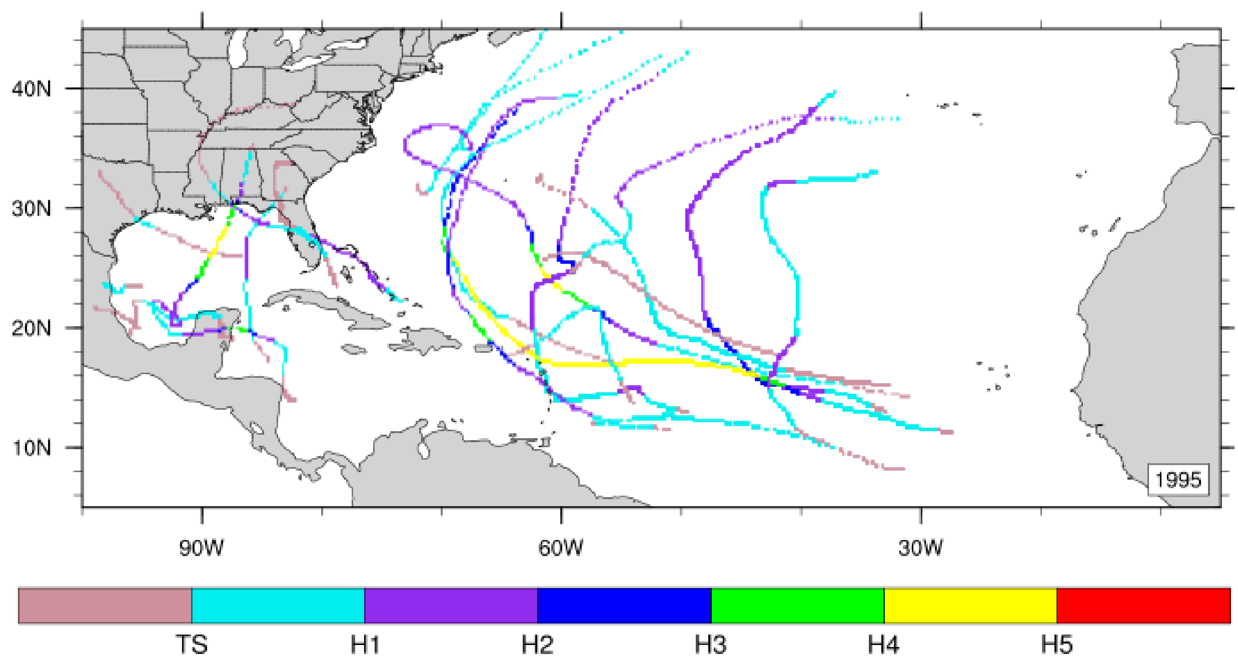

Hurricane Season 1996

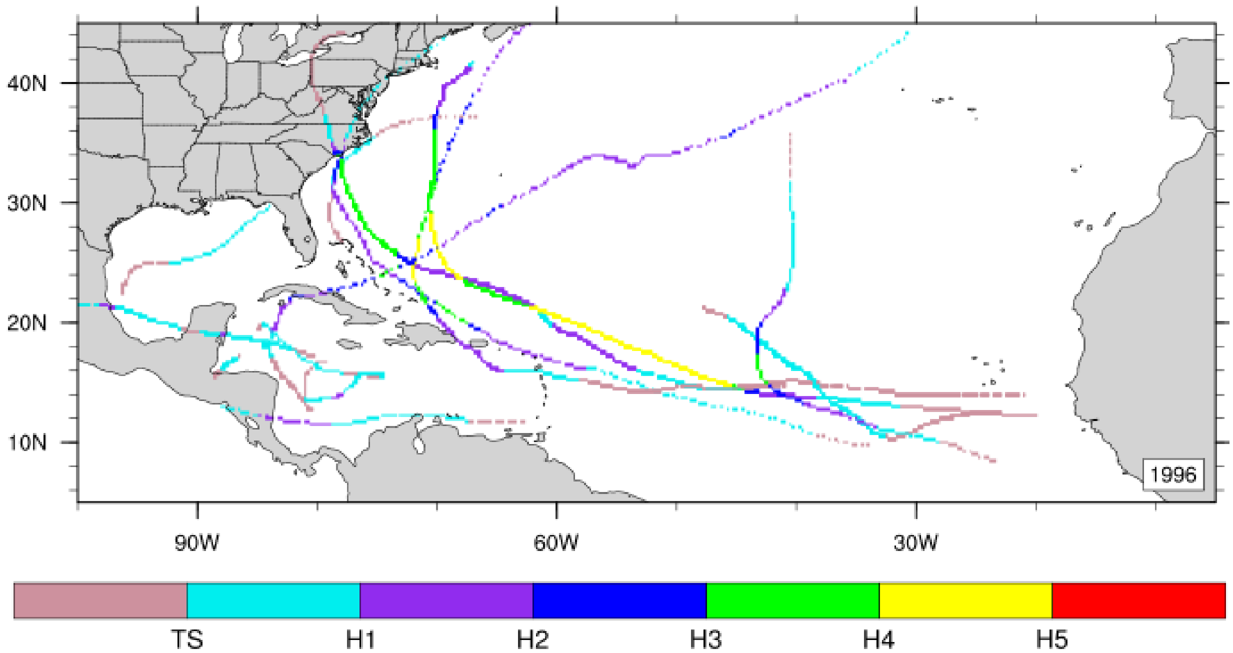

Hurricane Season 1997

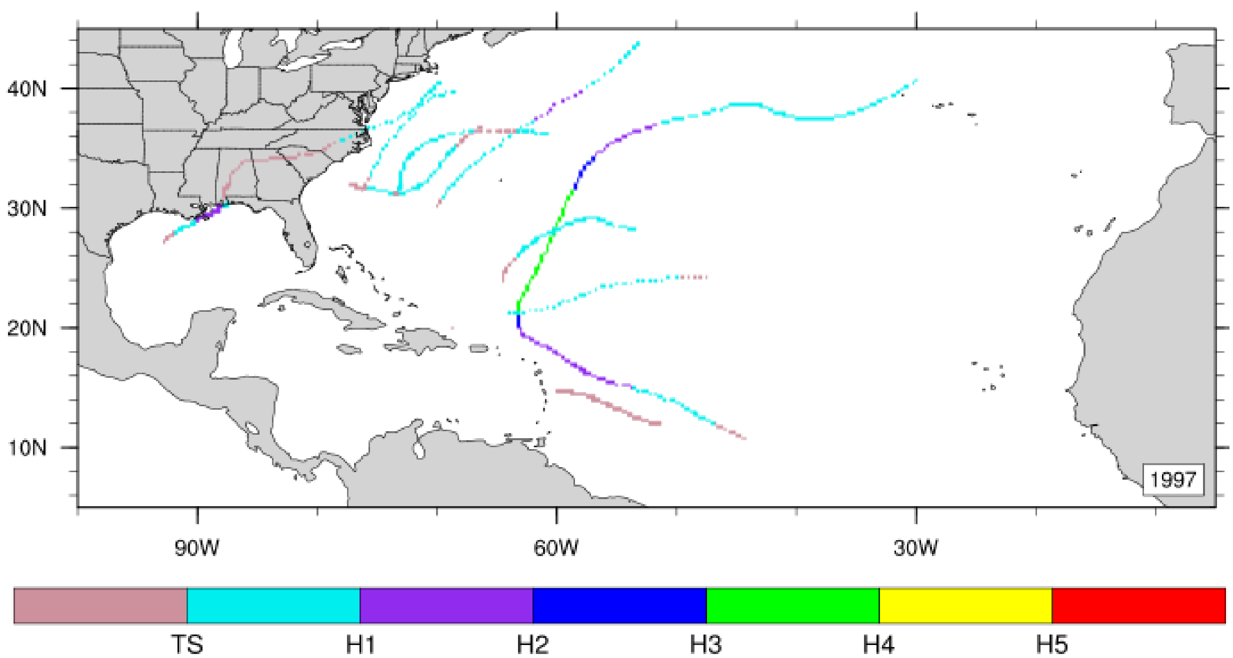

Hurricane Season 1998

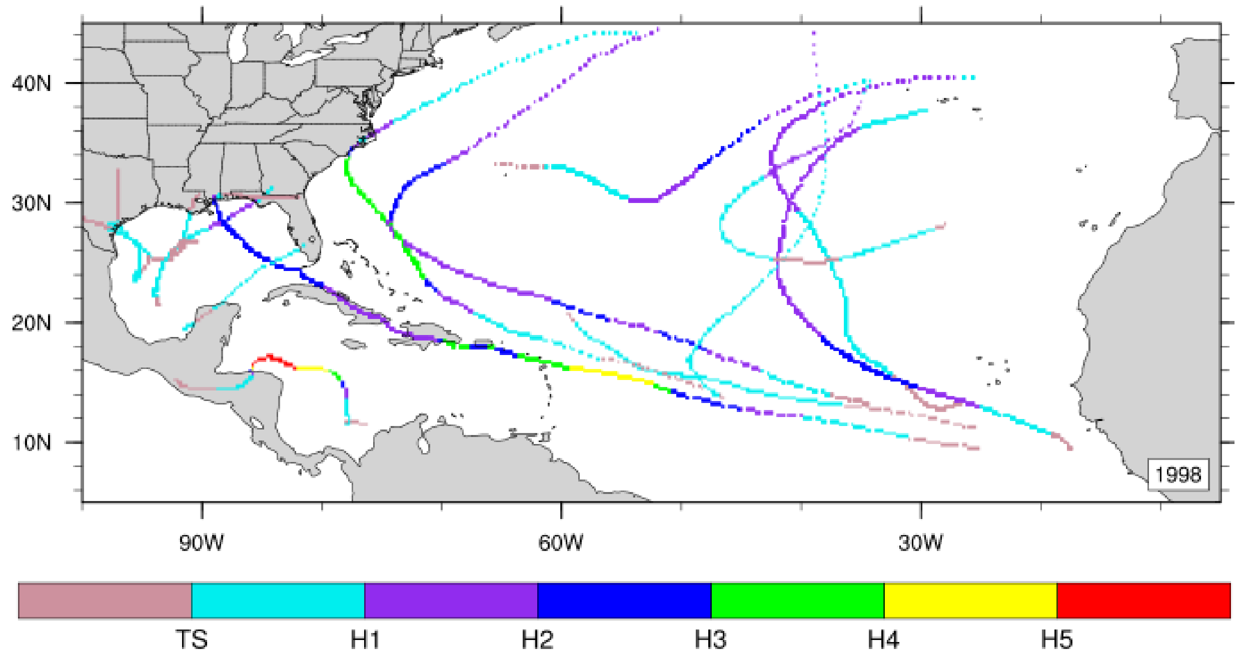

Hurricane Season 1999

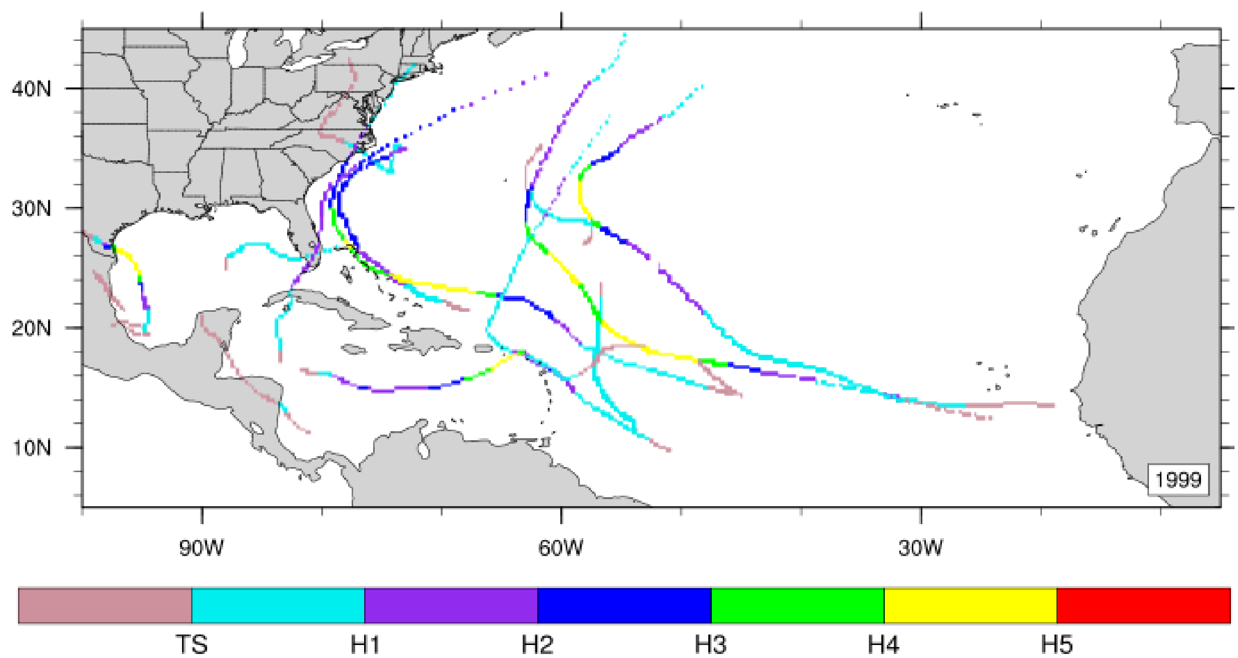

Hurricane Season 2000

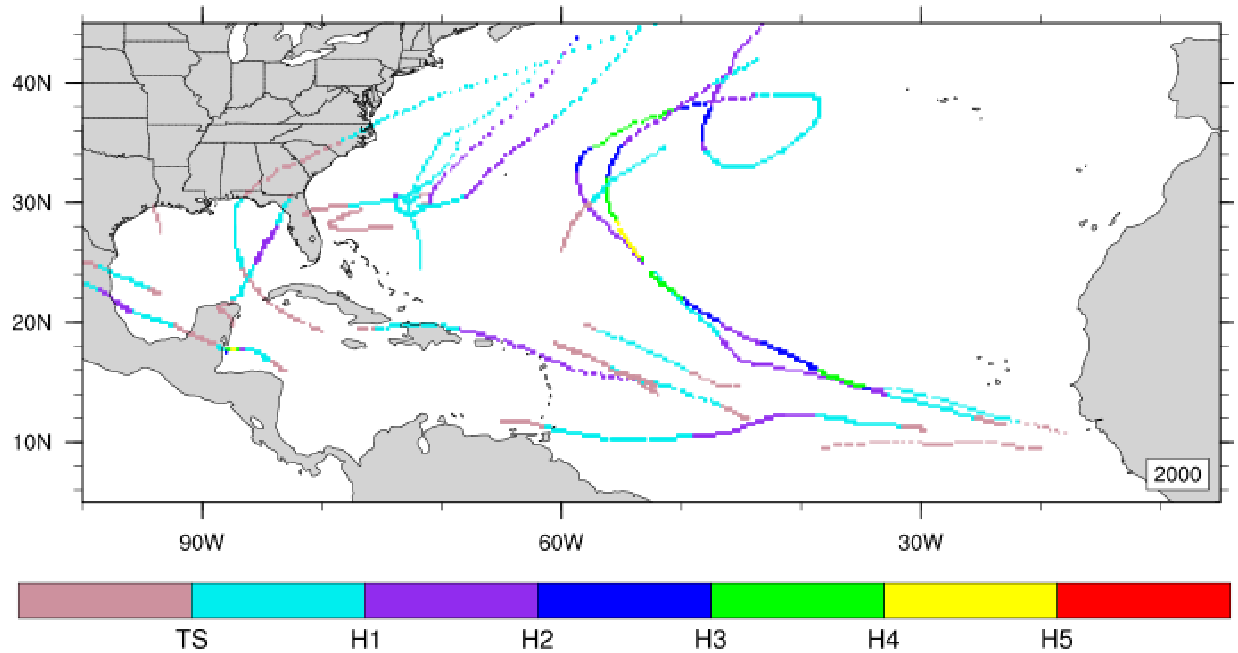

Hurricane Season 2001

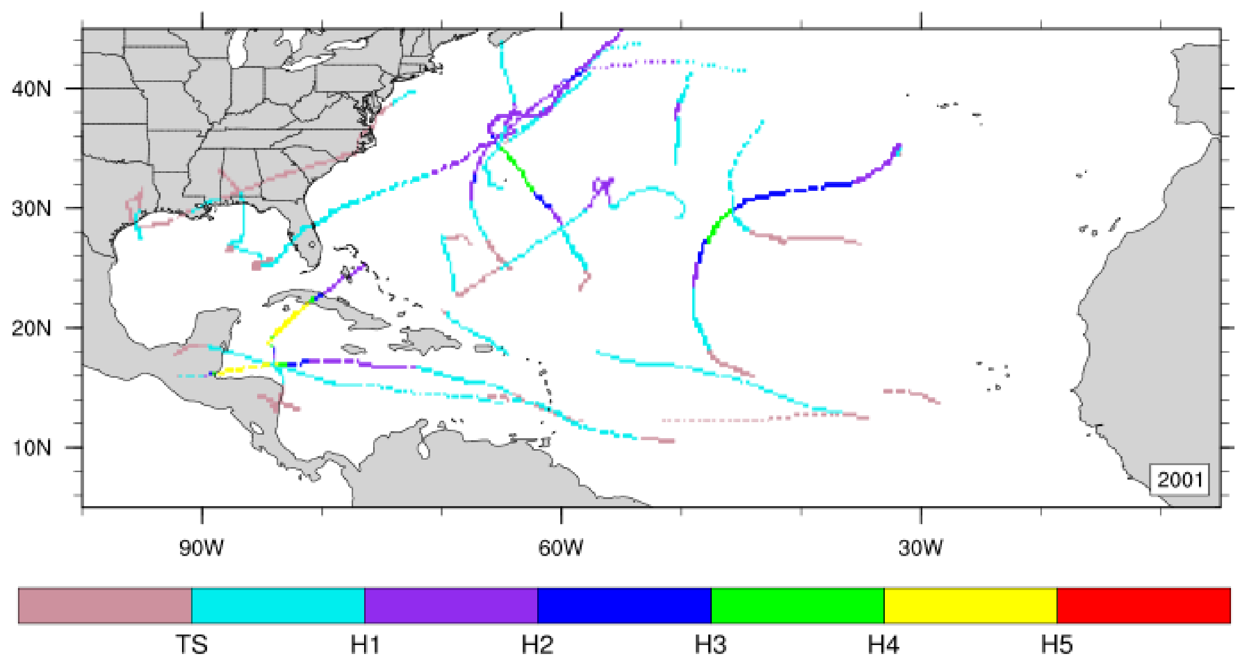

Hurricane Season 2002

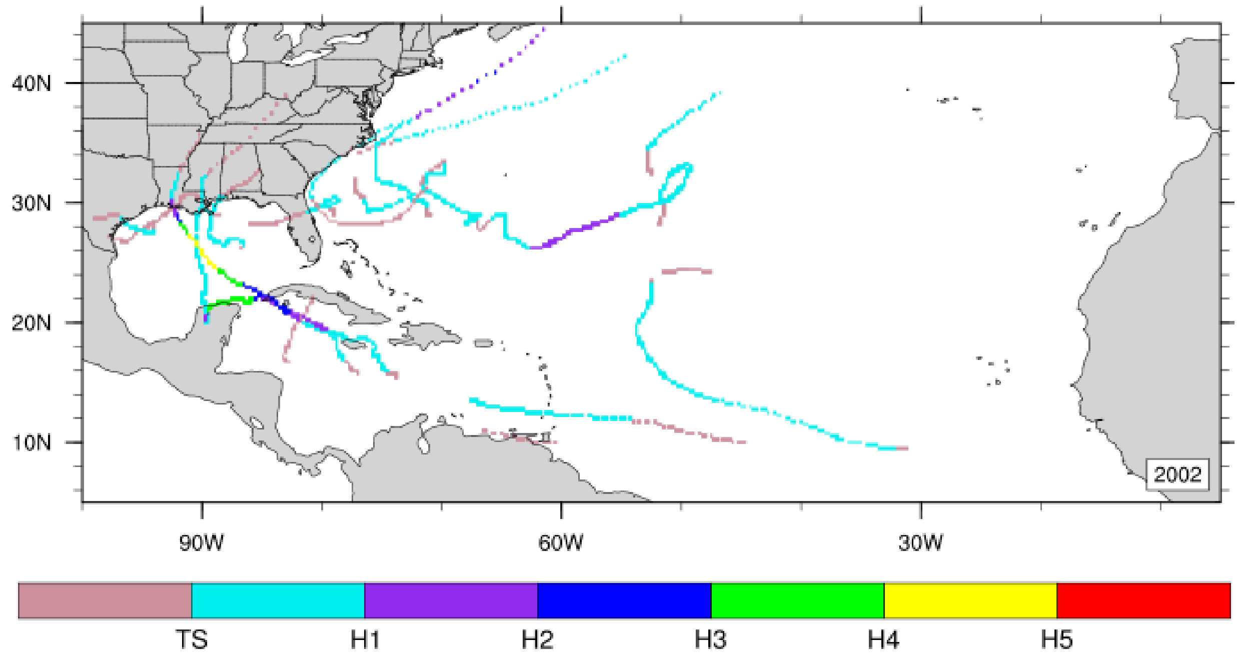

Hurricane Season 2003

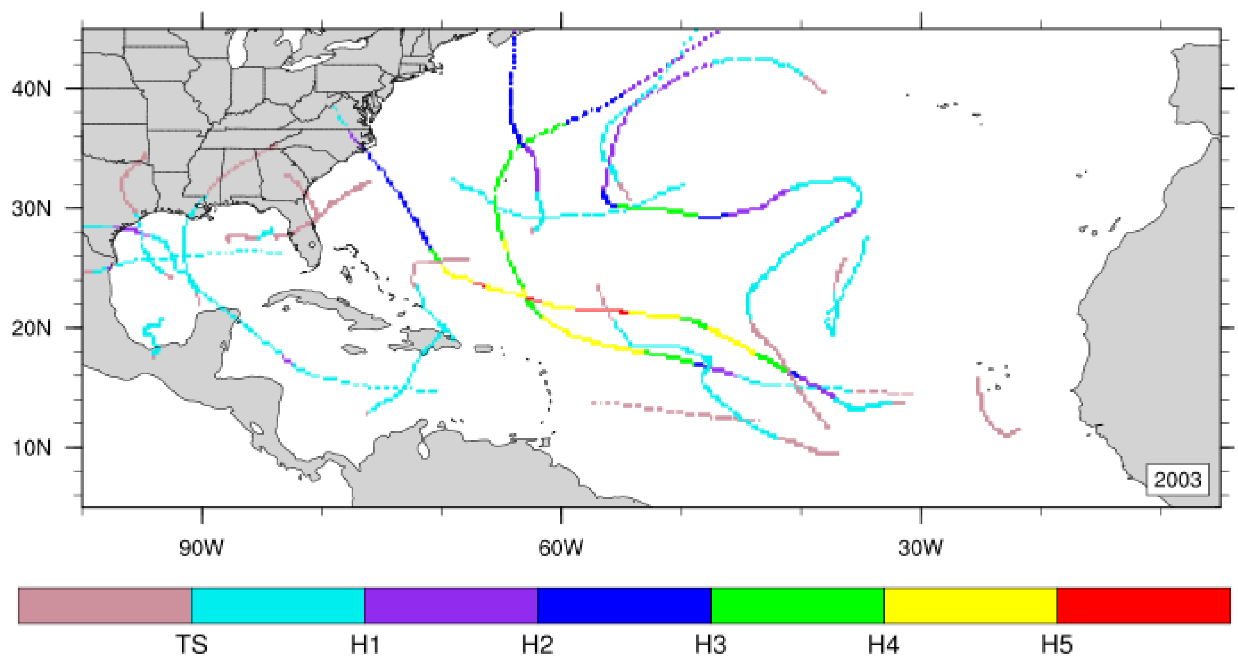

Hurricane Season 2004

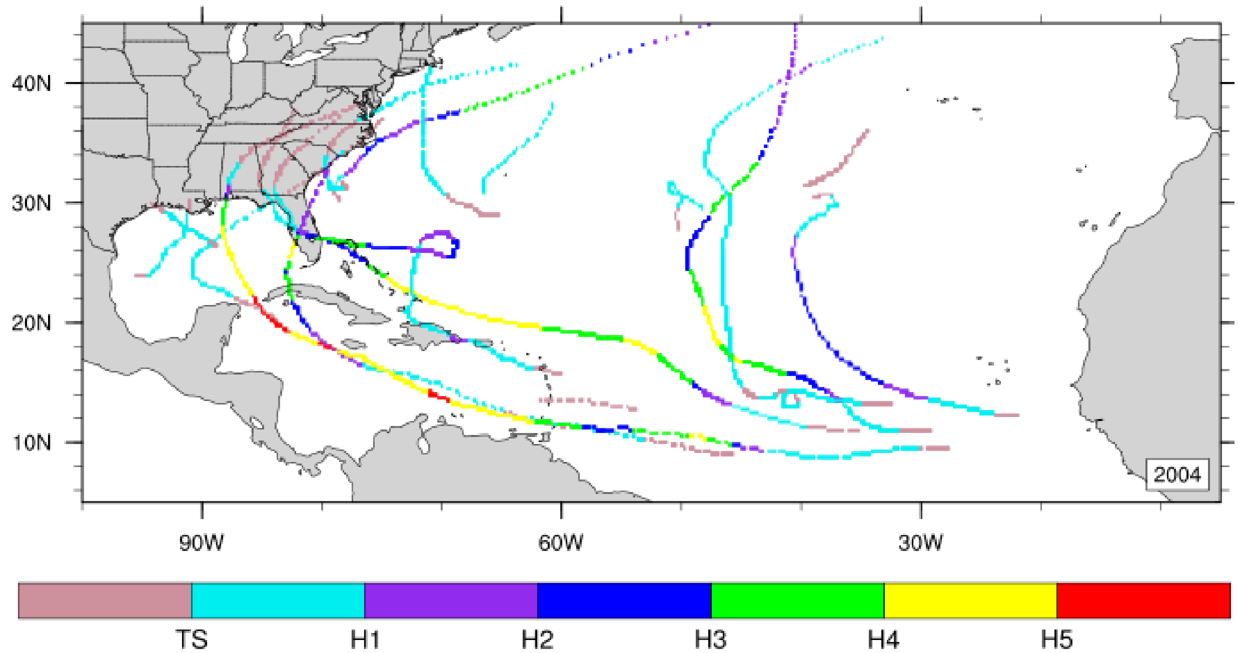

Hurricane Season 2005

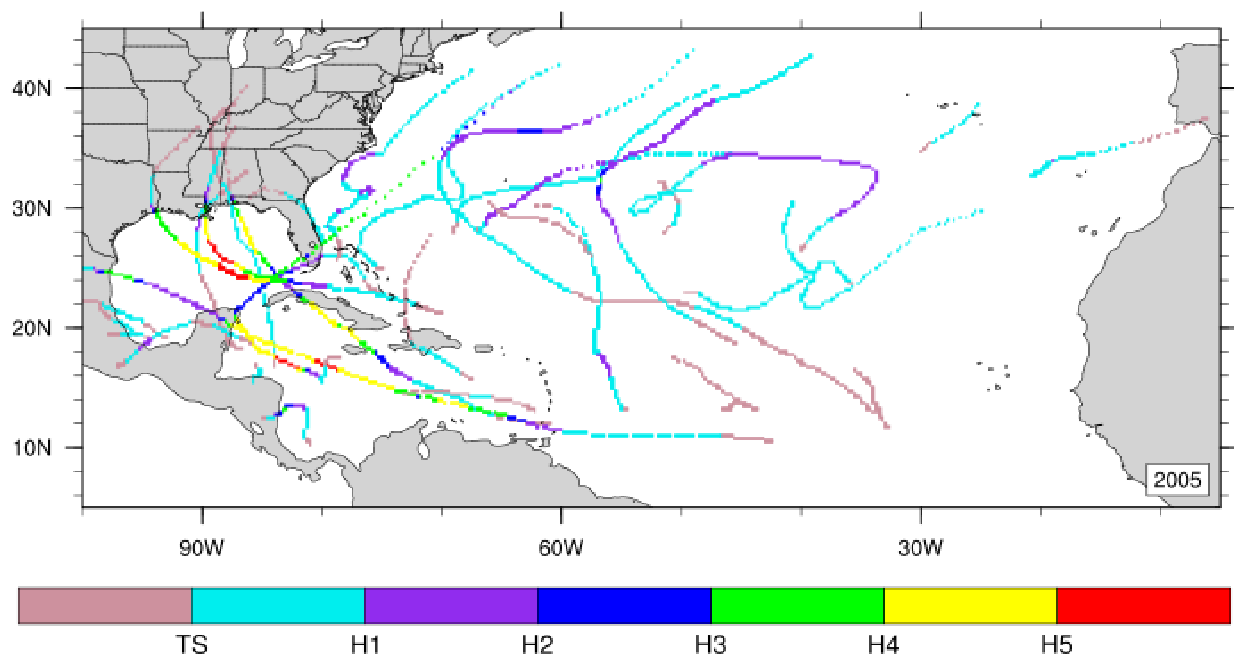

Hurricane Season 2006

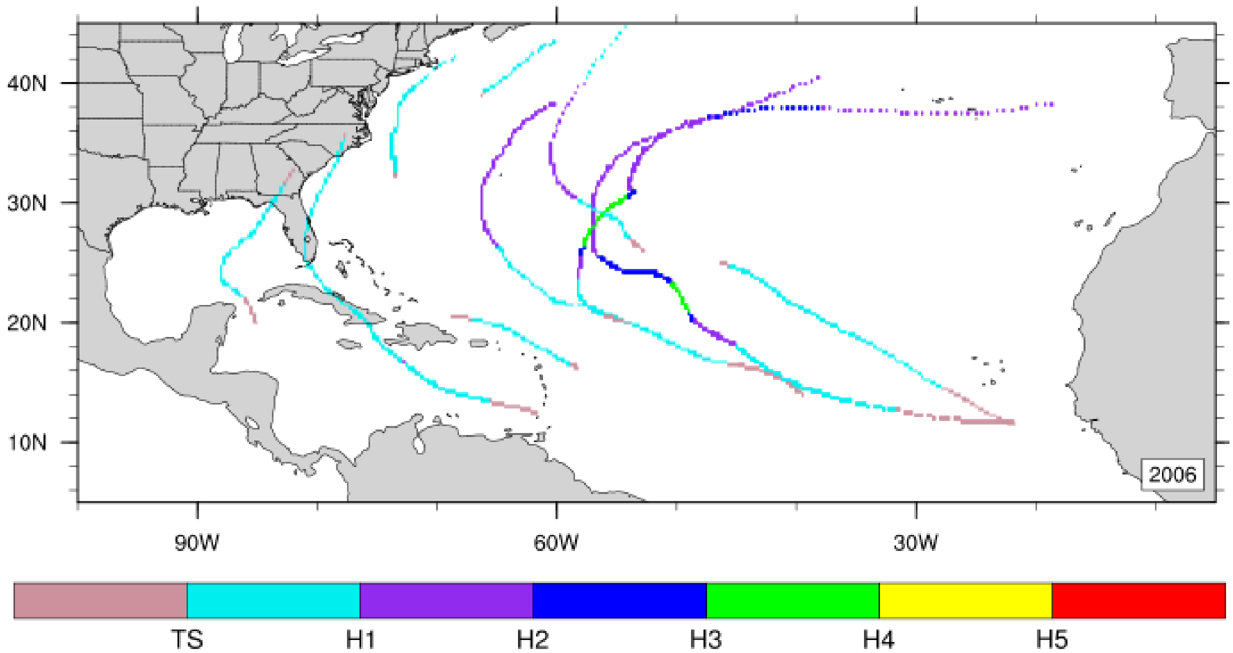

Hurricane Season 2007

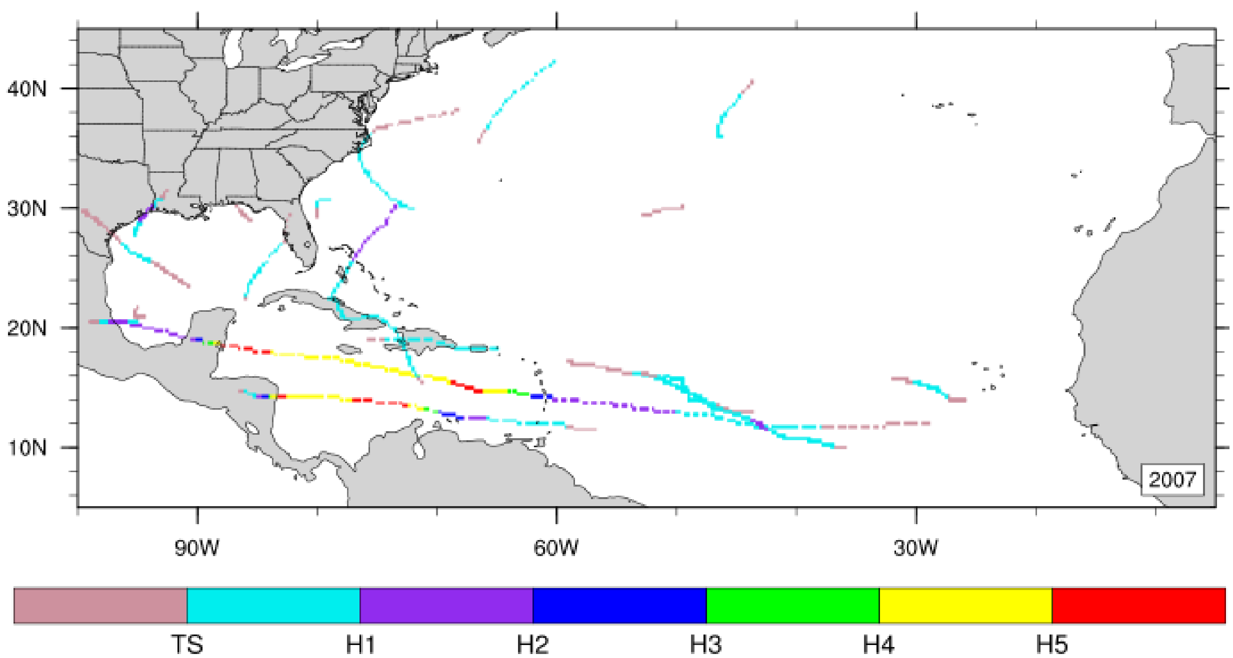

Hurricane Season 2008

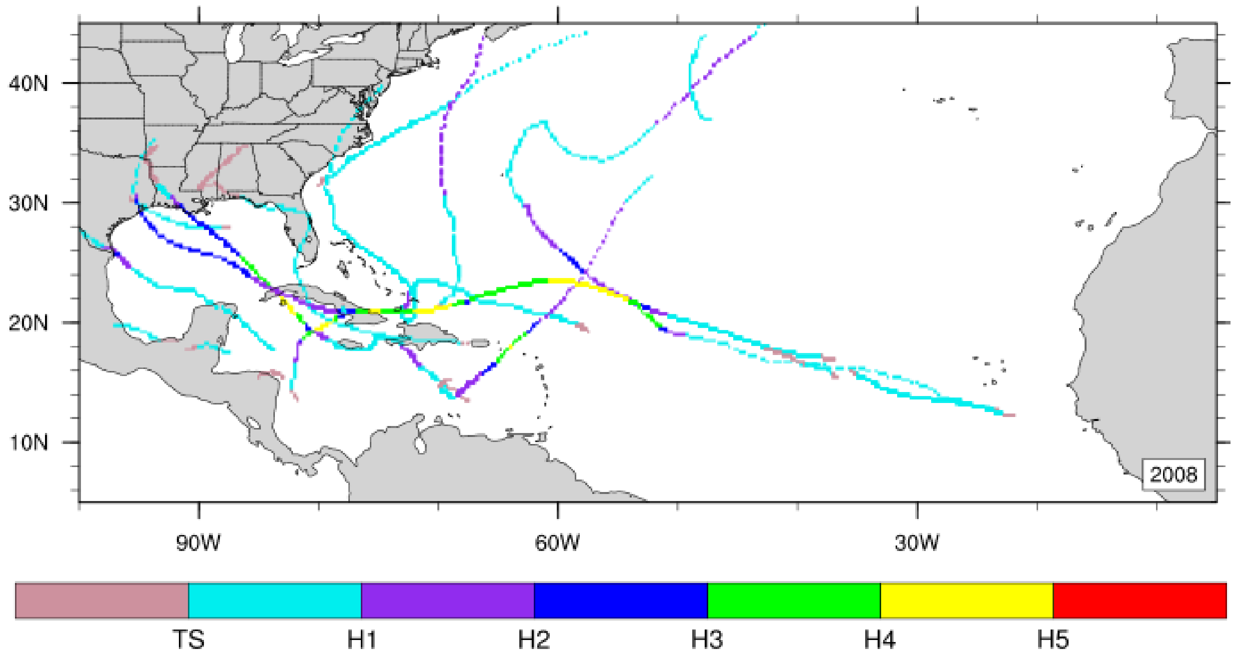

Hurricane Season 2009

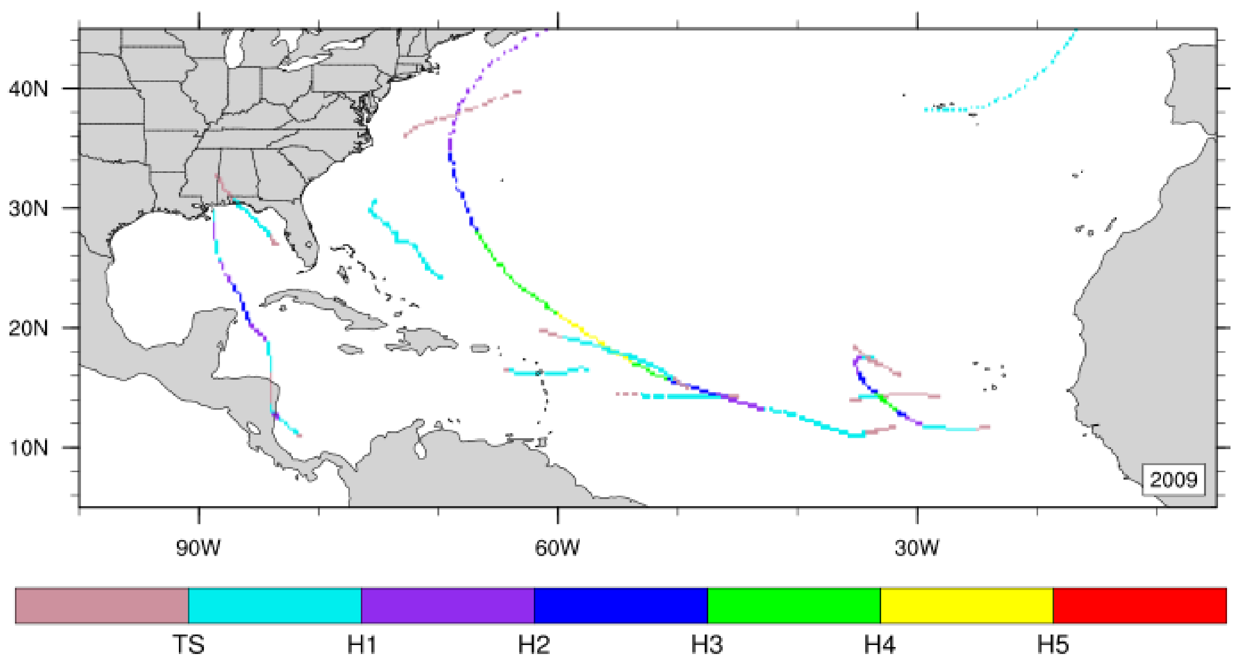

Hurricane Season 2010

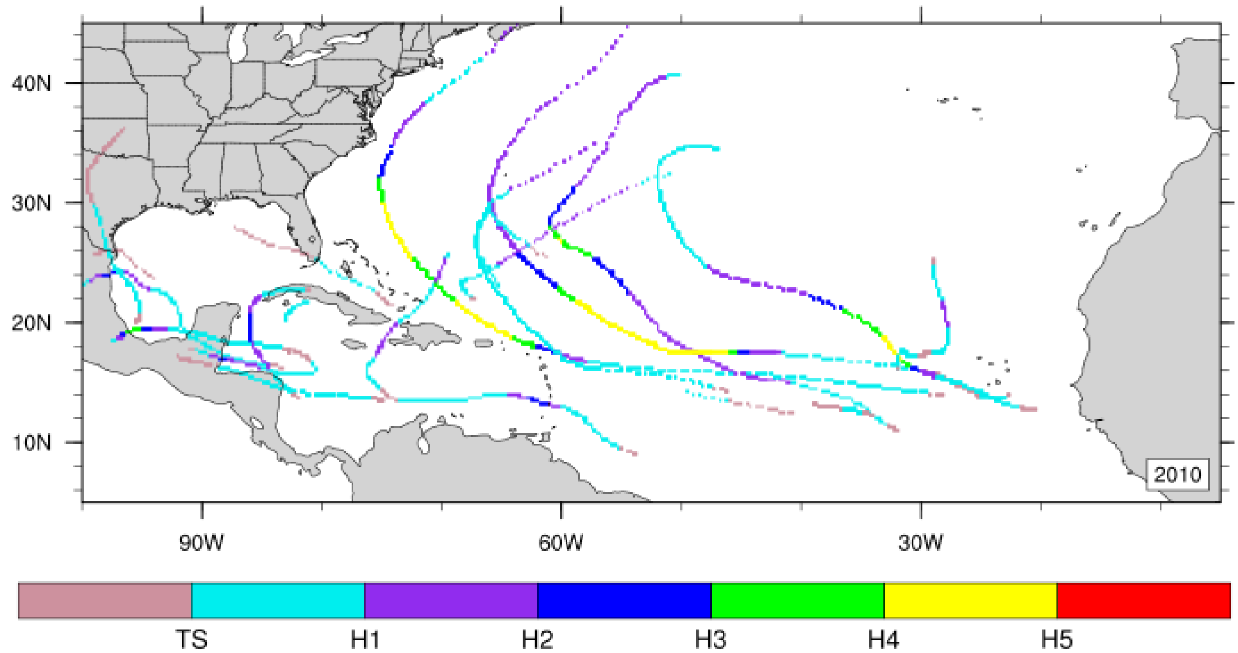

Hurricane Season 2011

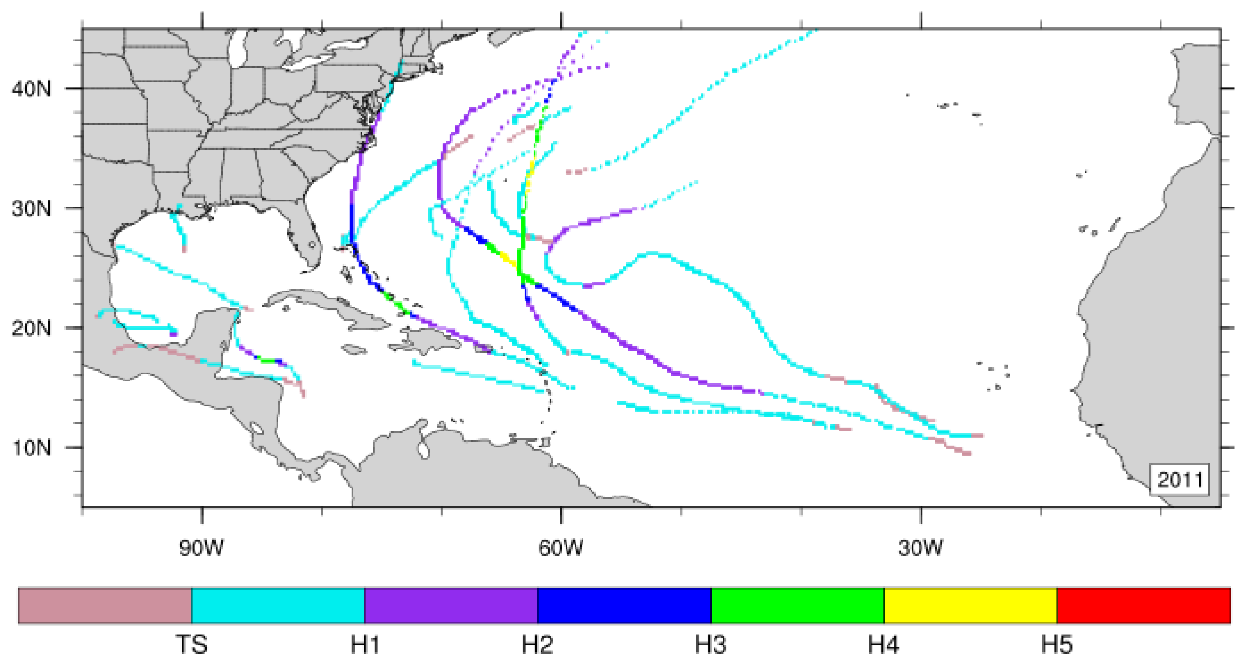

Hurricane Season 2012

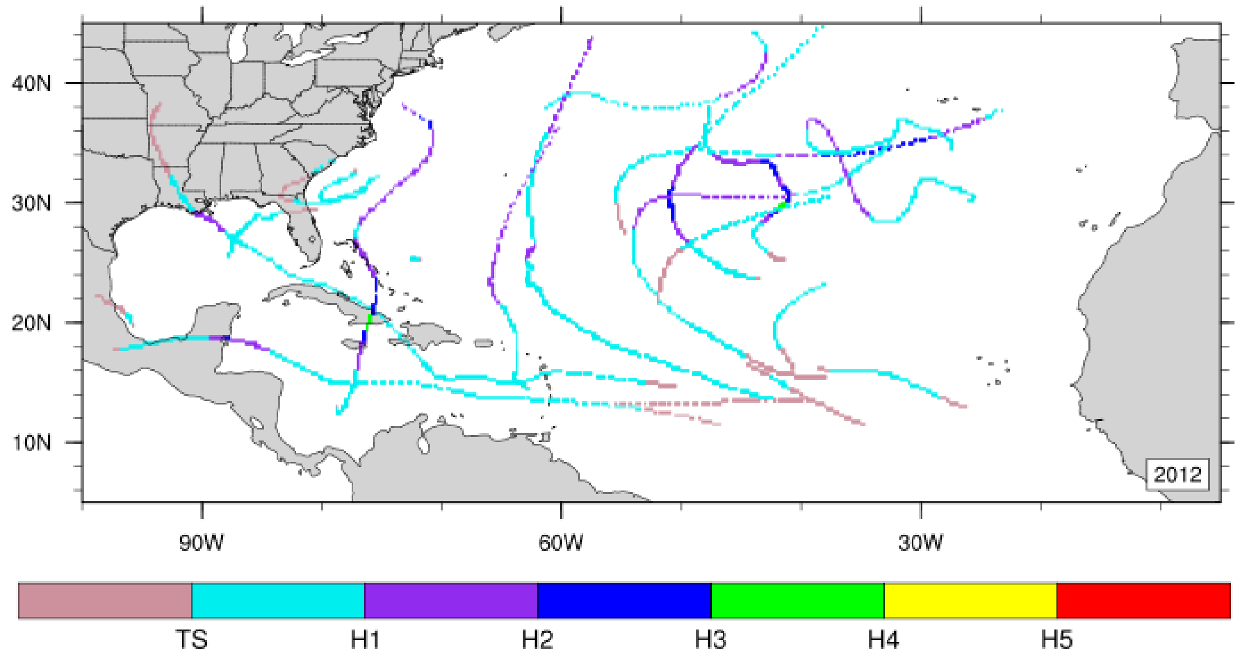

Hurricane Season 2013

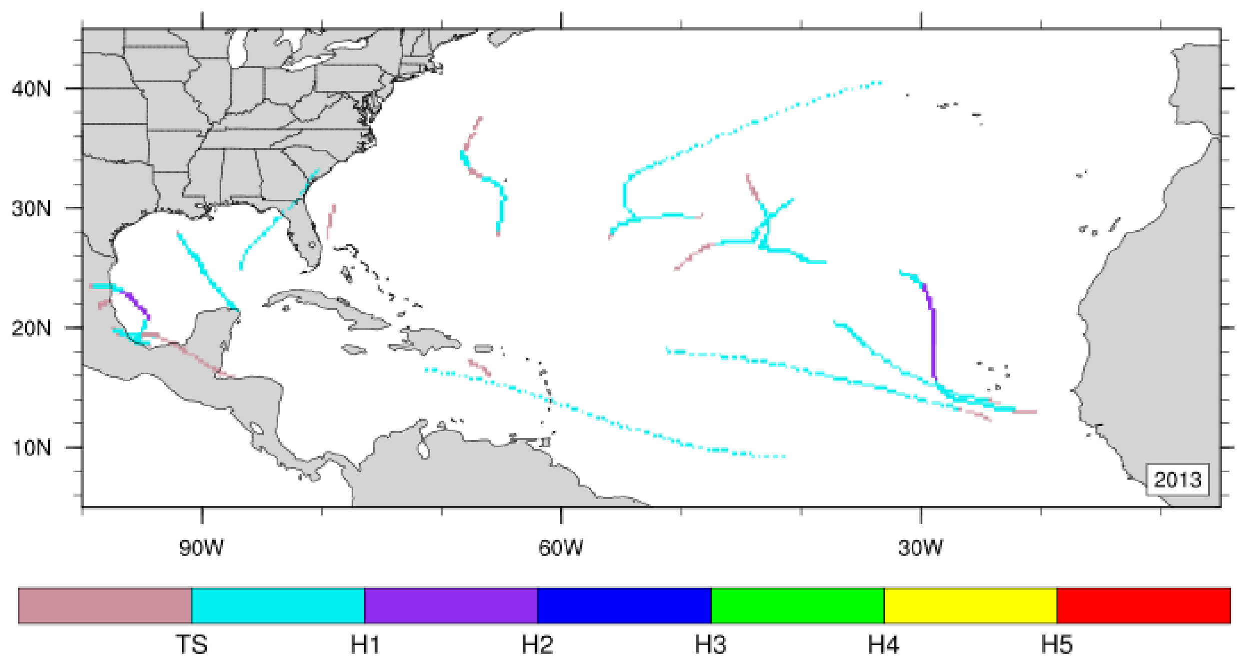

Hurricane Season 2014

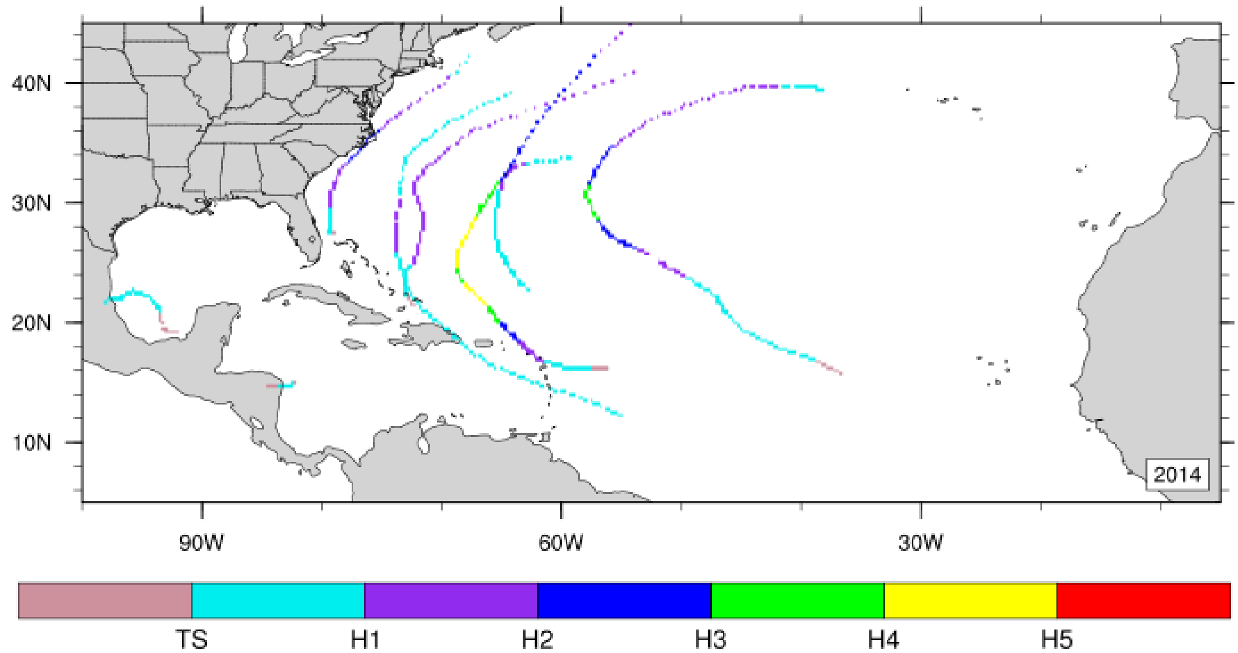

Hurricane Season 2015

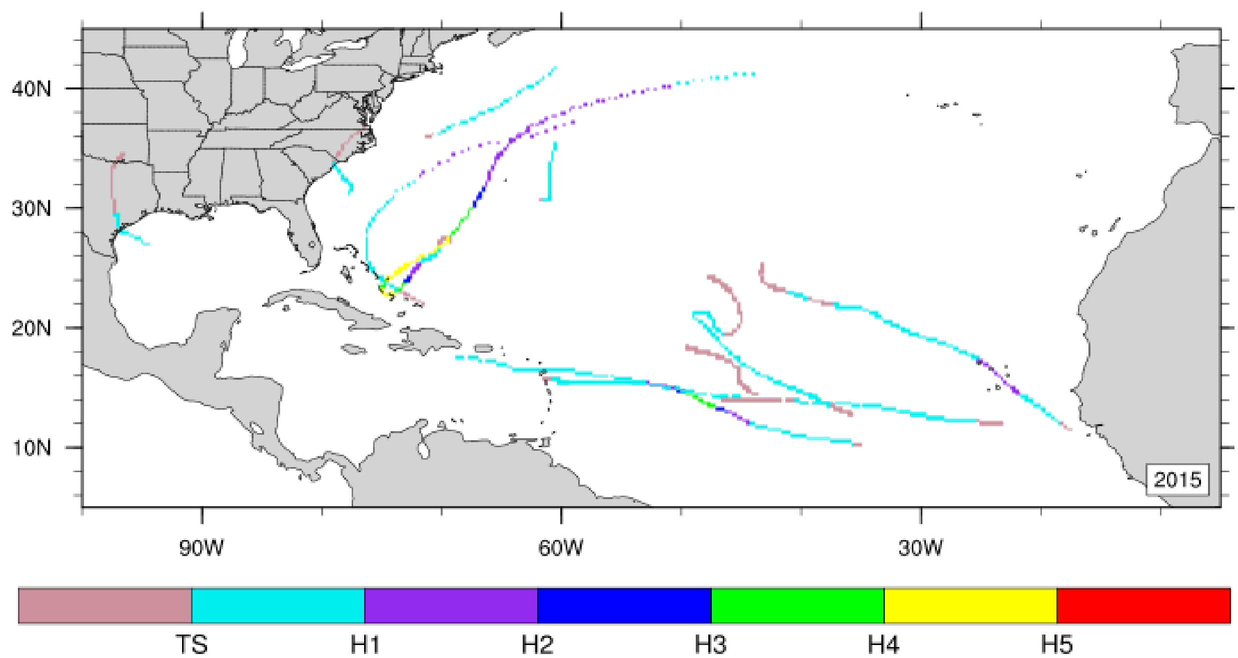

Hurricane Season 2016

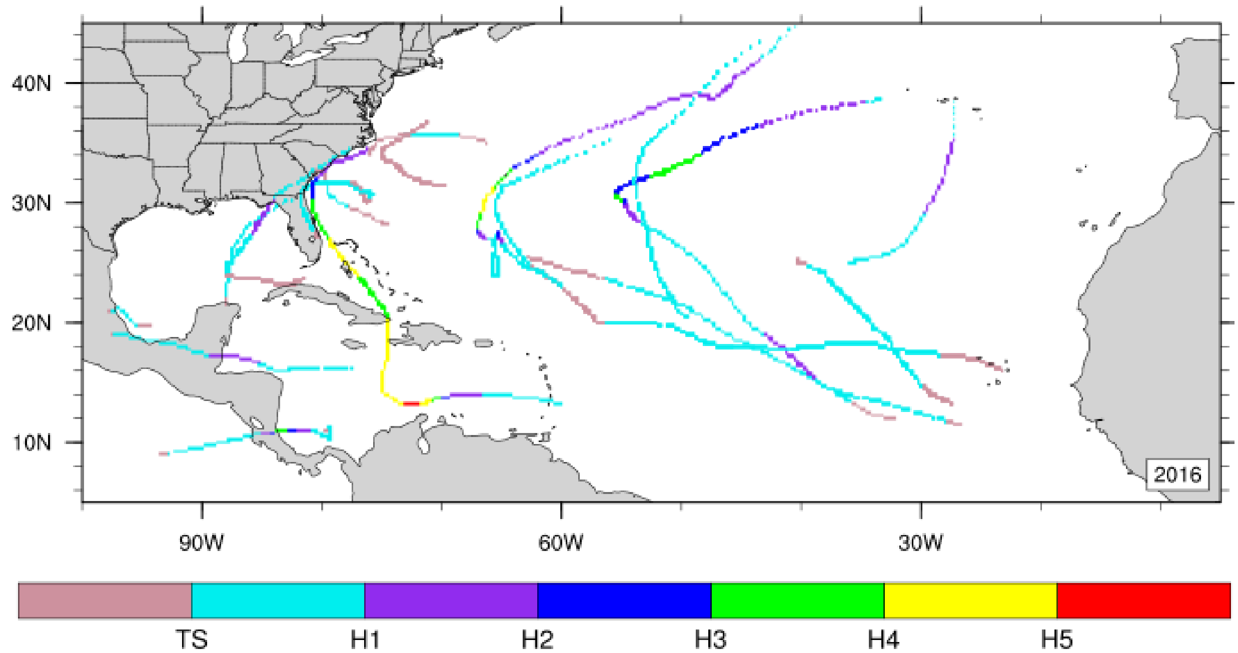

Hurricane Season 2017

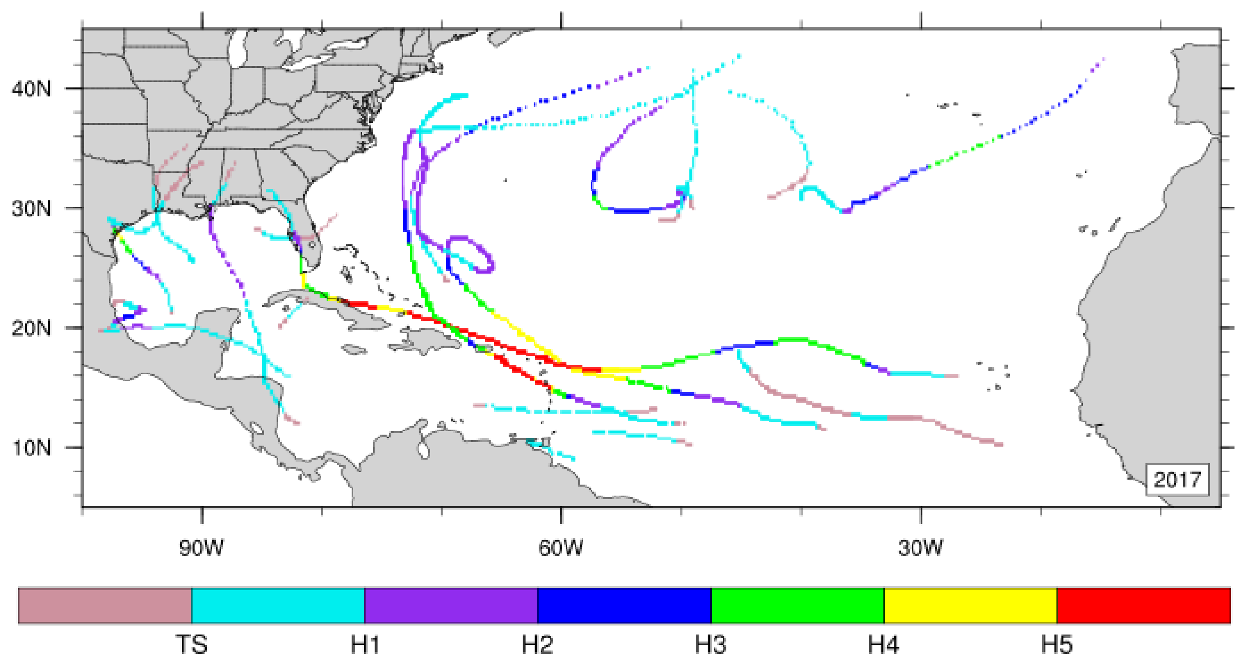

Hurricane Season 2018

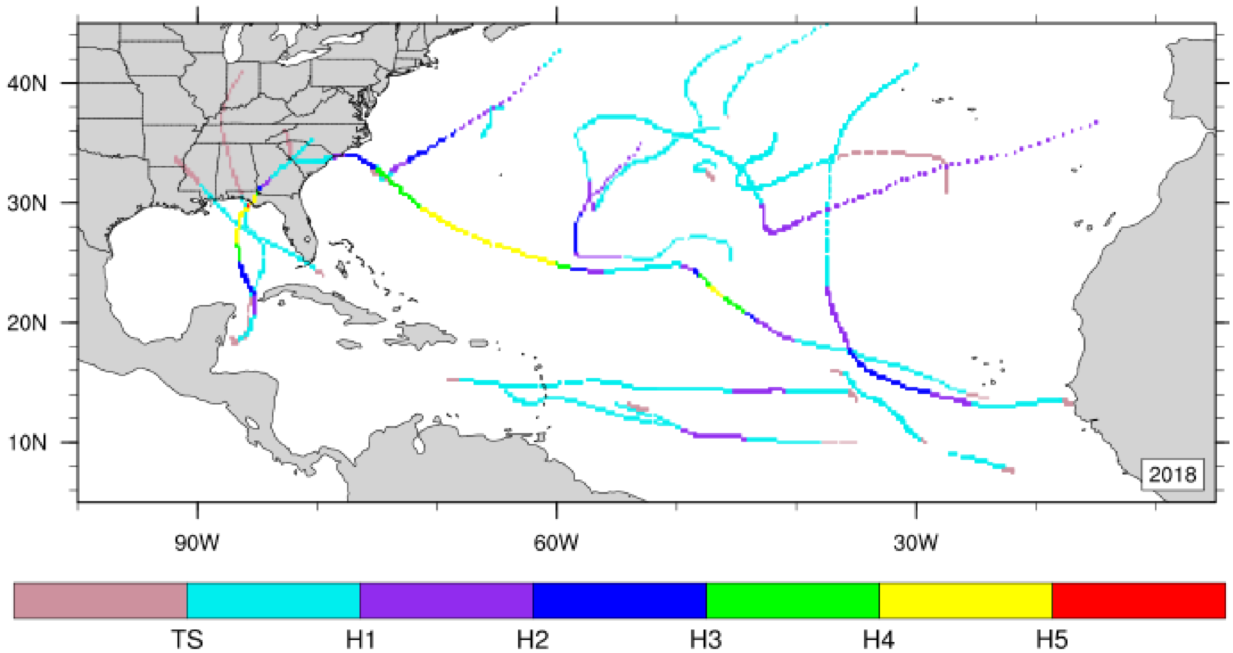

Hurricane Season 2019

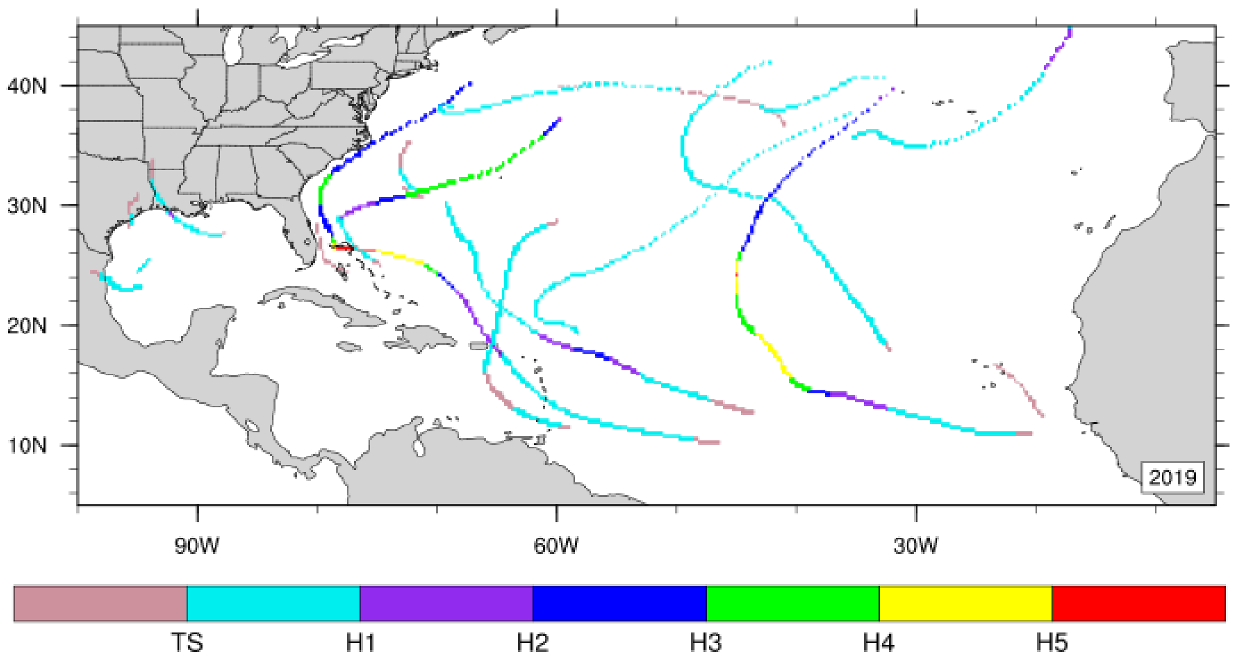

References

Baade, R. A., R. Baumann, and V. Matheson, 2007: Estimating the economic impact of natural and social disasters, with an application to Hurricane Katrina. *Urban Studies*, **44,** 2061-2076.

Beever, E. A., S. A. Sethi, S. Prange, and D. A. DellaSala, 2019: Introduction: Defining and Interpreting Ecological Disturbances. *Disturbance Ecology and Biological Diversity*, CRC Press, 3-38.

Bell, G. D., and M. Chelliah, 2006: Leading tropical modes associated with interannual and multidecadal fluctuations in North Atlantic hurricane activity. *J Climate*, **19,** 590-612.

Bosma, C. D., D. B. Wright, P. Nguyen, J. P. Kossin, D. C. Herndon, and J. M. Shepherd, 2020: An intuitive metric to quantify and communicate tropical cyclone rainfall hazard. *B Am Meteorol Soc*, **101,** E206-E220.

Cane, M. A., and Coauthors, 1997: Twentieth-century sea surface temperature trends. *science*, **275,** 957-960.

Carrasco, C. A., C. W. Landsea, and Y.-L. Lin, 2014: The influence of tropical cyclone size on its intensification. *Weather and Forecasting*, **29,** 582-590.

Chavas, D. R., N. Lin, W. Dong, and Y. Lin, 2016: Observed tropical cyclone size revisited. *Journal of Climate*, **29,** 2923-2939.

Elsner, J. B., J. P. Kossin, and T. H. Jagger, 2008: The increasing intensity of the strongest tropical cyclones. *Nature*, **455,** 92-95.

Emanuel, K., 2017: Assessing the present and future probability of Hurricane Harvey's rainfall. *Proceedings of the National Academy of Sciences*, **114,** 12681-12684.

Enfield, D. B., A. M. Mestas-Nuñez, and P. J. Trimble, 2001: The Atlantic multidecadal oscillation and its relation to rainfall and river flows in the continental US. *Geophysical Research Letters*, **28,** 2077-2080.

Ford, F. A., 2009: *Modeling the environment: an introduction to system dynamics models of environmental systems.* 2nd ed. Island press.

Gori, A., N. Lin, D. Xi, and K. Emanuel, 2022: Tropical cyclone climatology change greatly exacerbates US extreme rainfall–surge hazard. *Nature Climate Change*, **12,** 171-178.

Hall, T. M., and J. P. Kossin, 2019: Hurricane stalling along the North American coast and implications for rainfall. *Npj Climate and Atmospheric Science*, **2,** 17.

Huang, Z., D. Rosowsky, and P. Sparks, 2001: Hurricane simulation techniques for the evaluation of wind-speeds and expected insurance losses. *Journal of wind engineering and industrial aerodynamics*, **89,** 605-617.

Knabb, R. D., J. R. Rhome, and D. P. Brown, 2005: *Tropical cyclone report: Hurricane katrina, 23-30 august 2005.* National Hurricane Center.

Knaff, J. A., S. P. Longmore, and D. A. Molenar, 2014: An objective satellite-based tropical cyclone size climatology. *Journal of Climate*, **27,** 455-476.

Knight, D. B., and R. E. Davis, 2009: Contribution of tropical cyclones to extreme rainfall events in the southeastern United States. *Journal of Geophysical Research: Atmospheres*, **114**.

Knutson, T., and Coauthors, 2019: Tropical cyclones and climate change assessment: Part I: Detection and attribution. *Bulletin of the American Meteorological Society*, **100,** 1987-2007.

Knutson, T. R., J. J. Sirutis, S. T. Garner, G. A. Vecchi, and I. M. Held, 2008: Simulated reduction in Atlantic hurricane frequency under twenty-first-century warming conditions. *Nature Geoscience*, **1,** 359-364.

Kossin, J. P., 2018: A global slowdown of tropical-cyclone translation speed. *Nature*, **558,** 104-107.

Kossin, J. P., K. R. Knapp, T. L. Olander, and C. S. Velden, 2020: Global increase in major tropical cyclone exceedance probability over the past four decades. *Proceedings of the National Academy of Sciences*, **117,** 11975-11980.

Kwit, C., W. J. Platt, and H. H. Slater, 2000: Post-Hurricane Regeneration of Pioneer Plant Species in South Florida Subtropical Hardwood Hammocks 1. *Biotropica*, **32,** 244-251.

Landsea, C. W., and J. L. Franklin, 2013: Atlantic hurricane database uncertainty and presentation of a new database format. *Monthly Weather Review*, **141,** 3576-3592.

Lau, K. M., Y. Zhou, and H. T. Wu, 2008: Have tropical cyclones been feeding more extreme rainfall? *Journal of Geophysical Research: Atmospheres*, **113**.

Li, A., and F. T.-C. Tsai, 2020: Understanding dynamics of groundwater flows in the Mississippi River Delta. *Journal of Hydrology*, **583,** 124616.

Lillo, S.: Tropycal. [Available online at https://tropycal.github.io/tropycal/#.]

Lupo, A. R., T. K. Latham, T. H. Magill, J. V. Clark, C. J. Melick, and P. S. Market, 2008: The interannual variability of hurricane activity in the Atlantic and East Pacific regions.

McCabe, G. J., M. A. Palecki, and J. L. Betancourt, 2004: Pacific and Atlantic Ocean influences on multidecadal drought frequency in the United States. *Proceedings of the National Academy of Sciences*, **101,** 4136-4141.

Murakami, H., T. Li, and P.-C. Hsu, 2014: Contributing factors to the recent high level of accumulated cyclone energy (ACE) and power dissipation index (PDI) in the North Atlantic. *Journal of climate*, **27,** 3023-3034.

Naqvi, Z. R., 2010: Using remote sensing to assess potential impacts of hurricanes on mosquito habitat formation : investigating the mechanisms for interrelationship between climate and the incidence of vector-borne diseases, Environmental Science, Baylor University.

National Oceanic & Atmospheric Administration National Centers for Environmental Information: Pacific Decadal Oscillation (PDO). [Available online at https://www.ncei.noaa.gov/access/monitoring/pdo/.]

National Oceanic & Atmospheric Administration Physical Sciences Laboratory: Climate Timeseries AMO (Atlantic Multidecadal Oscillation) Index. [Available online at https://psl.noaa.gov/data/timeseries/AMO/.]

——: Download Climate Timeseries, Nino 3.4. [Available online at https://psl.noaa.gov/gcos_wgsp/Timeseries/.]

Newman, M., and Coauthors, 2016: The Pacific decadal oscillation, revisited. *J Climate*, **29,** 4399-4427.

Nnamchi, H. C., M. Latif, N. S. Keenlyside, and W. Park, 2020: A satellite era warming hole in the equatorial Atlantic ocean. *Journal of Geophysical Research: Oceans*, **125,** e2019JC015834.

Nogueira, R. C., B. D. Keim, D. P. Brown, and K. D. Robbins, 2013a: Variability of rainfall from tropical cyclones in the eastern USA and its association to the AMO and ENSO. *Theoretical and applied climatology*, **112,** 273-283.

——, 2013b: Variability of rainfall from tropical cyclones in the eastern USA and its association to the AMO and ENSO. *Theoretical and applied climatology*, **112,** 273-283.

Pielke Jr, R. A., C. Landsea, M. Mayfield, J. Layer, and R. Pasch, 2005: Hurricanes and global warming. *Bulletin of the American Meteorological Society*, **86,** 1571-1576.

Pielke, R. A., and C. W. Landsea, 1998: Normalized hurricane damages in the United States: 1925–95. *Weather and forecasting*, **13,** 621-631.

Saffir, H. S., 1973: Hurricane wind and storm surge. *The Military Engineer*, **65,** 4-5.

Seneviratne, S. I., and Coauthors, 2021: 11 Chapter 11: Weather and climate extreme events in a changing climate.

Shearer, E. J., V. Afzali Gorooh, P. Nguyen, K.-L. Hsu, and S. Sorooshian, 2022: Unveiling four decades of intensifying precipitation from tropical cyclones using satellite measurements. *Scientific reports*, **12,** 1-15.

Shepherd, J. M., A. Grundstein, and T. L. Mote, 2007: Quantifying the contribution of tropical cyclones to extreme rainfall along the coastal southeastern United States. *Geophysical Research Letters*, **34**.

Shultz, J. M., J. Russell, and Z. Espinel, 2005: Epidemiology of tropical cyclones: the dynamics of disaster, disease, and development. *Epidemiologic reviews*, **27,** 21-35.

Sousa, W. P., 1984: The role of disturbance in natural communities. *Annual review of ecology and systematics*, **15,** 353-391.

Taylor, H. T., B. Ward, M. Willis, and W. Zaleski, 2010: The saffir-simpson hurricane wind scale. *Atmospheric Administration: Washington, DC, USA*.

Trenberth, K., 2005: Uncertainty in hurricanes and global warming. *Science*, **308,** 1753-1754.

Trenberth, K. E., 1996: El Niño southern oscillation (ENSO). *Sea*.

Trenberth, K. E., J. Fasullo, and L. Smith, 2005: Trends and variability in column-integrated atmospheric water vapor. *Climate dynamics*, **24,** 741-758.

Van Oldenborgh, G. J., and Coauthors, 2017: Attribution of extreme rainfall from Hurricane Harvey, August 2017. *Environmental Research Letters*, **12,** 124009.

Vickery, P., P. Skerlj, and L. Twisdale, 2000: Simulation of hurricane risk in the US using empirical track model. *Journal of structural engineering*, **126,** 1222-1237.

Vickery, P. J., F. J. Masters, M. D. Powell, and D. Wadhera, 2009: Hurricane hazard modeling: The past, present, and future. *Journal of Wind Engineering and Industrial Aerodynamics*, **97,** 392-405.

Villarini, G., and G. A. Vecchi, 2012: North Atlantic power dissipation index (PDI) and accumulated cyclone energy (ACE): Statistical modeling and sensitivity to sea surface temperature changes. *Journal of climate*, **25,** 625-637.

——, 2013: Multiseason lead forecast of the North Atlantic power dissipation index (PDI) and accumulated cyclone energy (ACE). *Journal of climate*, **26,** 3631-3643.

Wang, F., and Y. J. Xu, 2009: Hurricane Katrina-induced forest damage in relation to ecological factors at landscape scale. *Environmental Monitoring and Assessment*, **156,** 491-507.

Weinkle, J., C. Landsea, D. Collins, R. Musulin, R. P. Crompton, P. J. Klotzbach, and R. Pielke, 2018: Normalized hurricane damage in the continental United States 1900–2017. *Nature Sustainability*, **1,** 808-813.

Witman, J. D., 1992: Physical disturbance and community structure of exposed and protected reefs: a case study from St. John, US Virgin Islands. *American Zoologist*, **32,** 641-654.

Wolfe, S. H., 1988: *An ecological characterization of the Florida Panhandle.* US Department of the Interior, Fish and Wildlife Service.

Yu, J. Y., C. Chou, and P. G. Chiu, 2009: A revised accumulated cyclone energy index. *Geophysical research letters*, **36**.

Zhang, R., and T. L. Delworth, 2006: Impact of Atlantic multidecadal oscillations on India/Sahel rainfall and Atlantic hurricanes. *Geophysical research letters*, **33**.